



TWINLATIN

Twinning European and Latin-American River Basins
for Research Enabling Sustainable Water Resources
Management

Work Package 3

Hydrological Modelling and Extremes

D3.1 Hydrological modelling report

D3.2 Evaluation reports

February 2009



List of Contents

1. INTRODUCTION	1
2. BAKER (AND BIOBÍO) RIVER BASIN (CHILE).....	5
2.1 Description of basin	5
2.2 Choice of model.....	11
2.2.3 User interface	12
2.3 Data requirements	13
2.3.1 Input data.....	13
2.3.2 Output data	14
2.4 Scenario modelling.....	14
2.5 Model development.....	17
2.5.1 Overview	17
2.5.2 Model set-up.....	17
2.5.3 Input Data.....	20
<i>Topography.....</i>	<i>20</i>
2.6 Calibration.....	23
2.7 Validation	25
2.8 Evaluation of hydrological modelling (D3.2).....	27
2.9 Summary and recommendations.....	28
3. CATAMAYO-CHIRA RIVER BASIN (ECUADOR-PERU).....	30
3.1 Description of basin	30
3.1.1 Hydrology	30
3.2 Choice of model.....	31
3.2.1 Problems.....	31
3.3 Model development.....	32
3.4 Data requirements	35
3.5 Calibration.....	40
3.6 Validation	46
3.7 Results.....	48
3.8 Scenario modelling.....	54
3.9 Evaluation of hydrological modelling (D3.2).....	55
3.10 Summary and recommendations.....	56
4. CAUCA RIVER BASIN (COLOMBIA)	59
4.1 Description of basin	59
4.2 Choice of model.....	60
4.3 Data requirements	61

4.4	Model development.....	62
4.5	Calibration.....	64
4.6	Validation	65
4.7	Evaluation of hydrological modelling (D3.2).....	65
4.8	Summary and recommendations.....	68
5.	COCIBOLCA LAKE BASIN (NICARAGUA)	69
5.1	Description of basin	69
5.1.1	Introduction	69
5.1.2	The regional climate.....	71
5.1.3	Previous studies and TWINLATIN objectives	72
5.2	Choice of model.....	73
5.3	Data requirements	83
5.4	Scenario modelling.....	84
5.5	Model development.....	85
5.6	Calibration and validation	93
5.7	Evaluation of hydrological modelling (D3.2).....	111
5.8	Summary and recommendations.....	114
6.	QUARAÍ RIVER BASIN (BRAZIL)	115
6.1	Description of basin	115
6.2	Choice of model.....	115
6.3	Data requirements	116
6.4	Scenario modelling.....	118
6.5	Model development.....	118
6.6	Calibration.....	128
6.7	Validation	131
6.8	Evaluation of hydrological modelling (D3.2).....	133
6.9	Summary and recommendations.....	134
7.	CUAREIM RIVER BASIN (URUGUAY)	135
7.1	Description of basin	135
7.1.1	Location.....	135
7.2	Choice of model.....	146
7.2.1	Current administration.....	146
7.3	Data requirements	150
7.4	Scenario modelling.....	152
7.5	Model development: SWAT.....	161
7.6	Model development: MODSIM	165
7.7	Calibration of SWAT.....	172

7.8	Validation of SWAT	175
7.9	Evaluation of hydrological modelling (D3.2).....	176
7.10	Summary and recommendations.....	184
8.	NORRSTRÖM.....	185
8.1	Description of basin	185
8.1.1	Natural Setting.....	185
8.1.2	Hydrology.....	186
8.1.3	Water Resources	186
8.2	Norrström collection of source data	187
8.2.1	Data storage	187
8.2.2	Geographical input data.....	187
8.3.	Development of the new Watshman modelling system.....	189
8.3.1	Input data	190
8.3.2	Database design	190
8.3.3	Watshman system architecture	190
8.3.4	Point Source Data Analysis	191
8.3.5	Geo-processing	192
8.3.6	Hydrological modelling.....	193
8.3.6	Leakage modelling, scenario analysis and data presentation	193
8.4.	Hydrological modelling in Norrström subbasins	194
8.4.1	Results of hydrological modelling in Norrström subbasins.....	194
8.5	Results from flow proportional measurements conducted by IVL	196
8.5.1	Discussion of hydrological modelling results.....	199
9.	SOUTH AMERICA CONTINENTAL MODELLING	200
9.1	Description of basin	200
9.2	Choice of model.....	200
9.3	Data requirements	201
9.4	Scenario modelling.....	207
9.5	Model development.....	207
9.6	Calibration and validation	209
9.7	Results	215
9.8	Evaluation of hydrological modelling (D3.2).....	216
9.9	Summary and recommendations.....	217
10.	SUMMARY AND RECOMMENDATIONS	218
10.1	Key results and achievements.....	219
10.2	Discussions and recommendations	221
	REFERENCES	223

List of Figures

Figure 2.1	Location and topography of the Baker River Basin, Chile	5
Figure 2.2	Lakes, tributaries and the most important sub-basins in the Baker River Basin.....	6
Figure 2.3	Mean annual temperature and precipitation for the Baker River Basin (DGA, 1987).....	7
Figure 2.4	Extent and completeness (%) of the daily time series of precipitation data for the Baker River Basin.....	8
Figure 2.5	Daily and hourly precipitation stations from DGA.....	9
Figure 2.6	Extent and completeness (%) of the daily discharge data time series.....	10
Figure 2.7	DGA's fluviometric network in the Baker River Basin.....	10
Figure 2.8	Main interface window	12
Figure 2.9	View of thematic data layers in AVSWAT	13
Figure 2.10	Grid points from the RCM run conducted by DGF- CONAMA (2006); at each point a 30-year daily time series (2071 – 2100) is available.....	16
Figure 2.11	Location of the Lonquimay sub-basin within the Biobío Basin.....	17
Figure 2.12	Representation of the land phase of the hydrological cycle within SWAT	18
Figure 2.13	Meteorological stations used for modelling.....	21
Figure 2.14	Land use for the Lonquimay Basin.....	22
Figure 2.15	Monthly observed versus simulated flows at the Lonquimay gauging station during calibration	24
Figure 2.16	Monthly observed versus simulated flows at the Lonquimay gauging station during validation	25
Figure 2.17	MOD10A2 images.....	26
Figure 2.18	Percentage of disagreement between monthly model outputs and MODIS images, for the different sub-basin. For 2000 only the months from March to December are considered.....	27
Figure 3.1	Location of the basin	30
Figure 3.2	DEM, river network and study area for SWAT in the Catamayo-Chira basin.....	33
Figure 3.3	Location of the five measurement stations of used streamflows in the calibration of SWAT	34
Figure 3.4	Meteorological stations used to apply SWAT in the Catamayo-Chira basin	36
Figure 3.5	Visualisation of precipitation regime stations used for SWAT application: mean monthly precipitation in (a) Ecuador and (b) Peru	37
Figure 3.6	Land cover and actual soil use applied to SWAT	38
Figure 3.7	Soil types used in SWAT.....	39
Figure 3.8	Most sensitive parameters for the basin.....	40
Figure 3.9	Simulated and observed streamflows during calibration period (1970-1981):station Santa Rose (sub-basin Catamayo).....	42
Figure 3.10	Simulated and observed streamflows during calibration period (1973-1983):station Puente Internacional (sub-basin Macará).....	42
Figure 3.11	Simulated and observed streamflows during calibration period (1970-1983):station Alamor en Saucillo (sub-basin Alamor)	43
Figure 3.12	Simulated and observed streamflows during calibration period (1974-1983) station Paraje Grande (sub-basin Quiróz).....	43

Figure 3.13 Simulated and observed streamflows during calibration period (1976-1986):station Ardilla (inlet at Poechos).....	43
Figure 3.14 Accumulated flows at Ardilla station (inlet at Poechos) (1976-1986).....	44
Figure 3.15 Location of the two sediment measurement stations used in SWAT calibration.....	44
Figure 3.16 Simulated and observed sediments during the calibration period: station Puente Internacional (sub-basin Macará).....	45
Figure 3.17 Simulated and observed sediments during the calibration period: station Ardilla (inlet at Poechos).....	45
Figure 3.18 Simulated and observed streamflows during calibration and validation period (1970-1994): station Santa Rose (sub-basin Catamayo).....	46
Figure 3.19 Simulated and observed streamflows during calibration and validation period (1973-1994): station Puente Internacional (sub-basin Macará).....	46
Figure 3.20 Simulated and observed streamflows during calibration and validation period (1970-1994): station Alamor en Saucillo (sub-basin Alamor).....	47
Figure 3.21 Simulated and observed streamflows during calibration and validation period (1974-1992):station Paraje Grande (sub-basin Quiróz).....	47
Figure 3.22 Simulated and observed streamflows during calibration and validation period (1974-1994): station Ardilla (inlet at Poechos).....	47
Figure 3.23 Most sediment producing microbasins.....	50
Figure 3.24 Sediment production in the basin for different hydrological years.....	51
Figure 3.25 Water production in the basin for different hydrological years.....	52
Figure 3.26 Most water producing microbasins.....	53
Figure 3.27 Water production expressed in MCM.....	54
Figure 4.1 Study zone location.....	59
Figure 4.2 General structure of the HBV/IHMS model.....	61
Figure 4.3 HBV/IHMS model scheme in the basin.....	63
Figure 4.4 Location of the Tulúa River Basin in the Upper Cauca River Basin.....	64
Figure 4.5 Multiannual monthly comparison of estimated (red) and recorded (green) hydrography for the period 1974–1995 for Mateguadua station in the Tulúa River Basin.....	65
Figure 4.6 Monthly annual variations of recorded and estimated flows for the period 1974-1995.....	66-67
Figure 4.1 Study zone location.....	59
Figure 4.2 General structure of the HBV/IHMS model.....	61
Figure 4.3 HBV/IHMS model scheme in the basin.....	63
Figure 4.4 Location of the Tulúa River Basin in the Upper Cauca River Basin.....	64
Figure 4.5 Multiannual monthly comparison of estimated (red) and recorded (green) hydrography for the period 1974–1995 for Mateguadua station in the Tulúa River Basin.....	65
Figure 4.6 Monthly annual variations of recorded and estimated flows for the period 1974-1995.....	66-67
Figure 5.1 The Lake Managua, Lake Cocibolca and River San Juan basins, data from USGS (2006).....	69
Figure 5.2 Chronogram showing the temporal availability of daily mean temperature data for the Lake Cocibolca catchment and immediate surroundings.....	73
Figure 5.3 Influence of distance and level of temporal aggregation on the correlation between temperature data time series for the stations from the Lake Cocibolca Basin. Red and blue dots represent correlation values for	

monthly and daily mean temperature data, respectively; each dot represents a correlation between two stations plotted against the distance between these two stations.....	74
Figure 5.4 Daily and annual mean temperatures at the stations Aeropuerto Internacional Managua and Juigalpa. The mean annual temperatures (thick lines) are plotted at the first day of the year, therefore slightly more to the left than the corresponding daily data.	74
Figure 5.5 Comparison of annual precipitation and temperature variability. The thick blue and black lines represent the annual temperature from the stations Aeropuerto Internacional Managua and Juigalpa, respectively; the thinner lines the annual precipitation for stations with complete yearly records.	75
Figure 5.6 Number of stations per year for which complete precipitation time series datasets are available, before and after quality control and gap-filling (the difference between the black and the blue lines represents the amount of data that is of too poor quality to be used).	76
Figure 5.7 Mean annual precipitation for the stations with a $\geq 70\%$ complete dataset for the period 1970 – 1990 (the background image shows a shaded relief map for the study area).	77
Figure 5.8 Correlation between the data from all the precipitation stations with daily data plotted against distance for different levels of temporal aggregations. One data point represents the mean of 120 correlation coefficient values. There was a marked increase in correlation coefficient values for the 4-5 day data aggregation level as compared to daily data.	77
Figure 5.9 Discharge stations and sub-basins of the Lake Cocibolca basin.....	78
Figure 5.10 Chronogram showing the temporal availability of daily discharge data for the Lake Cocibolca basin	79
Figure 5.11 Chronogram showing the temporal availability of monthly discharge data for the San Juan River ..	79
Figure 5.12 Temporal availability of discharge on a daily and monthly time scale, including stations located on the San Juan River (downstream of the lake outlet).....	79
Figure 5.13 Temporal availability of data on climatic variables required for the evapotranspiration calculations (analysis based on daily data but plotted at the monthly level to facilitate viewing)	80
Figure 5.14 The schematic computational flow chart of the WASMOD model (Xu, 2002).....	81
Figure 5.15 Flow chart of the WATSHMAN-PCRaster model adapted for snow-free conditions, modified from Westerberg (2005).....	82
Figure 5.16 Example of sample semi-variogram with fitted curve	87
Figure 5.17 Number of stations with monthly data available within a 20 km radius of the Mayales catchment over time	90
Figure 5.18 Digital elevation model (720 m pixel size) and flow network for the upper part of the Mayales basin, elevation in metres	90
Figure 5.19 Soil types in the Mayales catchment, classification from Mapa Agroecológico 1:50,000, (MAGFOR)	91
Figure 5.20 Daily (unrevised) discharge data from the Jicaral station in the Mayales catchment	92
Figure 5.21 Results of the CCWM gap filling method at the station Rivas for the period 1995-2005, observed and filled in values have been converted to monthly values	93
Figure 5.22 Chronogram of original daily data converted to monthly data	94
Figure 5.23 Chronogram of monthly data after gap-filling with the CCWM method.....	94
Figure 5.24 Sample semi-variogram for mean annual precipitation 1995-99, calculated on stations with more than 50% data in that period.....	95
Figure 5.25 Sample semi-variogram for mean annual precipitation 1975-85, calculated on stations with more than 70% data in that period, for the whole basin (left), Costa Rican part (middle) and Nicaraguan part (right). 96	
Figure 5.26 Comparison of methods for mean yearly precipitation in 1975-1994 calculated on stations with more than 30% complete years of monthly precipitation; stations within the basin are shown as black dots.....	96
Figure 5.27 The range of monthly precipitation in the basin for the 20-year period 1975-1994 was calculated on the stations with more than 50% complete years of monthly precipitation.....	97

Figure 5.28 Mean monthly precipitation for the 20-year period 1975-1994 was calculated on stations with more than 50% complete years of monthly precipitation. January through March is shown in the upper row (left to right) and April through June in the lower row (left to right).	98
Figure 5.29 Mean monthly precipitation for the 20-year period 1975-1994 was calculated on stations with more than 50% complete years of monthly precipitation. July through September is shown in the upper row (left to right) and October through December in the lower row (left to right).	98
Figure 5.30 Gap-filled monthly precipitation for all stations and mean areal precipitation interpolated with the IDW-method.	99
Figure 5.31 Comparison of 8-day evapotranspiration calculated with the Full Penman-Monteith equation and from the MODIS project.	101
Figure 5.32 Comparison of 8-day evapotranspiration calculated with the Full Penman-Monteith equation and from the MODIS project.	101
Figure 5.33 Cross-comparison of evapotranspiration calculations and PanA evapotranspiration at Aeropuerto Internacional Managua, Juigalpa and Rivas stations.	102
Figure 5.34 Mean annual precipitation (left) and actual evapotranspiration from the MODIS project (right) for the years 2000-2005. In the precipitation map the location of the precipitation stations are included as dots. The interpolation of precipitation cannot be considered valid in the Costa Rican part of the basin.	103
Figure 5.35 Mean annual run-off 2000-2005 calculated with the simple water balance model. The dots represent the precipitation stations in the basin where there were at least three years of complete data in this period; they were used for the interpolation of precipitation. The water balance cannot be considered valid in the Costa Rican part of the basin as there were no precipitation stations there during this period, and the interpolation of precipitation there is thus very uncertain	103
Figure 5.36 Precipitation interpolated with Universal Kriging for the period 1975-1994, stations having more than 30% complete yearly data in that period were used for the interpolation and those stations located within the watershed boundary are shown as black dots. The precipitation is considerably higher in the Costa Rican part of the basin	104
Figure 5.37 Limits of acceptability around the observed monthly discharge (mm) in the Mayales catchment.	105
Figure 5.38 Discharge in mm for the calibration of WASMOD in the period 1970-1990, the top graph shows the simulated uncertainty bound for the Reff-criterion and the bottom graph the uncertainty bound for the limit of acceptability criterion. Most of the observed data (red rings) were within the uncertainty bounds. The red rings with a black cross mark months where the model fails and the observations fall outside the limits of acceptability, this occurs less frequently for the low flows for the limit of acceptability criterion.	106
Figure 5.39 Discharge in mm for the validation of WASMOD in the period 1991-2005, the top graph shows the simulated uncertainty bound for the Reff-criterion and the bottom graph the uncertainty bound for the limit of acceptability criterion. Observed discharge within the uncertainty bounds are shown as red rings and those outside as a ring with a cross in it.	106
Figure 5.40 Discharge in mm for the validation of WASMOD in the period 1970-1990, the top graph shows the simulated uncertainty bound for the Reff-criterion and the bottom graph the uncertainty bound for the limit of acceptability criterion. Observed discharge within the uncertainty bounds are shown as red rings and those outside as a ring with a cross in it.	107
Figure 5.41 Uncertainty in predicted yearly discharge (mm) 1970-1990 in the Mayales catchment for the R_{eff} (top) and the limit of acceptability criterion (bottom). Red rings are observed yearly discharge.	108
Figure 5.42 Uncertainty in predicted yearly discharge (mm) 1991-2005 in the Mayales catchment for the R_{eff} (top) and the limit of acceptability criterion (bottom).	108
Figure 5.43 Calibration results from 1968 to 1982 for the PCRaster model application in the Mayales sub-catchment	109
Figure 5.44 Calibration results for 1980-1981 for the PCRaster model application in the Mayales sub-catchment. The simulated discharge data do not match the observed discharge in the start of the rainy season during 1980 where there are no peaks in the simulated discharge, but model performance is acceptable around the peak flows	109
Figure 5.45 Accumulated groundwater flow (m3/s) simulated in the model during a precipitation event.	110

Figure 5.46 Validation results from 1982 to 1994 for the PCRaster model application in the Mayales sub-catchment.....	110
Figure 5.47 Validation results from 1986 (top) and 1989 (bottom) for the PCRaster model application in the Mayales sub-catchment. In 1986 the first observed discharge peaks are not matched by the model which might be because of errors in the response of the model, discharge or precipitation. In 1989 there were peaks in the modelled discharge, which were not in the observed data. This suggests a too-fast response in the model, errors in discharge data or that the registered precipitation events were local and not representative of the basin as a whole.....	111
Figure 6.1 Division of the Quarai river basin in three watersheds according to the availability of data at stream gauges, and in catchments (grey outlined polygons within each watershed).....	122
Figure 6.2 Land use map of the Quarai river basin.....	123
Figure 6.3 Water balance variables considered in the simulation of a reservoir.....	124
Figure 6.4 Relation between surface area and maximum reservoir volume and linear function adjusted to the data.....	125
Figure 6.5 Scheme of water fluxes in a rice field: rainfall (P); irrigation (Irr); evapotranspiration (ET); infiltration losses (Di); spilling losses (Dv).....	126
Figure 6.6 Calculated (red) and observed (black) hydrographs of the river Quarai at Artigas/Quarai gauging station during part of the calibration period.....	129
Figure 6.7 Calculated (red) and observed (black) hydrographs of the river Quarai at Artigas/Quarai gauging station during part of the calibration period (1994-95 – log scale to highlight low flows).....	129
Figure 6.8 Flow duration curves for observed (black) and calculated (red) streamflows at Quarai/Artigas from 1980 to 2004.....	130
Figure 6.9 Flow duration curve of the river Quarai at its outlet (Barra do Quarai) showing lower values of Q95 than further upstream (Artigas/Quarai) due to river water abstractions.....	131
Figure 6.10 Calculated (red) and observed (black) hydrographs of the river Tres Cruces at Javier de Viana gauging station (model validation).....	132
Figure 6.11 Calculated (red) and observed (black) hydrographs of the river Tres Cruces at Javier de Viana gauging station (logarithmic scale to highlight low flows).....	132
Figure 6.12 Water used in rice irrigation according to the hydrological model results from 1981 to 2006, considering total water use, rainfall and supplemental irrigation.....	133
Figure 7.1 Location of the Tres Cruces creek.....	135
Figure 7.2 Tres Cruces creek basin.....	135
Figure 7.3 Raingauges with influence in the Tres Cruces creek basin.....	136
Figure 7.4 Precipitation annual cycle for the 330 raingauge. Precipitation in mm on the vertical axes and Months from January to December on horizontal axes, being the last one Annual values. The grey bars are the monthly average precipitation and the red bars the standard deviation in mm.....	137
Figure 7.5 Precipitation annual cycle for the 1019 raingauge. Precipitation in mm on the vertical axes and Months from January to December on horizontal axes, being the last one Annual values. The grey bars are the monthly average precipitation and the red bars the standard deviation in mm.....	137
Figure 7.6 Geology of the Tres Cruces creek basin (Source: Geology map of Uruguay).....	138
Figure 7.7 Groups of soils in the Tres Cruces creek basin (Source: Altamirano et al., 1976).....	139
Figure 7.8 Apt areas for rice-pasture system in the Tres Cruces creek basin (In green soil very apt, in pink soil apt, in yellow soil moderately apt).....	140
Figure 7.9 Tres Cruces creek basin's topography. Heights in m. (Note: The reference zero for the heights is 21.2 m below the official zero, see section 7.1.5).....	141

Figure 7.10 3D representation of the DEM in an area of the Cuareim River basin	142
Figure 7.11 Measured points of SGM and heights of the NASA MDE (Source: “Proyecto Piloto de Gestión Integrada de Crecidas en la Cuenca del Río Cuareim/Quaraí – Uruguay/Brasil”, 2005).....	142
Figure 7.12 Correlation between SGM and NASA DEM levels (Source: “Proyecto Piloto de Gestión Integrada de Crecidas en la Cuenca del Río Cuareim/Quaraí – Uruguay/Brasil”, 2005).....	143
Figure 7.13 Correlation between the 60 geodetic vertices of the SGM and the NASA DEM (Source: “Proyecto Piloto de Gestión Integrada de Crecidas en la Cuenca del Río Cuareim/Quaraí – Uruguay/Brasil”, 2005).....	143
Figure 7.14 Aerial photo of the Tres Cruces creek (Source: Google Earth)	144
Figure 7.15 Photographic view of the Tres Cruces creek	144
Figure 7.16 Location of 155 gauging station (red dot).....	145
Figure 7.17 Scale at the 155 gauging station	144
Figure 7.18 Annual flow cycle of the Tres Cruces creek at the 155 gauging station. In vertical axis Flow m^3s^{-1} , in horizontal axis Months from January to December, and the last two bars correspond to the whole year. Bars in blue are average flow in m^3s^{-1} while bars in red are standard deviation.	145
Figure 7.19 Permanence curve of 155 gauging station. Vertical axis is Flow m^3s^{-1} and horizontal axis is Probability.....	146
Figure 7.20 Existing dams and direct intakes in the Tres Cruces creek basin (red squares are direct intakes and green triangles are reservoirs	147
Figure 7.21 Planted rice area per rice season. On vertical axis, irrigated area in hectares. On horizontal axis, rice season. On blue, reservoirs. On red, direct intakes	148
Figure 7.22 Raingauges (red) and meteorological station (yellow)	151
Figure 7.23 Flow measurements at Tres Cruces creek basin	151
Figure 7.24 Runoff in the 1932-2007 period, in the Tres Cruces creek basin (Vertical axis, runoff in thousands of m^3 per month, horizontal axis, month and year)	153
Figure 7.25 Annual runoff cycle in Tres Cruces creek basin (Vertical axis, flow in thousands or m^3 per month). Horizontal axis, Month from January to December and at the end Annual. Green bars are average flow in m^3 per month, and red bars are standard deviations in m^3 per month)	153
Figure 7.26 Histogram of the stored volume in October at an infinitive reservoir located at the outlet of the Tres Cruces creek basin (1932-2007). Vertical axis: frequency, Horizontal axis: Maximum volume in October (millions of m^3).....	154
Figure 7.27 Maximum volume in October that is reached with 100%, 90% y 80% frequency. Vertical axis: volume in October. Horizontal axis: basin. Red bar, 100% frequency, yellow bar 90%, and green 80%.	155
Figure 7.28 Histogram of the maximum area of rice that could be irrigated, considering that only rice is irrigated. Vertical axis: Frequency. Horizontal axis: Maximum area of rice.....	157
Figure 7.29 Histogram of the maximum area of rice that could be irrigated, considering that rice and pastures are irrigated. Vertical axis: Frequency. Horizontal axis: Maximum area of rice	158
Figure 7.30 Maximum area of rice that would be possible to irrigate with a frequency of 100%, 90% and 80%, considering only the irrigation of rice. Vertical axis: Maximum area of rice. Horizontal axis: Contributing basin. Red bar: 100% Frequency. Yellow bar: 90% Frequency. Blue bar: 80% Frequency.	159
Figure 7.31 Maximum area of rice that would be possible to irrigate with a frequency of 100%, 90% and 80%, considering the irrigation of both rice and pastures. Vertical axis: Maximum area of rice. Horizontal axis: Contributing basin. Red bar: 100% Frequency. Yellow bar: 90% Frequency. Blue bar: 80% Frequency.....	160
Figure 7.32 Studied sub-basins	162
Figure 7.33 Current land uses (Red: Native Forest, Yellow: Pasture, Orange: Rice, Green: Water).....	162
Figure 7.34 Soils in the basin.....	163
Figure 7.35 Hydrologic configuration system for the Tres Cruces creek basin in MODSIM.....	167
Figure 7.36 Basins that contribute to the existing reservoirs in the Tres Cruces creek basin	169

Figure 7.37 Remaining basins.....	170
Figure 7.38 Volume of water in the reservoir 32	170
Figure 7.39 Runoff, evaporation and volume of water in October – reservoir 32	171
Figure 7.40 Demand for reservoir 25	171
Figure 7.41 Monthly runoff in link N8_N7.....	172
Figure 7.42 Daily runoff for Javier de Viana in 2005. Vertical axis: relative sensitivity. Horizontal axis: SWAT parameters	173
Figure 7.43 Flow chart for calibration	173
Figure 7.44 Daily runoff for the period 01/07/2004 - 30/06/2005 at Javier de Viana. Blue graph: measured flow. Red graph: calculated flow. Black graph: precipitation.....	174
Figure 7.45 Daily runoff for the period 01/07/2005 - 30/06/2006 at Javier de Viana. Blue graph: measured flow. Red graph: calculated flow. Black graph: precipitation	174
Figure 7.46 Daily runoff for period 01/07/2006 - 30/06/2007 at Javier de Viana. Blue graph: measured flow. Red graph: calculated flow. Black graph: precipitation.	176
Figure 7.47 Daily runoff in period 01/07/2007 - 30/06/2008 for Javier de Viana	176
Figure 7.48 Relationship between a variation in precipitation and the corresponding variation in runoff. Green: Average. Red: Percentile 50. Blue : Percentile 95	177
Figure 7.49 Permanence curves	178
Figure 7.50 Annual runoff used by DNH vs annual average runoff for the subbasins (Temez). Vertical axis: Annual average runoff (mm). Green dots: Annual average runoff (Temez). Red line: Criterion DNH. Green line: Average annual average runoff.....	179
Figure 7.51 Sub-basins for the two reservoirs and MODSIM scheme.....	180
Figure 7.52 MODSIM output: dam 20's demand, current scenario	180
Figure 7.53 MODSIM output: dam 20's demand, assumed scenario	181
Figure 7.54 MODSIM output: dams 20AA's demand, assumed scenario	181
Figure 7.55 Basins of the reservoirs and MODSIM scheme.....	182
Figure 7.56 MODSIM output: reservoir 30's demand, current and assumed scenarios.....	183
Figure 7.57 MODSIM output: reservoir 30AA's demand, assumed scenario	183
Figure 8.1 The Lake Mälaren and its surrounding land use.....	185
Figure 8.2 Land use percentage of the modelled area.....	186
Figure 8.3 The user interface of the Watshman extension to ArcMap.....	189
Figure 8.4 Watshman system architecture and data flow	191
Figure 8.5 Interface of a step in the Point Source Data Analysis wizard	192
Figure 8.6 The first step of the Geo-processing wizard	192
Figure 8.7 The interface of the hydrological modelling module.....	193
Figure 8.8 Measuring stations used in the modelling.....	195
Figure 8.9 Measured and modelled water flow at Ransta measuring station 1996-2001	195
Figure 8.10 Lake Mälaren catchment as represented in the SWAT-model. Sub-basin division coincides with the Swedish national division system. The catchments where the flow-driven sampling stations are located are indicated with yellow.....	197
Figure 8.11 Hydrological results for Grillby.....	198

Figure 9.1	Illustration of the gridded river (thin line) and accumulated flow (thick line) networks	203
Figure 9.2	Derived landcover for four indicative vegetation classes	203
Figure 9.3	Comparison of wetland coverage for two datasets: left, GLCC/ IGBP classification and right, GLWD (Lehner & Doll, 2004) denoted by green areas	204
Figure 9.4	Mean number of climate stations used in the derivation of the CRU dataset for the period 1961 - 1990.	204
Figure 9.5	Summary of water withdrawals by sector for South America	205
Figure 9.6	Percentage of crop type by area that are irrigated across South America (source: FAO-AQUASTAT)	206
Figure 9.7	Location and coverage of calibration basin	210
Figure 9.8	Plots comparing the mean monthly flows (left) and annual biases between modelled and observed flows (right) for four basins in South America	213-214
Figure 9.9	Observed and modelled monthly streamflow for the Orinoco at Pte Angostura	212
Figure 9.10	Maps illustrating a) WAI Type 1 b) WAI Type 3 and c) WAI Type 4 for South America computed for the baseline period 1961-1990.	216

List of Tables

Table 1.1	Approach to hydrological modelling	3
Table 1.1	Hydrological models used during TWINLATIN WP3	4
Table 2.1	Input data sources	14
Table 2.2	Model output parameters	15
Table 2.3	Chilean land use and its equivalent in the SWAT database	22
Table 2.4	Sensitivity ranking of the snowfall/snowmelt parameters	24
Table 2.5	Statistical indicators of model performance (monthly output) calculated at the outlet of the Lonquimay Basin, considering different periods of evaluation	24
Table 2.6	Predicted and observed (bold) discharges, considering different scales of evaluation (calibration)	24
Table 2.7	Statistical indicators of model performance (monthly output) calculated at the outlet of the Lonquimay Basin, considering different periods of evaluation	25
Table 2.8	Performance (%) of MODIS versus model results considering monthly evaluation	26
Table 3.1	Land cover and type and soil use	38
Table 3.2	Most sensitive parameters used in calibration for the Catamayo-Chira basin	41
Table 3.3	Statistical parameters and variation of outlet volume for model calibration	42
Table 3.4	Statistical parameters	44
Table 3.5	Statistical parameters and variation in outlet volume for model validation	45
Table 3.6	Classification of years by water contribution	48
Table 3.7	Sediment contribution in five measurement stations in yearly mass contribution	49
Table 3.8	Most contributing microbasins in different hydrological conditions/years	49

Table 3.9	Water production in microbasins	53
Table 4.1	Model calibration stages	62
Table 5.1	Data requirements of the different models	83
Table 5.2	Soil type parameter values for the soils in the Mayales basin.....	92
Table 5.3	Mean error measures at all stations for the evaluation of gap-filling methods.....	95
Table 5.4	Cross-validation errors for interpolation of mean annual precipitation data in the whole basin 1975-1994.....	97
Table 5.5	Mean areal monthly precipitation amounts.....	99
Table 5.6	Cross-validation errors for interpolation of monthly precipitation data in the whole basin 1965-2005. Errors are given as observed minus interpolated.....	100
Table 5.7	Cross-validation mean statistics of monthly data for different interpolation methods and observed data 1965-2005.....	100
Table 5.8	Comparison of mean evapotranspiration values (mm) for 2000-2005.....	100
Table 5.9	Model validation results.....	107
Table 6.1	Hydrological scenarios analysed in the Quaraí river basin (marked cells refer to aspects that were included in the model during each scenario).....	119
Table 6.2	Land cover and vegetation areas within the Quaraí river basin	123
Table 6.3	Values of parameters used in the simulation of rice fields within the MGB-IPH model.....	127
Table 7.1	Selected raingauges.....	137
Table 7.2	Main features of soils in the Tres Cruces creek basin (Source: Altamirano et al., 1976).....	139
Table 7.3	Characteristics of the dominant soil profile units present in the Tres Cruces creek basin (Source: Altamirano et al., 1976)	139
Table 7.4	Areas apt for rice-pasture system in the Tres Cruces creek basin (Source: Molfino et al., 2000).....	140
Table 7.5	Gauging station details.....	144
Table 7.6	Main features of existing dams in the basin.....	148
Table 7.7	Main features of existing direct intakes in the basin.....	148
Table 7.8	Irrigated areas based on annual sworn declaration.....	149
Table 7.9	Average planted area in the sworn declarations.....	149
Table 7.10	Raingauges.....	150
Table 7.11	Measured parameters at the meteorological station in Artigas.....	150
Table 7.12	Contributing areas at flow measuring points.....	151
Table 7.13	Flow measurements.....	152
Table 7.14	Maximum volume in October that is reached with 100%, 90% and 80% frequency.....	155
Table 7.15	80% Volume vs volume of existing reservoirs	156
Table 7.16	Frequency with which the current reservoirs reach their maximum volume	156
Table 7.17	Maximum area of rice that would be possible to irrigate with a frequency of 100%, 90% and 80%, considering only the irrigation of rice	159

Table 7.18 Maximum area of rice that would be possible to irrigate with a frequency of 100%, 90% and 80%, considering only the irrigation of both rice and pasture.....	160
Table 7.19 Area of rice 80% vs area of rice that is possible to water with the maximum volume of the existing dams.....	161
Table 7.20 Land use parameters.....	163
Table 7.21 Soil parameters.....	164
Table 7.22 Weather generation station parameters for Artigas station.....	165
Table 7.23 Basin parameters.....	166
Table 7.24 Basin parameters.....	175
Table 7.25 Values of the calibrated parameters in the basin.....	175
Table 7.26 Values of the objective function for the calibration period.....	175
Table 7.27 Values of the objective function for the validation period.....	175
Table 7.28 Volume calculated by DNH and frequency of occurrence for the contributing areas to the existing reservoirs.....	179
Table 7.29 Area of the basin/Area of rice for volumes of 80% and 100% frequency.....	182
Table 8.1 Input data to the AVSWAT model and its resolution.....	188
Table 8.2 Hydrological results for Lake Mälaren.....	196
Table 8.3 Results for flow proportional measurements and Ransta.....	197
Table 9.1 Summary of data requirements and sources for GWAVA.....	202
Table 9.2 An example of a cropping calendar for Argentina showing crop area as percentage of the total area equipped for irrigation by month (Source: FAO AQUASTAT).....	206
Table 9.3 Parameter values used to define soil moisture stores.....	208
Table 9.4 Cropping coefficients for six major irrigated crops grown in South America.....	209
Table 9.5 Summary of gauges and data used to calibrate the model.....	211
Table 9.6 Summary of water availability indices for surface water, groundwater and combined sources as computed in GWAVA.....	215
Table 10.1 Outcomes from hydrological modelling.....	218

1. Introduction

Water use has almost tripled over the past 50 years and in some regions the water demand already exceeds supply (Vorosmarty *et al.*, 2000). The world is facing a “global water crisis”; in many countries, current levels of water use are unsustainable, with systems vulnerable to collapse from even small changes in water availability. The need for a scientifically-based assessment of the potential impacts on water resources of future changes, as a basis for society to adapt to such changes, is strong for most parts of the world. Although the focus of such assessments has tended to be climate change, socio-economic changes can have as significant an impact on water availability across the four main use sectors i.e. domestic, agricultural, industrial (including energy) and environmental. Withdrawal and consumption of water is expected to continue to grow substantially over the next 20-50 years (Cosgrove & Rijsberman, 2002), and consequent changes in availability may drastically affect society and economies.

One of the most needed improvements in Latin American river basin management is a higher level of detail in hydrological modelling and erosion risk assessment, as a basis for identification and analysis of mitigation actions, as well as for analysis of global change scenarios. Flow measurements are too costly to be realised at more than a few locations, which means that modelled data are required for the rest of the basin. Hence, TWINLATIN Work Package 3 “Hydrological modelling and extremes” was formulated to provide methods and tools to be used by other WPs, in particular WP6 on “Pollution pressure and impact analysis” and WP8 on “Change effects and vulnerability assessment”. With an emphasis on high and low flows and their impacts, WP3 was originally called “Hydrological modelling, flooding, erosion, water scarcity and water abstraction”. However, at the TWINLATIN kick-off meeting it was agreed that some of these issues resided more appropriately in WP6 and WP8, and so WP3 was renamed to focus on hydrological modelling and hydrological extremes.

The specific objectives of WP3 as set out in the Description of Work are:

- To contribute to the understanding of the importance and interaction between different key processes in the generation of water and contaminant flows, and of their relation with specific human activities (soil and water use) in the study basins, through the application of physically-based and/or spatially distributed mathematical models.
- To assess the dynamics of the flooding problems in the Catamayo-Chira, Cauca and Quaraí/Cuareim river basins and create a basis for flooding scenario modelling based on climate change effects in all basins, through GIS based monitoring and modelling tools.
- To provide validated modelling tools, as well as results from the application of these tools, required for identification of corrective actions and their impact as well as for assessment of actual and future ecological status of the water bodies.

1.1 Hydrological modelling in TWINLATIN

The requirement to manage water resources in an integrated and sustainable manner has become a driving force behind the use of models in understanding how basin hydrology will be affected by change. Accurate hydrological modelling is a necessary basis for all Integrated Water Resource Management (IWRM) phases. Considerable research efforts are needed to enable hydrological modelling in some of the Latin-American basins, and depend very much on local conditions (ranging from tropical to polar climate zones), observed or expected problems and the availability of historical datasets in each basin. Hence, the activities described in this work package report vary substantially between the different basins and, in some cases, diverge from the originally stated ambitions as various limitations forced reassessments of modelling strategies as the project evolved. At the same time, the demands on the hydrological modelling component and its level of detail are similar in the basins, creating a natural opportunity for twinning approaches through the exchange of knowledge and expertise. These exchanges are both between the Latin-American basins themselves, and between the

Latin-American basins and the two European reference basins, the Norrström and the Thames, in which no further modelling activities took place as part of TWINLATIN.

Hydrological modelling applications have five principal stages, once the model itself is selected, namely: data collation and pre-processing, model set-up and configuration, calibration, validation and evaluation. The model is then ready to use for whatever purpose it has been developed and implemented. Data requirements may differ considerably, but are often extensive. Ideally, a long-term, wide-ranging, systematic monitoring system will have been in place in the basin, with a quality-controlled database, maintained by the central authority with the mandate to disseminate the data to users as required. Unfortunately, this is rarely, if ever, the case, and WP2 was charged with compiling and assessing all available data from current and earlier monitoring programmes in each basin, in order to design and implement a monitoring programme for TWINLATIN, with the aim of providing the data needed for other WPs, including WP3.

It should be noted that data are of many different types and originate from many different measuring devices and different sources. In simulating the behaviour of a catchment and river system, the hydrological model integrates these data, and inconsistencies can lead to errors in the computations, which may or not be evident in the output. Investigation of data and model uncertainty is largely beyond the SCOPE of TWINLATIN, though was examined as part of the modelling activities in the Lake Cocibolca basin.

WP3 activities very much followed the five stages in hydrological modelling applications, with milestones to complete model development, calibration, validation and evaluation in good time to feed into other WPs. This report combines deliverables D.1, reporting the hydrological modelling in each basin, with D3.2, evaluating the modelling accuracy and implications. The ambitious goal was hydrological models with an accuracy that allows analysis of the efficiency of local actions and global change scenarios, with errors in runoff calculations known at sub-basin level and not exceeding 20% of mean monthly flow.

1.2 Approach to hydrological modelling

In each of the Latin American river basins, a questionnaire was used to identify the problems to be solved and, therefore, the most urgent research needs under WP3. This had the added benefit of guiding the TWINLATIN partners, several of whom had little experience of hydrological modelling at the start of the project, through a thought process to assist them in clarifying the various issues to be considered in model selection, development and application. The questionnaire sought information on the reasons for modelling, the spatial and temporal scales for the modelling, and the data that were or would be available (see WP2 report). Recognition of the aims, data and resources available for the hydrological modelling lead to a choice of appropriate model(s).

In some basins, obviously, these changed through the lifetime of the project, as a result of developments in other work packages and also external factors, such as different priorities identified by stakeholders during public participation activities. Tables 1.1 summarises the final outcomes from this exercise, which are explored further in section 9 of this report, together with other issues such as the exchange of modelling experience between basins, the relevance of the modelling approaches to other non-TWINLATIN basins, and the wider applicability within the Latin American region.

The table reveals that there is a lot of similarity between the current water uses in each basin, the priority issues to be addressed during TWINLATIN generally, and WP3 specifically, and the future application of the modelling. In all the river basins water is used for supply to the domestic and agricultural sectors, the Baker and Cauca also mentioning some industrial users. Environmental concerns were raised in the Baker and Lake Cocibolca basins where conservation was raised as an issue. Common topics as priority issues in the majority of the basins included water availability, water quality, waste disposal, water rights and erosion and sedimentation. Similarly, all basins were interested in the impacts of climate and land use change, including water resource developments.

Table 1.1 Approach to hydrological modelling

Issue	Baker Chile	Catamayo-Chira Ecuador-Peru	Cauca Colombia	Lake Cocibolca Nicaragua	Cuareim/Quaraí Brazil-Uruguay
Area (km ²)	26,726	17,200	62,000	24,000	14,800
Transboundary?	yes	yes	no	yes	yes
Why model?					
Current water uses	Water supply, irrigation, mining, conservation	Water supply, irrigation	Water supply, irrigation (coffee, sugar cane), industry (paper)	Water supply, fishing, navigation, conservation, tourism	Water supply, irrigation (rice fields)
Priority issues	Lack of data, glacier/snowmelt issue, HEP development	Water demand, WQ/ sediment, reservoir siltation, deforestation, intensive agriculture	WQ, pollution from industry & intensive agriculture, waste disposal, water rights	Water availability, WQ/sediment, deforestation, intensive agriculture, waste disposal, navigation, water rights	Water availability, WQ, urban flooding, low flows/droughts, small farm dams, water rights
Modelling applications	Land use/ climate change	Land use/ climate change impacts on WQ/erosion	Land use/ climate change	Land use/ climate change	Water resource scenarios, land use/ climate change
Data availability and modelling time interval					
Data availability	Very poor in Baker, mixed in amount & quality in BioBío	Poor amount & quality	OK amount of data, quality poor	Poor amount & quality	Global datasets available, local data mixed in amount & quality
Time interval	Daily	Monthly	Daily	Daily/monthly/annual	Daily
Spatial scale	1 sub-basin of Biobío	Basin & 4 sub-basins	1 sub-basin	Basin & 1 sub-basin	Basin & 1 sub-basin
Model selection					
Choice of model	SWAT to Lonquimay sub-basin of BioBío to further develop snow/ glacier/ TWINBAS work	SWAT to 4 sub-basins in upper & mid basin, & outlet	HBV/IHMS to basin – for TWINLATIN work to Tulua sub-basin of Cauca	Simple WB & WASMOD WB for basin WATSHMAN-PCRaster in Mayales sub-basin & GLUE uncertainty	SWAT, MODSIM to Tres-Cruces sub-basin MGB-IPH large-scale distributed hydrological model to basin
Data requirements	Topography, met data, rain, snow, flow, land use, soils (daily)	Topography, met data, rain, flow, land use, soils (monthly)	Topography, met data, rain, flow, soils, veg (daily)	Topography, met data, rain, flow, soils (daily)	Topography, met data, rain, flow, land use, soils, veg, x-sections, reservoir & small farm dam data (daily)

where: HEP – hydroelectric power, WQ – water quality, WB – water balance, x-section – cross-section

Table 1.2 Hydrological models used during TWINLATIN WP3

Model	Description	Basins
GWAVA	Large-scale distributed model	South American continent
HBV/IHMS	Hydrodynamic forecasting model	Cauca
MGB-IPH	Large-scale distributed model	Cuareim/Quaraí
MODSIM	Water allocation model	Cuareim/Quaraí
SWAT	Physically-based rainfall-runoff model	Biobío, Catamayo-Chira, Cuareim/Quaraí
WASMOD	Water balance model	Cocibolca
Water balance	Water balance model	Cocibolca
WATSHMAN	Distributed rainfall-runoff model	Cocibolca

Issues unique to the Baker basin were the general lack of data, including glacier and snow melt information, for modelling to assess the impacts of hydropower development in a predominantly natural basin. Whilst “data” *per se* subsequently proved to be an important issue for many of the basins, as Table 1.1 indicates, the implications for modelling in the Baker within the timeframe of TWINLATIN were particularly significant, as it quickly became clear that meaningful spatially distributed hydrological modelling was simply not feasible. Instead, an alternative strategy was implemented, developing a hydrological model for the snow-fed Lonquimay sub-basin in the Biobío river basin, thereby further developing the work started under TWINBAS. Experience gained from this effort can then be transferred to the Baker basin as part of future, post-TWINLATIN, activities.

Apart from the Baker, all Latin American partners chose to model the entire basin, in addition to at least one sub-basin, usually selected by importance and/or data availability. Apart from the Catamayo-Chira, all partners chose to model at a daily time step. In the end, six different hydrological models were used by Latin American partners under WP3, ranging from a simple water balance to a large-scale distributed model, as listed in Table 1.2. SWAT was used in three of the basins, who benefitted greatly from the exchange of knowledge and experience. Despite the model being used, common data requirements in the basins included topographic data, meteorological data, flow data, and land use and/or soils data (Table 1.1).

Each of the TWINLATIN study basins varies dramatically in terms of climate, geography, hydrological response and the issues faced by the inhabitants e.g. flooding, water quality, sustainable water resources, soil erosion and development, amongst others. Basin-scale modelling ambitions focus on specific localised issues. A continental approach can provide a wider regional context for some of the problems faced, in particular water resources. It can also provide an opportunity for climate change impacts to be examined and compared at the continental, regional and basin scales. Therefore, the Global Water AVailability Assessment (GWAVA) model (Meigh *et al.*, 1998; Meigh *et al.*, 1999) was applied to the South American continent (excluding Nicaragua) enabling a broader regional picture of hydrology and spatial extents of water scarcity to be examined. The continent-wide approach means that a consistent methodology can be applied across four of the subject basins in the TWINLATIN project (Baker, Catamayo-Chira, Cauca and Quaraí/Cuareim) as well as the regions in between.

2. Baker (and Biobío) River Basin (Chile)

2.1 Description of basin

The bi-national Baker River Basin (Figure 2.1) is located in Patagonia, Southern South America, between 46°00' and 48°00' Southern Latitude and between 71°00' and 73°30' Western Longitude. With a total drainage area of 26,726 km² (IGM, 1984), it is the second largest river basin in Chile (only the Loa River Basin located in Northern Chile is bigger, with a total surface area of 33,865 km²). Unlike most other Chilean basins further north, the Baker River Basin starts off on the upper eastern slope of the Andes - which are largely covered by the Northern Patagonian Icefield - and stretches out across the international border into the plains of the Argentinean Steppe (pampa). At its southwestern tip, the basin drains into the Chilean fjord system, which in turn connects it to the Pacific Ocean. Maximum elevations in the basin are well above 3,000 masl, while the mean elevation is around 900 masl.

Most of the basin's surface area falls within the Chilean region of Aysén, but approximately 5,850 km² are located within the Argentinean province of Santa Cruz. As a consequence of the highly pronounced precipitation gradient that exists from east to west, the presence of a well-developed perennial river network is mostly restricted to the Chilean part of the basin. Work in TWINLATIN focuses on the Chilean part only.

2.1.1 Hydrography

The dominant hydrographic feature within the Baker River Basin is the Lago General Carrera (Figure 2.2). This lake has a total surface area of 1,848 km², of which approximately 850 km² are located in Argentina (where it is called Lake Buenos Aires). The lake is located at approximately 200 masl. It

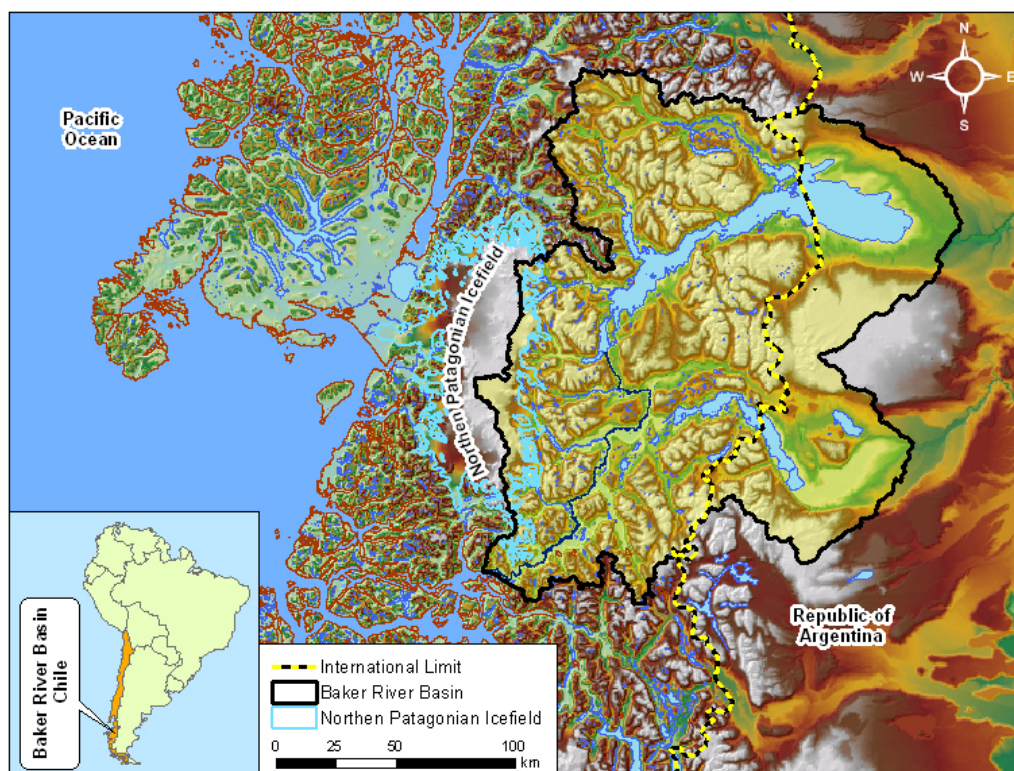


Figure 2.1 Location and topography of the Baker River Basin, Chile

receives the contributions of a multitude of rivers and streams, but almost all important contributions come from the Chilean side, mainly through a series of tributaries located on its northern shore: the Ibáñez, Avellanos, Murta, Engaño and Leones rivers. On its southern shore, the main contribution to the lake comes from the Jeinimeni River (in the southeast, on the Chilean-Argentinean limit); several other smaller rivers and streams exist in this area, most of them located to the west of Jeinimeni. The General Carrera Lake connects to the southwest to Lake Bertrand (50 km²), from which the Baker River springs. The Baker River drains into the Chilean fjord system (Pacific Ocean) through a three-armed delta located just north of the village of Caleta Tortel, after flowing south-southwestwards for approximately 170 km. The Baker River has the highest mean annual discharge rate of all Chilean rivers (1,133 m³s⁻¹; DGA, 1987). Its most important direct tributaries are: the Nef, de la Colonia and Ventisquero rivers, which drain from the Northern Patagonian Icefield located in the west, and the Chacabuco, Cochrane, del Salto and de los Ñadis rivers, which flow to the Baker from the east. Covering almost 3,000 km², the biggest sub-basin is that of the Cochrane River, which drains from Lake Cochrane (350 km²; called Pueyrredón in Argentina).

2.1.2 Basin geomorphology

The geomorphology of the Baker River Basin is the consequence of tectonic activity, the action of glaciers and of volcanism (northwest part), as well as of other less intensive, but nonetheless significant continuous agents such as precipitation, winds and the influence of the sea. The most important morphological unit is the Patagonian Andes Mountain Range (Cordillera de los Andes Patagónicos), which rises up to heights well above 3,000 masl within the Basin. Probably the most remarkable feature of the Cordillera is the presence of the vast Northern Patagonian Icefield (Campo de Hielo Norte), which stretches out for about 4,600 km², of which approximately 1600 km² are located within the Baker River Basin itself. From here, glaciers such as the Los Leones, Soler and La Colonia flow down eastwards and give rise to rivers of the same name. Present-day geomorphology of the Baker River Basin is also characterised by the presence of two major, currently separated lakes,

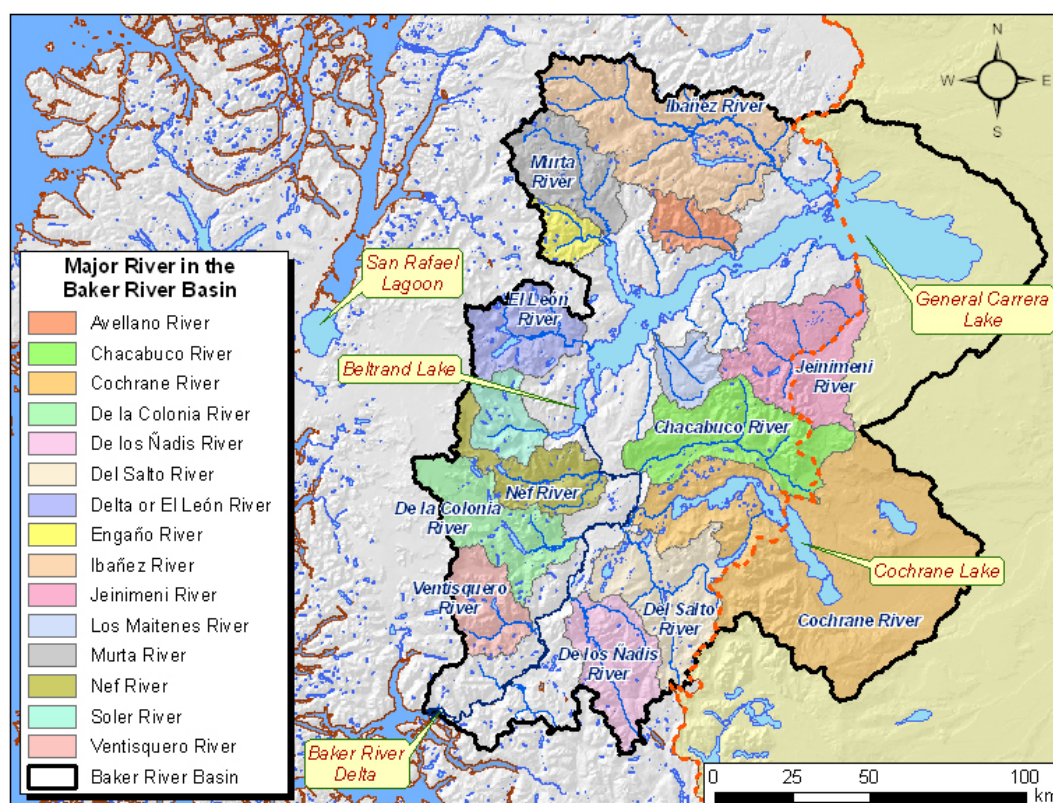


Figure 2.2 Lakes, tributaries and the most important sub-basins in the Baker River Basin

the Lago General Carrera and the Lago Cochrane. Diversion of the drainage direction of both lakes from the Atlantic to the Pacific occurred during the deglaciation (15-16 ka – 12.8 ka) of the eastern flank of the Northern Patagonian Icefield (going through the intermediate stage of a unified lake). This deglaciation process explains to a big extent the current geomorphology of the basin, and is described in detail in Turner *et al.* (2005).

2.1.3 Climate

Mean annual temperature and precipitation for the Baker River Basin are shown in Figure 2.3. Three of the five main Köppen climate classes are represented in the basin (source: http://www.puc.cl/sw_educ/geografia/cartografiainteractiva/):

- Cold climate class, represented in the basin by the EFH (Polar Highland Ice Caps) climate type, and mainly present in the area of the Northern Patagonian Icefield.
- Temperate climate class, represented in the basin by both the Cfc (Maritime SubArctic) climate type and the Cfbs (Maritime Temperate) climate type (precipitations throughout the year for both types, but more regularly distributed towards the coast). This class covers most of the basin.
- Dry climate class, represented in the basin by the Bsk (Middle-Latitude, Semi-Arid Steppe with Winter Precipitations) climate type, and typical for the area around Chile Chico.

The Agroclimatic Map of Chile (Mapa Agroclimatico de Chile; INEA, 1989) differentiates between five main climate types in the Baker Basin:

- Polar Marine Climate (Clima Marino Polar), represented in the basin by the Cerro Benete Agroclimate.
- Humid Alpine Polar Climate (Clima Polar Alpino Húmedo), represented in the basin by the Cordillera Austral Agroclimate.
- Humid Marine Patagonian Climate (Clima Marino Húmedo Patagónico), represented by the Río Baker Agroclimate.
- Polar Alpine Climate (Clima Polar Alpino), represented in the basin by the Hielo Perpetuo Agroclimate.
- Cold Mediterranean Climate (Clima Mediterraneo Frío), represented in the basin by the Chile Chico Agroclimate.

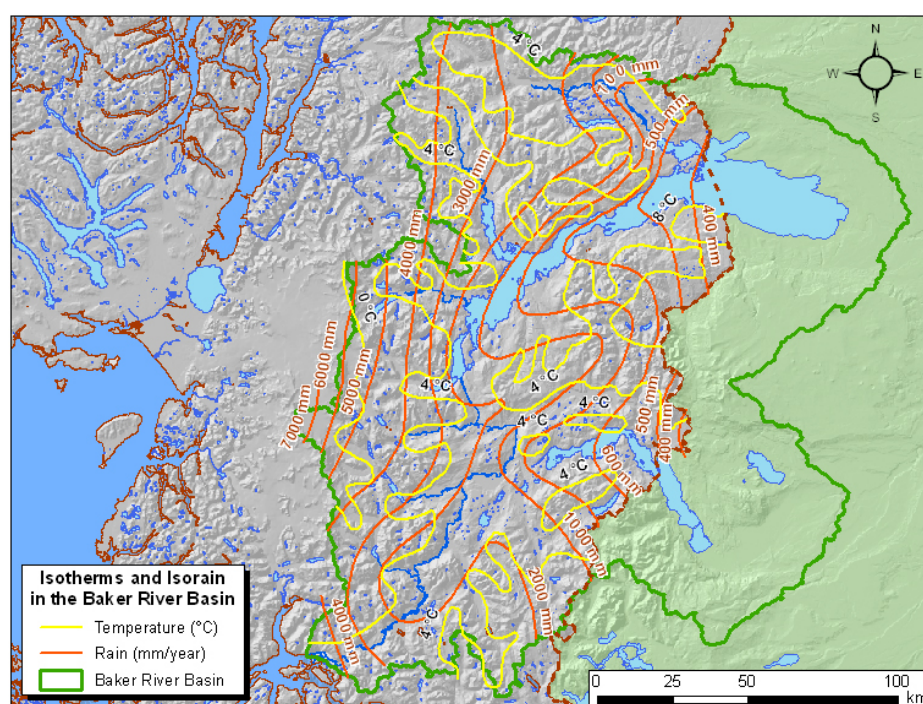


Figure 2.3 Mean annual temperature and precipitation for the Baker River Basin (DGA, 1987)

2.1.4 Hydrology

The hydrological regime of the river network in the Baker River Basin is of the mixed type, with contributions to the individual river hydrographs both from glacial and snow melt, and from direct rainfall; the relative importance of these contributions varies widely and is highly dependent on both season and geographical location. The Ibáñez River constitutes the most important tributary on the northern shore of the General Carrera Lake. It originates from a glacier that comes down from the glaciated Massif of Cerro Hudson. The Murta River constitutes - due to its length and discharge rate - together with the Ibáñez River, one of the most important tributaries to the General Carrera Lake. It receives the waters from numerous small glacial streams, and is mostly flanked by high mountains; in its lower reaches it meanders through an alluvial plain and reaches the lake through its estuary at Murta Bay. The Jeinimeni River is the most important tributary to the southern shore of the General Carrera Lake; it originates from the Jeinimeni Lake. Its middle and lower reaches constitute the international border between Chile and Argentina. Jeinimeni discharge rates are highly variable throughout the year. High discharge rates due to glacial and snow melt are typically observed in December, while winter rainfall contributes to higher values between July and September. The Del Baño Stream is located to the west of the village of Chile Chico; this small sub-basin is monitored by DGA because of its strategic importance for the mining and irrigation activities in the area. Its hydrological regime is similar to that of the Jeinimeni River. The Cochrane River tributates to the Baker River 24 km downstream (east) from its source, the Lake Cochrane (Pueyrredón Lake in Argentina). It runs through a big depression that starts on the Patagonian plateau and penetrates between the Chacabuco (to the north) and Esmeralda (south) Mountain Range. The Baker River itself sprouts from the Bertrand Lake, which in turn receives the draining waters from the General Carrera Lake. The fluviometric station on the first segment of the Baker River downstream from Lake Bertrand (Angostura sector) clearly shows the regulating power of these lakes on the hydrology of the upper Baker River. The most important tributaries to this segment are the Nef and Chacabuco rivers. The combination of snowmelt and rainfall contributions lead to peak values which are typically observed during summer (February).

2.1.5 Data availability

Meteorological data

Due to the complicated climatological conditions and the isolated geographic location of the Baker River Basin, the monitoring network is relatively poorly developed in comparison to many other Chilean Basins. The meteorological network within the basin consists of eight stations for which daily rainfall data are obtained (Figures 2.4 and 2.5). Of these eight stations, at present seven stations are active.

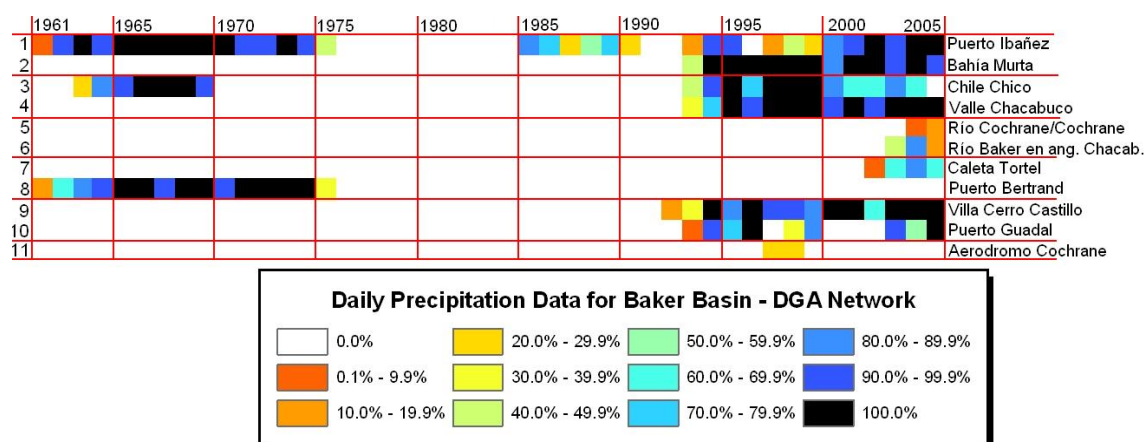


Figure 2.4 Extent and completeness (%) of the daily time series of precipitation data for the Baker River Basin

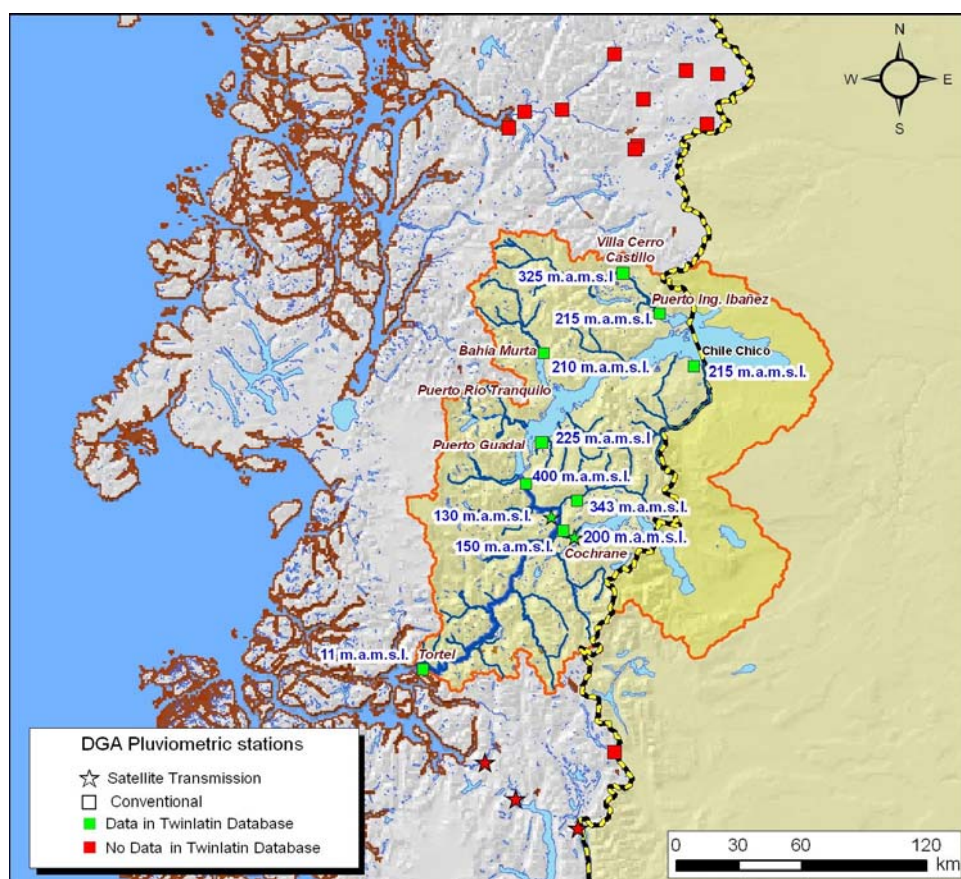


Figure 2.5 Daily and hourly precipitation stations from DGA

The spatial distribution of the measuring network (Figure 2.5) shows that the stations are mainly located at lower elevations, generally in the vicinity of urban settlements. The current measurement network does thus not cover the altitudinal gradients that most certainly exist within the basin. This fact complicates the establishment of water balances at the (sub-)basin level, and immediately limits possibilities for modelling applications. Time series for the different stations are highly discontinuous and, even for those years for which information is available, data gaps are common and considerably large (Figure 2.4).

Fluviometric data

The spatial distribution of the fluviometric monitoring network is given in Figures 2.6 and 2.7. At present, nine stations are operational in the basin. Of these, six have been recently equipped with satellite data transmission, and now register at the hourly time step.

Implications for modelling

It became clear that meaningful spatially distributed hydrological modelling applications for the Baker River Basin (suggested in the planned activities for WP3 in the original DOW) - using the outcome from the priority setting exercise done under WP1 (based on an analysis of potential conflicts, knowledge gaps and the existence of other past/ongoing/upcoming projects) and considering the results from the analysis on data availability for the Baker Basin under WP2 (now also including the newly available datasets from Endesa) - were not feasible under TWINLATIN due to the non-representativeness of the available input information providing very limited possibilities for model calibration and validation. This conclusion takes into account EULA's previous experience in hydrological modelling under limited conditions of data availability (e.g. TWINBAS where modelling was successful but data availability – though also limited - was much better; see Stehr *et al.*, 2008).

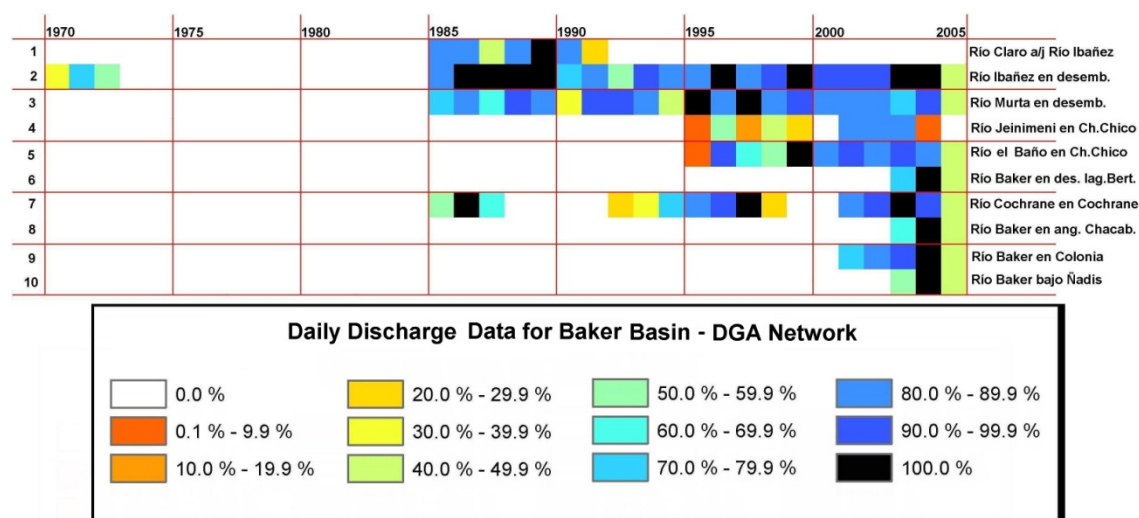


Figure 2.6 Extent and completeness (%) of the daily discharge data time series

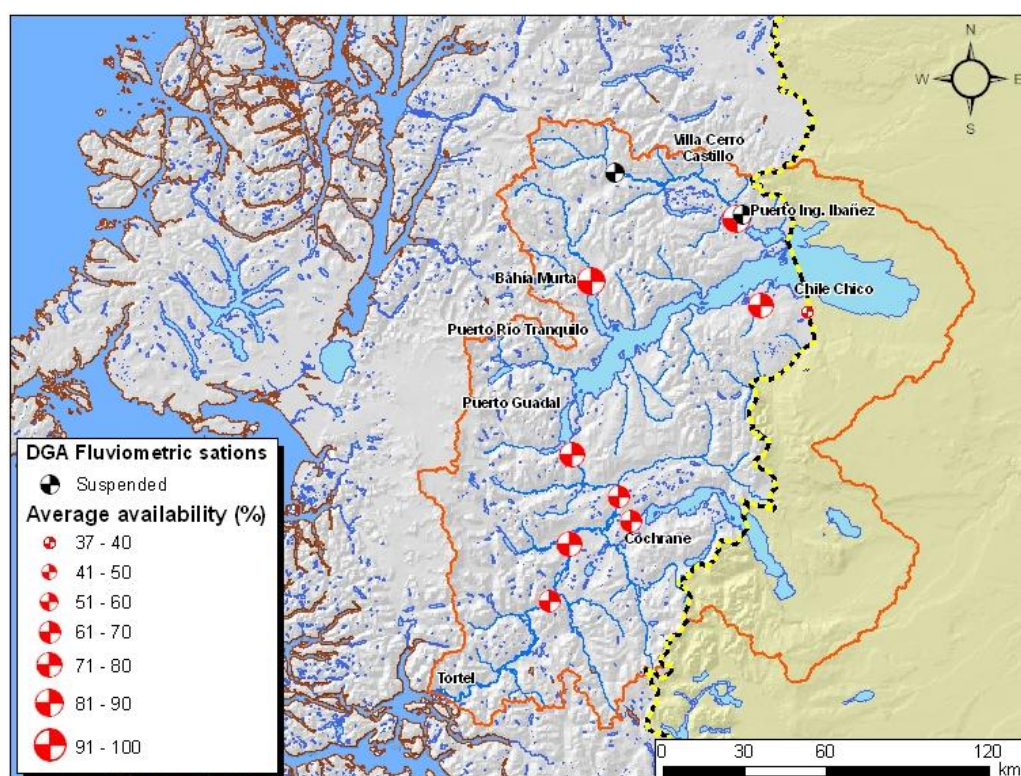


Figure 2.7 DGA's fluviometric network in the Baker River Basin

It was further also perceived that the outcome from such a modelling exercise is currently not the information most needed by the stakeholders, for the general purpose of immediate and near-future decision-making in the basin.

Considering the former conclusions with respect to the current feasibility of a distributed modelling approach in the Baker Basin, an alternative modelling strategy was implemented: based on the slightly better data availability (allowing calibration and validation) for certain snow-fed sub-basins in the upper part of the Biobío Basin (see TWINBAS WP4, in which non-snowfed sub-basins in the Central Part of Biobío were modelled), and due to the similarity of processes of these sub-basins with many

sub-basins in the Aysén Region (and the Baker River Basin), it was decided to develop a modelling application for the snow-fed Lonquimay sub-basin in Biobío.

Experiences gained from this effort can then be used to evaluate the potential future usefulness of transferring the applied modelling approach to the Baker River Basin, as well as to plan further (post-TWINLATIN) developments which will be required in the Baker Basin in order to allow for the successful implementation of such a modelling approach. In this sense, considerable advances have been obtained in the modelling of the Lonquimay sub-basin (using the SWAT model), a manuscript on results of this modelling effort has been prepared, and results from the exercise are documented in this report. In addition, a presentation on results from this work at the last SWAT User Conference has been made.

2.2 Choice of model

2.2.1 Model category

For practical applications in macro-scale basins, in Chile as in many other places in the world, the typical availability of meteorological data at the daily time scale immediately restricts the number and type of models that can potentially be applied. It is from this perspective that research efforts within TWINLATIN – continuing with efforts undertaken in the context of TWINBAS, another EC FP6 project - are centred on a versatile, semi-distributed hydrological model based on the SCS Curve Number (USDA SCS, 1972) technique. Model development itself is not an objective of work here. Instead, the existing SWAT model (Soil & Water Assessment Tool; Arnold *et al.*, 1998; Neitsch *et al.*; 2002^a; Neitsch *et al.*, 2002^b) is chosen for application. It is generic, freely downloadable, user support is available from the developers, and graphical user interfaces (GUI) exist for commonly used GIS packages (e.g. ArcView, ArcGIS 9.1, GRASS). Besides being a hydrological modelling tool (hydrograph simulations, water balance calculations), SWAT also includes additional modules which allow the assessment of the impact of land use management options on, for example, erosion and water quality. A stochastic weather generator is incorporated, and options for sensitivity analysis and automated calibration (e.g. van Griensven & Bauwens, 2005) are included in a recent version. The SWAT model is subject to continuous development, and has been successfully applied in many countries (e.g. (Chaubey *et al.*, 2005; Hattermann *et al.*, 2005).

Within the framework of TWINLATIN, the SWAT model is being applied to the Lonquimay Basin (to gain experience and insight in minimum input data requirements for future applications for the Baker), Norrström Basin, and Catamayo-Chira Basin. Exchange of information and practical experience in both directions (twinning) has facilitated implementation in the different basins.

2.2.2 Specific model system

SWAT was developed by the United States Department of Agriculture (USDA) in the 1990s. It is a physically-based hydrological and water quality model designed to route water, sediments and contaminants from individual basins through the whole of the river basin systems (i.e. from meso-scale to macro-scale). It can be used to predict the impact of land management practices on water, sediment and agricultural chemical yields in large complex basins with varying soils and land use and management conditions, over long periods of time.

When used with ArcView3.2 (AVSWAT-X), the model can be classified as semi-spatially distributed, as it uses a mixed vector- and raster-based approach: the basin is divided into sub-basins, and meteorological input data are organised at this level. Sub-basins can be further subdivided into Hydrologic Response Units (HRUs): these consist of lumped land areas within the sub-basin comprised of specific land cover, soil and management combinations. These are the spatial units at which calculations occur, as the HRUs are assumed to be homogeneous with respect to their hydrologic properties (Neitsch *et al.*, 2002^a). The HRUs are semi-automatically derived by the model, based on Land Use, Soil Type and Elevation GIS data layers, and certain decision criteria that can be defined by the user.

The hydrology of the basin is conceptually divided into two major phases: the land phase of the hydrological cycle and the river routing phase. Contributions to discharge in the sub-basin's main river reach is controlled by the land phase. The river routing phase then determines the movement of water through the channel network towards internal control points (e.g. where limnigraph data may be available for calibration and validation) and towards the basin outlet. Manning's equation is used to define the velocity of flow. Two methods can be used for routing: the variable storage method or the Muskingum river routing method. Both the variable storage and Muskingum routing methods are variations on the kinematic wave model (Neitsch *et al.*, 2002^a).

Evapotranspiration in the SWAT model can be calculated by one of the three following methods: Penman–Monteith, Hargreaves or Priestley–Taylor. Penman–Monteith offers a better process description but has high input data requirements which are generally hard to fulfil. Hargreaves and Priestley–Taylor provide coarser approximations but have the advantage of needing fewer input variables. Under minimum conditions of data availability, Hargreaves can even be used with temperature as the only required measured input time series (Heuvelmans *et al.*, 2005). For the surface runoff estimation, SWAT gives two alternatives: the SCS Curve Number procedure (USDA SCS, 1972) and the Green & Ampt infiltration method; for the latter input data at a finer-than-daily time resolution are required, whereas the Curve Number method is lumped over time (Johnson, 1998); it is typically applied using daily rainfall values.

Runoff contributions from snowmelt can be incorporated by means of the use of a temperature index. This method is commonly used for resource management purposes (Walter *et al.*, 2005). SWAT gives two alternatives: firstly, the use of corrected temperature and precipitation values considering orographic effects produced by elevation gradients (for that purpose the basin is subdivided in elevation bands); or secondly, the direct assignment of observed temperature and precipitation data to the different sub-basins, without further correction for orographic effects.

2.2.3 User interface

The most popular interface for use with the SWAT model is the AVSWAT GUI (Di Luzio *et al.*, 2002), integrated in ArcView3.2. The interface allows for both pre- and post-processing of data. Both GIS thematic data layers and attribute tables can be used, and connections with external databases can be established. The SWAT model itself runs in DOS, but model runs can be initiated and results can be analysed through the GUI.

A detailed user manual for AVSWAT can be downloaded for free from the internet (<http://www.brc.tamus.edu/swat/index.html>). Some examples of screen prints from the SWAT GIS interface are shown below (Figures 2.8 and 2.9).

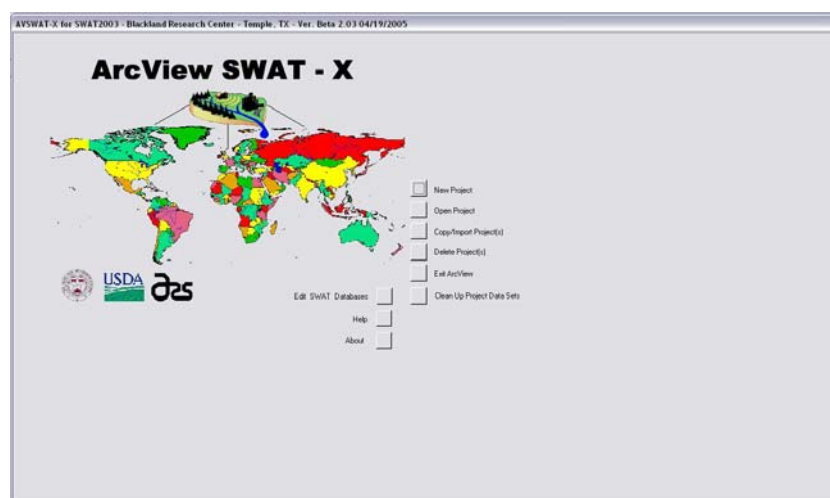


Figure 2.8 Main interface window

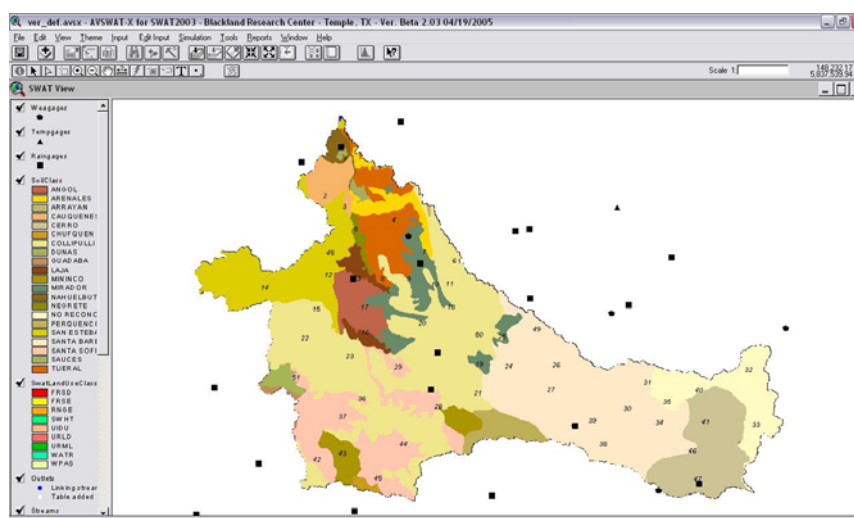


Figure 2.9 View of thematic data layers in AVSWAT

Selection of SWAT for application under TWINLATIN is thus based on, amongst others, the following considerations:

- good user documentation which facilitates transfer to interested stakeholders (e.g. DGA);
- feasibility of applying the model under restricted availability of input data e.g. daily precipitation and temperature data only;
- sensitivity and automated calibration procedures integrated;
- integration within a GIS interface;
- availability of snowmelt module, which is highly relevant for the modelling of Andean / Patagonian basins.

Useful outputs consist of:

- daily and/or monthly evaluations of water balance components at different points of interest within the basin;
- possibility for analysing impacts of change scenarios e.g. climate change.

In the latter context, future applications of SWAT within the Baker River Basin may be useful to analyse how climate change might impact (sub)basin hydrology in this area. For this purpose, however, use of the SWAT model and its snowmelt component should first be trained in sub-basins where a minimum of input data availability exists. For this purpose, under TWINLATIN, the Lonquimay Basin is being modelled, and possibilities (including evaluation of minimum data requirements) for meaningful transfer to the Baker River Basin are being analysed.

2.3 Data requirements

2.3.1 Input data

Data requirements for hydrological modelling applications typically depend on: firstly, the dimensions of the system being modelled, and the scale at which modelling is conducted, secondly, the variety and/or complexity of the hydrological processes involved; and finally – and especially - on the ultimate use that will be given to the model outcome. These points, together with data availability, should influence directly in the choice of model for any given application. In this sense, SWAT is a versatile tool, as it allows the user to choose between different options for describing the different components of the hydrological cycle. That choice will typically be based on local data availability, as well as on the previously cited considerations.

Table 2.1 *Input data sources*

Type	Source
Topography	SRTM
Precipitation data	BNA-DGA, DMC
Temperature data	BNA-DGA
Land use	National Inventory of Vegetational Resources of Chile (<i>Catastro y Evaluación de los Recursos Vegetacionales Nativos de Chile</i> ; CONAF-CONAMA-BIRF, 1995).
Soil Type	Agrological Study of the VIII and IX Region (<i>Estudio Agrológico de la VIII y IX Región</i> ; CIREN, 1999 ^a ; CIREN, 1999 ^b)
Flow	DGA

As in this case, the modelling concerns a sub-basin of the Biobío (to gain experience in modelling using the SWAT snowmelt module), input data for the modelling exercise were obtained from the environmental database constructed under TWINBAS (Table 2.1).

2.3.2 Output data

A number of output files are generated in every SWAT simulation. Average daily values are always printed in the HRU, sub-basin and reach files, but the time period they are summarised over will vary. Depending on the print option selected, the output files may include all daily values, daily amounts averaged over the month, daily amounts averaged over the year, or daily amounts averaged over the entire simulation period. The output data describe the evapotranspiration process, surface water flows and subsurface flow. Data types are listed in Table 2.2. The outputs are given at the sub-basin, HRU, and reach level. All outputs are given for the selected print time period.

Additional post-processing of the outputs may be carried out using, for example, a spreadsheet. The model output data may be written as text file and can be seen directly using the AVSWAT interface in ArcView; alternatively a user-selected software can be used to process them.

2.4 Scenario modelling

2.4.1 Climate change scenarios

As a first approximation, under TWINLATIN climate change scenarios for the Baker River Basin will be prepared based on output from the MAGICC-SCENGEN v4.1 scenario modelling tool, as part of a harmonised approach towards scenario generation which will be followed by the different TWINLATIN partners. In the case of the Baker Basin, this information will allow for a basic, preliminary and semi-quantitative assessment of the potential impact of climate change on water resources in the basin. In a similar way, information will also be obtained from the MAGICC-SCENGEN tool for the Lonquimay Basin (Biobío). This information will be more directly used to perturb observed meteorological time series for this basin, which can then be used for a quantitative impact assessment (sensitivity analysis of the hydrological model) by means of the SWAT hydrological model application.

Output from MAGICC-SCENGEN will consist of change signals (reference period 1961-1990) for temperature (absolute change) and precipitation (% change) for the future 30-year time window 2071-2100 (mean values). Obtained change signals will be used to perturb a baseline for temperature and precipitation for the Lonquimay Basin, in order to perform an analysis of the sensitivity of the hydrological model to meteorological (climate) input datasets and as such make a first evaluation of the potential impacts of plausible climate change scenarios on (sub)basin hydrology.

Table 2.2 *Model output parameters*

	Parameter	Level
1	Total amount of precipitation (mm H ₂ O)	HRU; Sub-basin
2	Irrigation (mm H ₂ O). Amount of irrigation water applied	HRU
3	Potential evapotranspiration (mm H ₂ O)	HRU; Sub-basin
4	Actual evapotranspiration (soil evaporation and plant transpiration) (mm H ₂ O)	HRU; Sub-basin
5	Soil water content (mm H ₂ O)	HRU; Sub-basin
6	Water that percolates past the root zone (mm H ₂ O)	HRU; Sub-basin
7	Recharge entering aquifers (total amount of water entering shallow and deep aquifers) (mm H ₂ O)	HRU
8	Deep aquifer recharge (mm H ₂ O)	HRU
9	Water in the shallow aquifer returning to the root zone in response to a moisture deficit during the time step (mm H ₂ O)	HRU
10	Irrigation from shallow aquifer (mm H ₂ O)	HRU
11	Irrigation from deep aquifer (mm H ₂ O)	HRU
12	Shallow aquifer storage (mm H ₂ O)	HRU
13	Deep aquifer storage (mm H ₂ O)	HRU
14	Surface runoff contribution to streamflow in the main channel (mm H ₂ O)	HRU; Sub-basin
15	Transmission losses (mm H ₂ O)	HRU
16	Lateral flow contribution to streamflow (mm H ₂ O)	HRU
17	Groundwater contribution to streamflow (mm H ₂ O)	HRU; Sub-basin
18	Water yield (mm H ₂ O)	HRU; Sub-basin
19	Leaf area index at the end of the time period	HRU
20	Average daily streamflow into reach (m ³ s ⁻¹)	Reach
21	Average daily streamflow out of reach (m ³ s ⁻¹)	Reach
22	Average daily rate of water loss from reach by evaporation (m ³ s ⁻¹)	Reach
23	Average daily rate of water loss from reach by transmission through the streambed (m ³ s ⁻¹)	Reach

In addition to this, temperature and precipitation time series (0.5° x 0.5° grid cells) for both the reference period 1961-1990 and the future time window 2071-2100 from the Chilean RCM exercise “Study of the Climatic Variability in Chile in the XXI Century” (CONAMA-DGF, 2006) are made available for the Baker Basin. These time series can also be used for a finer resolution change effects assessment. In this study, the HadCM3 GCM (mean resolution 300 x 300 km) was used to indirectly force the regional simulations: the atmospheric model that is forced at the surface level with the output from this model is HadAM3, which represents very similar characteristics but at a major spatial resolution. Output from this last model finally is used to force the regional simulations which are executed with the PRECIS model, at a spatial resolution of 25 km. The different output variables from this model (e.g. mean, maximum and minimum temperature, and precipitation) are available for each grid point within the spatial domain 18°S – 57°S and 62°W – 85°W. Three 30-years time series are available for each point: the reference climate and two future climatic time series for the period 2071-2100, corresponding to the A2 and B2 emission scenarios, respectively (see Figure 2.10).

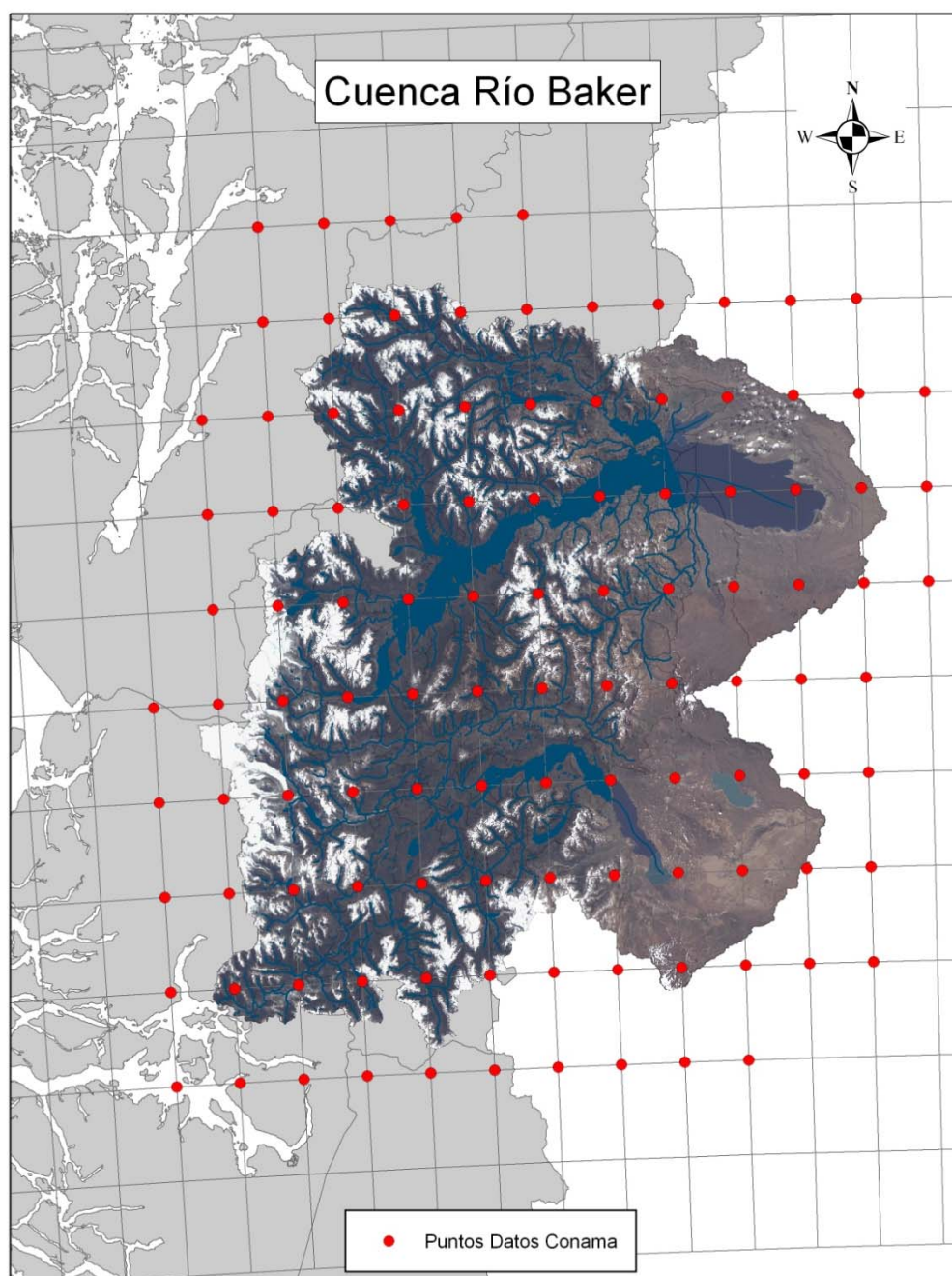


Figure 2.10 Grid points from the RCM run conducted by DGF- CONAMA (2006); at each point a 30-year daily time series (2071 – 2100) is available

2.4.2 (Land) use change scenarios

A considerable part of the Baker River Basin is contained in the National System of Protected Areas (SNASPE), another part belongs to a private reserve, and an important portion of the remaining surface area is snow- or glacier-covered, or offers little opportunities for human exploitation. From this perspective, only more localised land use changes are foreseen to take place in the near future (e.g. mining activities, forestry plantations in specific sub-sectors of the basin), which are expected to have a more local rather than a basin-scale impact. Undoubtedly the change with major impacts for the next decade is the planned hydropower development in the basin. Activities under TWINLATIN do not foresee any modelling approach to evaluating the impacts of such development, as this would be part of the Environmental Impacts Assessment (EIA) studies that are to be provided by the implementing

company. TWINLATIN tries to provide new knowledge on topics that are currently not being dealt with by other initiatives; attention under TWINLATIN for this work package has, therefore, been focussed on the topic of hydrological impacts of climate change in snow-fed basins in Chile (similar to many of the ones present in Baker).

2.5 Model development

2.5.1 Overview

As previously mentioned, in the context of TWINLATIN, the rainfall-runoff modelling application focuses on one sub-basin of Biobío, namely the Lonquimay Basin (455 km²). Through the application of the previously described SWAT model, monthly and annual water yield at the sub-basin level can be obtained and can be used later on to assess the impact of change scenarios on basin hydrology. Groundwater flows will not be explicitly modelled (detailed hydrogeological data which would allow the application of a separate groundwater model are lacking), but it is possible to derive the magnitude of the exchange between surface and groundwaters through analysis of the water balances calculated by SWAT.

Through the modelling of the Lonquimay Basin, TWINLATIN will thus set the basis for future modelling efforts in the Baker River Basin. Figure 2.11 shows the location of the Lonquimay Basin. This sub-basin occupies approximately 2% of the total surface area of the Biobío Basin.

2.5.2 Model set-up

The hydrological cycle as simulated by SWAT is based on the following water balance equation:

$$WYLD = PP - ET - \Delta SW - (PERC - GWQ)$$

Where: *WYLD* is the water yield of the (sub)basin (*WYLD* includes surface runoff, lateral flow and base flow), *PP* is precipitation, ΔSW is change in soil water content (vadose zone), *PERC* is flux to the groundwater and *GWQ* is baseflow contribution to the river discharge.

The subdivision(s) of the basin enables the model to reflect the influences of local characteristics (e.g. soil type, land use type, etc.) on the different components of the water balance.

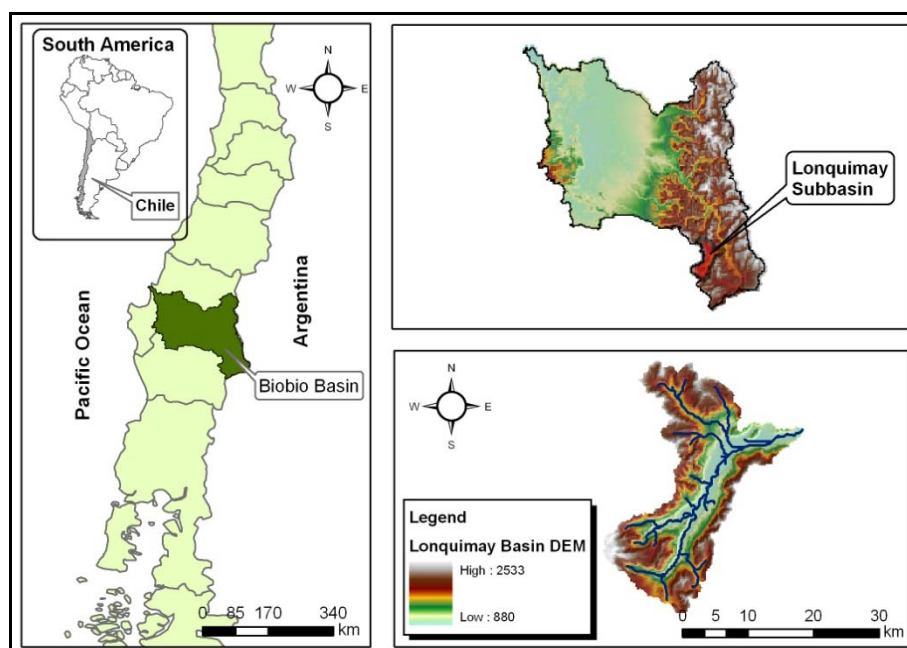


Figure 2.11 Location of the Lonquimay sub-basin within the Biobío Basin

Climate

The climate of a basin provides the moisture and energy inputs that control the water balance and determine the relative importance of the different components of the hydrological cycle. The climatic variables used by SWAT consist of precipitation, air temperature, solar radiation, wind speed and relative humidity. Minimum requirements (i.e. in case of the use of the SCS Curve Number (CN) technique for runoff, and the Hargreaves equation for evapotranspiration) are: daily precipitation, and minimum and maximum daily temperature. The data can be input from records of observed data, or can be generated by means of a stochastic weather generator. Currently available input data for the Lonquimay Basin consist of 11 years of daily precipitation and temperature time series observed at six stations. Data from one limnigraph is available for calibration and validation. The SCS CN and the Hargreaves method are thus used, together with the observed time series, for the modelling of runoff and evapotranspiration, respectively, in the Lonquimay Basin.

Hydrology

Precipitation may be intercepted and held by the vegetation canopy, or fall to the soil surface. Water on the soil surface will infiltrate into the soil profile or flow overland as runoff. Runoff moves relatively quickly towards a stream channel and contributes to short-term stream response. Infiltrated water may be held in the soil and later evapotranspired, or it may slowly make its way to the surface-water system via underground paths. The potential pathways of water movement simulated by SWAT in the HRU are illustrated in Figure 2.12.

For the modelling of the Lonquimay Basin, the model is set up in such a way that the following components are considered in the calculations: precipitation as rain and snow; snow accumulation and melt, surface runoff, transmission losses; infiltration, soil storage, evapotranspiration, sublimation, lateral flow and percolation, shallow and deep aquifer, return flow and streamflow.

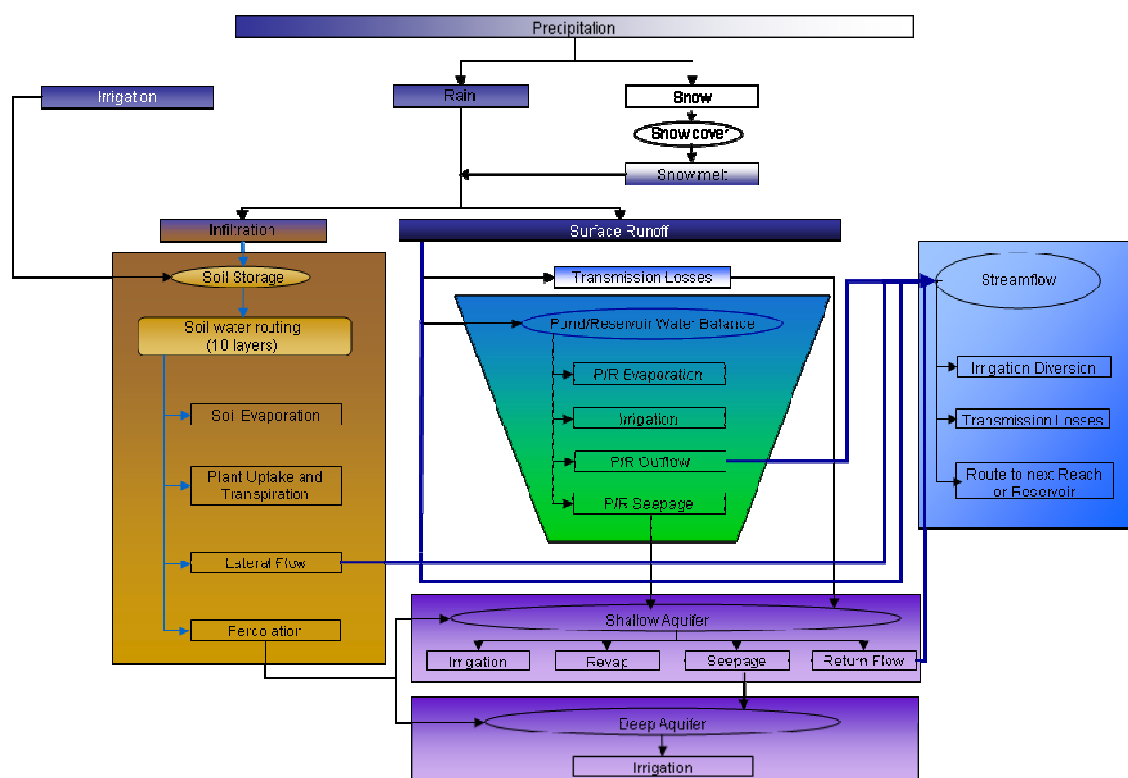


Figure 2.12 Representation of the land phase of the hydrological cycle within SWAT

Evapotranspiration

Evapotranspiration is a collective term for all processes by which water in the liquid or solid phase at or near the earth's surface becomes atmospheric water vapour. Evapotranspiration includes evaporation from rivers and lakes, bare soil, and vegetated surfaces; evaporation from within the leaves of plants (transpiration); and sublimation from ice and snow surfaces. The model computes evaporation from soils and plants separately as described by Ritchie (1972). Potential soil water evaporation is estimated as a function of potential evapotranspiration and Leaf Area Index (LAI; area of plant leaves relative to the area of the HRU). Actual soil water evaporation is estimated by using exponential functions of soil depth and water content. Plant transpiration is simulated as a linear function of potential evapotranspiration and LAI. More details (equations, additional references, etc.) can be obtained from the SWAT Theoretical Manual.

Lateral subsurface flow

Lateral subsurface flow, or interflow, is the streamflow contribution which originates below the surface but above the saturated zone. For calculation purposes, the (unsaturated) soil profile can be subdivided into a maximum of 10 layers. In this way, variability in soil characteristics such as conductivity can be accounted for (if such information is available). Lateral subsurface flow in the soil profile (0-2 m) is then calculated simultaneously with the redistribution of water within the soil profile. A kinematic storage model is used to predict lateral flow in each soil layer. Typically, under limited availability of information on the variability of soil characteristics within the vertical soil profile, a single soil layer is used for modelling. This is thus, consequently, also the case for the Lonquimay Basin model application.

Surface runoff

Surface runoff, or overland flow, is flow that occurs along a sloping surface. Using daily rainfall amounts, SWAT simulates surface runoff volumes for each HRU. Surface runoff volume for the Lonquimay Basin is thus computed using the modified version of the CN method (USDA Soil Conservation Service, 1972) incorporated in SWAT. In this method, the curve number varies non-linearly with the moisture content of the soil. The curve number drops as the soil approaches the wilting point and increases to near 100 as the soil approaches saturation.

River network

The river network in the implementation of SWAT for the Lonquimay Basin is generated from the Digital Elevation Model (DEM), using a minimum contributing area of 5 km². The extracted river network was compared with official shapefiles from the DGA, and a very good correspondence between “real” and “extracted” river network was observed.

Within the SWAT application, two types of channels are considered: the main channels and the tributaries. Tributary channels are minor or lower order channels branching off the main channel within each sub-basin. A tributary channel drains only a portion of the sub-basin and does not receive groundwater contribution to its flow. All flow in the tributary channels is released and routed through the main channel to the outlet of the sub-basin. SWAT automatically calculates the attributes for each channel from the DEM and uses these to determine the time of concentration for the sub-basin.

Transmission losses (i.e. losses of surface flow via leaching through the streambed) may occur in ephemeral or intermittent streams. SWAT uses Lane's method (USDA Soil Conservation Service, 1983) to estimate transmission losses. Losses are a function of channel width, length and flow duration. Both runoff volume and peak rate are adjusted when transmission losses occur.

Baseflow

Baseflow is the volume of streamflow originating from groundwater. SWAT partitions groundwater into two aquifer systems: a shallow, unconfined aquifer which contributes return flow to streams within the sub-basin, and a deep, confined aquifer which contributes return flow to streams outside the sub-basin (Arnold *et al.*, 1993). Water percolating past the bottom of the root zone is partitioned into two fractions, and each fraction becomes recharge for one of the aquifers. In addition to return flow, water stored in the shallow aquifer may replenish moisture in the soil profile in very dry conditions or

be directly removed by plants. Water in the shallow or deep aquifer may be removed by pumping. In the current model application for the Lonquimay Basin, no pumping is considered. The model considers transfer from the shallow to the deep aquifer by means of a parameter called “Deep aquifer percolation fraction”. As no information regarding the properties of shallow and/or deep aquifers for the Lonquimay Basin was available, the model parameters were calibrated.

Flood routing

As water flows downstream, a portion of it may be lost due to evaporation and transmission through the bed of the channel. Another potential loss is removal of water from the channel for agricultural or human use. Flow may be supplemented by rainfall on the channel itself and/or addition of water from point source discharges. Flow is routed through the channel by choosing between a variable storage coefficient method (Williams, 1969) or the Muskingum routing method. In the Lonquimay Basin application, the variable storage coefficient method was chosen for flow routing. Water abstraction points in this sub-basin of Biobío are limited, so as a first approximation no water extraction was modelled. The calibrated/validated model can then later be used to assess the impact of abstraction on water availability in other sub-basins.

Spatial Scale

The SWAT version integrated in ArcView3.2 is semi-spatially distributed: the user uses several options to set the level of detail or spatial scale, in accordance with the specific requirements of a particular application. For the application to the Lonquimay Basin, a 90m x 90 m DEM was used as a basis for the delineation of the basin. Automated extraction of the river network was done by using a threshold value of 5 km² for the upstream contributing area. A total of 45 sub-basins were defined, 44 of which were close to the different intersections in the river network, and one which was close to one point where limnigraph data are available (outlet of the whole basin), a requirement for calibration and validation purposes. A total of 87 HRUs were generated within the different sub-basins.

Temporal Scale

Considering the availability of input data at the daily time scale, a time step of one day was used for the model calculations. Output data are also generated at the daily level. The daily data can then be aggregated to the monthly or annual level, in order to obtain the corresponding water balances and runoff volumes. In TWINLATIN, monthly data are used to evaluate model performance. Aggregation of output data at the monthly time scale gives a clear overview of the inter-annual and intra-annual variability of the water yield of the different sub-basins.

2.5.3 Input Data

Topography

The DEM used in the modelling process has a pixel of 90 x 90 m. It is based on the datasets from the Shuttle Radar Topography Mission (SRTM), available through the web site of the USGS. Voids in the datasets due to signal shading caused by locally abrupt topography were filled using a radial basis function: a spline with tension with a weight of 0,1 and a minimum of 20 data points was applied using data rings surrounding the No Data areas in order to interpolate the missing values. Extreme elevation values detected as outliers were replaced by the mean elevation of a 3x3 pixel neighbourhood. A preliminary global assessment of SRTM data accuracy by Rodriguez (2005) gave a vertical accuracy of 6.2 m (90% error) for South America. The DEM for the Lonquimay Basin was projected to UTM Zone 19, datum WGS1984, using Cubic Convolution for resampling.

Meteorological data

The SCS CN method was chosen for runoff calculations, due to the availability of rainfall input data at the daily time step only. For evapotranspiration, the Hargreaves method was used. This method requires a minimal amount of input data i.e. daily series of maximum and minimum temperature. Input data were obtained from the Banco Nacional de Aguas of the Chilean General Water Administration (Dirección General de Aguas; BNA-DGA). In this phase, 11 years of data were used, corresponding to the period 1992 – 2002.

Data gaps in the precipitation time series were filled using the Inverse Distance Weighting (IDW) interpolation technique:

$$P_{fill} = \frac{\sum_{i=1}^n \frac{1}{d_i} \cdot P_i}{\sum_{i=1}^n \frac{1}{d_i}}$$

where: n corresponds to the number of stations without data gaps for the day under consideration, P_i is the precipitation of station i and d_i is the distance between the station to be filled and station i .

For the daily temperature time series (maximum and minimum), a temperature lapse rate was used. This lapse rate was estimated using temperature data and elevation for the available temperature measurement stations. The lapse rates used were $-0.008 \text{ }^\circ\text{Cm}^{-1}$ for maximum temperature and $-0.002 \text{ }^\circ\text{Cm}^{-1}$ for minimum temperature.

$$T_{fill} = (Z_{fill} - Z_i) * \frac{\Delta T}{\Delta Z} + T_i$$

where: Z_{fill} corresponds to the elevation of the station with the data gap, Z_i is the elevation of the closest station in terms of height, $\Delta T/\Delta Z$ corresponds to the temperature lapse rate and T_i to the temperature elevation of the closest station.

Datasets are available for a total of six precipitation and temperature stations, located within or in the vicinity of the Lonquimay Basin. All these stations were considered for the filling of data gaps. However, for the modelling itself, only two precipitation and temperature stations were used (Figure 2.13). This is due to the fact that, in the current AVSWAT version, for each time step a single value for precipitation and Tmin and Tmax is assigned to each sub-basin. This single value is taken from the nearest station (minimum distance to the centroid of the sub-basin). For this reason, only the datasets from the two stations most closely located to the sub-basin centroids were considered by the model.

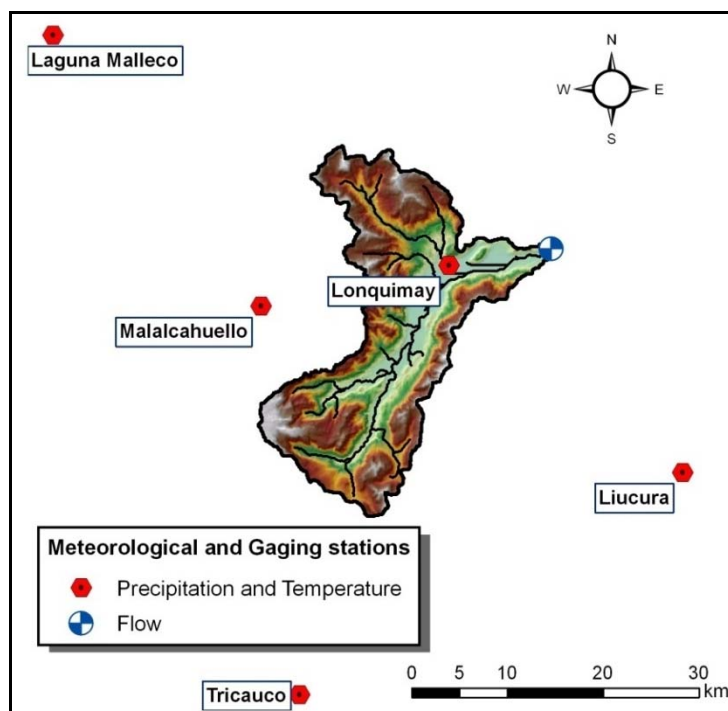


Figure 2.13 Meteorological stations used for modelling

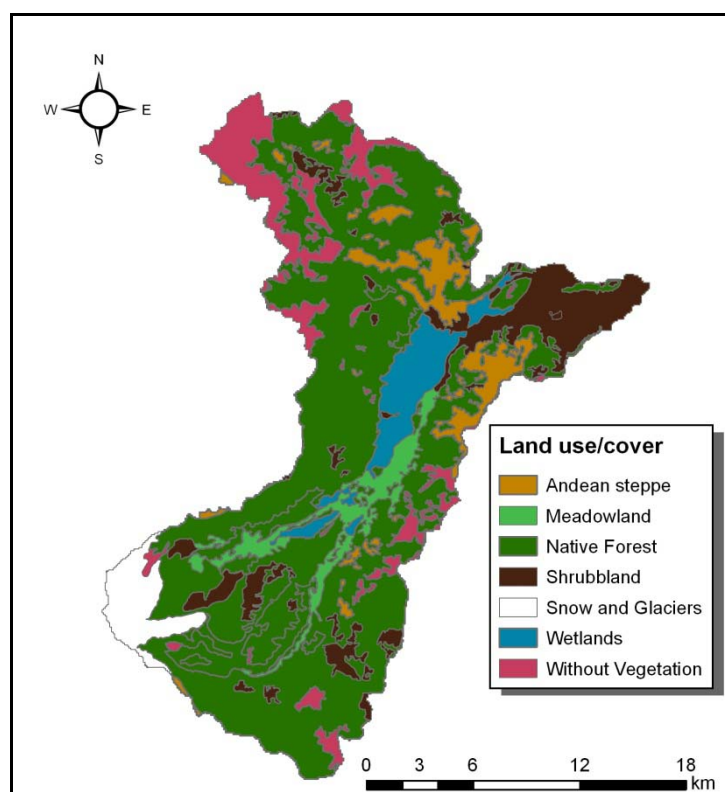


Figure 2.14 Land use for the Lonquimay Basin

Land use and soil types

The description of land use in the basin (Figure 2.14) used for modelling was based on the interpretation of aerial photographs (scale 1:70.000 and 1:115.000 from 1996-1998; INE, 1999), combined with information from the National Inventory of Vegetational Resources of Chile (*Catastro y Evaluación de los Recursos Vegetacionales Nativos de Chile*; CONAF-CONAMA-BIRF, 1995).

Due to the lack of availability of locally derived parameters values that describe the hydrological characteristics (e.g. SCS CN, LAI, etc.) of the different land use types observed in the basin, each locally observed land use was associated with a land use type contained in the SWAT model database. As a first approximation, the parameter values corresponding to those land use types were used in the model. Future research efforts in Chile should orient towards obtaining local and/or regional values for those parameters. The association of local land use with land uses container in the SWAT data base is given in the Table 2.3.

Table 2.3 Chilean land use and its equivalent in the SWAT database

Chilean land use classification	SWAT database	Code
Native Forests	Forest-Deciduous	FRSD
Areas Without Vegetation	Summer Pasture	SPAS
Andean steppe	Summer Pasture	SPAS
Meadowland	Summer Pasture	SPAS
Wetlands	Wetlands-Non-Forested	WETN
Shrubland	Range-Grasses	RNGE
Snow and Glaciers	Pasture	PAST

The hydrological group of a soil series (required for the application of the CN method) was derived from the soil texture contained in the official description of soil series of the Agrological Study of the VIII and IX Region (*Estudio Agrológico de la IX Región*; CIREN, 1999^b), according to the recommendations given by the US Department of Agriculture (USDA, 1986). Granulometric data for the different soil series were also extracted from the previously mentioned study; conductivity values were obtained from Liu *et al.* (2002), cited by Campos (2005). For the Lonquimay Basin the soil type is described as not recognised, so considering the lack of information for this area, as a first approximation it is assumed that the soil properties are the same as those of the nearest defined soil type, in this case Santa Barbara (Silt Loam).

Channel flow

For calibration and validation, time series from the only limnigraph station in the sub-basin (outlet) were used (Figure 2.14). These time series correspond to the period 1995-2002.

Snow

For snow modelling purposes, ten elevation bands - each one of them covering 10% of the sub-basin area - were considered for each one of the 45 sub-basins. Parameterisation of the snowmelt module (e.g. mean air temperature at which precipitation is equally likely to be rain as snow, threshold temperature for snow melt, maximum and minimum melt factors) was initially based on data from the Chilean literature (Peña *et al.*, 1985; Escobar, 1992), after which a calibration procedure was applied. Precipitation and temperature lapse rate were obtained using available meteorological data (local measurements) in combination with information derived from the Land Surface Temperature/Emissivity Daily L3 Global 1km MOD11A1 product.

2.6 Calibration

The SWAT model includes a large number of parameters describing hydrological characteristics distributed across the basin under study. In order to obtain model results that reflect actual process behaviour in the field, the model parameters are subject to adjustments as part of a calibration process. The parameter ranges in the calibrated model must be physically reasonable, within pre-specified ranges, in order to support the application of the model for impact assessment.

For calibration purposes, available time series from a limnigraph located at the outlet of the basin were used. The model was run with rainfall and temperature data from 1992-1998 as input. The first three years were reserved for model warm-up; calibration was performed using the last four years of data available from these time series (Figure 2.15).

Before calibration, a sensitivity analysis considering only the snowfall/snowmelt routine parameters was done for ranking purposes (Table 2.4). This ranking of most sensitive parameters was established by means of a LH-OAT analysis (Latin Hypercube Sampling - One at A Time; incorporated in the latest model version, SWAT2005; van Griensven *et al.*, 2006). With these results, a manual calibration was then done, which was followed by a second sensitivity analysis, considering all 28 parameters included in the SWAT sensitivity analysis module. The resulting six most sensitive model parameters were: baseflow alpha factor, channel effective hydraulic conductivity, initial SCS CN II value, surface runoff lag time, available water capacity and Manning's n value for the main channel. After this, the automated calibration procedure implemented in SWAT2005 called PARASOL (Parameter Solution Method; van Griensven & Bauwens, 2003) was applied for calibration. To obtain the optimum solution the Sum of the Squares of the Residuals (SSQ) was used. Model calibration was evaluated at the level of monthly output data. Statistical indicators used for evaluating model performance are: Nash-Sutcliffe Modelling Efficiency Index (EF), Goodness of fit (R^2) and the % of deviation from observed streamflow (PBIAS).

The closer the values of RRMSE and ABSERR are to zero, and those of R^2 and EF to unity, the better the model performance is evaluated (Abu El-Nasr *et al.*, 2005). For PBIAS, the optimum value is 0; a negative value indicates an overestimation of observed discharge values, whereas a positive value indicates underestimation. Tables 2.5 and 2.6 show results for different periods of model evaluation.

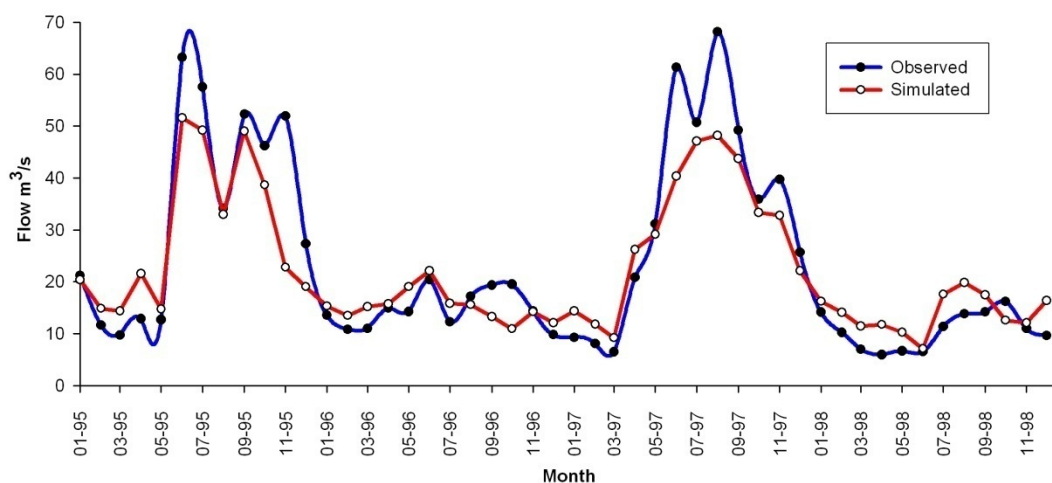


Figure 2.15 Monthly observed versus simulated flows at the Lonquimay gauging station during calibration

Table 2.4 Sensitivity ranking of the snowfall/snowmelt parameters

Place	Sensitivity analysis 1		Value	Unit
1	Snowfall temperature	SFTMP	0.9	°C
2	Maximum melt factor for snow	SMFMX	5.0	mm H ₂ O/°C-day
3	Minimum melt factor for snow	SMFMN	1.244	mm H ₂ O/°C-day
4	Snow melt base temperature	SMTMP	1.57	°C
5	Snow pack temperature lag factor	TIMP	1.0	
6	Temperature lapse rate	TLAPS	-5.0	°C

Table 2.5 Statistical indicators of model performance (monthly output) calculated at the outlet of the Lonquimay Basin, considering different periods of evaluation

Index	Calibration						All
	Su ¹	A ²	W ³	Sp ⁴	SA [*]	WS ^{**}	
EF	0.14	0.82	0.86	0.51	0.83	0.76	0.81
R ²	0.89	0.92	0.93	0.66	0.93	0.83	0.87
PBIAS	-28.24	0.45	7.60	19.58	-9.01	12.8	4.88

¹: Summer; ²: Autumn; ³: Winter; ⁴: Spring; *: Summer – Autumn; **: Winter – Spring

Table 2.6 Predicted and observed (bold) discharges, considering different scales of evaluation (calibration)

Year	Seasonal flow (m ³ s ⁻¹)				Mean annual flow (m ³ s ⁻¹)
	Summer	Autumn	Winter	Spring	
1995	16.02	22.81	46.45	30.66	29.13
	14.61	19.04	54.27	44.41	33.45
1996	15.00	18.95	15.58	12.34	15.24
	13.65	15.78	15.49	16.07	14.78
1997	12.20	29.46	44.74	31.59	29.94
	8.47	30.07	59.72	35.84	33.99
1998	15.41	10.06	17.57	12.45	13.89
	12.26	6.30	12.40	12.41	10.58
Mean	14.66	20.32	31.08	21.76	22.05
	12.24	17.80	35.47	27.18	23.20

2.7 Validation

Time series from the 1996-2002 period were used for model validation. Again, the first three years of data from these time series are used for model warm-up. Evaluation of model performance is thus based on output for the 1999-2002 period (Figure 2.16). Table 2.7 shows results for different periods of model evaluation.

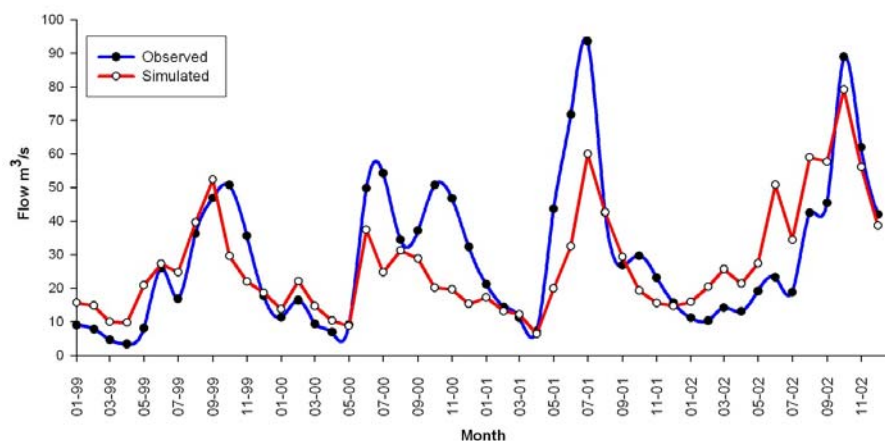


Figure 2.16 Monthly observed versus simulated flows at the Lonquimay gauging station during validation

Table 2.7 Statistical indicators of model performance (monthly output) calculated at the outlet of the Lonquimay Basin, considering different periods of evaluation

Index	Validation						All
	Su ¹	A ²	W ³	Sp ⁴	SA [*]	WS ^{**}	
EF	-1.27	0.32	0.34	0.38	0.36	0.36	0.56
R ²	0.24	0.32	0.35	0.77	0.37	0.51	0.57
PBIAS	-39.01	3.08	2.2	29.55	10.96	15.87	7.86

¹: Summer; ²: Autumn; ³: Winter; ⁴: Spring; *: Summer – Autumn; **: Winter – Spring

2.7.1 Snow Cover Area (SCA) validation

The MODIS snow cover products are one of the many geophysical products derived from MODIS data. Global snow extent has been mapped by MODIS since shortly after the launch of the Terra satellite, and a global, daily snow-cover map has been produced since February 2000. The MODIS snow cover products are provided daily and as 8-day composites at 500 m resolution over the Earth's land surfaces, using an algorithm based on the normalised difference of a visible and a shortwave infrared band (Hall *et al.*, 2002). The MOD10A2 products (Figure 2.17) are composites of eight days of snow maps in the sinusoidal grid, produced by compositing from two to eight days of the MOD10A1 and MYD10A1 snow products. An 8-day compositing period was chosen because that is the exact ground track repeat period of the Terra and Aqua platforms.

To validate the snow cover area estimated by the model, the MOD10A2 snow product (Hall *et al.* 2006, updated weekly) was used. Firstly, images were reprojected (WGS84 UTM 19S) using the MODIS Reprojection Tool (MRT). Basin images were reclassified as (1) snow and (0) no snow, and then aggregated at the monthly time scale.

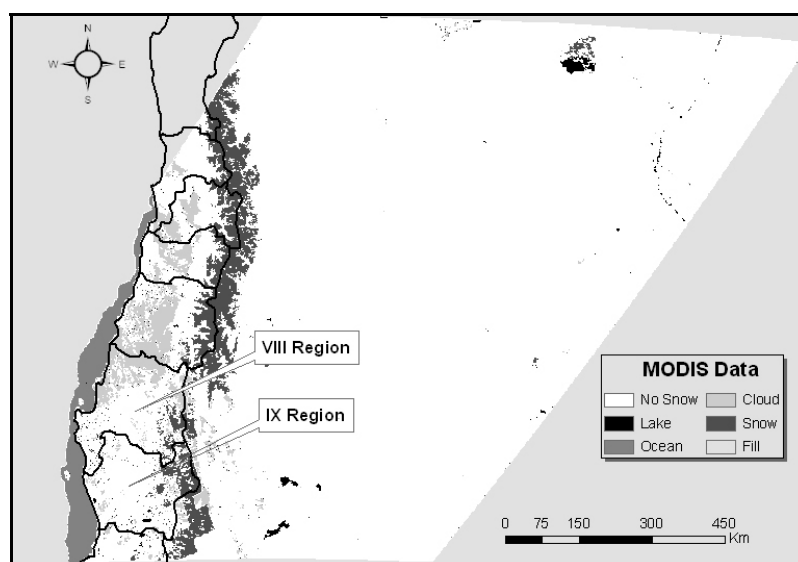


Figure 2.17 MODIS images

Considering the limited existing overlap between locally observed time series for the Lonquimay basin and available MODIS imagery, three years of MODIS images (2000–2002) could be used for the SCA validation. Cells with snow presence in each sub-basin are counted for each month and multiplied by the cell area, as to obtain the snow area for the sub-basin. Then, sub-basins were reclassified as (1) snow or (0) no snow. Snowpack was calculated using values obtained for snowfall, snowmelt and sublimation. As in the case of MODIS, model values were also reclassified as (1) snow or (0) no snow for each sub-basin; in this case a zero value was assigned only if snowfall, snowmelt, sublimation and snowpack were zero. After reclassification, values from the modelling results were subtracted from the MODIS-based results; a zero value indicates that the image and model are in agreement, -1 indicates that model results reveal snow presence whereas the MODIS image does not, and 1 indicates that model does not estimate snow whereas the MODIS image signals the presence of snow. Table 2.8 and Figure 2.18 summarise the results of the comparison exercise.

Table 2.8 Performance (%) of MODIS versus model results considering monthly evaluation

	Results in agreement			Modelling no; MODIS yes			Modelling yes; MODIS no		
	2000	2001	2002	2000	2001	2002	2000	2001	2002
January		84	100		16	0		0	0
February		98	93		2	7		0	0
March	29	89	98	71	11	2	0	0	0
April	29	85	71	4	13	27	67	2	2
Mai	89	96	87	4	0	0	7	4	13
June	96	53	98	4	0	2	0	47	0
July	93	91	96	7	0	0	0	9	4
August	91	87	96	2	13	0	7	0	4
September	93	76	98	2	24	2	5	0	0
October	44	36	62	56	64	36	0	0	2
November	85	33	56	13	67	44	2	0	0
December	80	100	71	20	0	29	0	0	0

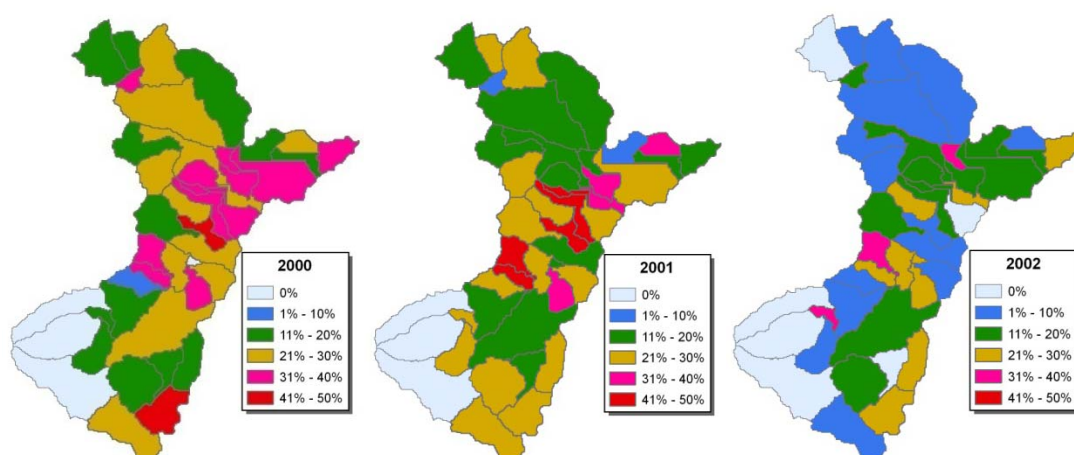


Figure 2.18 Percentage of disagreement between monthly model outputs and MODIS images, for the different sub-basin. For 2000 only the months from March to December are considered.

2.8 Evaluation of hydrological modelling (D3.2)

Sections 2.7 and 2.8 report the calibration and validation of the SWAT model for the Lonquimay sub-basin of the Biobío River Basin. Good overall calibration and validation period model performance was obtained for discharge data at the Lonquimay basin outlet for the PBIAS (% of deviation from observed streamflow) criterion, whereas performance for EF (Nash-Sutcliffe Modelling Efficiency Index) ranged from Good to Satisfactory only, for the calibration and validation period, respectively.

A more detailed look at Table 2.7 and Figure 2.16 shows that at the monthly, seasonal and annual level the model tended to underestimate the higher flows (mainly winter and spring), whereas low flows (which mostly occur during summer and autumn) were typically overestimated. Analysis of results for the different seasons by means of the EF, R^2 (Goodness of fit) and PBIAS criteria (Table 2.7) shows that the best overall performance occurs during winter (in terms of correspondence between observed and modelled river flows). Representation of summer discharges for both the calibration and validation period would be considered as only Satisfactory (as compared to Good for the other seasons) for PBIAS, and as Not Satisfactory for EF. The total runoff water balance over the modelled period is slightly positively biased (meaning an underestimation of total outflow).

Validation of snow results given by the model using MODIS images shows that there is a good average agreement of 79% between modelled and observed snow cover over the 3-year period 2000-2002. In 5% of the cases, the model predicts snow where the image does not, whereas in 16% of all cases images represent snow where the model does not (Table 2.8). As can be seen from Figure 2.18, the biggest and smallest discrepancies between model and images corresponded to the years 2000 and 2002, respectively. Especially noticeable is the increase in units represented as having a snow cover by the model where the image does not for 2000. However, the main difference still is the lack of representation of MODIS-snow covered areas in SWAT (Table 2.8). The higher discrepancies for the year 2000 may be related to the precipitation input patterns for the basin, where the total modelled water balance input to the basin for 2000 is approximately half that of 2002 (perhaps due to more erratic rainfall patterns under dry/drier years). However, a considerably higher number of modelled years would be needed in order to enable the establishment of sound conclusions with regard to this last point. From Table 2.8 it can be observed that at the monthly level, October and November presented the greatest number of discrepancies between results based on SWAT versus MODIS. Also in these cases, in general the model does not represent part of the snow cover detected by MODIS. Modelled discharge values for this period (October and November; years 2000 and 2001) are also typically below the measured monthly values (high positive PBIAS), whereas summer discharges are typically overestimated by the model.

Considering also the fact that peak flows during the wet season as well as total model period runoff are underestimated by the model, at least a partial explanation for unsatisfactory or sub-optimal model behaviour may be found in the inadequate representation of the spatial precipitation fields used in this application. This would be caused by the reduced number of available meteorological stations (a problem common to many Latin-American river basins), and by the absence of meteorological stations in the higher parts of the basin (where both precipitation values and variability are expected to be high). In addition to this, a potentially inadequate representation of soil types and profiles for the Lonquimay Basin by means of the Santa Barbara Series (a consequence of the lack of locally determined soil type information) might lead to an overestimation of infiltration and groundwater storage, especially for the steep and high-lying areas which would both have a thin (or even no) soil cover and thus, in reality, cause considerable contributions to the quick flow component. The underestimation of snow cover over such areas during spring may also lead to a higher groundwater recharge contributing to (overestimated) baseflows at a later stage, and to an under-representation of snow accumulation and snow melt dynamics and, thus, reduced contributions from snowmelt during spring (the effects of snow melt on observed mean river flows for October-November can clearly be observed from Figure 2.15 and 2.16).

Even when certain problems (such as the ones described above, many of which seem to be related to the limited amount and spatial coverage of input and calibration and validation datasets) could be detected with regard to the model performance in the Lonquimay Basin, the model does represent the major intra- and inter-annual variability of discharge values in the basin relatively well. From this perspective, by applying the necessary caution in the interpretation of the results, the model can indeed already be used to make a first assessments by means of model simulations of the possible impacts of climate change scenarios in a mixed-regime (rainfall and snow-fed) river basin from central Chile, and conclusions from this assessment can be used to foresee potential impacts under similar climate change scenarios in similar sub-basins of the Baker (see WP8 report).

2.9 Summary and recommendations

The hydrological component of the Soil and Water Assessment Tool SWAT was applied to a sub-basin of Biobío located in the Andes of south-central Chile. The very limited availability of traditional input and calibration and validation datasets for this sub-basin is typical of many Andean (sub)basins in Chile. Results obtained from this model application for the Lonquimay basin show a good to satisfactory general model performance in terms of representation of long term or annual mean discharge at the basin outlet.

Besides the traditional calibration and validation based on river flow, MODIS snow products were used to evaluate the representation of snow cover extent as it is generated by means of the calibrated SWAT model snow routine. Although a reasonable description of snow cover extent could be obtained under most circumstances, the present case study shows the limitations inherent to modelling under situations of low station density in areas with high (topography-induced) precipitation gradients. Location and density of monitoring stations undoubtedly play a determinant role in the general accuracy of model results, and the present case study provides an example quantitative indication of how good a model may perform under limited availability of input meteorological datasets. Improvements in model behaviour may, however, still be obtained in future work through the incorporation of an improved description of basin soil types and characteristics (especially for those parts of the basin that can be reasonably assumed to have a very thin or non-existing soil cover), as well as through the use of differential seasonal temperature lapse rates (analysis of temperature data obtained from MODIS produced a different lapse rate value for the different seasons).

By applying the necessary caution in the interpretation of the results (see also Chapter 9 for evaluation), the model can indeed already be used to make a first assessments by means of model simulations of the possible impacts of climate change scenarios in a mixed-regime (rainfall and snow-fed) river basin from central Chile, and conclusions from this assessment can be used to foresee potential impacts under similar climate change scenarios in similar sub-basins of the Baker (see WP8 report).

Especially with regard to its usefulness for the Baker Basin, future work should also more explicitly address the aspect of glacier melt contributions. For this purpose, the glacier melt module proposed by Schaper *et al.* (1999) can be adapted and incorporated in SWAT.

In the current work, the MODIS snow products have been used for validation purposes only. This has allowed gaining improved insight into the performance of the SWAT model and of its snowfall– snow melt routine. Future efforts may be directed towards the incorporation of MODIS information directly into the process of model parameter calibration itself, in an attempt to further improve model results. Such incorporation would depart from the inherent assumption that the MODIS representation of snow cover is good.

With regard to the water authorities in the Baker River Basin (and in general), the following recommendations can be made:

- Well-thought and strategic (long-term/goal-oriented) improvements in the hydrometeorological monitoring networks should urgently be considered (longer time series are generally required for model calibration and validation, and maximum benefits from improvements in the monitoring network will not be obtained immediately; even so such improvements should not be postponed); such improvements can be balanced and combined – out of cost considerations - with the search for alternative data sources such as, for example, those generated from remote sensing. In order to evaluate the potential importance of such alternative data sources, additional research will be required.
- Capacity building in the use of hydrological models for government stakeholders has been conducted in the past (e.g. in the Biobío Basin under TWINBAS). For the Chilean case, in the immediate future, however, the execution of modelling work is mainly situated within the academic or consultant environment, where specific modelling tasks can be conducted upon request by water stakeholders and authorities. The outcome from such work is clearly of high interest to the water stakeholders, who can use information from the modelling in their decision-making. Conducting the modelling applications at government institutions themselves, however, may be feasible in the future; under current conditions, government organisations will typically lack staff – or available staff will lack time - to conduct such modelling work themselves. This may change in the near future, as modelling support for decision-making becomes more and more required. Creating awareness among government stakeholders with regard to the possibilities and limitations of modelling work, however, is important, as it will help them to better evaluate the real value of model outcome, and to better direct and specify requests for consultancy work or research. Attention has been given to this aspect under TWINLATIN (e.g. through the public participation workshops), and this awareness building should also be further developed in ongoing and future interactions between academics and authorities (or other basin stakeholders). Providing training on simplified modelling case studies may also be helpful in this sense.

3. Catamayo-Chira River Basin (Ecuador-Peru)

3.1 Description of basin

This study is conducted in the binational Catamayo-Chira River Basin, which has an extension of 17,199.18 km². 7,212.37 km² are situated in Ecuadorian territory (66.82% of the province of Loja); the Peruvian part occupies an area of 9,986.81 km² and it is located in the department of Piura (corresponding to 30% of the department) (Figure 3.1).

The river basin is located between 03°30' and 05°08' south latitude and 79°10' and 81°11' west longitude, with a altitudinal rank that goes from sea level, in the outlet of the Chira river (in the Pacific Ocean), to 3,700 m in the Podocarpus National Park (Loja). The river basin limits to the north with the binational river basin Puyango-Tumbes, east with the Zamora-Chinchipe province in Ecuador, south with the provinces of Piura and Huancabamba in Peru, and west with the Pacific Ocean.

The basin houses eleven life zones (Holdridge classification system), ranging from tropical desert to mountainous rain forest. Mean temperatures vary from a relatively high 24° C in the lower part of the basin to temperatures about 7° C in the higher parts, at altitudes above 3200 masl, being about 20° C the mean temperature in the middle zone.

The forest vegetation predominates with 698,602.12 ha (it supposes 40.62% of the river basin). Next grazing with 501,639.10 ha (29,17%), followed by the bush vegetation with 232,277.54 ha (13.51%); farming occupies 177,731.35 ha (10.33%) and Andean desert has an area of 25,740.44 ha (1.50%). Finally there are areas dedicated to other uses (eroded areas or in erosion process, urban areas, water bodies, etc.) which occupy an area of 83,927.06 ha (4.88%).

3.1.1 Hydrology

The Catamayo-Chira River Basin is constituted by the sub-basins of Quiroz (3,108.77 km², 18%), Chipillico (1,170.27 km², 7%), Alamor (1,190.27 km², 7%), Macará (2,833.29 km², 17%), Catamayo (4,184.03 km², 24%) and the Chira System (called this way because it includes a lot of small sub-basins draining to the Chira river (4,711.90 km², 27%).

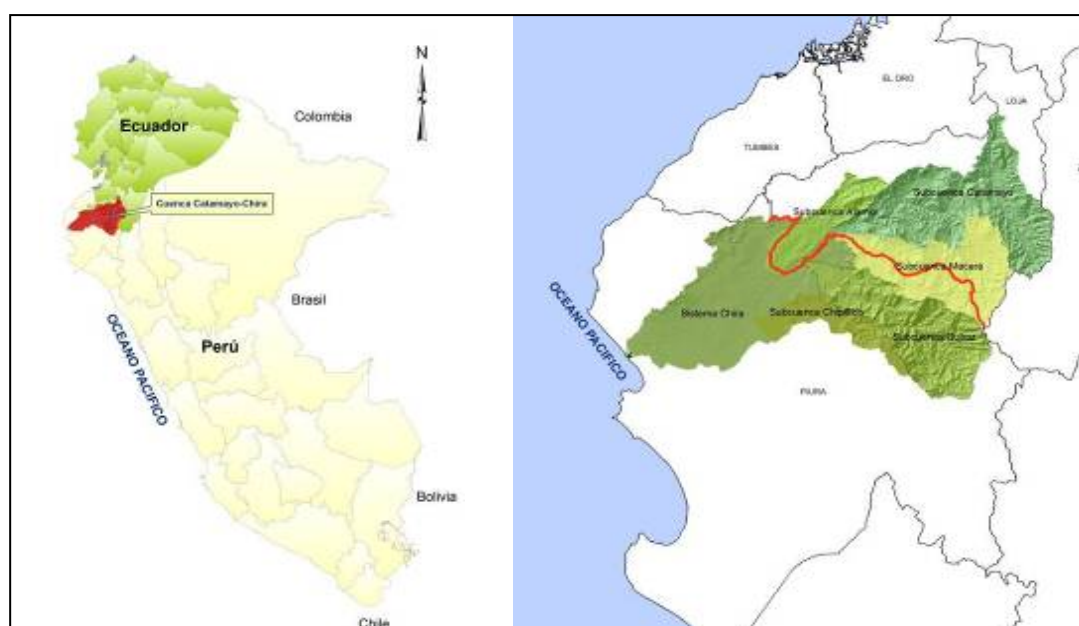


Figure 3.1 Location of the basin

The basin has dendritic characteristics, showing good drainage. The main course is the Catamayo Chira river, with an overall length of 315 km, of which 196 km are located in Ecuadorian territory, in which it takes the name of Catamayo river, and the other 119 km in Peruvian territory, where from the confluence of the rivers Catamayo and Macará it takes the name of Chira river. Downstream it receives the contribution of the Quiroz river, flowing in a south-east to north-west direction, and the Alamor river from the north. Further downstream, the Chipillico river enters the main course as well as smaller creeks activated in the rainy season.

The river basin precipitation and temperature present noticeable variations in space and time. In the lower river basin the rainy periods are short and scarce and, with the exception of the years of the phenomenon El Niño, it rains from January to April with an annual average of 10 to 80 mm. In the river basin medium zone the rainy period goes from December to May with annual average precipitations of 500 to 1000 mm. On the other hand, in the high river basin, rains happen from October to May with annual averages greater than 1,000 mm.

Evaporation spatial variation ranges from 6 mm per day in the lower part, to 3 mm per day in the upper zone.

With regard to temperature, the annual average temperatures of the river basin oscillate between 24°C in the low river basin, 20°C in the medium river basin and 7°C in the high part of the river basin.

A strong influence from the oriental climate regime is evident in the upper zones, in contrast to the coastal regime that dominates the lower part, where the ENSO-influence is remarkable.

The greatest flows are from the Catamayo sub-basin with a mean monthly flow of 31.1 m³s⁻¹ (Santa Rosa station) and the Macará sub-basin with a mean monthly flow of 40.9 m³s⁻¹ (Puente Internacional station). These flows represent 70% of the total basin flow.

3.2 Choice of model

3.2.1 Problems

The Catamayo-Chira is a basin that has been strongly operated upon. As a result there is high pressure on natural resources, especially water. Natural land cover also has been altered considerably due to agricultural and livestock producing activities conducted by local inhabitants along the river basin, and a high deforestation degree.

This problem is heavier in the higher and middle part of the basin, due to increasing superficial runoff, washing away of nutrients, water erosion and sediment transportation along the river flows into the Pochos reservoir and lower land river beds (e.g. Chira), increasing infrastructure vulnerability in the valley during the rainy season, due to inundation and loss of agricultural soil and changing the hydrological regime of the basin.

The objective for a hydrological model in the Catamayo-Chira river basin is determined in the first place by the need to gain a better knowledge about the hydrological behaviour of the basin, due to limited availability of flow measurements, except in a few strategic zones in the basin. With this tool, specific areas at micro-basin level that are the main water production entities can be detected, as well as erosion processes quantified and the main sediment production zones determined.

The basin's response to different coverages and land uses can be evaluated which allows analysing the influence of the land use change dynamics on erosion and the impact on water production. In this way the model will provide a tool for planning and evaluating land and water use in the basin.

3.2.2 Model selection

One of the objectives of the TWINLATIN project was applying a hydrological and erosion model in the binational basin, adapted to local characteristics thus allowing solving of problems and designing of proposals for better basin management.

The SWAT model was chosen because it had already been applied to big and complex Andean basins, comparable to the Catamayo-Chira basin, offering acceptable results. It is true that the available data

show a lack of information e.g. soil cover data, but at the same time this provides an opportunity to conduct further necessary investigations.

Also the climatic and hydrological data availability could be a limitation for model application, due to time and space scale reasons. The model needs a representative scale that describes adequately the special variability over the basin during a certain (long) period. This was controlled by working closely with local institutions administrating these data, collecting available (digital) data, and digitising paper data in order to get a representative measurement station density.

SWAT is also a relatively efficient model that can be run easily on a PC. It is shareware, working on the ArcView-Gis 3.2 platform, a software in which the project personnel had experience. In addition, SWAT offers the possibility to extend the hydrological model by sub-models to analyse sediments, and allows evaluation of different land uses and their impact.

However, being a complex model, it was impossible to analyse the whole extent of the Catamayo-Chira basin, because data needs are enormous. This is why the following criteria were used to prioritise the modelling area:

- Availability of information: amount
- Assessment of collected data: quality and spatial range
- Zones suffering erosion problems and water production zones
- Zones without relevant data for the model

3.2.3 User interface

For this study, an ArcView 3.2 Software extension, integrating SWAT, called AVSWAT-X was used. ArcView offers the necessary tools before and after model application, allowing graphical and numerical database edition. It also allows delimitation of sub-basins, definition of hydrological response units, location of measurement stations and calibration of simulation results.

3.3 Model development

3.3.1 The SWAT model

The SWAT model (Soil and Water Assessment Tool) has been developed by the USDA-ARS (Agricultural Research Service) in collaboration with the University of Texas to predict the impact of soil management and land cover on water production, sediments in complex basins presenting soil, land cover and land use variability over long periods. The model consists of a set of sub-models, used to simulate different hydrological processes. The model is based upon the general hydrological balance equation. Division of the basin into sub-basins and hydrological response units allows introduction of different evapotranspirations, due to different land cover and soil types.

Runoff is assessed by the model for each hydrological response unit (HRU). These HRU are created by the model on sub-basin level, improving representation and defining smaller zones having more homogenous physical and climatic characteristics, which allows SWAT to produce a better physical description of the hydrological balance.

The necessary parameters to estimate daily potential evapotranspiration, whether using Hargreaves or Penman-Monteith, are calculated based upon monthly values of climatic data included in the model, using internal equations managed by SWAT.

SWAT includes in its modelling the curve number procedure, in which it relates superficial runoff with different soil types and land uses. This curve number depends upon land use and the hydrological group to which the soil belongs, being the A, B, C or D group, depending from various factors such as infiltration permeability or drainage capacity.

SWAT uses a special treatment for soil cover. Vegetative growth is an important factor for the model, so a lot of biophysical parameters needed to be adapted from the original SWAT database for the Catamayo-Chira basin as this information could not be collected for the study zone.

3.3.2 Study area

As a study area for the hydrological and erosion analysis the whole basin area was originally considered, being 17,199.19 km². However, this exercise was limited to only a 68% of the total basin area, being 11,790.33 km². This was decided based upon the following criteria:

- Data availability and evaluation, as SWAT has highly demanding data requirements. Quantity, quality and spatial resolution of available information were assessed in order to permit a good model application, and subsequent calibration and validation.
- Prioritisation of zones presenting erosion problems and water production zones. This explains the attention paid to middle and higher parts of the basin. One important aspect concerning the lower part is its dryness. Precipitation is very scarce, except for the ENSO phenomenon, and in consequence water erosion is about zero.
- Zones that do not contribute, with relevant data for the model. In the lower part of the basin two huge reservoirs are located. Downstream from these reservoirs, the rivers practically disappear. Most of the release water flows through channels that cannot be modelled because they do follow contour lines, and are also regulated (opened and closed) in a (for the model) irregular way.

One of the reservoirs, San Lorenzo, used to irrigate the San Lorenzo settlement, is 90% located in the neighbouring Piura basin, and releases most of its water to this basin. There is no information available about what percentage of drainage water returns to the Chira basin, and what percentage is evacuated through the Piura basin. There is a minimum flow entering the river Chira by the Chipillico sub-basin, normally just reservoir overflow in heavy precipitation periods. All this would cause a significant distortion in the results.

Based upon these considerations, it was determined that the SWAT model could be implemented in the middle and higher parts of the basin, and for this reason the study area does not include the territories downstream from the reservoirs Poechos and San Lorenzo (Figure 3.2).

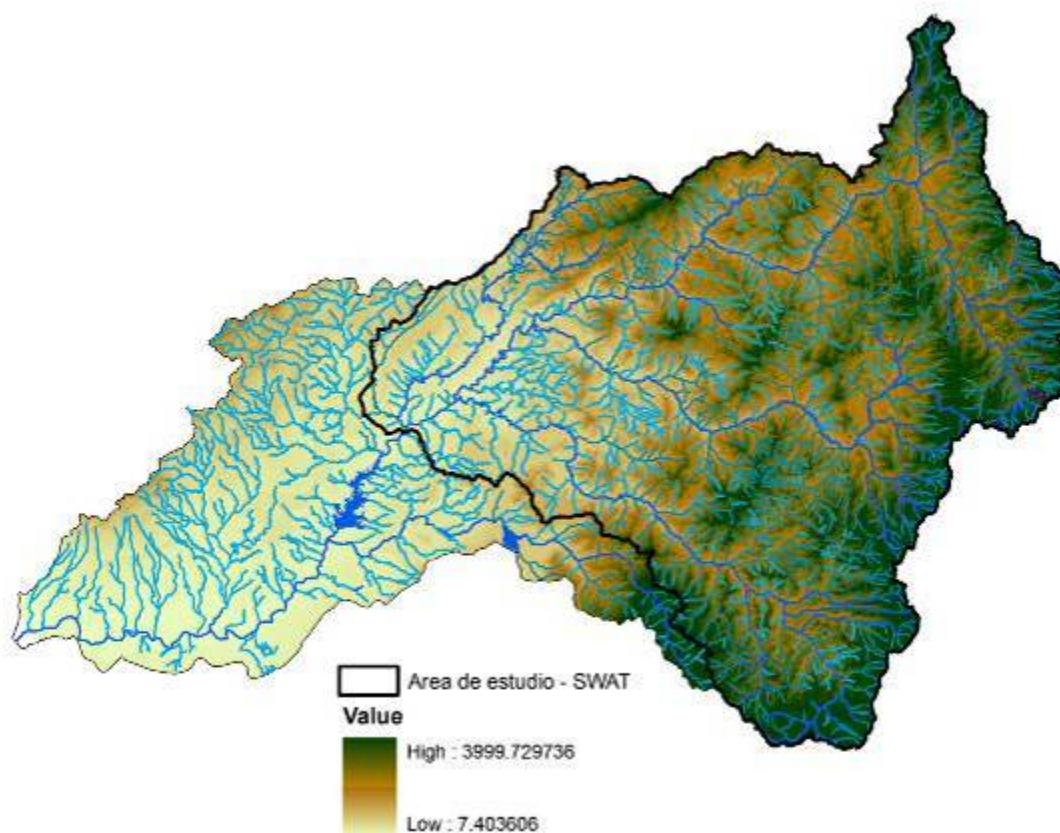


Figure 3.2 DEM, river network and study area for SWAT in the Catamayo-Chira basin

3.3.3 Model configuration

The model was calibrated for the four sub-basins located in the middle and higher part of the basin (measurement stations Catamayo, Alamor Saucillo, Puente Internacional and Paraje Grande), and at the measurement station Ardilla, located at the Poechos reservoir's inlet, which includes the contribution of these four sub-basins as well as other important contributions. In order to get results in the simulation that reflect data from measured streamflows at these measurement stations, the model was calibrated. This calibration consisted in adjusting parameters that describe hydrological conditions used by the model.

Applying SWAT to the whole study area, the Ardilla measurement station was considered as control point (Poechos reservoir inlet). This station receives the contributions from the four sub-basins already calibrated as well as contributions from other microbasins (Figure 3.3). The methodology used for calibration at the Ardilla station consisted of introducing values for the parameters adjusted at the level of each hydrological response unit in the four sub-basins already calibrated, and only adjusting values for the rest of microbasins.

This method was necessary due to the huge extension of the basin and because it was decided to use five hydrometric stations for calibration to reduce uncertainties. For this reason it was necessary to apply and calibrate SWAT in each sub-basin separately.

This resulted in a slower but more accurate process, due to easier data treatment at sub-basin level and reduced data uncertainty compared to treatment in only one calibration point.



Figure 3.3 Location of the five measurement stations of used streamflows in the calibration of SWAT

3.4 Data requirements

To start working with SWAT it was necessary to recollect and generate information, which in a lot of cases were not available e.g. soil information and precipitation data available only written on paper. Digitising and generating necessary information was a huge part of the implementation process. SWAT needs a lot of information, the most important items are described below.

3.4.1 Digital Elevation Model

The Digital Elevation Model (DEM) basically permitted definition of the drainage system and the sub-basin borders. Contour lines at 200 m, at a 1:250,000 scale, were the initial available information for the basin. To improve the accuracy of the DEM it was necessary to improve the scale of the base map. For that purpose, additional topographical information was processed at a 1:50,000 scale with contour lines every 40 m on the Ecuadorian side of the basin and at a 1:100,000 scale with contour lines every 50 m on the Peruvian side. An integration of the contour lines was done that resulted in a single map with contour lines every 40 m. This matching was done in ArcView, using curve interpolation techniques. The greatest difficulty was the difference of detail between topographical maps (contour lines) generated in both countries. It was a long and difficult job integrating both maps' information in a single map for the basin.

The DEM used for SWAT was elaborated in ArcView 3.2 and was generated using a 100 m x 100 m cell width.

3.4.2 Hydrography

A validation of the river network was done in vector format. Basically correspondence between new 40 m contour lines and existent river network was verified. During this analysis some inconsistencies were found (especially in the Ecuadorian part, due to different information sources) such as rivers crossing contour lines, incomplete river courses usually due to lagoons.

To correct these errors, information at 1:50,000 at the Ecuadorian side was used, which allowed matching the information with the information used for the contour lines. Not all of the existing rivers could be used because this would have generated big differences at the border, as the Peruvian river network information was on a bigger scale. A new visual validation was done to obtain a product adjusted to the needs of the model. The river network is useful to compare to the calculated network.

3.4.3 Climate and hydrological data

A quality analysis of climatic and hydrological daily and monthly data from the 19 Peruvian and 24 Ecuadorian stations was realised.

Process simulation requires a considerable amount of climatic, meteorological and hydrological data, including precipitation, temperature, wind speed, dew point temperature, and solar radiation, all on daily and monthly level. This information is used by the model to simulate model entries and outputs. Additionally streamflow and sedimentation data are required for use in the calibration and validation phase. Statistical procedures were used to obtain 15 monthly parameters which characterised the climate of the area, to prepare the model for the basin (*Annex 1.0. Caracterización Climática, Meteorológica e Hidrológica de la Cuenca Binacional Catamayo Chira*).

To determinate evapotranspiration, the Hargreaves method was used. This methods requires basically minimum and maximum temperatures.

The analysed pluviometric stations present a rainy period between October and April, with March being the wettest month. The stations in the lower part of the basin present the biggest absolute difference between dry and wet months, in comparison to the stations in the higher part where precipitation is more uniformly distributed through the year. In the lower stations, the ENSO effect is much more significant.

To determinate evapotranspiration, the Hargreaves method was used. This methods requires basically minimum and maximum temperatures.

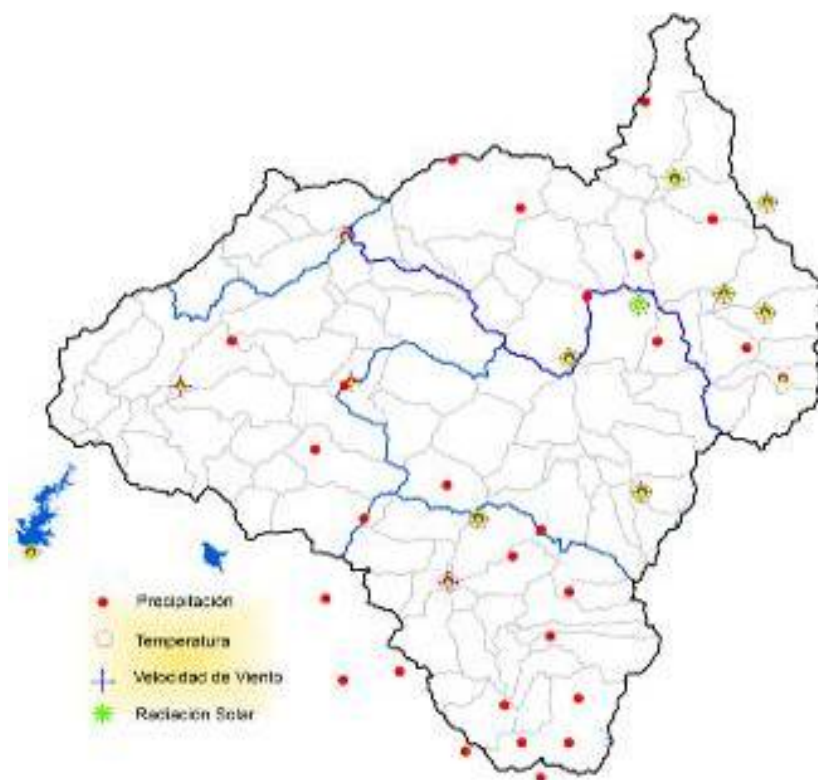


Figure 3.4 Meteorological stations used to apply SWAT in the Catamayo-Chira basin

The analysed pluviometric stations present a rainy period between October and April, March being the wettest month. The stations in the lower part of the basin present the biggest absolute difference between dry and wet months, in comparison to the stations in the higher part where precipitation is more uniformly distributed through the year. In the lower stations, the ENSO effect is much more significant.

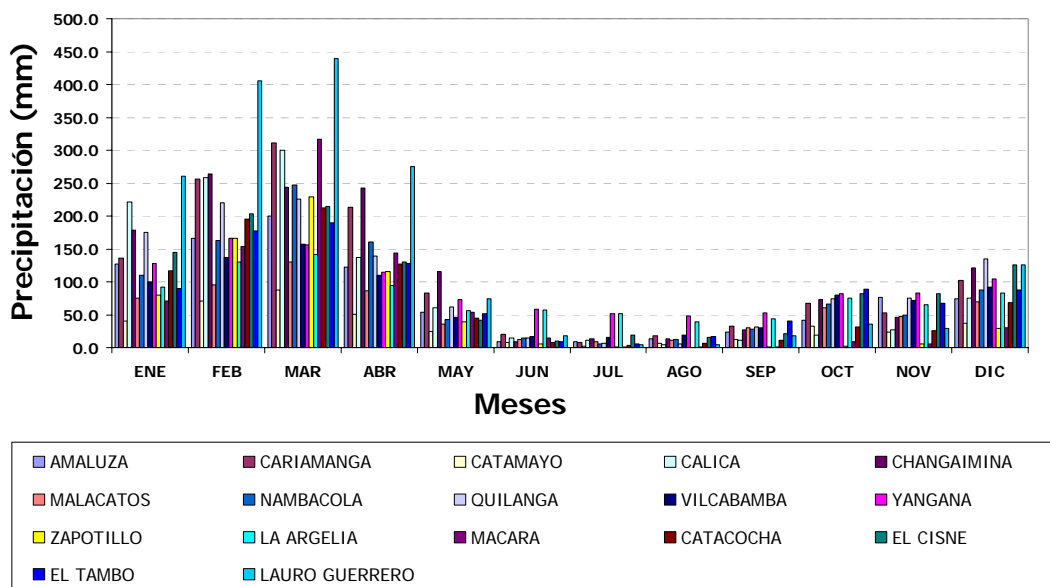
3.4.4 Soil use

Basic information was the soil use map, elaborated by the Catamayo-Chira project in 2002. This map was actualised with Landsat TM Images from 2006 and field verification was done. The biggest problem in this part of the process was the lack of values for the biophysical parameters, describing the hydrological characteristics of the different soil types in the basin, and which are needed for SWAT.

The SWAT developer-generated database does not consider crops nor soil uses as present in the study zone (such as coffee, banana, or dry forest). Therefore it was necessary to introduce these data in the SWAT database. However, for these crops no Curve Number (CN), Leaf Area Index (LAI), Cover and crop managing factor (USLE C) and other parameters were available. To cover these lack of information, these parameters were estimated, comparing existent crops in SWAT and local partial existent studies.

In the basin, 20 land cover types were determined as detailed in Table 3.1 and Figure 3.6.

(a)



(b)

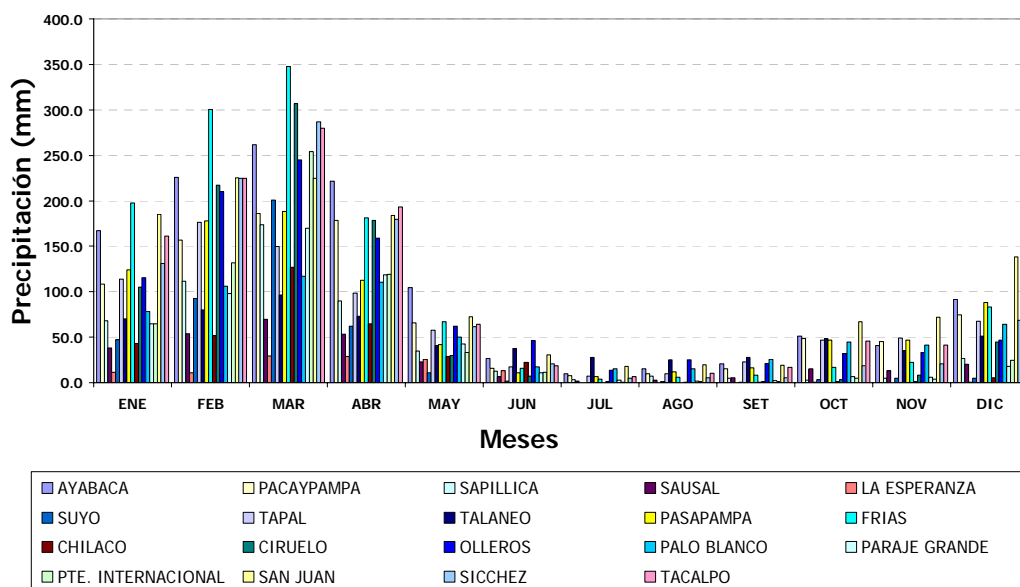
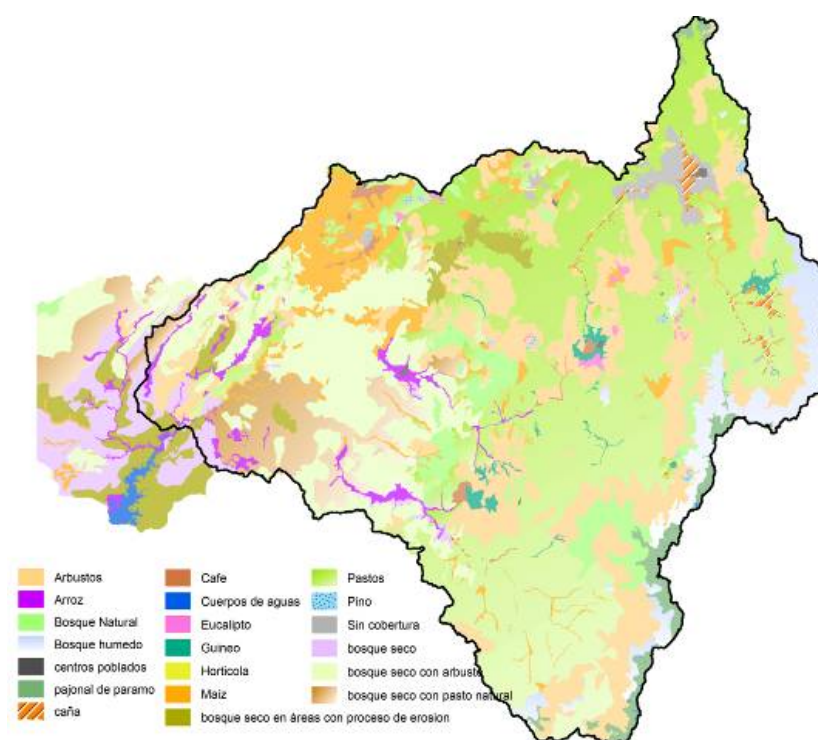


Figure 3.5 Visualisation of precipitation regime stations used for SWAT application: mean monthly precipitation in (a) Ecuador and (b) Peru

Table 3.1 Land cover and type and soil use

Nº	SWAT code	Description	%
1	rice	Rice	1.62
2	pasp	Pajonal de páramo	1.91
3	arbu	Bush	16.25
4	bohu	Humid Forest	4.01
5	bona	Natural Forest	4.12
6	bose	Dry Forest	4.65
7	bsca	Dry Forest with bush	12.83
8	bspn	Dry Forest with grazing	6.67
9	bser	Dry Forest in zones with erosion processes	4.37
10	suga	Sugar cane	0.60
11	cafe	Coffee	0.43
12	urld	Urban centres	0.09
13	watr	Water bodies	0.44
14	euca	Eucalyptus	0.31
15	bana	Banana	0.70
16	toma	One year crops	0.09
17	corn	Maize	5.13
18	paso	Grazing	34.38
19	pino	Pine	0.19
20	bare	No cover	1.21

**Figure 3.6** Land cover and actual soil use applied to SWAT

3.4.5 Soil types

As a start a soil map realised in the year 2002 by the Catamayo-Chira project was used. This map was based upon various studies carried out by different institutions in both countries (Peru and Ecuador), but this information was not detailed enough for SWAT, basically because the most important information needed were hydrophysical data of the different soil units identified on the map.

For this reason a specific soil study was planned, to incorporate data into SWAT, and concentrated in the area, determined for the study (*Annex 2.0: Validación y Complementación de los Estudios de Suelos de la Cuenca Binacional Catamayo Chira con miras a Implementar El Modelo SWAT*). General characteristics, soil unit descriptions (including morphological, physical and chemical soil aspects and taxonomic classification), and verification and correction of soil units were obtained from the field samples and the laboratory analysis profile characterisation (Figure 3.7). This permitted generation of a database that could be used for SWAT (*Anexo 3.0: Propiedades de las unidades de suelo incorporadas al Modelo SWAT*).

The K factor, defined as soil resistance to erosion by direct impact of rain drops, was calculated for this study using the EPIC model (Sharpley & Williams, 1990):

$$K = \frac{1}{7.6} \left\{ 0.2 + 0.3 \exp \left[-0.0256 SAN \left(1 - \frac{SIL}{100} \right) \right] \right\} \left(\frac{SIL}{CLA + SIL} \right)^{0.3} \left(1.0 - \frac{0.25OM}{OrgC + \exp(3.72 - 2.95OM)} \right) \left(1.0 - \frac{0.7SN}{SN + \exp(-5.51 + 22.9SN)} \right)$$

Where: K is in $(\text{ton ha h ha}^{-1} \text{ MJ}^{-1} \text{ mm}^{-1})$, SN is $1.0 - SAN/100$ and SAN , SIL , CLA , OM and $OrgC$ are percentages of sand, lime, clay, organic matter and organic carbon content, respectively.

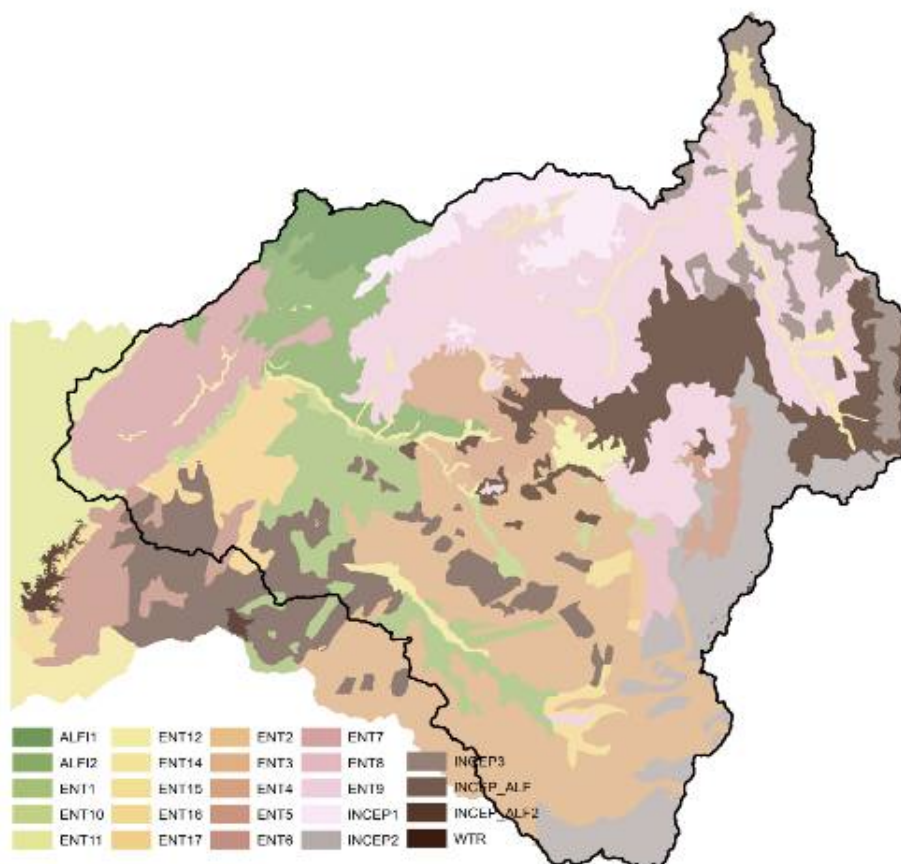


Figure 3.7 Soil types used in SWAT

3.5 Calibration

Calibration consists in adjusting model parameters based upon comparing simulated and observed or measured data in the existing stations in the basin. For calibration the parameters with the greatest incidence were manipulated.

In a first run, significant differences between the simulated and measured flows were observed. Therefore it was necessary to apply a sensitivity analysis, using the correlation coefficient R^2 (Sincich *et al.*, 1999) and efficiency EF (Nash & Sutcliffe, 1970). For this analysis, multiple runs were compared to analyse how results respond in function of variation of the principal parameters. In this way, 19 SWAT parameters were analysed, resulting in a total of 7 sensible parameters (Figure 3.8): Mean Slope Length (SSLSBSN), Alpha Baseflow Factor (ALPHA_BF), Ground Water Delay Time (GW_DELAY), Minimum Ground Water Height Needed in Superficial Aquifer (GWQMN), Ground Water Recharge Coefficient: "revap" (GW_REVAP), Curve Number (CN), and Lateral Flow Travel Time (LAT_TIME). It was decided not to manipulate parameters related to soil characteristics as these were measured and validated in the field.

It has to be taken into account that this sensitivity analysis for the Catamayo-Chira basin was realised modifying a single parameter in each run, in other words interaction between parameters was not considered. However, during the calibration process this effect could be analysed, observing variation in the simulation after manipulating different parameters at the same time and analysing comparative hydrograms between simulated and measured streamflows.

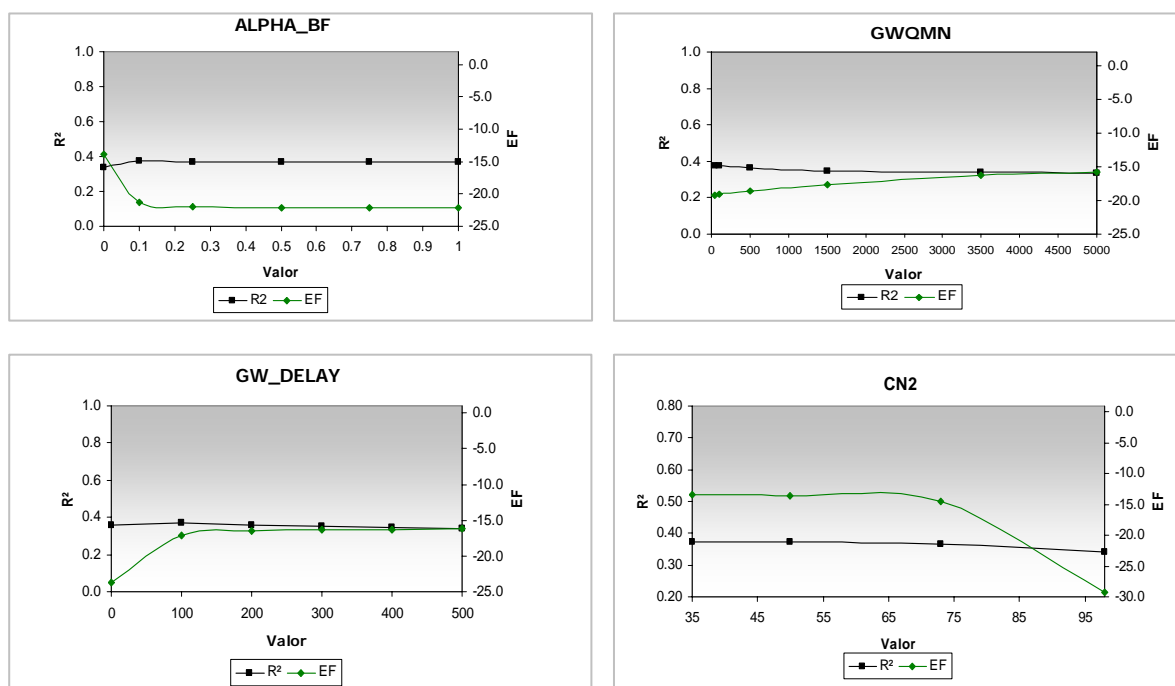


Figure 3.8 Most sensitive parameters for the basin

Manual calibration was applied to the basin, using the sensitivity analysis as a guideline. SWAT was applied for a simulation period over 16 years (including the calibration and validation period) at the five identified calibration points. The analysed period is different between calibration points, due to availability of historical data for each station. Parameter adjustment was only done in the calibration period, the validation process being carried out by simply running the model for the different time periods, using the parameters determined during calibration. It is important to mention that for calibration the value ranges (Table 3.2) of sensitive parameters have been determined without losing their physical meaning.

SWAT carries out the simulation of the hydrological cycle on a daily, monthly and annual basis for each HRU. In the present study a monthly analysis of the information was carried out, due to the conclusion of the quality analysis that there was little correspondence between daily pluviometric data and streamflows. For this reason it was not possible to calibrate SWAT with the daily information available. On the other hand, evaluation of the simulation on a monthly basis proved to show very representative statistic efficiencies.

The proposed methodology for calibration of the basin consisted in calibrating in a first step the four sub-basins (Catamayo, Alamo, Quiroz and Macará), corresponding to the higher and middle part of the basin, defined in function of the availability of data from streamflow measurement stations. In a second step the adjustments made to these four measuring points were introduced in the model for carrying out a calibration in the Ardilla measurement station, located on the inlet of the Pochos reservoir. Aside from these four sub-basins, other important contributions enter this station (Figure 3.3).

The statistical adjustment criteria used were the Correlation Coefficient R^2 and Efficiency EF (Nash & Sutcliffe, 1970). In addition the error of accumulated outlet volume for the calibration period was calculated. The data used for the calibration in each station were drawn from different periods, due to availability of historical data (Figures 3.9-3.13). Calibration results are shown in Table 3.3.

Table 3.2 Most sensitive parameters used in calibration for the Catamayo-Chira basin

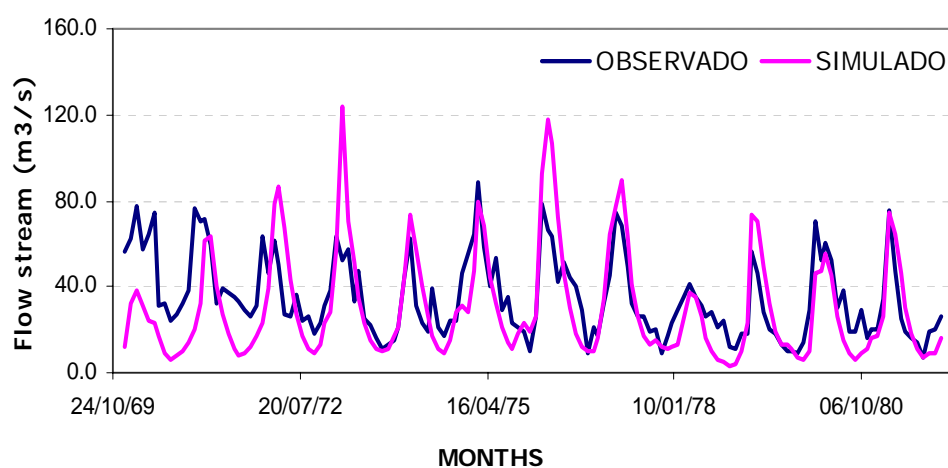
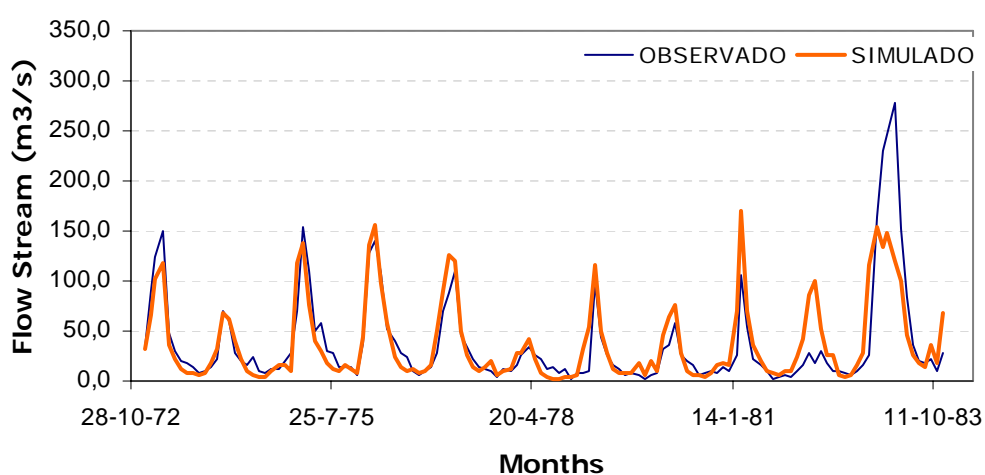
Calibrated parameters in SWAT	Unity	Default value	Range calibrated values	Sensitivity grade	Influence on streamflows
<u>Streamflow calibration</u>					
Mean slope length (SLSUBBSN)	m	0.05	25 - 35	High	Superficial flow Baseflow
Alpha Baseflow Factor (ALPHA_BF)	days	0.048	0.1 – 0.2	High	Baseflow
Groundwater Delay (GW_DELAY)	days	31	100 - 200	Medium	Baseflow Superficial flow
Lateral Flow Time (LAT_TIME)	days	0	7 – 8	High	Superficial flow Baseflow
Groundwater required minimum Height in superficial aquifer (GWQMN)	mm H2O	0	0 - 100	Medium	Baseflow
Groundwater recharge “revap” coefficient (GW_REVAP)	-----	0.02	0.02 – 0.2	Medium	Baseflow
Curve Number (CN2)	-----	*	**	High	Superficial flow Baseflow
<u>Sediment calibration</u>					
Sediment retention exponent (SPEXP)	-----	1.0	0.0004	High	Sediment production

* Values corresponding to the different existing soil cover types.

** The optimal value for CN2 varies in function of the hydrological soil group within a certain soil use type.

Table 3.3 Statistical parameters and variation of outlet volume for model calibration

	Calibration period	R ²	EF	ΔV (%)
Santa Rosa Station	1970 – 1981	0.47	0.02	13.10
Puente Internacional Station	1973 – 1983	0.70	0.70	0.96
Alamor en Saucillo Station	1970 – 1983	0.68	0.68	6.83
Paraje Grande Station	1974 – 1983	0.77	0.76	3.30
Ardilla Station	1976 – 1986	0.77	0.76	2.10

**Figure 3.9** Simulated and observed streamflows during calibration period (1970-1981): station Santa Rosa (sub-basin Catamayo)**Figure 3.10** Simulated and observed streamflows during calibration period (1973-1983): station Puente Internacional (sub-basin Macará)

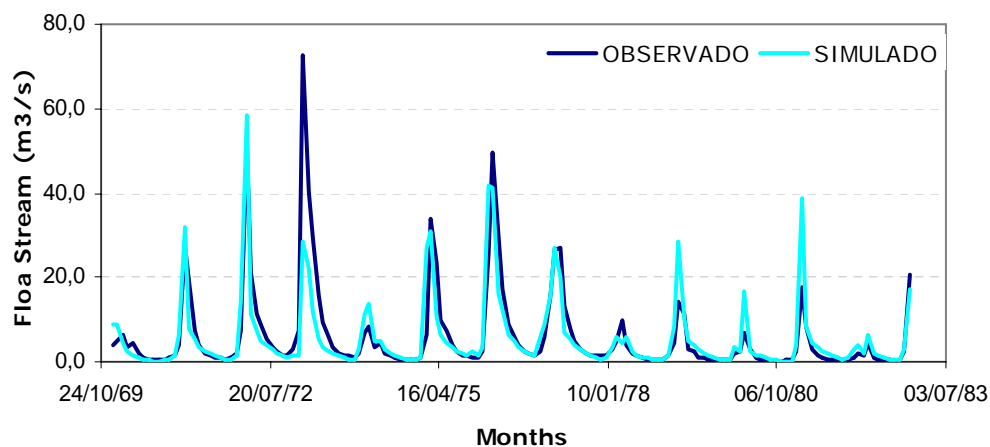


Figure 3.11 Simulated and observed streamflows during calibration period (1970-1983): station Alamor en Saucillo (sub-basin Alamor)

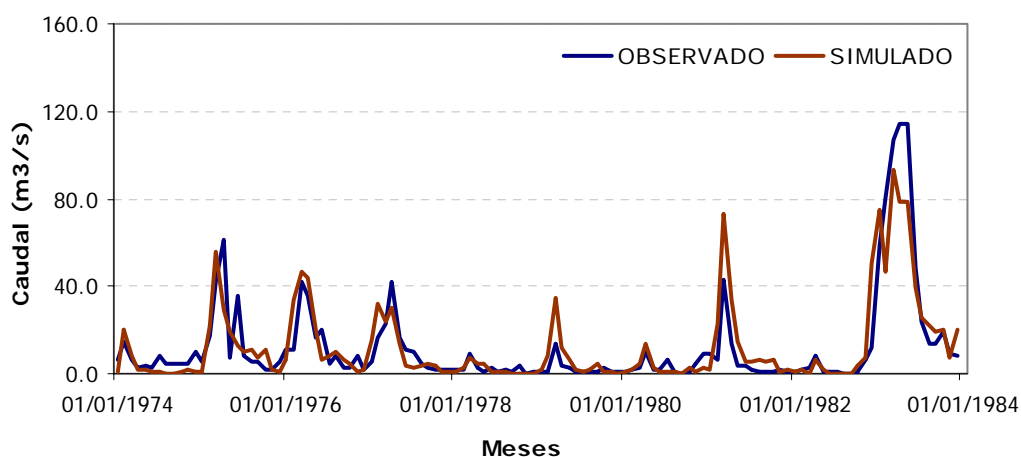


Figure 3.12 Simulated and observed streamflows during calibration period (1974-1983): station Paraje Grande (sub-basin Quiróz)

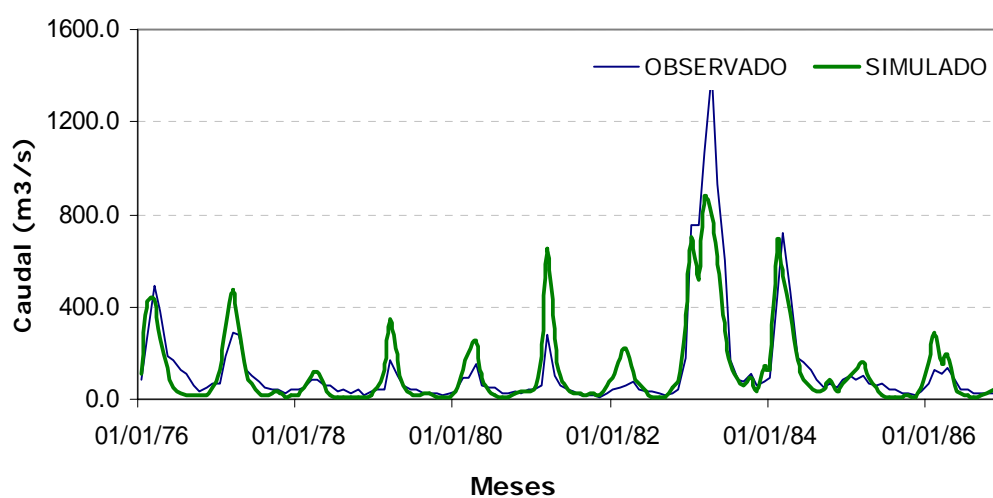


Figure 3.13 Simulated and observed streamflows during calibration period (1976-1986): station Ardilla (inlet at Poechos)

In Table 3.3 the evaluation of the performance of the model at the five calibration points is shown in summary. Generally speaking, the model simulates adequately the outlet flows, as also can be seen in Figures 3.9 to 3.13. However, the best calibration results are obtained in the Ardilla station, at the Poechos reservoir inlet (Figures 3.13 and 3.14).

Sediment production was analysed at two calibration points (Figure 3.15). Data were available from the stations Puente Internacional and Ardilla (both at the Peruvian side of the border). A problem was the limited availability of sediment data. Information available on the Peruvian side corresponds to short periods of time (a few years) or years with incomplete information, not allowing validation of the model. In Table 3.4 model performance at the two calibration points is shown.

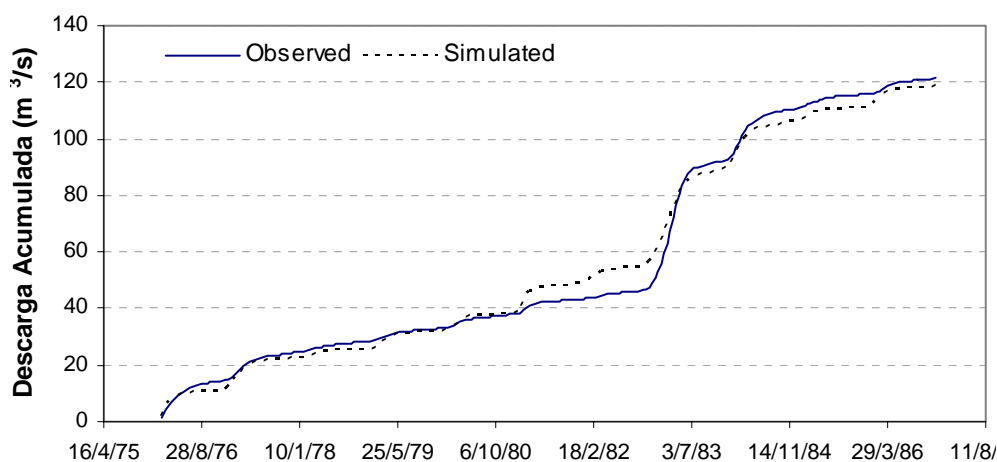


Figure 3.14 Accumulated flows at Ardilla station (inlet at Poechos) (1976-1986)



Figure 3.15 Location of the two sediment measurement stations used in SWAT calibration

Table 3.4 Statistical parameters

Station	Calibration period	R ²	EF
Station Puente Internacional	1973 – 1982	0.67	0.65
Station Ardilla	1984 – 1988	0.62	0.21

Figures 3.16 and 3.17 show the comparison between simulated and measured sediment production on a monthly basis. It can be observed that at the station Puente Internacional the model was able to simulate sediment production with a reasonable precision. Statistical correlation is acceptable (Table 3.4). In the case of Ardilla, the same efficiency was not reached; on the contrary a very little representative EF value was obtained. In this case, the model simulates parts of the observed sediment load well, but huge overestimations, basically in humid periods, are also present.

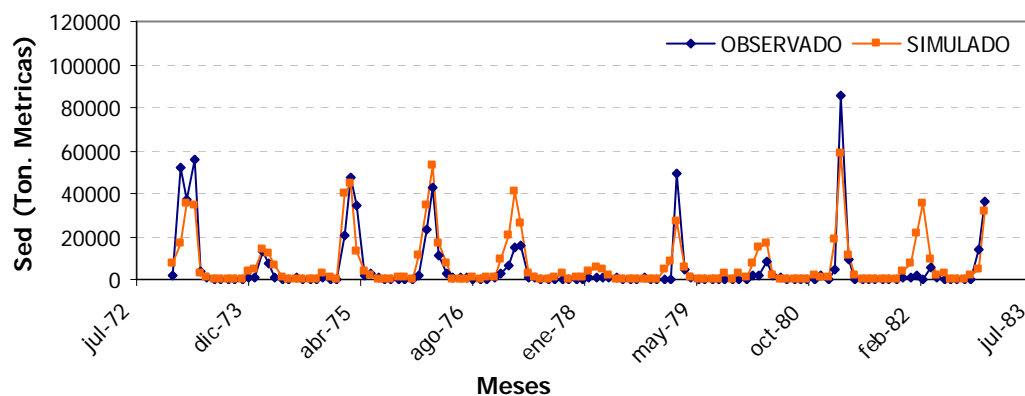


Figure 3.16 Simulated and observed sediments during the calibration period: station Puente Internacional (sub-basin Macará)

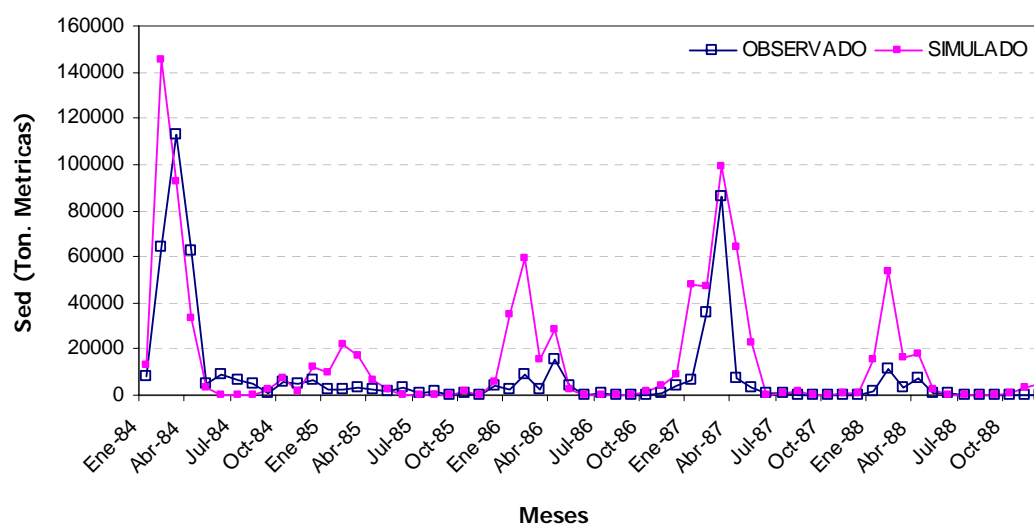


Figure 3.17 Simulated and observed sediments during the calibration period: station Ardilla (inlet at Poechos)

Table 3.5 Statistical parameters and variation in outlet volume for model validation

Station	Validation period	R ²	EF	ΔV (%)
Station Santa Rosa	1982 – 1994	0.47	-3.10	27.16
Station Puente Internacional	1984 – 1994	0.75	0.75	6.67
Station Alamor en Saucillo	1984 – 1994	0.53	0.42	9.83
Station Paraje Grande	1984 – 1992	0.63	0.52	42.0
Station Ardilla	1987 – 1994	0.76	0.74	7.18

3.6 Validation

The validation of the model consists of measuring the predictive capacity of the model making a comparison between calculated and observed streamflows, using the calibration phase determined parameters, but for a different time period. Table 3.5 shows the statistical evaluation carried out for the basin and the model validation. The streamflow estimation was carried out in the five measurement stations, used for calibration (Figures 3.18 to 3.22).

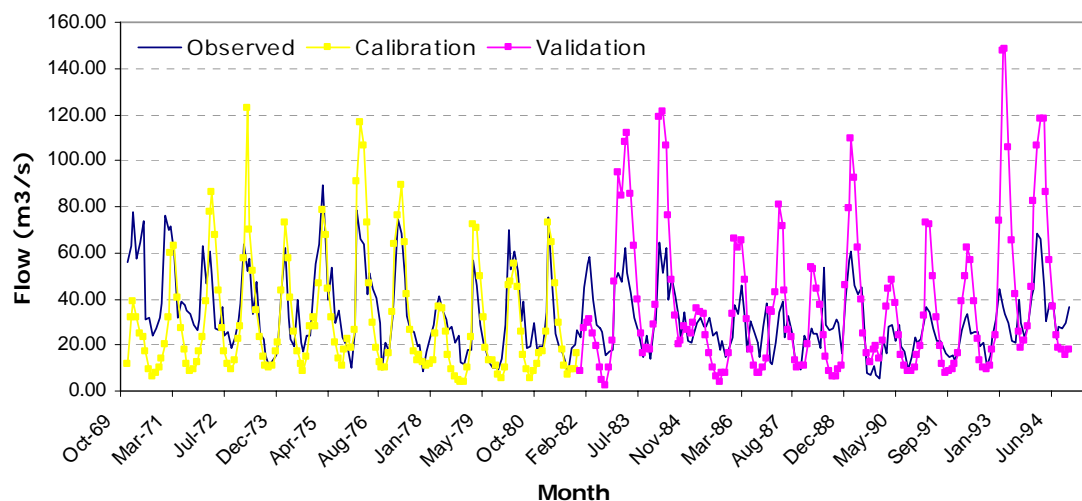


Figure 3.18 Simulated and observed streamflows during calibration and validation period (1970-1994): station Santa Rose (sub-basin Catamayo)

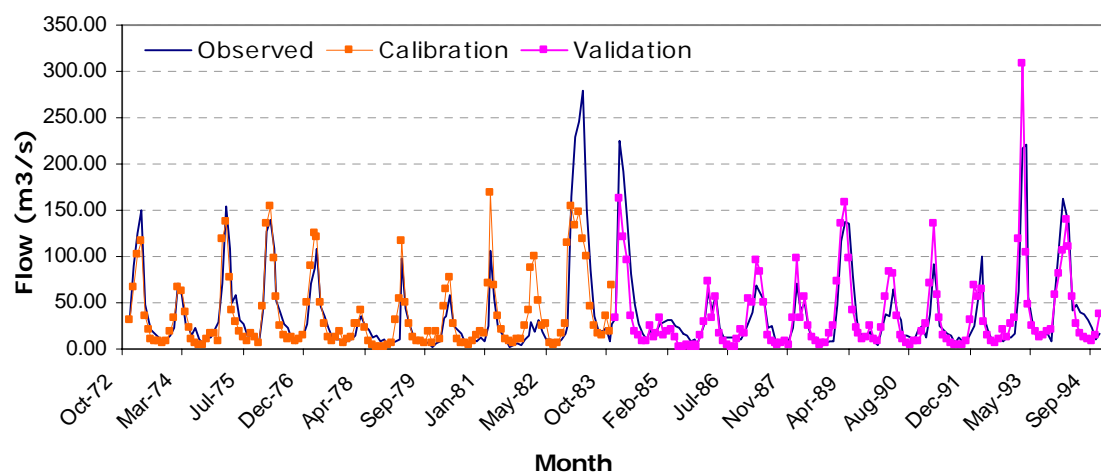


Figure 3.19 Simulated and observed streamflows during calibration and validation period (1973-1994): station Puente Internacional (sub-basin Macará)

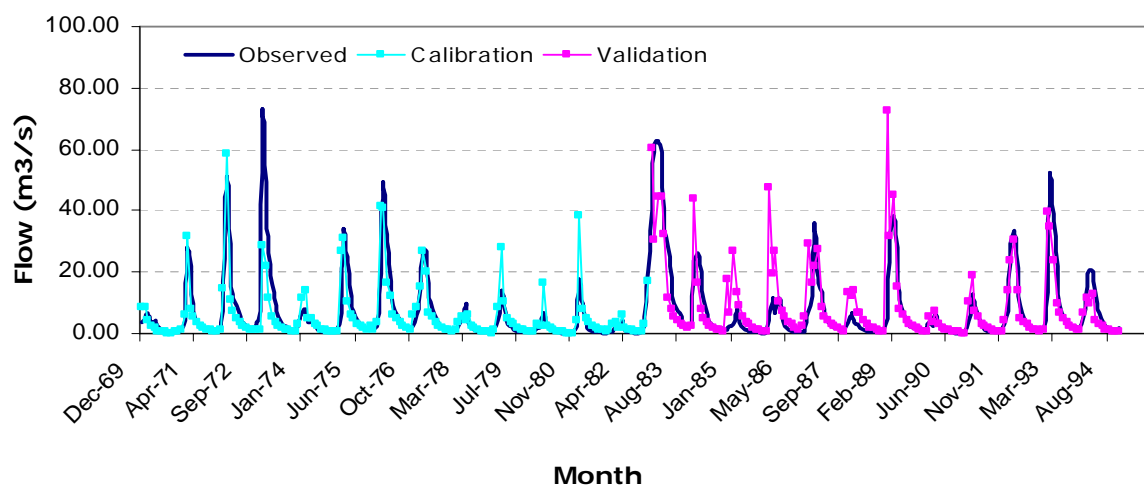


Figure 3.20 Simulated and observed streamflows during calibration and validation period (1970-1994): station Alamor en Saucillo (sub-basin Alamor)

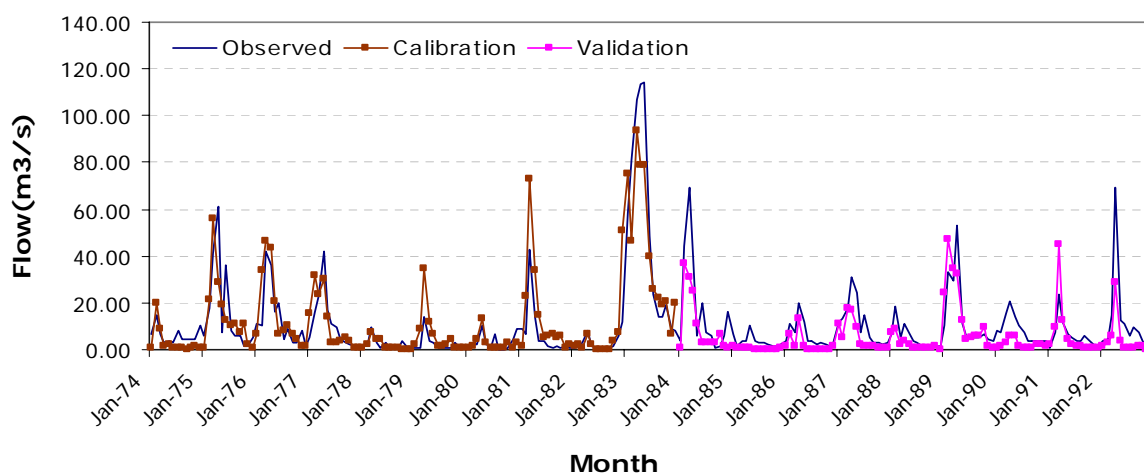


Figure 3.21 Simulated and observed streamflows during calibration and validation period (1974-1992): station Paraje Grande (sub-basin Quiróz)

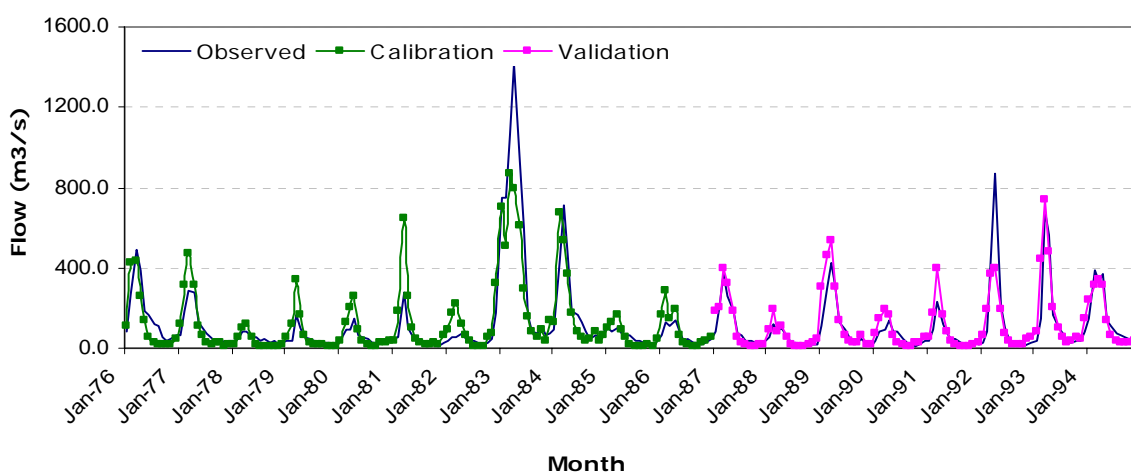


Figure 3.22 Simulated and observed streamflows during calibration and validation period (1974-1994): station Ardilla (inlet at Poechos)

3.7 Results

SWAT is a rather powerful model and produces a lot of output information. These output data depend on the type of simulation applied - daily, monthly or annual - for each HRU, and for each sub-basin. Reports generated by the model were imported into Excel to allow a better analysis of the results. In this study a monthly analysis of the information was made for each of the 111 defined microbasins. The model calculated for each one the net amount of water contributed by the microbasin to the flows, expressed in mm water, and the sediment production in ton/ha, beside some other hydrological variables characterising the water cycle.

Data are organised according to the hydrological year (September-August) to better represent hydrological behaviour in the basin and to allow comparing results with results from the WaTEM/SEDEM application, run in the same study area.

Years are classified based upon water contributions in very dry years, dry years, wet years, normal years and ENSO years (Table 3.6). This was done to differentiate and analyse hydrological behaviour of the basin in different periods and climatologic conditions.

Concerning sediment production in dry and normal years, erosion rates of 37.26 ton/ha/yr were calculated. In wet years, erosion rates were about 60.99 ton/ha/yr. The maximum erosion rate for the analysed periods was 185.68 ton/ha/yr during the period September 1982 - August 1983 (ENSO year), which represents a rather high erosion rate.

In the same manner the annual contribution in ton was estimated at five different river sections for the years 1976 to 1988. Results can be seen in Table 3.7. It can be observed that an ENSO year (1983) delivers the highest sediment rates, due to greater runoff and the consequently greater erosion, basically in the middle part of the basin. This year contributions are up to 20,043,617.60 which is 3 to 10 times more than a wet and a dry year, respectively. Likewise, 1983 registers the highest sediment contributions compared to other years for all analysed points.

From these results, the 15 microbasins that most contribute to sedimentation generation were determined (Table 3.8 and Figure 3.23). The discrimination criterion was 3 ton/ha/yr, considering that less is a low erosion rate. For this a historical series was analysed by SWAT (1976 – 1988) representing different hydrological conditions.

Table 3.6 Classification of years by water contribution

Period		Classification of years		
Sep	1976	Aug	1977	Normal year
Sep	1977	Aug	1978	Dry year
Sep	1978	Aug	1979	Dry year
Sep	1979	Aug	1980	Dry year
Sep	1980	Aug	1981	Dry year
Sep	1981	Aug	1982	Very dry year
Sep	1982	Aug	1983	ENSO year (FEN)
Sep	1983	Aug	1984	Wet year
Sep	1984	Aug	1985	Dry year
Sep	1985	Aug	1986	Dry year
Sep	1986	Aug	1987	Normal year
Sep	1987	Aug	1988	Very dry year
Sep	1988	Aug	1989	Normal year
Sep	1989	Aug	1990	Dry year
Sep	1990	Aug	1991	Dry year
Sep	1991	Aug	1992	Normal year
Sep	1992	Aug	1993	Normal year
Sep	1993	Aug	1994	Normal year

Table 3.7 Sediment contribution in five measurement stations in yearly mass contribution

Year	Metric tons (yearly uass)				
	Station Santa Rosa	Station Puente Internacional	Station Alamor en Saucillo	Station Paraje Grande	Station Ardilla (inlet at Poechos)
1976	2,149,647.03	2,741,987.41	768,185.24	416,598.49	7,844,674.68
1977	1,165,959.31	1,678,083.94	463,187.32	278,773.72	6,119,269.33
1978	78,092.83	540,949.98	69,276.50	32,435.78	877,663.05
1979	584,147.21	1,277,856.25	326,718.24	50,317.49	2,517,391.82
1980	460,190.51	698,063.39	122,633.48	45,450.90	2,888,220.97
1981	775,588.99	2,068,855.34	351,933.22	240,215.55	5,760,970.41
1982	330,556.61	2,246,234.19	206,817.38	119,463.46	4,575,773.78
1983	2,302,537.99	3,490,550.99	1,705,591.16	541,839.86	20,043,617.60
1984	1,885,625.43	2,748,078.24	570,061.77	145,985.81	8,875,487.54
1985	192,733.68	598,780.16	281,689.94	3,056.62	1,774,978.10
1986	685,798.23	895,794.29	797,790.16	23,600.12	3,483,040.74
1987	610,755.65	1,290,597.50	683,154.76	124,955.34	6,896,996.46
1988	650,559.71	1,039,416.19	231,555.80	21,200.37	2,260,666.96

Table 3.8 Most contributing microbasins in different hydrological conditions/years

Sub-basin	Micro basin	Area (Ha)	Normal	ENSO			Multiannual Mean
			year 76-77	Dry year 80-81	year 82-83	Wet year 83-84	
Ton/ha/year (SYLD)							
Alamor	15	13076.00	14.325	10.185	50.943	12.579	22.376
Alamor	16	14610.00	13.693	8.844	42.493	11.201	20.19
Catamayo	28	8438.00	21.378	8.833	9.116	5.215	10.386
Catamayo	33	19500.00	37.152	19.665	185.686	13.636	34.24
Macará	45	17980.00	3.119	14.295	0.829	7.418	6.393
Macará	48	13560.00	2.550	1.751	1.984	6.111	4.303
Macará	59	19333.00	2.066	2.748	2.031	5.607	4.72
Macará	60	13607.00	13.934	6.829	9.848	4.679	8.337
Macará	66	2760.00	2.123	1.180	7.552	1.104	2.936
Macará	72	3060.00	9.239	4.729	6.073	2.792	5.658
Macará	77	8133.00	7.517	3.694	5.131	2.390	5.479
Alamor	105	14035.00	6.223	4.940	26.157	5.984	14.149
Alamor	106	3522.00	13.933	10.693	55.802	12.978	22.909
Alamor	107	11586.00	11.141	4.751	51.184	2.368	5.567
Alamor	109	7091.00	5.624	2.942	2.289	1.957	4.937
Total		170,291.00					

Areas with a greater erosion grade at sub-basin level were located in Alamor, Catamayo and Macara, representing an area of 170,291.00 ha. These corresponded to microbasins 33, 15 and 106 and were the ones representing the biggest soil losses, with a mean of 36.5 ton/ha/yr.

Superposing the 170,291.00 ha supposedly affected by erosion with the soil cover and actual use map, it can be seen that these zones are located in Alamor in the maize and coffee areas, on hill sides with moderate slopes. The identified zones in the Catamayo and Macara sub-basins are those corresponding to depredated forest with trees and scarce pastures.

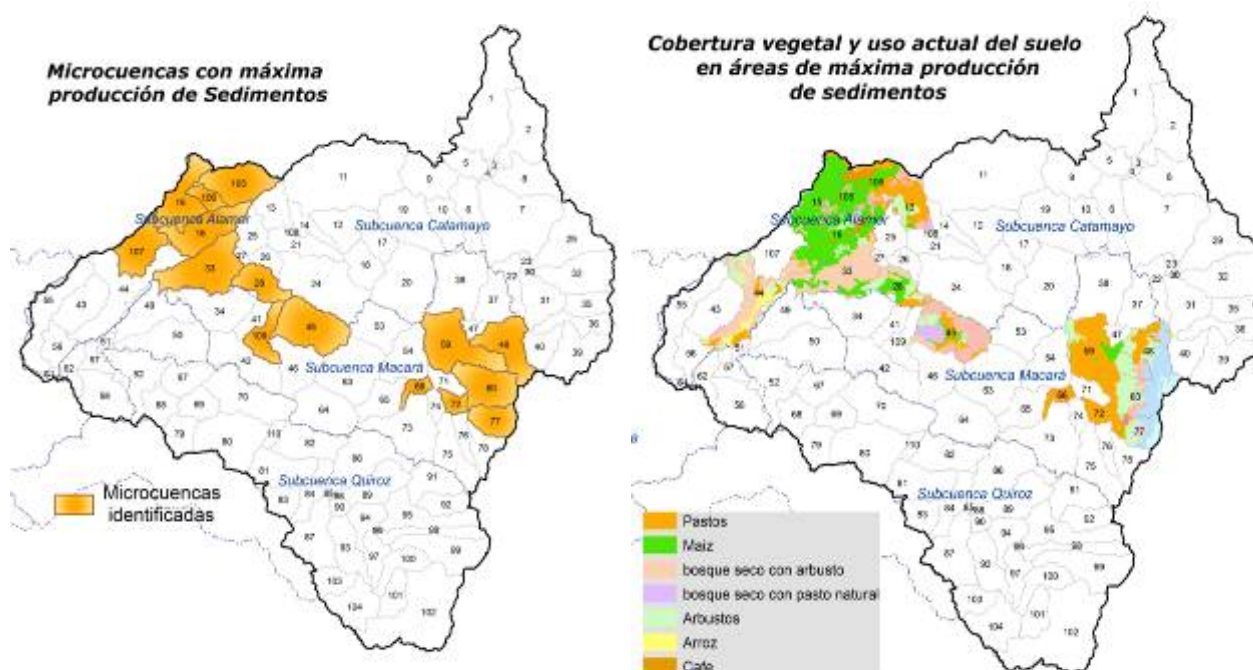


Figure 3.23 Most sediment producing microbasins

Hence, as can be observed (Figure 3.24) in dry year conditions (September 1980 – August 1981), as well as in normal year conditions (September 1986 – August 1987), there is no remarkable difference related to most contributing microbasins. Even so for wet and dry years, sub-basins Alamo, Macara and Catamayo always represent the biggest contributions. Analysis of the contributions' erosion rates from the different microbasins reveals a real difference, especially between a normal or dry year and a wet one. Production per ha is almost duplicated, and in an ENSO year it reaches extremes such as 186 ton/ha, or five times the normal year production. Another relevant aspect is that despite the differences between years there are microbasins that are always affected.

In the maps (Figure 3.25) water production for each microbasin can be seen, for different hydrological years. In this case the difference in spatial distribution between an ENSO year and other years is notorious. A big production in lower and middle part areas can be seen as a direct consequence of the climate alterations caused by ENSO, resulting in heavy rains in the normal dry coastal area. On the other hand, under normal conditions in dry years and wet years, the spatial distribution of water production in the middle and higher parts of the sub-basins Catamayo, Macara and Quiroz is more similar, contributing up to 1443,912 mm water during the period September 1983 to August 1984.

Based upon these results, 20 microbasins were determined as contributing the most to the basin. For this, a historical series of 21 years (1976 – 1994) which represents different hydrologic conditions was simulated in SWAT. Table 3.9 shows the water production for each sub-basin, ordered by water contribution. Production in four different hydrologic periods is compared. The table shows the amount of water expressed in mm water (WYLD is the sum of runoff, lateral flow and subterranean water contribution, less transmission losses) which results in the net water contribution of the microbasin to the flows.

As can be seen in Figure 3.26, the 20 micro basins identified as hydrologically important are located in the sub-basins Catamayo, Macara and Quiroz, the most important ones being the microbasins 25, 26 and 27 in the sub-basin Catamayo.

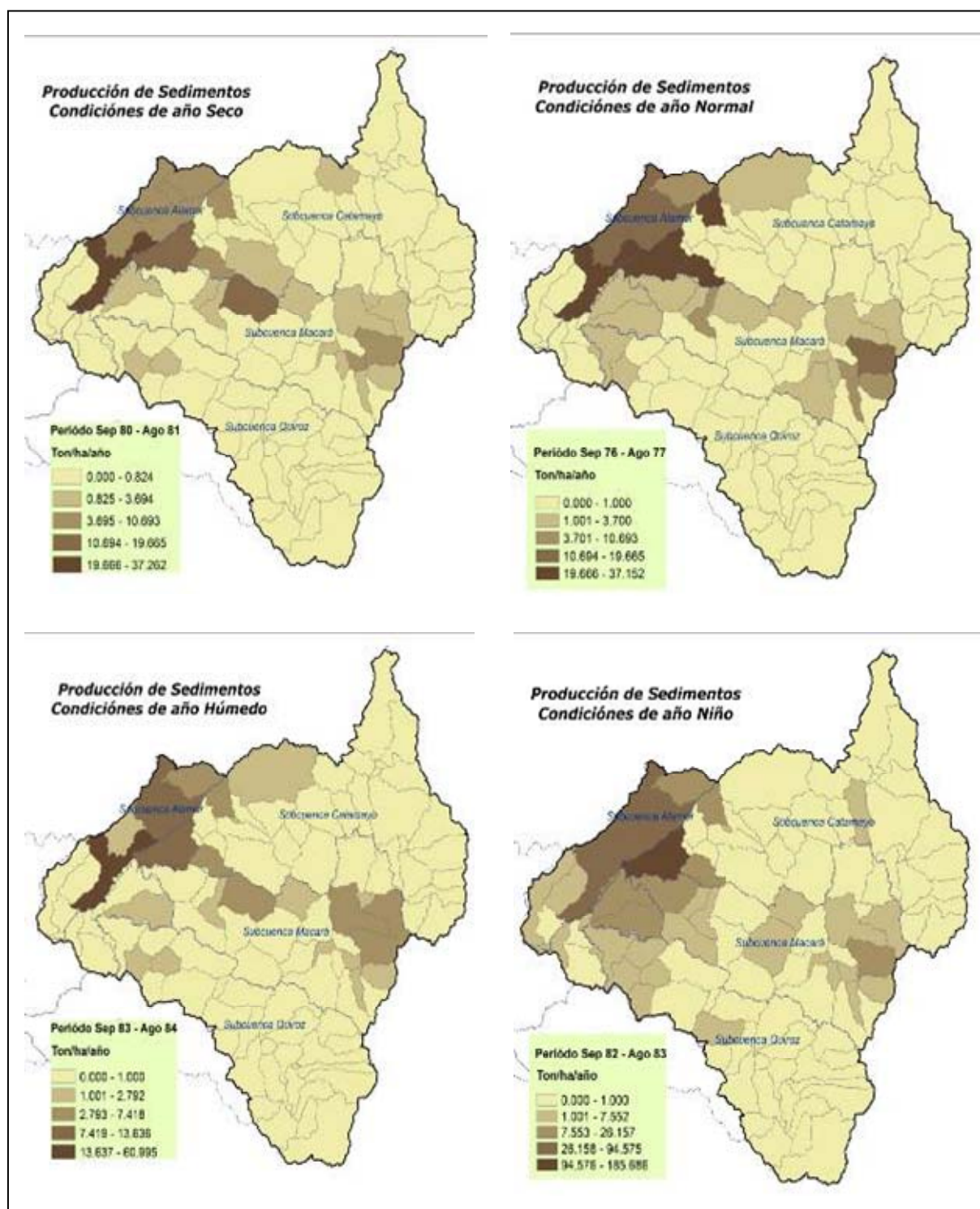


Figure 3.24 Sediment production in the basin for different hydrological years

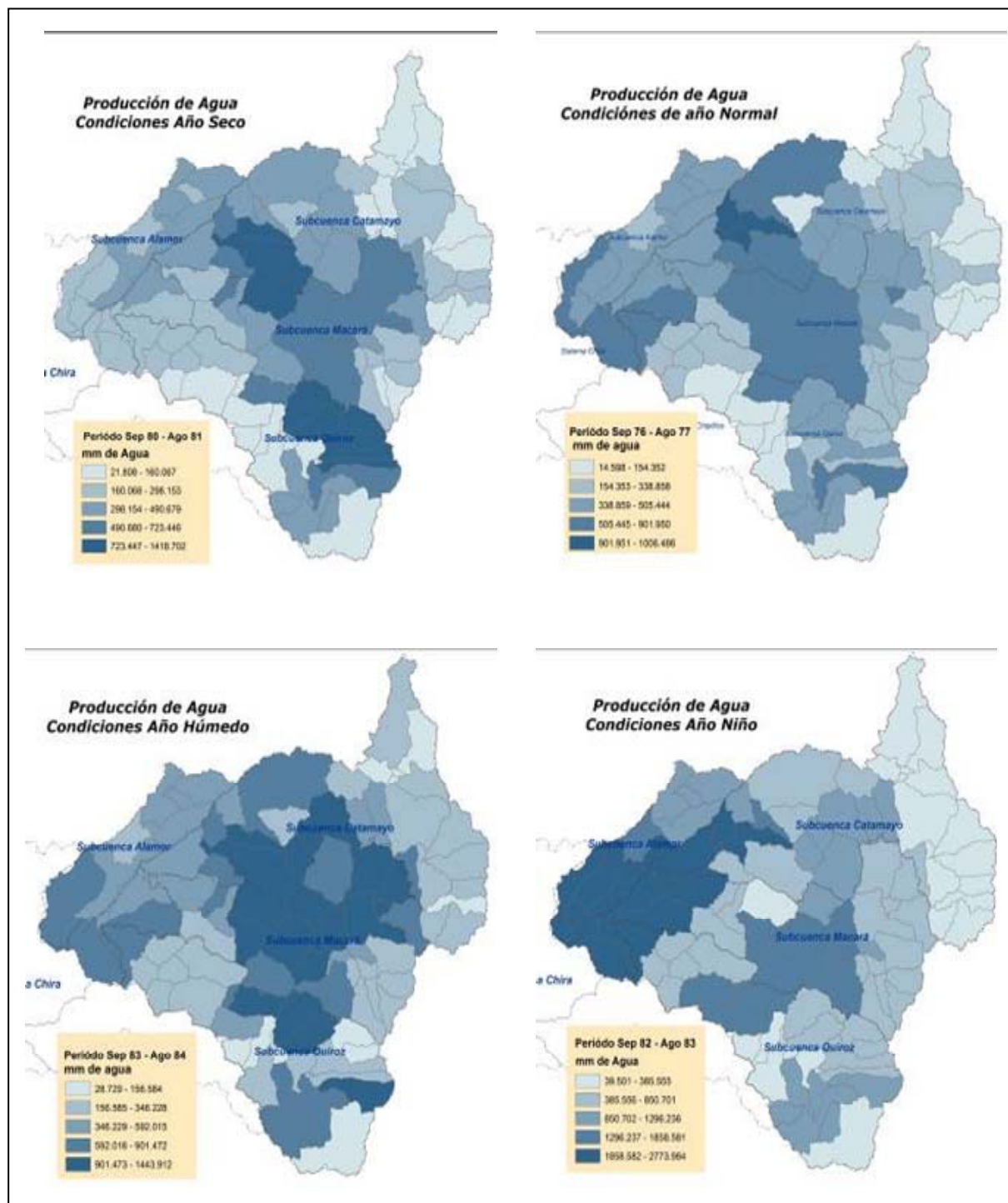


Figure 3.25 Water production in the basin for different hydrological years

Table 3.9 Water production in microbasins

Sub-basin	Micro basin	Area (Ha)	Normal year	Dry year	ENSO year	Wet year	Multiannual Mean *
			76-77	80-81	82-83	83-84	
mm (WYLD)							
Catamayo	14	5,086.00	659.155	466.627	1462.599	670.259	626.778
Catamayo	21	8,411.00	1006.063	756.654	2340.973	935.901	970.521
Catamayo	24	25,762.00	719.495	1418.702	494.301	1443.912	671.327
Catamayo	25	6,825.00	953.305	723.446	2294.628	893.005	932.662
Catamayo	26	3,946.00	1003.938	756.210	2340.019	934.903	969.496
Catamayo	27	1,092.00	1006.486	757.566	2340.609	936.667	970.866
Catamayo	28	8,438.00	758.561	682.995	825.002	731.663	538.831
Macará	37	9,625.00	381.180	540.876	587.157	1078.313	543.255
Macará	38	19,181.00	484.437	648.858	692.314	1224.872	647.333
Macará	41	4,608.00	737.403	664.223	817.415	722.372	527.784
Catamayo	45	17980.00	576.030	1138.793	385.555	1138.692	616.620
Macará	53	11,855.00	630.139	574.965	1296.236	992.240	596.586
Macará	54	12,903.00	660.950	612.306	1381.019	1044.297	631.623
Macará	59	19,333.00	459.728	619.954	656.946	1197.761	620.523
Macará	65	8,927.00	606.684	578.494	1708.006	1244.596	693.570
Macará	73	18,598.00	577.067	634.776	1389.526	625.859	547.654
Quiróz	86	17,402.00	468.689	837.736	805.326	1041.587	764.027
Quiróz	89	11,816.00	466.536	841.878	811.667	1049.220	769.175
Macará	99	2,300.00	727.013	519.876	1145.460	912.708	442.030
Catamayo	108	495.00	630.877	442.807	1398.000	645.402	596.919

* Multiannual mean of the 21 simulated years

**Figure 3.26** Most water producing microbasins

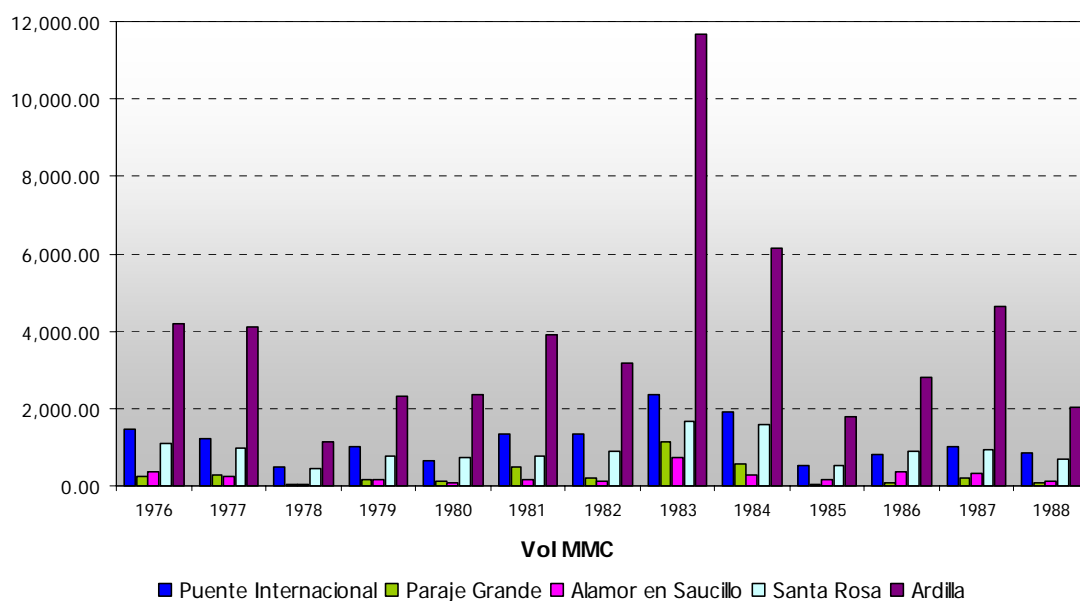


Figure 3.27 Water production expressed in MCM

In Figure 3.27 the amount of water expressed in million cubic metres (MCM) for each modelling year can be appreciated, with the year 1983 the most contributing one. This was an ENSO year, summing up to 12,000.00 MCM. For a year in normal conditions, the mean contribution is 4,000 MCM, measured in Ardilla at the Poechos inlet. Nevertheless, the most important contributions are from the Macara sub-basin (Puente Internacional station) with contributions up to 2,400.00 MCM per year and the Catamayo sub-basin (Santa Rosa station) with contributions up to 1,500.00 MCM per year. These two sub-basins represent a 70% contribution.

3.8 Scenario modelling

SWAT quantifies the impact of land uses management on water production and soil erosion. In the framework of TWINLATIN, two types of changes are being modelled. First, those related to land use change, measuring the impact that different scenarios of land use would have on the sediment and water production. Second, those related to climate change. Different scenarios of greenhouse-induced climate change will be evaluated, calculating the impacts of every one of them on the sediment and water production.

The land use changes in this study are absolute changes between defined land use classes and do not imply land use modifications, like intensification of agriculture or forest degradation. The modelled climate changes are absolute changes in temperature and relative changes in precipitation, including data that can be generated from this change like the changes in intensity of rainfall. The effects that those changes have on the study area are assessed by the analysis of production of sediments as well as the production of water.

3.8.1 Land use change

The most impacting land use changes in the last century in the Catamayo-Chira basin has been the deforestation to open up new agricultural, especially pastoral, areas. Often this process ended up with degraded and eroded soils, especially in areas with steep slopes. The documentation of this phenomenon is difficult as the maps available are not very detailed and use different legends. Nevertheless for the Ecuadorian part of the basin, Feijó & Chalan (2008) describe a forest area to pasture conversion of 20,000 ha between 1992 and 2002, while for the sub-basin Quiroz on the

Peruvian side a conversion of forest and brush area to cultivated land of 6,592 ha is reported by Gruber (2008) for the period 1994 – 2007.

The land use change scenarios applied in this study, therefore, also focus on these aspects, particularly production activities that carry forward this trend, as well as protection and conservation activities that display possibilities to go against this trend. The scenarios are developed both by expert judgment of actual tendencies and by an ecologic/economic landscape value study (*'Zonificación Ecológica – Económica de la Cuenca Catamayo-Chira'*). The detail of each of these scenarios are described in the WP8 report.

3.8.2 Climate change

The scenarios of climatic change are elaborated with the model MAGGIC / SCENGEN that consists of the one-dimensional climate Model MAGICC (Model for the Assessment of Greenhouse Induced Climatic Change) and that estimates the mean global change in temperature up to a specified date. This happens on basis of different scenarios of green house gas emission.

The years 2025, 2050 and 2080 have been chosen as timeframe for climate change simulations, even if the following analysis of change effects only concentrates on the year 2050. The model SWAT needs some years of fore-running to adjust to the local hydrologic conditions, embodied by the provided soil, vegetation and climate data, so it was considered to elaborate climate change data for a period at least 5 years before the reference year 2050. In this context the model is used to simulate the hydrologic effects of the climate change from 2045 – 2055 with the central year 2050. The detail of each of these scenarios are described in the WP8 report.

3.9 Evaluation of hydrological modelling (D3.2)

3.9.1 Precision and level of detail

The results of the statistical analysis carried out by sub-basin are different from one another, but it can be concluded that calibration and validation on a monthly basis show generally acceptable results for the basin. In the same way the graphics show that simulated streamflows maintain the measured streamflow tendencies.

However, in the case of the basin, SWAT tends to overestimate the streamflows compared to measured values. This is more accentuated in the sub-basins Catamayo and Alamor (Figures 3.18 and 3.20, respectively), and is most likely caused by the rainfall interpolation method i.e. in the whole basin 41 pluviometric stations were used, but in the different sub-basins the spatial distribution of the (same) pluviometric stations was probably not representative enough.

It is necessary to mention that streamflow and sediment data corresponding to the station Ardilla have been carried out as direct measurements until 1975. From 1976 when the Poechos reservoir went into operation, data were obtained by calculating hydrological water balances, which probably deforms streamflow and sediment results simulated by the model for wet and very wet years (ENSO), due to high precipitations in the middle and lower part of the basin during these periods. In the same way and taking into account the distance between the reservoir outlet and the inlet at the station Ardilla (25 km), different dry streams from both river sides contribute in these periods with considerable flows which are not quantified.

All simulations were done on a monthly scale, as during the information quality control it was established that no correspondence existed between daily data, which made it impossible to calibrate SWAT with the available daily data. On the other hand, evaluation of monthly simulation showed representative statistic efficiencies. In the same way, climatic data such as minimum and maximum temperatures, solar radiation, relative humidity and wind speed were obtained from reducing monthly to daily data.

3.9.2 Most important limitations

The most time-consuming aspect was the gathering and digitisation of climatic and hydrologic information for the basin, as more than an 80% of the information used was physical hard-copy information. Efforts were concentrated on processing daily precipitation and pluviograms, considering these the most important input information for this kind of model. However, more climatic data exist that could not be digitised, due to limitations in time and resources.

It was noticed that the Ecuadorian side of the basin presents a limited hydrometeorological station network where no sediment measurements are made, as well as a limited technical application for streamflow measurements, carrying out a direct measurement every trimester and daily limnometric readings (water level) on any moment of the day. This results in a high degree of uncertainty in the information and has a direct consequence on the quantity and quality of the results of the model.

In the Peruvian part, detailed hydrometeorological and sedimentation information exist from 1972 to 1990. From this date on some stations went out of order, which reduces information availability for some areas in the basin.

Another problem was the lack of information related to biophysical parameters, describing the hydrological characteristics of the different soil use types in the basin and that have to be incorporated in SWAT. The SWAT developers'-generated database does not consider crops and soil uses on a lot of soil covers in the basin (e.g. coffee, banana, dry forest, amongst others). Therefore it was necessary to introduce these new uses in the SWAT database, although information for CN, LAI, USLE C and some other specific parameters was not available. Instead, they were associated with other existing crops in the SWAT database and drawn from a few existing studies developed in the basin.

The existing soil information showed a lot of inconsistencies such as a lack of correspondence between similar zones on both sides of the border (it may be unlikely that a soil type changes with political border) which generated a lot of uncertainty about the information included in the maps. This conclusion, together with the absence of hydrophysical data on each soil type, motivated the production of a soil study to homogenise available information at Great Group level and focus results on hydrological model implementation.

3.9.3 Next steps and further applications

Although the model has been prepared to be applied in the basin, a lot of topics still can be worked out in order to analyse the impact of soil use changes and climate changes on water and sediment production. Some of these topics have been started and will be explained in the WP8 report.

3.10 Summary and recommendations

SWAT was applied in the Catamayo-Chira basin on a monthly time scale, and acceptable results were produced to simulate streamflows in the basin. Nevertheless it is possible to improve results, introducing more data into the model. As mentioned before, one of the limitations was the paper format of the climatic data, and the consequently large digitalisation process. There is still a lot of paper information available that could be introduced into the model.

The methodology used was the most appropriate because of the large extension, and because it was decided to use five hydrometric stations to calibrate the model in the whole basin. This resulted in a larger process, but it allowed better results, as these were obtained by sub-basin which reduced uncertainties; furthermore, analysis by sub-basin was less complicated than a single calibration point would have been.

Preliminary tests and a sensitivity analysis allowed identification of the most influencing parameters in the basin, which was useful to avoid using a huge number of parameters, reducing in this way to the analysis of the most sensitive parameters that were adjusted during the calibration process. Seven sensitive parameters were identified.

A manual calibration was carried out. This is a rather complex process, because it supposes experience and a vast knowledge of the territory. In this case, the project benefitted from team members from the Binational Technical Group with a lot of their experience on erosion and hydrology.

The rain interpolation method used is not recommended for the basin due to its orographic characteristic; it considers the closest station to the centroid of each sub-basin and assumes data of this station to distribute the rainfall, which can affect the quality of the results if these data are not representative for this sub-basin, especially rain being one of the most relevant data for this kind of model.

The obtained results can be considered a useful tool for management and planning activities. It will allow a first assessment of impacts on water and sediment production due to soil use and climatic changes in the basin.

It is important to keep on investigating to improve results produced by the model and carry on working on topics like improving spatial and temporal resolution of climatic information, and to carry out studies to determine the curve number and other biophysical parameters of the different soil cover types in the basin.

It is also necessary to increase the number of climatic stations and analyse their redistribution, basically using automatic stations to avoid data loss or incorrect registration.

3.10.1 Institutional activities

Binational Technical Group (Grupo Técnico Binacional, GTB)

To obtain a shared tool that can be used as a complementary instrument for studies, investigations, projects and decision-making in each of the institutions involved in basin management, a technical binational group (GTB) about erosion and hydrology was organised. This group should allow sustainability and optimal use of this tool.

In 2007 initial formation of the GTB by technicians from the different institutions was started. On the Peruvian side these institutions were: Servicio Nacional de Hidrología y Meteorología (SENAMHI), Proyecto Especial Chira Piura, Gobierno Regional Piura y Autoridad Autónoma de las cuenca hidrográficas Chira Piura and in the case of Ecuador: PREDESUR, UTPL, CINFA, Consejo Provincial de Loja. These technicians were experienced in different techniques, but basically in SWAT.

In January 2008, the Peruvian part of the GTB, with support of their institutions, started a participatory implementation of the SWAT model. A working plan was designed, and periodic meetings were organised to work with the multidisciplinary group put into practice the acquired skills, combined with the personal background and experience of all participants. This allowed fulfilling one of the goals of TWINLATIN i.e. the transference of development planning and decision-making tools to local institutions involved in the basin's management.

At this moment, the technicians are able to run SWAT and have completed the TWINLATIN work. However, it is important to keep on supporting this kind of investigations. There are still a lot of aspects that can be improved to obtain even better results e.g. a detailed study to determinate the curve number for different soil uses in the basin or digitisation of the hard-copy daily climate data.

The results of this study, apart from those already mentioned, are an evaluation of the impact of soil use changes, climate change and the hydrologic response of the basin to these changes. These are detailed in the WP8 report. This impact evaluation should allow to design proposals to face these changes.

Model familiarisation and technology transference

A technician from the project participated in a model familiarisation session in IVL in Sweden as a twinning activity. This session was organised from the 16th of April 2007 till the 4th of May 2007. Representatives of the following basins participated: Catamayo Chira (Peru – Ecuador), the Cuareim - Quarai basin (Uruguay) and the Cocibolca Lake basin (Nicaragua).

As a part of the follow-up, Peter Wallenberg, an IVL expert realised a visit to the basin, where he made a trip across the basin and took part in several meetings in Piura and Loja to see the advances in the model implementation. This visit was carried out in September 2007. A hydrological modelling expert from PROMAS, from the University of Cuenca in Ecuador, also gave periodical assistance. Specific support was given for the climatic, meteorological and hydrologic characterisation of the basin, in the area of hydrology by staff from the Universidad Técnica Particular de Loja.

4. Cauca River Basin (Colombia)

4.1 Description of basin

The Cauca River is the second most important river artery of Colombia with a longitude of 1,204 km, draining a basin of 59,074 km². More than 16 million inhabitants live there, representing 25% of the Colombian population. The Cauca River flows through the departments of Cauca, Valle del Cauca, Quindío, Risaralda, Caldas, Antioquia, Córdoba, Sucre and Bolívar.

The Cauca River has three very important sections: the Upper, Middle and Lower Cauca. The Upper Cauca covers the area from its origin in the department of Cauca, until the municipality of La Virginia, in the department of Risaralda. The Middle Cauca goes from La Virginia until the municipality of Puerto Valdivia, in the department of Antioquia. The Lower Cauca goes from Puerto Valdivia down to the Brazo de Loba, in the department of Bolivar. As well as human settlements, an important sector of Colombia's south-western manufacturing industry (mainly paper manufacturing), the sugar cane agro-industry and part of the coffee growing zone, are also located in the Upper Cauca area.

The Upper Cauca River section goes from Salvajina Dam, in the department of Cauca, down to La Virginia, in Risaralda (Figure 4.1), covering an extension of 569 km, and having an average width of 100 m. The river bank depth ranges from 3.5 m to 8 m. The most serious water quality problems are found here due to contaminated discharges, especially near the city of Cali. One of the main environmental authorities in the Upper Cauca River Basin is the Corporación Autónoma Regional del Valle del Cauca (CVC), an institution in charge of water quality improvement.

Standardisation and other control strategies have been associated with information on the river's behaviour, contamination and expected quality levels according to water resource usage. Considering variables involved in this type of decision and complex relationships among such variables, mathematical modelling has been used as a planning and control tool.

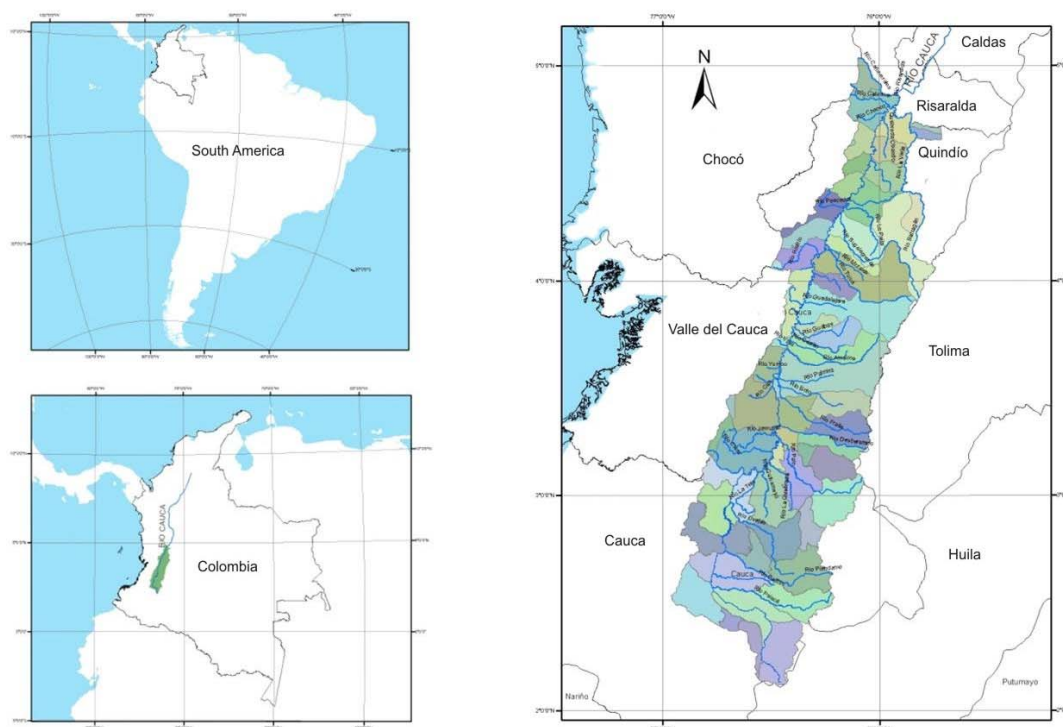


Figure 4.1 Study zone location

4.2 Choice of model

Mathematical models are built based on equations that represent or simulate the essence of a process or system. An adequately calibrated model allows simulation of the behaviour of a modelled process or system, predicting results under different analysis conditions or alternatives.

Runoff water is the result of the transformation process of rainfall over the basin. This process involves other hydro-climatic phenomena, such as evapotranspiration, infiltration and groundwater. Conceptual rainfall-runoff models, through the quantification of more relevant physical processes and mathematical functions, are able to continuously simulate water flows for periods of time as long as the available series of the entry data.

There are multiple and different mathematical formulas to simulate the rainfall-runoff process, through which it is possible to quantify the water flow at the required site in the basin. These equations are used to build models for the analysis and optimisation of water resources usage. The model implementation and application requires data on the hydrology regime, as well as the environmental conditions of the basin.

Several studies have been performed in the Upper Cauca River Basin, considering the implementation of a mathematical model in order to have a better understanding of the hydrology, hydrodynamics, sediments, morphology and water quality processes.

In order to maximise Salvajina dam's operations, in 1987, CVC selected and implemented the hydrological mathematical model HBV/IHMS (Hydrologiska Byråns Vattenvalansavdelning) of the Swedish Meteorology and Hydrology Institute (SMHI), for the forecast of flows (SMHI, 2005). It has also implemented it as a support tool for studies and projects related to water resources management in the Upper Cauca River basin.

4.2.1 HBV/IHMS model

CVC purchased and implemented the HBV/IHMS (Hydrologiska Byråns Vattenbalansavdelning - Hydrological Bureau Water balance) model for the application of the hydrology model in the Upper Cauca River Basin. The HBV/IHMS software was developed by the Swedish Meteorological and Hydrological Institute (SMHI) during the 1970s (SMHI, 2005). The model was updated in 1996 and 2005 and is currently used in more than 40 countries of the world.

The first version of the HBV/IHMS model was purchased and implemented in 1987, to optimise Salvajina Dam's operations. The license was renewed in 1998, and the corresponding training course and license were received. In 2005, the new Windows version was purchased, and the model's calibration was reviewed.

HBV/IHMS is a rainfall-runoff model applied to simulate water flow and hydrological forecast. The main entry in rainfall-runoff models is precipitation data, which together with other physical and climatic variables and with the quantification of hydrology processes using mathematical models, permanently explain basin water storage and continuously simulate the water flows.

The application of the HBV/IHMS model as a support tool has the following purposes:

- Salvajina Dam operation: The HBV/IHMS model allows short, medium and long-term forecasts of flows going from the Cauca River to the Salvajina Dam, as well as to the hydrometric stations of the Cauca River, under the jurisdiction of CVC. This model uses real-time information coming from the automatic stations in the monitoring network, as well as complementary stations.
- Quality control on information related to rainfall and water flow: The HBV/IHMS model is very versatile on data management. The graph module allows rapid detection of inconsistencies.
- Detailed hydrology studies: The HBV/IHMS model allows studies on water flows in large basins, larger than 40 km². It is possible to generate daily or monthly water flow series at any location of the sub-basins of interest.

Figure 4.2 depicts the basic structure of the HBV/IHMS model, describing its general working routines and functions:

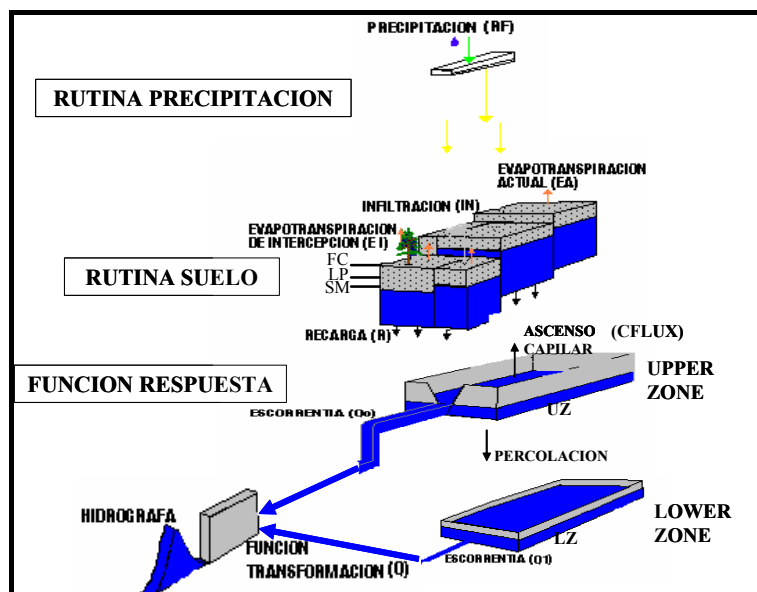


Figure 4.2 General structure of the HBV/IHMS model

Rainfall and snow melting routine

Rainfall and snow are calculated separately, taking into consideration the temperature threshold. Given the region of study zone's climate conditions, snow-related aspects were not taken into consideration.

Soil routine

The HBV/IHMS model is based on a tank theory modification that assumes statistical distribution of the basin's storage (soil humidity). The HBV/IHMS model has gradually developed a semi-distributed model that allows dividing the basin into sub-basins. Each of these sub-basins has a runoff distribution, according to its elevation and vegetation.

Response or Runoff Assessment Function

The response function transforms excess soil water into runoff, including the direct effect of rainfall and evaporation. It simulates surface and underground runoff conditions.

Runoff Transformation Routine

Runoff generated by the response function is managed through a transformation function, allowing the retention of runoff values throughout time i.e. it provides hydrography data at the basin's exit.

4.3 Data requirements

The following type of information was required for the implementation of the HBV/IHMS model:

- Model components: Model components are the physical characteristics of the basin, such as elevation, coverage, area.
- Status variables: Those indicate the degree of impact caused by the pluviometric stations in the basin under analysis. For example, the station weight is the impact or influence level of an identified pluviometric station located in the basin under analysis.
- Entry variables: Rainfall, water flow and evaporation data obtained from the stations in the corresponding basin.

Rainfall

This is the most important parameter of the model. For its implementation in CVC, a careful selection of pluviometric stations was done, comparing 145 stations from CVC's computer database. Once the

statistical analyses from these stations were completed, a data base consisting of 108 stations was developed.

Evaporation

Evaporation records from the stations represent this variable behaviour in the basin.

Flow

Records from the hydrometric stations in the Cauca River and its tributaries are used.

4.4 Model development

The implementation of the HBV model in the Upper Cauca River Basin was analysed for the development in three work areas:

- Salvajina Dam operation: The objective is generating short, medium and long-term forecast series for the Cauca River flow into Salvajina Dam and the hydrometric Cauca River stations.
- Hydrology studies: Hydroclimatic information provides a tool for the hydrological characterisation of all model scheme basins.
- Determination of water flow duration curves: Necessary records for basins lacking water flow information can be generated for projects related to surface water distribution in basins under CVC's jurisdiction.

Table 4.1 describes the calibration runs performed in order to meet the initial goals, identifying three information levels.

Table 4.1 *Model calibration stages*

Calibration	Information	Stations	Objective	Calibration period	Validation period
First level	Real-time daily rainfall	25 Alert network rainfall stations	Daily forecast on short, médium and long-term inflow to Salvajina Dam		
Second level	Daily rainfall	41 rainfall stations	Optimisation of the hydroclimatic network		
Third level	Daily rainfall	107 rainfall stations, 57 flow stations	Water flow studies in Valle del Cauca basins	1 Jan 1973 to 3 Dec 1982	1 Jan 1983 to 31 Aug 1999

For the implementation of the model, information is required from 107 pluviometric (rainfall) stations, three evaporation stations and 57 water flow stations.

Based on available cartography, it was possible to map water divisions for main flows going to existing limnigraphic stations (sub-basins). This also identified points of interest for water flow generation. Average elevation, coverage and sewage areas for each sub-basin were also determined.

Rainfall data are the most important variable for model application. Therefore, a more comprehensive analysis on existing information was performed. Missing rainfall data were determined in search for a common period for stations. Statistical tools were used to complete missing rainfall data. On the other hand, in stations where it was not possible to determine rainfall series, information was obtained using existing correlation with nearby and similar stations in order to establish substitute stations. Once the entry series for each of the stations was determined, their corresponding weight was assessed for the different configurations.

The model scheme is shown in Figure 4.3, including the distribution of available entry information for the implementation of the model in the study zone (Upper Cauca River basin).

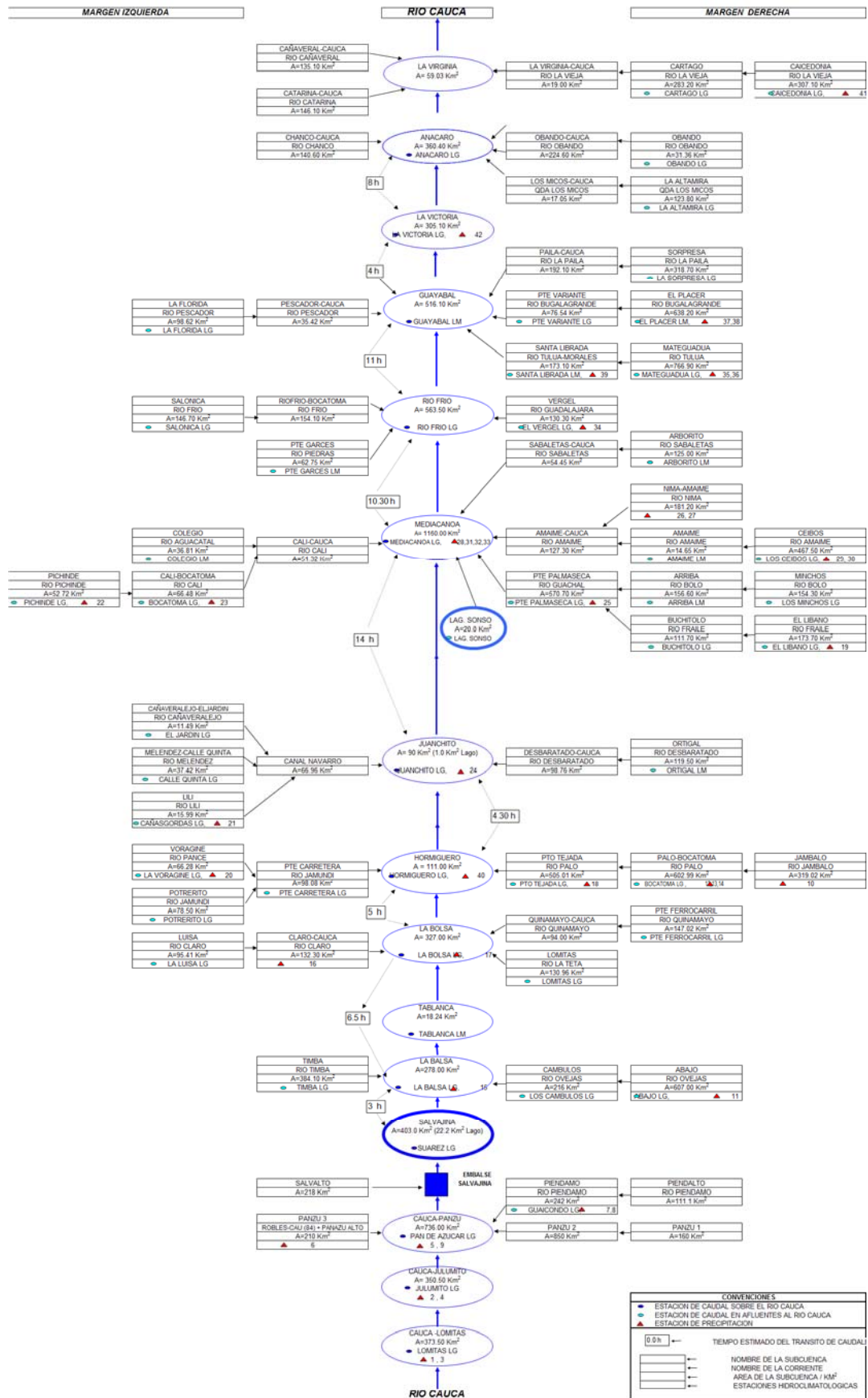


Figure 4.3 HBV/IHMS model scheme in the basin

For the execution of the HBV/IHMS model as a support tool in the development of WP8 on global changes, the hydrological modelling is used to obtain the basin's water resource variation data, according to climate planning results provided by climate change models. Calibration and validation were revised at the pilot basin of the Tulúa River located in the middle zone of the Upper Cauca River Basin.

4.5 Calibration

The calibration process is fundamentally based on three criteria that allow the adjustment of hydrography measures with those generated by the model, according to information on rainfall and basin conditions. The following criteria were taken into consideration at the Mateguadua Station to calibrate the pilot basin of the Tulúa River (pilot basin for integrated water resources management):

- Visual inspection of generated and registered hydrography;
- Continuous observation of accumulated differences between the modelled and observed flows;
- Analysis of variance using Nash-Sutcliffe efficiency criterion (Nash-Sutcliffe, 1970) and R2 Goodness of fit which should be between 0.8 and 0.95 for a good fit.

The model was calibrated for the pilot project for integrated water resources management in the Tulúa River Basin (Figure 4.4).

The multiannual monthly hydrographic behaviour was calculated (in red) and recorded (in green) for the calibration period of the HBV/IHMS model between 1974 and 1995, as shown in Figure 4.5.

General similarity in trends (shape) and volumes estimated by the model have been observed.

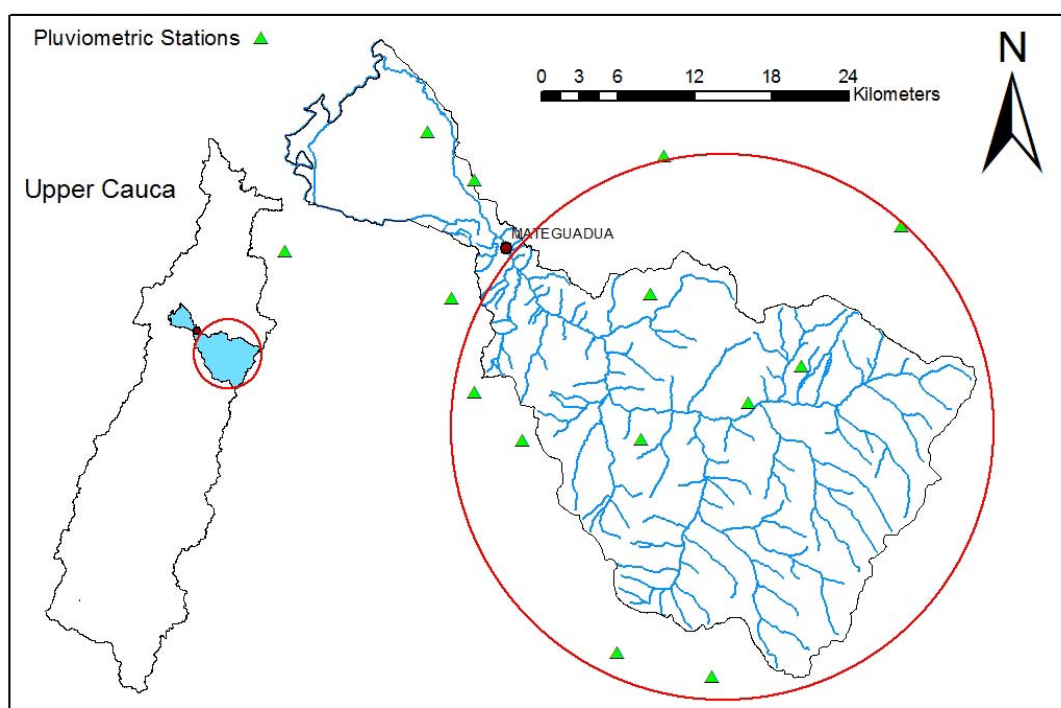


Figure 4.4 Location of the Tulúa River Basin in the Upper Cauca River Basin

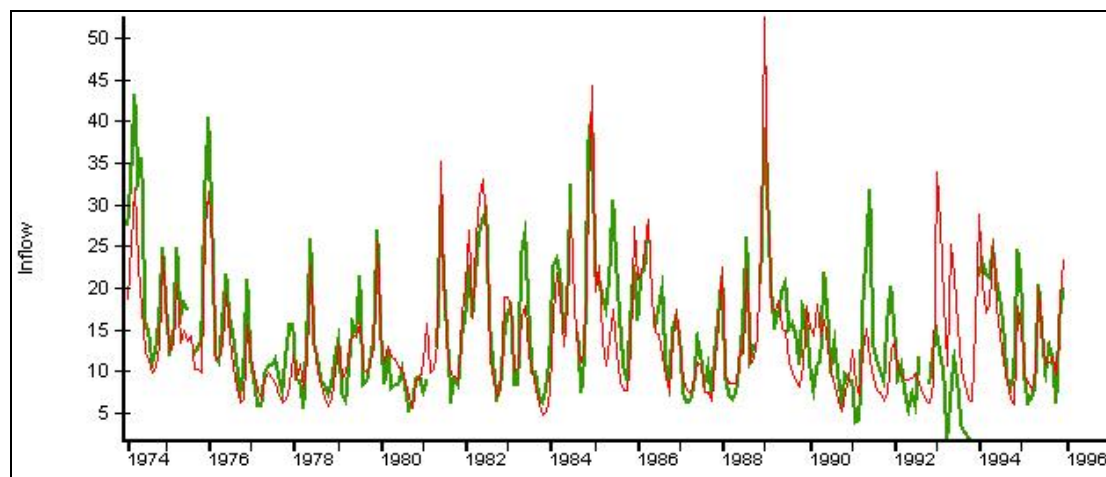


Figure 4.5 Multiannual monthly comparison of estimated (red) and recorded (green) hydrography for the period 1974–1995 for Mateguadua station in the Tulúa River Basin

4.6 Validation

Model results were validated for the period between 1996 and 2004. The statistical results calculated included the accumulated difference between the observed and modelled flows of -570 mm and the R^2 Goodness of fit of 0.46. The accumulated difference value is considered high for the validation period, and shows that the model tends to underestimate the flows. The Goodness of fit is considered low for the validation period.

4.7 Evaluation of hydrological modelling (D3.2)

The evaluation of validation results demonstrate limitations found in the initial entry information. One of the problems initially found corresponds to data deficiencies in certain pluviometric stations, where data are missing for certain periods of time. Despite using statistical techniques for their completion, sometimes it is not possible to fill the gaps and, therefore, it is necessary to determine substitute stations to fill in that information. This leads to the introduction of uncertainties into the model, which later are reflected in differences found between model predictions and field data.

Physical characteristics definitions were initially mapped with existing cartography information, from digital maps on a 1:300.000 scale. This generated errors in mapping water divisions and defining drainage areas. These errors have been corrected, improving the working scale, as well as base cartography extracted from digital cartography generated and substituted by photo-interpretation and satellite image processing, providing a better definition and measurement precision in basin areas.

A source of calibration information is the flow data collected in stations located on the Cauca River. In many cases, water flow values are distorted by floods caused by increased water levels. Another problem found is water flow data estimates based on level data obtained through the rating curve which, in many cases, contains a high uncertainty for curve extrapolated data. These situations may be corrected by the improvement of the calibration curves quality, both in the Cauca River, as in its tributaries, through field campaigns aimed to collect larger amounts of information on high and low extreme flow values that lead to reduce uncertainties in flow data information.

One of the model's applications as a management tool for hydrology forecast is the generation of a series of short, medium and long-term forecasts on flows pertaining to tributaries entering Salvajina Dam. It is also possible to generate water flow series for basins lacking flow information or in basins that have downstream intake stations that, therefore, are not representative of their natural hydrological behaviour, to be used for studies on water resources availability and to develop water distribution projects in Valle del Cauca.

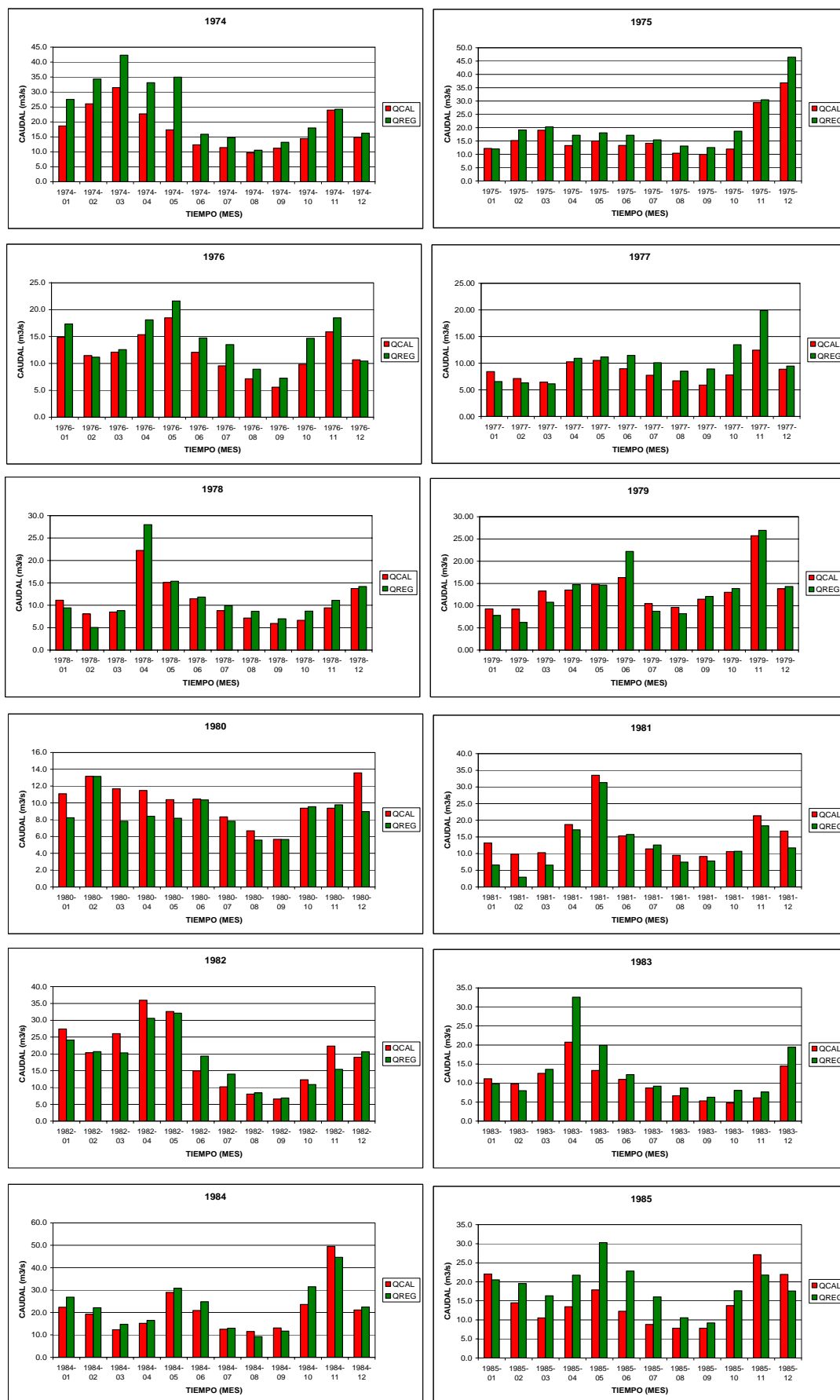


Figure 4.6 Monthly annual variations of recorded and estimated flows for the period 1974-1995



Figure 4.6 continued Monthly annual variations of recorded and estimated flows for the period 1974-1995

4.8 Summary and recommendations

Complete information on the basin's pluviometer series is necessary to overcome the need to use substitute stations, which adds a degree of uncertainty to the model's forecast results.

Revision of existing correlations between the pluviometer stations in the Upper Cauca River Basin are necessary given the fact that the model requires having substitute stations for those where it may not be possible to collect full data.

It is necessary to analyse space distribution and coverage of pluviometer stations currently located in the zone and review pluviometric data during dry seasons since data may be directly influenced by climate phenomena such as El Niño.

Revision of calibration curves of the Mateguadua station on the Tulúa River is necessary, as well as water flow records quality control. Constant updating of inflow information is key in order to have more precise rating curves, uncertainty reduction and updated field record information.

5. Cocibolca Lake Basin (Nicaragua)

5.1 Description of basin

5.1.1 Introduction

Lake Cocibolca, also called Lake Nicaragua, is the largest lake in Central America and an important freshwater resource in the region. It covers approximately 7,800 km² and has a mean depth of only around 13 m. Lake Xolotlán or Managua, which is located further north-west (Figure 5.1), sometimes connects directly with the Cocibolca Lake via the Tipitapa River. Today this process occurs infrequently e.g. during extreme precipitation events such as the hurricane Mitch of October 1998; before the middle of the 19th century the two lakes were regularly connected.



Figure 5.1 The Lake Managua, Lake Cocibolca and River San Juan basins, data from USGS (2006)

The drainage basin of Lake Cocibolca is transboundary, with the southern part located in Costa Rica. The Lake Managua and Lake Cocibolca watersheds form part of the larger San Juan River Basin which has a total drainage area of approximately 42,000 km², making it the largest basin located in more than one Central American country. It is the drainage area of the Cocibolca Lake itself (approximately 24,000 km², without the contributions from and to the Managua Lake and San Juan River, respectively) which is the object of study in the TWINLATIN project¹.

Both the San Juan River and Cocibolca Lake have since long been important for transportation in Nicaragua, and there have been various plans throughout the years of constructing an inter-oceanic route connecting the Caribbean and the Pacific Ocean (Montenegro-Guillén, 2006). Besides this, Lake Cocibolca has played a variable role for the national fishing industry throughout Nicaraguan history. More recently, it is increasingly becoming important as a national and international tourism attraction. The lake and its surrounding wetlands are also an important pool of biodiversity, with the lake itself presenting some very particular conditions such as the presence of Bull sharks (of which the conservation status within the lake is uncertain at present).

Lake Cocibolca is not nearly as heavily polluted as Lake Managua, which receives the waste waters from the Nicaraguan capital. However, it is generally acknowledged amongst the Nicaraguan public opinion that the quality of the waters of the Cocibolca Lake has deteriorated significantly over the past decades. Several theories that try to explain this deterioration are on hand, one of the main ones being the progressive deforestation and land use conversions in the terrestrial part of the basin. This deforestation would have led to an increase in erosion and thus sediment, pesticide and nutrient loads towards the rivers and lake. Local stakeholders also frequently express their perception of severe impacts of this land cover/land use conversion (which mainly consists of the transition from forest cover to livestock breeding grounds) on local (sub-basin) hydrology. Studies confirming or quantifying these impacts, however, are limited in scope or non-existing at all.

Other threats include the lack of (mainly) urban waste water treatment (e.g. City of Granada), contamination from navigation and a particularly noticeable problem of (solid) waste disposal. On top of this are the added threats associated to volcanic activity and hurricanes (Montenegro-Guillén, 2006). Some societal actors also point a finger at the Tilapia breeding cages located directly in the Lake, in the vicinity of the Ometepe Island.

Even though the lake itself stores a tremendous volume of freshwater, provision of drinking water within the basin has and keeps on being problematic e.g. in many of the (higher lying) localities of the north-east part of the basin, where rivers become intermittent as an effect of the prolonged dry season, and where groundwater wells may be contaminated with arsenic (i.e. high natural background levels). Water shortage problems in the area are frequent and expected to increase in the future under different highly probable scenarios, such as the ongoing southwards expansion of the city of Managua and a potentially significant reduction of precipitation rates under climate change. It is probable that the lake under such circumstances will become an important potential source for the provision of freshwater in this region, as it is the only large superficial freshwater supply in this highly populated and semi-arid part of Central America (OAS, 2007). As an example of this, it can be noted that at this moment works have started to provide the City of Juigalpa with drinking water that originates from the lake. Preparations are currently being made to provide the rapidly growing coastal town of San Juan del Sur (which is located outside of the basin and is one of Nicaragua's main tourism destinations) with water from the lake; other locations may soon follow with similar initiatives. In this perspective, it becomes clear how a further deterioration of water quality in the Cocibolca Lake may jeopardise these development plans. Awareness at the Central Government level about the potential strategic

¹In Figure 5.1, the Río Frío watershed is included as part of the Cocibolca Lake Basin. However, the Río Frío drains from the South directly into the San Juan River. This occurs almost at the point where the San Juan River starts (i.e. immediately downstream from the lake outlet). The Frío River may therefore exert a certain influence on the lake.

importance of the Cocibolca Lake is reflected in the fact that a complete article of the new National Water Law (May 15, 2007) is specifically dedicated to the protection and conservation of the Cocibolca Lake.

5.1.2 The regional climate

The regional climate of Central America is characteristic of the tropics: it presents a low seasonal variability in temperature and a high seasonal variability in precipitation. The surrounding oceans have a large impact on the climate, but there is a greater spatial and temporal variability in precipitation than might be expected in such a case (Alfaro, 2000; Portig, 1976). The configuration of the coastline in relation to seasonal flow patterns and orographic lifting at the high mountain range which stretches through the region explain a large part of this variability (Hastenrath, 1967). Central America is located in the North Atlantic trade wind belt and is also influenced by the northward migration of the Inter-Tropical Convergence Zone (ITCZ) (Amador *et al.*, 2006; Hastenrath, 1967). Significant seasonal changes in wind direction only occur in the western and southern parts of Central America, which are affected by the Pacific Ocean; in general wind speeds are small (Portig, 1976).

In the boreal winter the easterly trade winds dominate the lower levels of the atmosphere and the ITCZ is at its southernmost position (Hastenrath, 1967). During the first half of winter the trade winds are occasionally interrupted by northerly winds (Nortes) associated with outbreaks of cold air from the North American continent; these winds produce precipitation on the windward sides of the mountains (Hastenrath, 1967; Portig, 1976). The differences in the precipitation regimes between the Caribbean and Pacific coasts are large; there is no distinct dry season on the Caribbean coast while the leeward position relative to the trade winds and the Nortes gives little precipitation on the Pacific coast during the boreal winter.

Maximum annual temperatures occur around April before the start of the rainy season (Portig, 1976); the temperature then decreases during the wet season until January and this intra-annual variation is strongly related to the seasonal variability of precipitation (Aguilar *et al.*, 2005). The diurnal temperature range is much larger than the annual temperature range, and increases with distance from the coast (Portig, 1976). The rainfall regime in most of the Cocibolca Basin, as on most of the Pacific coast of Central America, is clearly bimodal (Alfaro, 2000); it presents a long dry season followed by a first rainfall maximum in early summer (June), after which there is a decrease in rainfall, called the midsummer drought (*la canícula*), around July-August. The second and largest rainfall maximum occurs in the middle of September and the absolute minimum takes place in March. The midsummer drought is brought on by a strengthening of the easterly trade winds that results in maximum precipitation on the Caribbean coast, as orographic lifting takes place at the mountain range; at the same time there is a decrease in precipitation on the Pacific coast (Magaña *et al.*, 1999). During June and again in September-October the atmospheric influences from the Pacific Ocean are predominant (Hastenrath, 1967); this is also when wet spells occur most frequently, the trade winds are weak and the cross-equatorial flow in the eastern Pacific is strong (Peña & Douglas, 2002). Transient weather disturbances such as hurricanes, tropical storms and depressions, easterly waves and meridional displacements of the ITCZ create the largest part of the synoptic variability in precipitation during the rainy season (Peña and Douglas, 2002). The climate in the Cocibolca Basin is classified as continuously wet (mainly the extreme southern and eastern parts) and wet-and-dry climate (the majority of the basin) (McGregor & Nieuwolt, 1998).

Several earlier studies have shown strong correlations between inter-annual climatic variations in Central America and oceanic climate-variability indices such as ENSO (El Niño Southern-Oscillation) indices and Atlantic sea-surface temperatures (Aguilar *et al.*, 2005; Diaz *et al.*, 2001; Enfield & Alfaro, 1999). The El Niño effect on temperature is clear as there is warming throughout the year during El Niño years (Diaz *et al.*, 2001). The predominant effect on precipitation is a reduction in precipitation amounts and thus a risk for sustained droughts; the drying signal is strongest during summer and autumn (Diaz *et al.*, 2001).

5.1.3 Previous studies and TWINLATIN objectives

Little previous work exists on water balance modelling for the Lake Cocibolca Basin. One major (series of) study(ies) corresponds to the PROCUENCA San Juan Project, a Costa Rican – Nicaraguan cooperation project sponsored by UNDP and OAS (OAS, 2007) which focused on the concept of integrated river-basin management (no major attention was given to the basin's water balance). The final aim of this project was to formulate certain general recommendations for a strategic action plan for sustainable management of the water resources in this bi-national basin. However, limited baseline information was available for this purpose. Results from PROCUENCA have been taken into consideration in TWINLATIN (e.g. in WP5). After hurricane Mitch, the USGS had a large project in Central America (including Nicaragua) that focused on the development and use of GIS infrastructure and know-how, satellite data and on the construction and remediation of the hydrological monitoring network which was severely damaged by the floods occurring during the hurricane (USGS, 2002). Collaboration in Nicaragua was carried out in cooperation with the institutions INETER (Instituto Nicaragüense de Estudios Territoriales) and MAGFOR (Ministry of Agriculture and Forestry), amongst others. However, the links that had been established to clearinghouses (e.g. <http://www.clearinghouse.gob.ni/>) and other information sites are dysfunctional at the time of writing. Currently, in the framework of the newly established Nicaraguan Water Law (May 2007), increased interest exists at the Hydrology Direction of the INETER with respect to improving the water balances for the different Nicaraguan River Basins. It is in this context that TWINLATIN aims to provide a distinct contribution through the provision of knowledge and products, obtained from the work conducted under WP3.

The scope of the work to be conducted under WP3 is a function of not only the local stakeholders' interest, but also of the feasibility of the different methodological approaches. In this context, it is important to indicate how the effects of civil war and other destabilising events in Nicaragua can be clearly seen in the lack of and decrease in data quality, especially around 1990 (see, for example, Figure 5.6). In general, quality control of hydrometeorological time series data (described in more detail in the WP2 report) showed that: firstly, data quality was low for many precipitation stations; and that, secondly, especially discharge time series were highly discontinuous or, in the best cases, contained a lot of data gaps. The former aspects immediately limit the possibilities for hydrological modelling applications in the basin, and the accuracy of results from spatial interpolation of, for example, precipitation, can be expected to vary as a function of the time window considered in the analysis; this is a consequence of the amount of available data.

One of the main objectives of the hydrological modelling work that was developed under WP3 relates to the development and implementation of a methodology which allows for an improved estimation of the basin water balance, and of the uncertainties involved. Transfer of the methodology developed for this case study to the Nicaraguan government institution INETER (which holds the national mandate for the establishment of (sub)basin water balances under the new Water Law) constitutes a big contribution of the project to INETER's role in the future management of the Cocibolca Basin, but also holds the potential for further extension of the developed methodology to other parts of the national territory. National interest in improved water balance modelling is, amongst other reasons, related to the provisions with regard to the extension of water use rights which are contained in this new National Water Law. Considering the long-term potential strategic importance of the Cocibolca Lake, certain interest also exists in the assessment of impacts of plausible climate change scenarios on the basin water balance.

In order to achieve the former goals, a simpler, long-term water balance estimation method was compared to the results of a monthly water balance model applied with uncertainty estimation.

The feasibility of hydrological modelling with a daily time step was assessed in a sub-basin (Mayales River) where sufficient coincident meteorological and hydrological data were available. The modelling study, therefore, also serves as an evaluation of the coherence and quality of the hydro-meteorological data. Within the Nicaraguan part of the Lake Cocibolca basin, the Mayales sub-basin was the only sub-basin for which data availability approached the minimum conditions for which meaningful results from such a modelling approach could be anticipated. Theoretically, the particular

type of model that will be applied here should under ideal conditions allow for an assessment of impacts from land use and climate change; however, the feasibility of this will be highly conditioned by the availability and quality of input and calibration/evaluation datasets.

5.2 Choice of model

5.2.1 Available data and preconditions for modelling

For a specific study site, the applicability of any given model will be highly conditioned on the available data and its quality and characteristics. Therefore, this section starts with an analysis and description of available datasets for the Cocibolca Basin. Availability and quality of data are described at different spatial and temporal scales, and departing from this analysis, a justification is given for the selection of models.

Temperature data

Intra-annual variation in daily mean temperature in the basin was low (the deviations between maximum and minimum temperatures were around 10-15°C for most stations). In general a decline in temperature with altitude could be observed. For the Nicaraguan part of the catchment, temperature data were only available for 19 stations. Many times series end in the 1990s (Figure 5.2).

Correlation between temperature time series from different stations was relatively high, both for monthly and daily data, and there was a general decline in correlation with distance between the stations (Figure 5.3).

A linear regression analysis of the two stations with the longest time series (Juigalpa and Aeropuerto Internacional Managua) showed that there was a significant warming trend (95% confidence level) in the annual mean temperature with time. From 1971 to 2003 the trend was 0.033°C per year ([0.022, 0.044] 95% confidence bounds) for the station Aeropuerto Internacional Managua and 0.030°C per year ([0.019, 0.042] 95% confidence bounds) for the Juigalpa station. This upward tendency corresponds to the regional results obtained by Aguilar *et al.* (2005) who found an increasing trend in the temperature extremes for all of Central America of 0.2 to 0.3°C per decade for the period 1971 to 2003. However, in the decade prior to 1970, a decreasing trend can be observed (Figure 5.4).

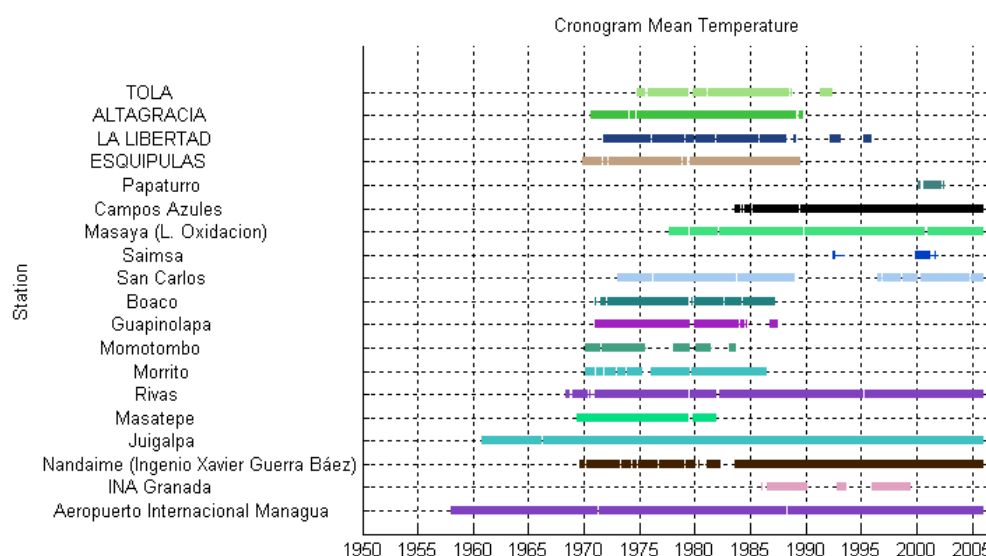


Figure 5.2 Chronogram showing the temporal availability of daily mean temperature data for the Lake Cocibolca catchment and immediate surroundings

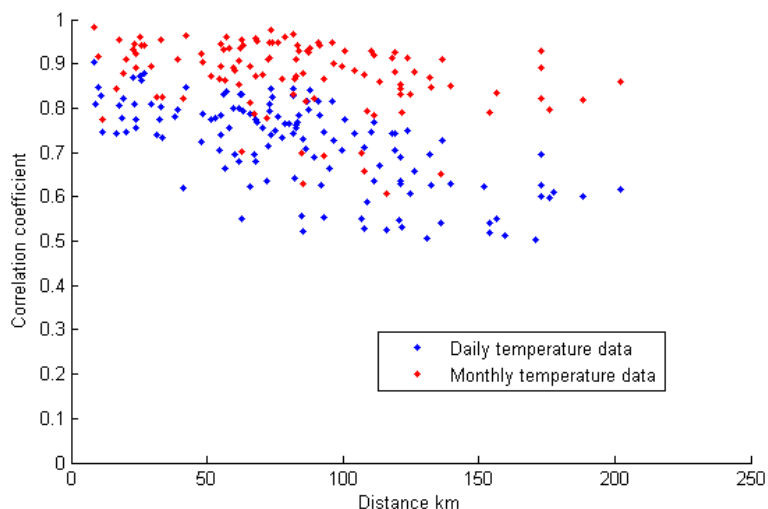


Figure 5.3 Influence of distance and level of temporal aggregation on the correlation between temperature data time series for the stations from the Lake Cocibolca Basin. Red and blue dots represent correlation values for monthly and daily mean temperature data, respectively; each dot represents a correlation between two stations plotted against the distance between these two stations.

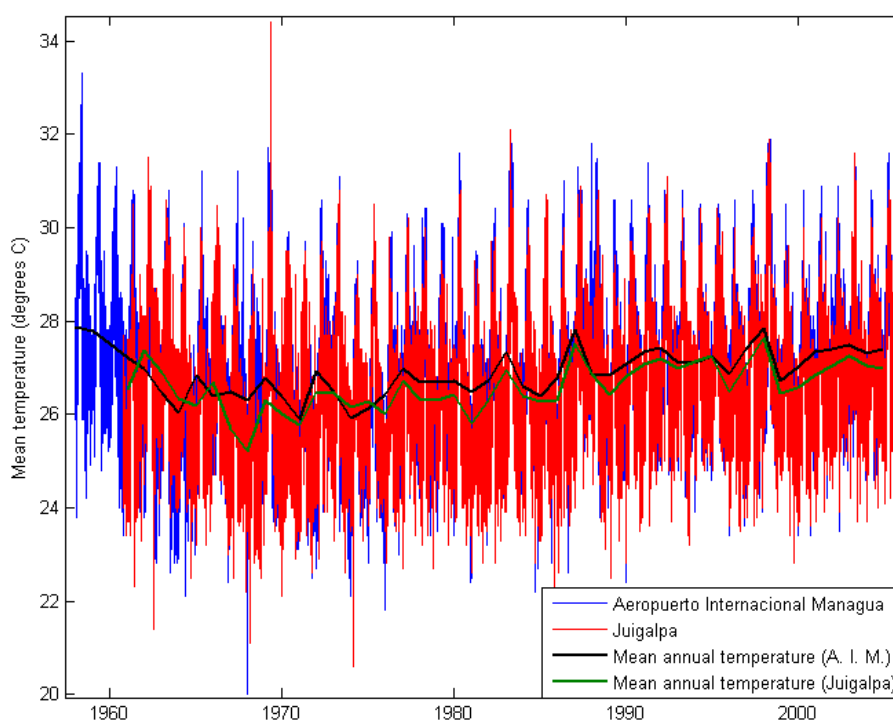


Figure 5.4 Daily and annual mean temperatures at the stations Aeropuerto Internacional Managua and Juigalpa. The mean annual temperatures (thick lines) are plotted at the first day of the year, therefore slightly more to the left than the corresponding daily data.

Mean annual temperature data were consistent with the El Niño/La Niña variations. El Niño years like 1969-70, 1972-73, 1982-83, 1986-88, 1997-98 showed higher temperatures and La Niña years like 1974-76, 1984-85 and 1999-2000 lower temperatures (El Niño/La Niña events were retrieved from the Climate Prediction Centre Internet Team (2007)).

A comparison of annual precipitation for all stations in the Nicaraguan part of the basin (complete yearly datasets only), to annual temperature for the two stations with longest records showed that precipitation was generally low during El Niño years, when temperature was high. For most precipitation stations, a clear inter-annual variability could be observed (Figure 5.5).

Precipitation data

Available precipitation time series contained many data gaps and several other quality problems were also identified; therefore, a thorough quality control had to be carried out during the construction of the basin's environmental database (for greater detail see WP2). In short, the quality-control process consisted of: comparing double-mass curves and time-series plots for nearby stations; identification of too-frequent and too-low data; checking doubtful extreme values with the values of all other stations; and visual inspection of all time series. The main quality problem that was identified was lacking homogeneity i.e. showing, for instance, too many too-frequent values because of misread or typed data. The high inter-annual variability in the basin (Figure 5.5) makes it important to include only stations that cover a sufficient number of years in the analysis e.g. in the interpolation of mean annual precipitation for a certain time period.

A total of 81 stations with daily precipitation data - mostly from the Nicaraguan part of the basin - were included in the database. Additionally, 54 stations with monthly precipitation data - predominantly from the Costa Rican part of the basin - were obtained and incorporated into the database. Time series for nine more precipitation stations were obtained; however, these datasets have been rejected during the quality control, as they contained too many erroneous data. Because of similar reasons, parts of the data were deleted from the time series of several of the stations that were kept in the final version of the database.

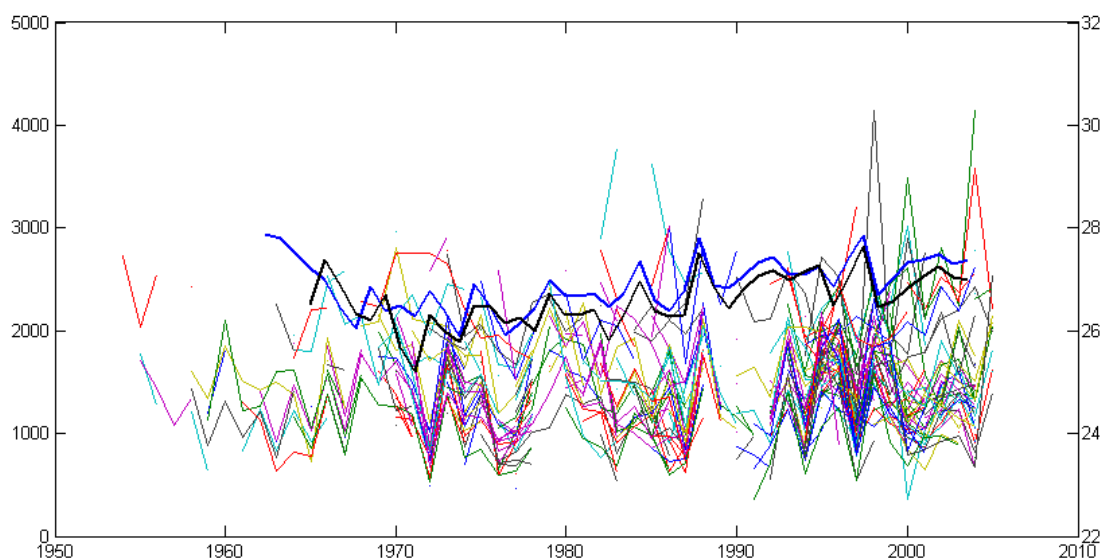


Figure 5.5 Comparison of annual precipitation and temperature variability. The thick blue and black lines represent the annual temperature from the stations Aeropuerto Internacional Managua and Juigalpa, respectively; the thinner lines the annual precipitation for stations with complete yearly records.

In this final database, data availability at the monthly time scale was much better than at a daily time scale. A sharp drop in the number of stations with data available for the 1990s could be observed (Figure 5.6). Furthermore, it was also noticeable that a considerable percentage (as much as 15% during some years) of the daily data were of too-poor quality to be used, and that this percentage increased in later years.

An analysis of mean annual precipitation from 1970 to 1990 for stations with a >70% complete dataset for this period (Figure 5.7) showed that the mean annual precipitation was lower in the north-western part of the basin than in the southern and eastern part. The precipitation was especially high in the mountainous southern part of the basin located in Costa Rica. Unfortunately, for this part of the basin time series were only available until 1993. This means that the calculation of areal precipitation, and thus also the water balance calculations for the entire basin, are less accurate from 1994 and onwards².

Correlations between time series from different stations were markedly higher on a 4-5 day time aggregation level, as compared to a daily time scale (Figure 5.8). This initial increase in correlation was much more important than when moving from the 4-5 day aggregation level to the level of monthly aggregated data. There was a general decline of correlation with distance, and stations far away from each other were no longer significantly correlated on a daily time scale. This spatio-temporal correlation structure was calculated from daily data and was, thus, representative only of the Nicaraguan part of the basin.

The spatial and temporal characteristics of the precipitation regime are described in detail in section 5.6.2, as this corresponds to the results obtained from work under WP3.

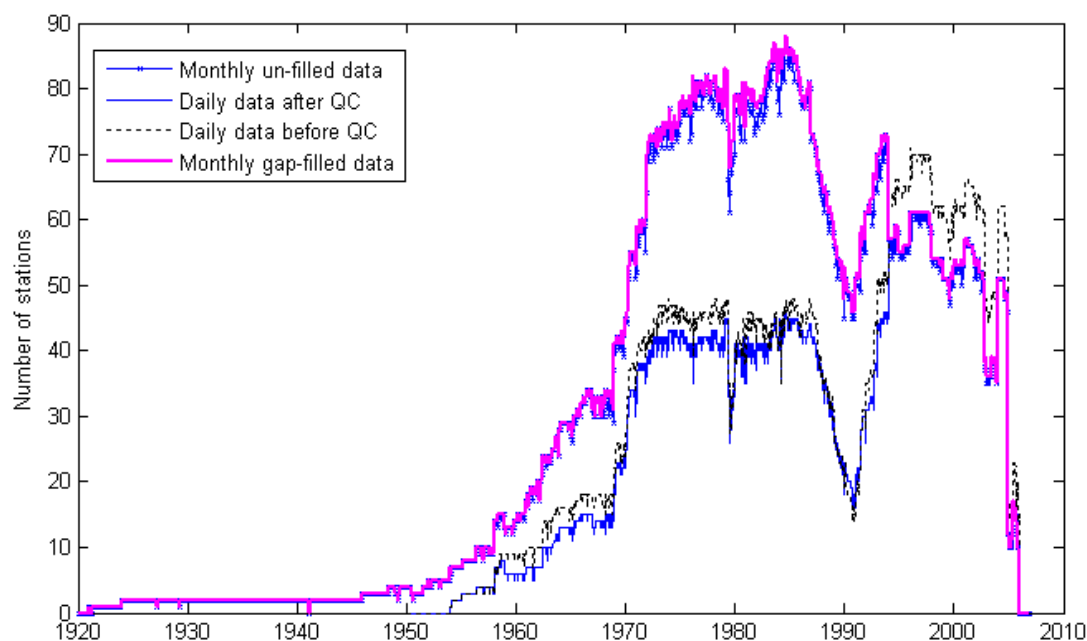


Figure 5.6 Number of stations per year for which complete precipitation time series datasets are available, before and after quality control and gap-filling (the difference between the black and the blue lines represents the amount of data that is of too poor quality to be used).

² The cluster of observational points in the southernmost tip of the Basin correspond to the drainage area of the Río Frio; the Frio river drains directly to the Río San Juan immediately downstream from the Lake outlet; depending on the purpose, contributions from this sub-basin may be eliminated from the water balance.

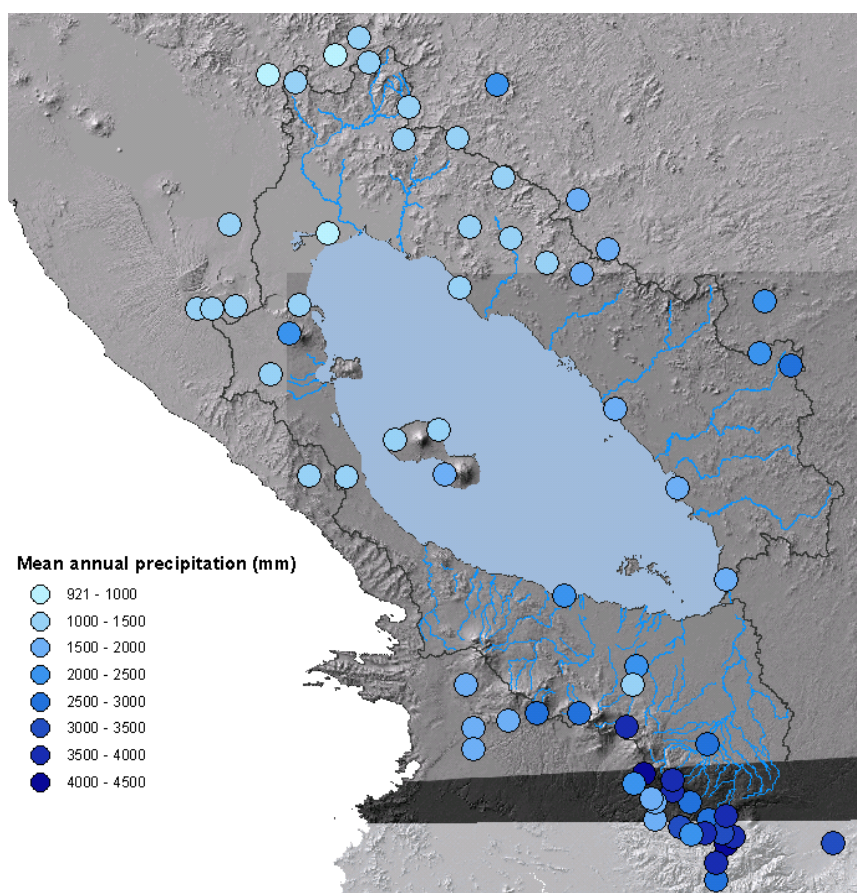


Figure 5.7 Mean annual precipitation for the stations with a $\geq 70\%$ complete dataset for the period 1970 – 1990 (the background image shows a shaded relief map for the study area).

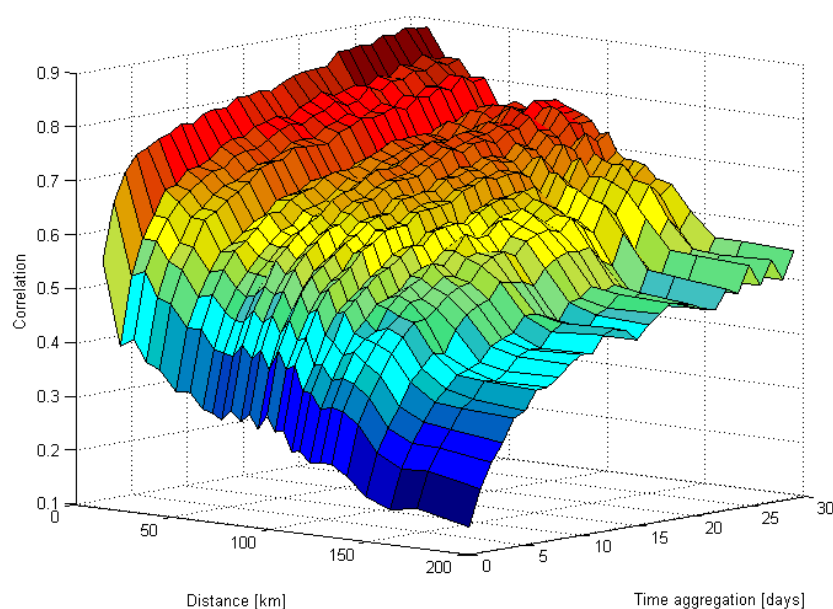


Figure 5.8 Correlation between the data from all the precipitation stations with daily data plotted against distance for different levels of temporal aggregations. One data point represents the mean of 120 correlation coefficient values. There was a marked increase in correlation coefficient values for the 4-5 day data aggregation level as compared to daily data.

Discharge data

Daily discharge time series were available mainly for the sub-basins in the northern part of the basin. In addition to this, time series of water level from the Lake Cocibolca in Paso Panaloya, and on the San Juan River just downstream from the lake outflow at San Carlos, and further downstream at El Castillo, were also available (Figure 5.9). Most discharge records contained numerous data gaps and/or were of relatively short duration (Figures 5.10 and 5.11).

The San Carlos station is located at the outflow of the Lake Cocibolca. The El Castillo station is located some distance away from the Cocibolca Basin, further downstream on the San Juan River which has received the contributions from a series of tributaries at this point. However, considering the partially different time periods for which data were available from both stations, simultaneously measured specific discharge at El Castillo holds interesting information as it could be related to the value at San Carlos for water balance validation purposes. As can be seen from Figure 5.12, shorter time periods exist for which no discharge measurements are available at all for the basin.



Figure 5.9 Discharge stations and sub-basins of the Lake Cocibolca basin

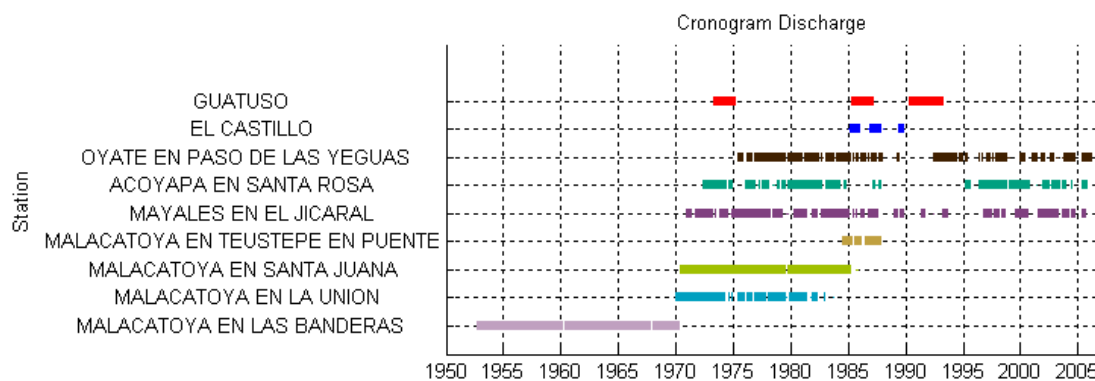


Figure 5.10 Chronogram showing the temporal availability of daily discharge data for the Lake Cocibolca basin

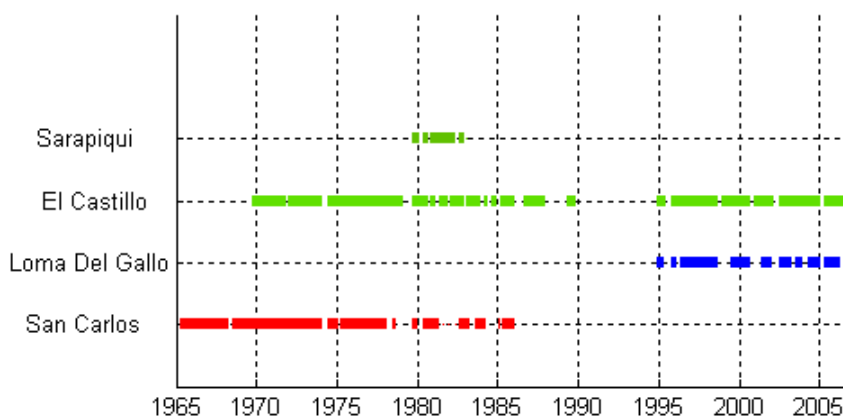


Figure 5.11 Chronogram showing the temporal availability of monthly discharge data for the San Juan River

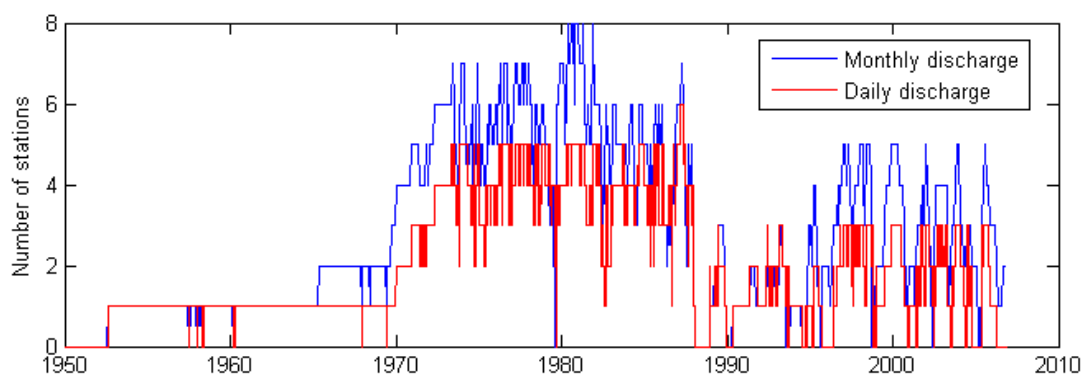


Figure 5.12 Temporal availability of discharge on a daily and monthly time scale, including stations located on the San Juan River (downstream of the lake outlet).

Meteorological data for calculation of evapotranspiration

In addition to temperature data (described above), data for climatic variables needed for the calculation of evapotranspiration with the Penman method were simultaneously available at a maximum of 8 stations (Figure 5.13). Most of these stations were located in the eastern part of the basin. For only five of these stations, the simultaneous availability of data were sufficient for the calculation of evapotranspiration in the 2000–2005 period.

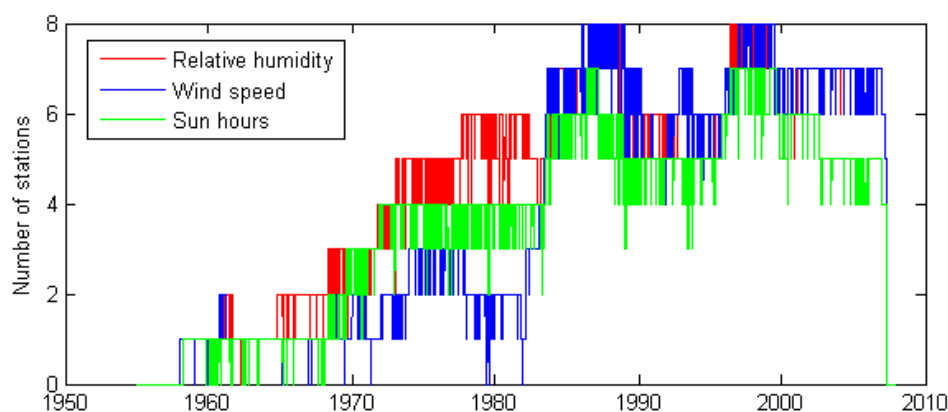


Figure 5.13 Temporal availability of data on climatic variables required for the evapotranspiration calculations (analysis based on daily data but plotted at the monthly level to facilitate viewing)

5.2.2 Water balance modelling and uncertainty estimation

In order to obtain a more complete monthly precipitation dataset for the water balance calculations, shorter gaps in the time series were filled first. Two methods for gap-filling that use a weighted combination of data from surrounding stations were evaluated: the Coefficient of Correlation Weighting Method CCWM (Teegavarapu & Chandramouli, 2005) and the Inverse squared Distance Weighted interpolation (IDW; e.g. Isaaks & Srivastava, 1989). The aim of the water balance modelling was to establish the long-term water balance for the whole basin, comparing the application of a simpler method to that of a more advanced. The rationale of the comparison was to test the applicability, limitations and uncertainties of the simpler approach, as it is of interest to establish a straightforward methodology that can be applied to the estimation of available water resources also in other parts of Nicaragua (water balance calculations are required for the whole country by the new water law - *Ley General de Aguas Nacionales* - that was passed in May 2007). Uncertainty estimation was important especially as data quality and availability often were low. The simple method was comprised of calculation of the long-term (mean annual) water balance as the subtraction of an evapotranspiration GIS layer from a precipitation GIS layer (based on an interpolation of measured station data). Several interpolation methods were assessed for the interpolation of precipitation to find the method that worked best in this basin, and to evaluate the additional gain in using more advanced geo-statistical methods like kriging instead of the simpler IDW method.

Evapotranspiration is hard to estimate if flux measurements are not available; in the basin sufficient meteorological data to calculate potential evapotranspiration were available at five stations. A spatially distributed calculation of evapotranspiration from these data would require spatially distributed modelling using distributed meteorological forcing data and land use parameters derived from satellite data with high temporal resolution. This was not possible in this project; however, spatially distributed evapotranspiration data were available from the MODIS-project (Mu *et al.*, 2007) for evaluation purposes in the TWINLATIN project. These data were compared to evapotranspiration values calculated with the full Penman-Monteith method (Monteith, 1965) and the FAO56 Penman-Monteith method (Allen *et al.*, 1998) based on the locally measured meteorological datasets. Calculation of distributed evapotranspiration can also be achieved using distributed meteorological

forcing variables from global datasets such as the NCAR/NCEP reanalysis data and vegetation parameters derived from satellite data. This approach is similar to the one used in the MODIS-evaporation project (a part of the NASA/EOS-project). In all cases, the limitations inherent to the different approaches should be duly considered prior to any use of the obtained results.

MODIS (MODerate resolution Imaging Spectroradiometer) is a key instrument aboard the Terra (EOS AM) and Aqua (EOS PM) satellites. Data from MODIS provide detailed information on vegetation and surface albedo, which has been used to develop a remotely sensed evapotranspiration model (Mu *et al.*, 2007). With a combination of the Penman-Monteith equation, remote sensing and global meteorology data the algorithm was developed to estimate both surface resistance and evapotranspiration at a 0.05 degree resolution and with an 8-day time step. These high resolution global datasets are expected to be made available globally in the future, and may thus constitute an interesting future source of information on regional evapotranspiration. This dataset can thus also prove useful for INETER's practical water balance calculations in other parts of Nicaragua, where observed meteorological datasets may be even sparser. The evaluation of the potential for using the MODIS-derived datasets in Nicaragua, therefore, constitutes a valuable contribution of the TWINLATIN project. These data were compared temporally and spatially to the evapotranspiration calculated at the meteorological stations in the basin. Water balance calculations were compared to observed and modelled discharge data at the sub-basin level, for those cases where complete yearly datasets were available. Based on an analysis of the available precipitation data time series, the time window 1965-2005 was selected as a feasible time window for modelling purposes; however, a more complete precipitation dataset i.e. covering the whole basin including the Costa Rican part, was available for the time window 1975-1994 only. Unfortunately, evapotranspiration estimates from MODIS were not available for this period. In the end, the 2000-2005 period was selected for the simple water balance calculations, based on the availability of the actual evapotranspiration data. A qualitative comparison was made with a mean annual precipitation map for the basin based on the 1975-1994 (whole basin) precipitation dataset.

A more complex water balance calculation was conducted by means of the 3-parameter monthly conceptual rainfall-runoff model WASMOD (Xu, 2002), which was applied within an uncertainty estimation framework (Figure 5.14). The model has previously been used in a large number of catchments, under many different climatic conditions and at a multitude of scales (e.g. Widen-Nilsson *et al.*, 2007; Xu & Halldin, 1997).

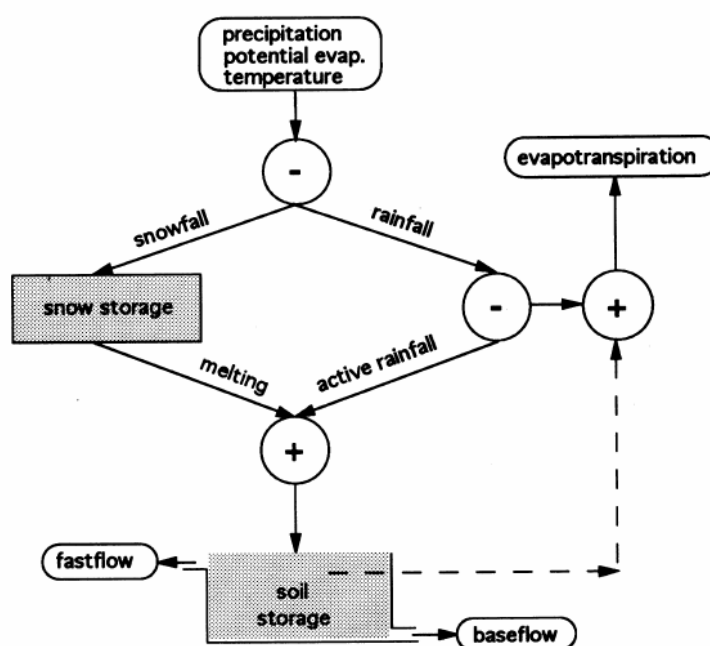


Figure 5.14 The schematic computational flow chart of the WASMOD model (Xu, 2002)

When potential evapotranspiration is given as input (as is the case in this WP3 application), only three model parameters are needed in snow-free catchments. The low number of parameters results in a low computational cost, which enables a better uncertainty estimation (i.e. many Monte Carlo simulations can be performed in a short time). The calibration of the model is here performed within an uncertainty estimation framework using the Generalised Likelihood Uncertainty Estimation (GLUE) method (Beven & Binley, 1992). In short, the GLUE method of estimating parameter uncertainty consists of running Monte Carlo simulations for parameter values in defined possible intervals, and then accepting all parameter sets that produce acceptable results according to some user-defined evaluation criteria e.g. the Nash-Sutcliffe criteria (Nash & Sutcliffe, 1970). The predicted discharge values from each accepted parameter set are then sorted according to the likelihood of that simulation and uncertainty bounds are constructed from the 5 and 95% quantiles of the cumulative density function of the predicted discharge values.

5.2.3 Distributed hydrological modelling in the Mayales catchment

As a third approach, the applicability of a daily distributed hydrological model was tested in the Mayales sub-basin. This model application serves as an evaluation of data quality and coherence; based on the obtained results, the feasibility of, firstly, modelling ungauged catchments in the basin and, secondly, scenario modelling, can be assessed. The application also allows for a description of the hydrological characteristics of the Mayales sub-basin. The attempt to conduct a distributed hydrological modelling approach for this sub-basin acquires additional relevance as (drinking) water shortages problems occur frequently here; analysis of plausible future scenarios could be conducted in the future with the model under the conditions that the results from the calibration and evaluation exercise are good enough.

The GIS-based distributed hydrological model (Westerberg, 2005) used in this case study is a part of the WATSHMAN modelling system. It was developed in the PCRaster software – which is a GIS integrated with a dynamic programming module (van Deursen, 1995). The model simulates runoff from a catchment based on daily mean values of temperature and precipitation (Figure 5.15).

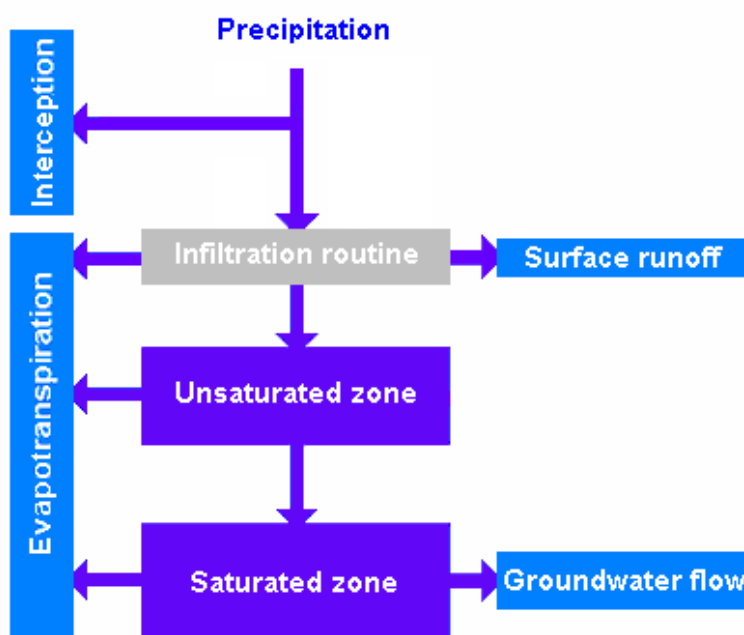


Figure 5.15 Flow chart of the WATSHMAN-PCRaster model adapted for snow-free conditions, modified from Westerberg (2005)

The GIS input data consist of maps of soil type, land use, lakes, rivers and a Digital Elevation Model (DEM). The model is a hybrid between a conceptual and a physical model, having relatively few calibration parameters and using information directly derived from the DEM. Groundwater is modelled assuming a linear reservoir and the flow routing is done with the kinematic wave equation combined with Manning's equation. The GIS and the hydrologic model are embedded in each other, allowing the calculation of each variable in all grid cells. The output from the model consists of raster maps for each time step for a pre-defined variable, or a time series for a variable at a specified grid cell. The flow network is generated from the DEM, and defines the water flow patterns at the grid scale.

The model was originally developed for Swedish conditions. However, as there were no lakes in the Mayales sub-basin, both the snow and the lake routine were excluded for this case study. Another change was that in the case of the Mayales sub-basin, meteorological time series were available which allowed for the calculation of potential evapotranspiration with the FAO56 Penman-Monteith equation (Allen *et al.*, 1998). The WATSHMAN-PCRaster model has also been embedded in an uncertainty estimation framework, as the quality issues with the precipitation data and the large expected uncertainties in discharge data make uncertainty estimation a crucial part of hydrological modelling in the basin. In section 5.2.1, it was shown how an increase in spatial correlation between rainfall stations was obtained when going from daily to 5-day accumulated precipitation data (Figure 5.8); thus better modelling results may be expected for modelling conducted at this time scale. Because of the assumptions underlying the daily model equations it was not possible to use a 5-day time step here; however, this is a topic that may be addressed in future work.

5.3 Data requirements

All hydrological models used in this study require evapotranspiration (potential or actual) as input. As there were sufficient data available at five stations, evapotranspiration could be calculated with the Penman-Monteith method (Monteith, 1965) or the FAO56 Penman-Monteith method (Allen *et al.*, 1998). These methods are preferable compared to other methods based on e.g. temperature or radiation alone (Xu & Singh, 1998). Areal estimates of temperature and precipitation were needed, and geo-statistical methods such as kriging were used for the interpolation. The data requirements of the different hydrological models/methods are specified in Table 5.1.

Table 5.1 Data requirements of the different models

Model	Data	Time scale of data
Simple water balance	Interpolated precipitation data Evapotranspiration data from the MODIS-project. Comparison with evapotranspiration calculated with the full Penman-Monteith and FAO56 Penman-Monteith methods based on wind-speed, mean temperature, relative humidity and sun hours at climate stations. Observed discharge for model evaluation.	Mean annual values of interpolated precipitation. Daily meteorological data for the Penman-Monteith methods.
WASMOD	Temperature, precipitation and potential evapotranspiration (calculated with the FAO56 Penman-Monteith method based on daily wind-speed, mean temperature, relative humidity and sun hour data)	Monthly data
WATSHMAN-PCRaster model	Climate data: Precipitation, temperature, potential evapotranspiration (calculated with the FAO56-Penman method based on wind-speed, mean temperature, relative humidity and sun hours). GIS data: Soil types, land use, rivers, DEM.	Daily data

5.4 Scenario modelling

It is a generalised perception within the Nicaraguan public opinion that deforestation has severely affected major parts of the national territory over the past decades. This tendency towards the uncontrolled removal of the original forest cover has not been an exception to the Cocibolca Lake Basin. The idea is widely spread amongst local stakeholders that deforestation in the basin is (one of) the main cause(s) for several major, specific problems such as: increased erosion, increased sediment, nutrient and pesticide loads into the Cocibolca Lake from the surrounding territory, changes in local (sub-basin) hydrology, as well as the general degradation of land and water resources within the basin.

It is also widely acknowledged that climate change may have severe impacts on the availability and quality of water resources in the region, as well as on the occurrence of extreme events. The former is especially relevant considering the fact that a major part of the basin has a long dry season, and that under current conditions severe problems with the provision of drinking water in many localities of the basin already exist.

This short introduction indicates the importance of work to be conducted under WP8, in which the impacts of various plausible change scenarios on water resources in the basin should be evaluated. Work under WP8, however, will need to take into account the results and conclusions from the modelling applications (and uncertainty analysis) developed under WP3. A long-term goal for the Cocibolca Lake Basin is the assessment of impacts from plausible climate and land use change scenarios by means of the application of calibrated and validated spatially-distributed mathematical modelling tools; however, the feasibility of such an approach under TWINLATIN is very much dependent on the results and conclusions that are obtained under the present work package; current results with regard to the magnitude of uncertainties indicate that under TWINLATIN a more simple approach, allowing for a first, basic assessment of change impacts will be required. More details on the followed approach for the scenario impact assessment are given in the WP8 report.

5.4.1 Climate change scenarios

As a first approximation under TWINLATIN, climate change scenarios for the Cocibolca Basin (to be used for impact assessment) will be prepared based on output from the MAGICC-SCENGEN v4.1 scenario modelling tool, as part of a harmonised approach towards scenario generation applied by the different TWINLATIN partners.

Output from MAGICC-SCENGEN will consist of change signals for temperature (absolute change) and precipitation (% change) with regard to the 1961-1990 reference period, calculated for future 30-year time windows (mean values). These change signals will be obtained for the following two 5°x5° cells which both contain parts of the Cocibolca Basin: [90°-85° W | 10° - 15° N] and [85°-80° W | 10° - 15° N]. In addition to this, precipitation time series (0.5° x 0.5° grid cells) for both the reference period 1961-1990 and the future time windows 2071-2100 obtained from the RCM runs which have been executed by the Cuban Meteorological Institute (PRECIS tool; SRES scenarios A2 and B2, covering Central America and the Caribbean (<http://precis.insmet.cu/Precis-Caribe.htm>)) will be analysed, and a first assessment of the impact of using downscaled versus coarse-scale change scenarios on the basin's water balance will be made.

5.4.2 Land use change scenarios

Currently, three GIS forest cover maps are available for the Cocibolca Basin corresponding to the years 1983, 1990 and 2000, respectively. Unfortunately, standards and classification schemes that have been handled to prepare these maps based on the available input satellite imagery were highly heterogeneous for the different years. For this reason, the use of these maps for projecting future land use (forest cover) changes (e.g. based on a logical regression approach) is not recommended. The strong inter-annual climatic variability as well as the limited availability and quality of the discharge time series make it further improbable that impacts from land use change can be deducted from the observational datasets. Land use changes would have the largest impact on peak flow dynamics and amounts, and these high flow discharge data are judged to be very uncertain in the Cocibolca Basin.

As a conclusion from the former, at present no work on this component is thus further included under TWINLATIN, instead the recommendation is formulated for, firstly, the development of a binational, well-established and agreed-upon protocol and uniform classification scheme for the preparation of land use data layers for the Cocibolca Basin in all future work and, secondly, the need for increased attention to the improvement of the quality of the hydro-meteorological measuring network (and in particular, the validity of the rating curves) .

5.5 Model development

The main model development for the Lake Cocibolca Basin concerns: geo-statistical interpolation, distributed hydrological modelling, and uncertainty estimation.

Geo-statistical interpolation routines have been set up for the interpolation of time series of climate data in the basin using the freeware Gstat (Pebezma & Wesseling, 1998). This program is called from MATLAB within which the input data files needed for each time step are produced. In the case of kriging interpolation, the fitting of a curve to the sample semi-variogram obtained from Gstat is also performed in MATLAB. These semi-variogram parameters are then used by Gstat for the interpolation. This solution allows fitting of a semi-variogram with a nugget. The nugget effect is related to the uncertainty in the measured dataset; therefore, this option is especially important for dry months when spatial auto-correlation is low. Routines were implemented for four different interpolation methods: Ordinary Kriging (OK), Kriging with external drift (KED), Universal Kriging (UK) with coordinate base functions, and Inverse squared Distance Weighted (IDW) interpolation. Two routines for filling shorter gaps in climate data, the Coefficient of Correlation Weighting Method (CCWM) and the Inverse squared Distance Weighting method (IDW), were also coded in MATLAB and evaluated.

The distributed hydrological model used for the modelling of the Mayales sub-basin was developed in the PCRaster software, which is a GIS integrated with a dynamic programming module. The adjustment of the model to Nicaraguan conditions was described in section 5.2.3.

The PCRaster model has also been embedded in an uncertainty estimation framework as the quality issues with the precipitation data and the large expected uncertainties in discharge data make uncertainty estimation a central issue in this study. The method employed here is the Generalised Likelihood Uncertainty Estimation method, GLUE (Beven & Binley, 1992), a widely used and straightforward method that can be applied for assessing parameter uncertainty as well as input data uncertainty. The GLUE routines were all written in MATLAB and the PCRaster program is called from MATLAB during the uncertainty estimation (essentially consisting of Monte Carlo simulations in which different parameter combinations are applied).

5.5.1 Simple water balance modelling set-up

Before any hydrological modelling could be carried out it was necessary to first fill shorter gaps in the daily meteorological time series, in order to obtain more complete monthly data. With regard to gaps in the temperature data time series, a certain number of missing data per month can be accepted when the monthly averages are calculated. For precipitation data, the problem is more complex and gap filling is required: for this purpose, two methods were evaluated in this study. After filling the gaps, the mean areal precipitation needed to be calculated from the station data, and distributed precipitation maps created from the station data through interpolation. Results from the four different interpolation methods mentioned above were, therefore, compared in order to identify the method that worked best with this dataset.

Filling of shorter gaps in the precipitation data series

Two methods were evaluated for the filling of gaps shorter than a month in the climate data series: the Coefficient of Correlation Weighting Method (CCWM) (Teegavarapu & Chandramouli, 2005) and Inverse squared Distance Weighted interpolation (IDW; e.g. Isaaks & Srivastava, 1989). The CCWM is similar to the IDW method but the correlation coefficient is used instead of squared inverse distance

to calculate the weights of the n surrounding stations. The following equation shows the CCWM method for gap filling:

$$\theta_m = \frac{\sum_{i=1}^n \theta_i R_{mi}}{\sum_{i=1}^n R_{mi}}$$

where: θ_m is the missing value to be filled in and R_{mi} is the coefficient of correlation between the i -th station and station m with the missing value

Datasets consisting of all observations which were simultaneously available at two given stations were used in the calculation of the correlation coefficient; a minimum of 730 days within each dataset was set as a criterion for the calculation of the correlation coefficient. The filling of gaps was done for months where there was at least one day with data, in order not to lose this information when the monthly time series were calculated (the monthly data were computed from complete monthly datasets). If, for instance, only one day, or 5 days, were missing, the rest of the values for that month were filled. Gaps longer than a month were not filled here; instead, under such conditions the precipitation data are generated through the spatial interpolation process. The gap filling methods were evaluated separately for two different time periods, as the distribution of available stations in the study area changed considerably over time. Finally, a program was made for later use at INETER, which was based on the gap filling method that performed best in the present case study.

Interpolation of precipitation

The aim of the interpolation was to produce a monthly mean areal precipitation dataset for the whole catchment, as well as distributed maps of mean yearly precipitation needed for the simple water balance method. A second objective was to obtain the mean monthly spatial distribution of precipitation in the catchment, in order to characterise the precipitation regime.

The accuracy of the precipitation-interpolation method is important as it influences the quality of the final water balance calculations; therefore, four different methods were evaluated: Ordinary Kriging (OK), Kriging with external drift (KED), Universal Kriging (UK) with coordinate base functions and Inverse squared Distance Weighted (IDW) interpolation. Co-Kriging was also tested for mean annual precipitation. The interpolation methods are based on the assumption of spatial autocorrelation; it was shown (Figure 5.8) that this autocorrelation is much higher for monthly data than for daily data and the results of the interpolation will therefore be better for the monthly data. The number of precipitation stations with data during the interpolation period 1965 to 2005 varied between the years and this influences the quality of the interpolation: this was particularly the case for the calculation of precipitation in the Costa Rican part of the basin (Figure 5.7), where no time series data were available from 1994 onwards, and where precipitation amounts were highest (thus also impacting the quality of the mean areal precipitation calculations).

IDW is a simpler method where the precipitation at a missing location is calculated as an average of the precipitation at the surrounding stations weighted against the inverse of the squares of their distances from the prediction location. The following equation shows the IDW method for interpolation:

$$R_x = \frac{\sum_{i=1}^N R_{xi} \cdot d_{xi}^{-2}}{\sum_{i=1}^N d_{xi}^{-2}}$$

where: R_x is the predicted precipitation, R_{xi} the precipitation at the i -th station, d_{xi} is the distance between the i -th station and the prediction location and N is the number of stations.

IDW has been shown to produce results comparable to that of more advanced methods like kriging when the sampling density is high (Dirks *et al.*, 1998) or when there is low spatial dependence between observations (Goovaerts, 2000). In geostatistical methods, the variable to be interpolated is treated as a random variable and an explicitly stated stationary random function model (that describes the pattern of spatial continuity) is used for the estimation at un-sampled locations (Isaaks & Srivastava, 1989). Kriging, also known as a Best linear Unbiased Estimator (BLUE) aims at

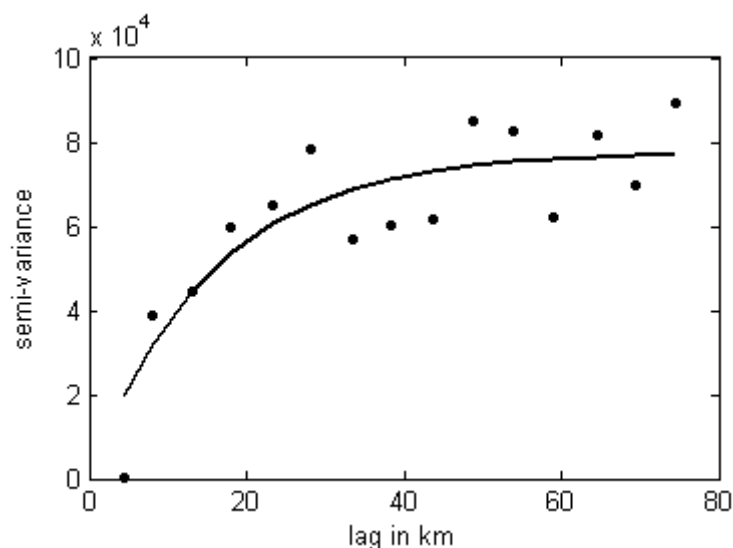


Figure 5.16 Example of sample semi-variogram with fitted curve

minimising the error variance and a zero mean residual error. To define the pattern of spatial continuity of the random function model a variogram is usually used. In practice the sample variogram – to which a curve is fitted – is calculated from half of the averaged squared difference between all pairs of observed data, which is then plotted against distance between data points (Goovaerts, 2000) (see Figure 5.16).

In ordinary kriging, the weights used in the estimation of the ungauged points are calculated from the ordinary kriging set of equations, and the co-variances for different distances are derived from the fitted semi-variogram. The precipitation at the prediction location is then calculated as:

$$R_x = \sum_{i=1}^N \theta_i R_i$$

where: R_x is predicted precipitation, R_i is precipitation at the i -th station, θ_i is weight for the i -th station and N is the number of stations.

For universal kriging, first a trend is modelled and subtracted from the data where afterwards the residual semi-variogram is calculated. For kriging with external drift, elevation is used as a secondary variable to estimate the trend locally, and the elevation information is used at all prediction locations where a digital elevation model is needed. In co-kriging a separate variogram is estimated for the auxiliary variable. In this study an exponential variogram with a nugget effect was used; the nugget parameter corresponds to the semi-variance at lag zero and is related to sampling error and short-scale variability (Isaaks & Srivastava, 1989). If the semi-variogram curve is modelled as a pure nugget (i.e. a straight horizontal line) the ordinary kriging method reduces to a simple averaging of the data i.e. there is no increase in semi-variance with distance and all stations thus get the same weight. The freely available geo-statistical software Gstat (Pebezmá & Wesseling, 1998) and the Gstat package in R (Pebezmá, 2004) were used for the interpolation of monthly time series data and mean monthly precipitation, but the automatic fitting of a curve to the sample semi-variogram was done in MATLAB using the polyfit function in order to improve the fitting of the nugget parameter. As low spatial autocorrelation was generally found for dry months, it was important that the method used for fitting a curve to the semi-variogram could include this nugget effect. The kriging was performed as block kriging with blocks the size of 900 m (chosen to be an even multiple of the DEM pixel size) and a discretising size of 100 points per block. The mean annual precipitation interpolation was performed with ArcGIS Geostatistical Analyst and anisotropic semi-variograms were used.

Calculation and analysis of evapotranspiration

Potential evapotranspiration was calculated with the full Penman-Monteith equation (ET_{FPM}) at the five meteorological stations which had sufficient data for this purpose for the period 2000-2005. ET_{FPM} was compared to: (i) FAO56 Penman-Monteith calculated from the same data (ET_{FAO}); (ii) measured PanA evapotranspiration, as well as to (iii) ET from the MODIS-project (where water availability have been taken into account in the ET-calculations) (Table 5.8).

The evapotranspiration was calculated using the Penman-Monteith equation (PM) in its full form (Monteith, 1965). Meteorological input data to Penman-Monteith are daily mean values of air temperature, relative humidity, wind speed and hours of sunshine.

Since the aerodynamic and surface resistance formulations are the main differences between the Penman-Monteith, FAO and MODIS algorithms, a short review of the calculations used in the full Penman-Monteith is given as a basis for the discussion in the following sections.

The aerodynamic resistance, r_a , is parameterised as:

$$r_a = \frac{\ln\left(\frac{z-d}{z_{0m}}\right) \ln\left(\frac{z-d}{z_{0v}}\right)}{\kappa^2 u_z}$$

where: z is reference height (m), d is zeroplane displacement height (m), z_{0m} is roughness length for momentum (m), z_{0v} is roughness length for water vapour (m), κ is von Karmann's constant 0.41 (-) and u_z is wind speed at reference height z ($m s^{-1}$).

The zeroplane displacement height, d , is given by:

$$d = \frac{2}{3} h$$

where: h is vegetation height (m)

The roughness length for momentum, z_{0m} , is given by:

$$z_{0m} = 0,123h$$

where: h is again vegetation height (m)

The roughness length for water vapour, z_{0v} , is calculated as:

$$z_{0v} = 0,1z_{0m}$$

The surface resistance for diffusion of water vapour through the stomata openings, r_s , is parameterised as:

$$r_s = \frac{r_{leaf}}{0,5LAI}$$

where: r_{leaf} is surface resistance for a single leaf ($s m^{-1}$) and LAI is leaf area index ($m^2 m^{-2}$)

Because only one side of the leaf has stomata openings the LAI is multiplied by the coefficient 0.5 in the last equation. The vegetation parameters used in the full Penman-Monteith were set to the same values – where applicable – as typically used by the FAO56 representing tall grass:

Reflection coefficient (albedo) $\alpha = 0.23$

$h = 0.12$ m

$r_{leaf} = 100$ $s m^{-1}$

$LAI = 3.0$ $m^2 m^{-2}$

Simple water balance

The long-term water balance, R , was calculated simply as interpolated precipitation minus evapotranspiration:

$$R = P - E$$

where: P is precipitation (mm) and E is evapotranspiration (mm)

The calculations were performed for the period 2000-2005 using the evapotranspiration data from the MODIS-project, as only these data had a sufficient coverage of the basin.

5.5.2 Model set-up for the Mayales sub-basin

Monthly water balance modelling

Monthly water balance calculations with uncertainty analysis were performed with the WASMOD-model for the Mayales sub-basin. The input to the WASMOD-model consisted of monthly values of temperature, precipitation and potential evapotranspiration calculated with the FAO56 Penman-Monteith equation (Allen *et al.*, 1998). Precipitation stations that were within a distance of 20 km from the sub-basin border were included in the interpolation; stations further away were not expected to influence the interpolation to a considerable degree. Because of the reduced number of precipitation stations that were available within and in the vicinity of the sub-basin, the monthly precipitation was interpolated with the IDW method instead of a more advanced geo-statistical method like kriging (Figure 5.17).

Model calibration was performed for two different evaluation criteria: the standard Nash-Sutcliffe (Nash & Sutcliffe, 1970), and limits-of-acceptability around the observed discharge (Beven, 2006). The limits of acceptability, that should be chosen prior to running the model (e.g. by evaluation of rating curve accuracy), are the acceptable deviations between simulated and observed values based on a consideration of the sources of observation and commensurability errors in the modelling process.

The limits-of-acceptability were calculated as a function of discharge, and allowed for a larger acceptable spread of simulated results around the observed discharge values for high flow conditions, and a much smaller for low flows. Ideal model performance should result in a simulated discharge which is within the limits of acceptability 100% of the time. Here the limits-of-acceptability criterion, R_{LA} , was calculated as the percentage of time that the simulated discharge was within the previously established limits of acceptability. These limits were defined as a percentage, P , around the observed discharge data:

$$R_{LA} = 1 - T_{LA}$$

where:

$$LA = Q_{obs} \pm Q_{obs} * P$$

and where:

$$P = e^{-300 \left(\frac{Q_{obs}}{\max(Q_{obs})} \right)^2} + 0.6$$

where: T_{LA} is the percentage of time that the observed discharge is not within the limits of acceptability, Q_{obs} is the observed discharge at a certain day, 300 is a scaling coefficient and 0.6 is the accepted error percentage (60%) for maximum discharge.

As rating curve data were not available for analysis of the uncertainty in observed discharge, these scaling coefficients were set purely based on an estimation of the uncertainties in input data and observed discharge.

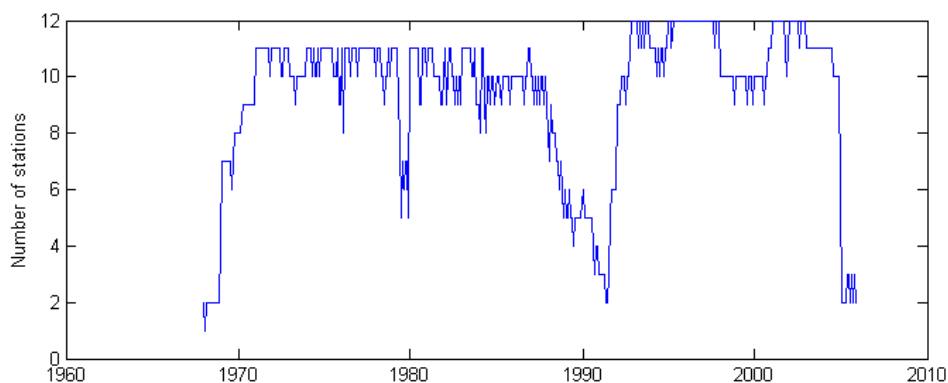


Figure 5.17 Number of stations with monthly data available within a 20 km radius of the Mayales catchment over time

A total of 200,000 simulations were made with the model and all model simulations achieving a higher value than the behavioural threshold were considered acceptable. The uncertainty bounds for the calibration period, which show the interval of the accepted discharge predictions, were calculated using the results from all acceptable model runs. The acceptable parameter sets were then used for the model application for the validation period: again all parameter sets that gave simulations better than the threshold values during the validation period, were used to construct the uncertainty bounds for this period.

Distributed daily modelling

For distributed rainfall-runoff modelling of the Mayales Basin with a daily time step, the WATSHMAN-PCRaster model was set up with a grid cell resolution of 720 m: a relatively coarse cell resolution was selected as a reasonable simulation speed was needed for the uncertainty estimation within GLUE, (the resolution of the available original SRTM DEM was 30 m). Flow patterns were derived from the Digital Elevation Model and in the model water is accumulated in this flow network and the stream network derived from it (Figure 5.18).

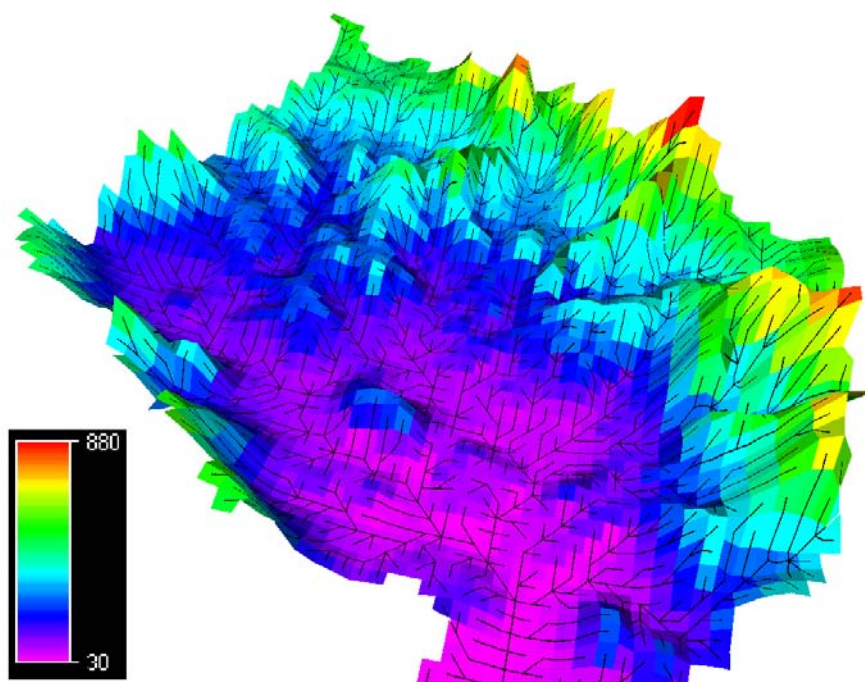


Figure 5.18 Digital elevation model (720 m pixel size) and flow network for the upper part of the Mayales basin, elevation in metres

Input data on soil type for the Mayales catchment consisted of four different soil classes which were obtained from the Mapa Agroecológico (1:50,000 resolution) from MAGFOR; these were reclassified into three main classes: Clay loam, Clay and Heavy clay (Figure 5.19).

Soil type parameter values and Manning roughness coefficients (Table 5.2) were taken from Chow *et al.* (1988) and Grip & Rodhe (1985). These values were then used as a guideline in the calibration process; model parameter values were sampled from intervals around these literature values.

The discharge data series (Figure 5.20) contained many gaps and the uncertainty in the data were judged to be high due to the difficulties to measure discharge in these types of rivers with unstable cross-sections (due to substantial erosion and sedimentation taking place in the river channel). Especially the high flow data can be considered to be very uncertain, as peak flows have a short duration and few measurements at very high flows are typically included in the existing rating curves. The discharge data time series were revised and inconsistencies and outliers removed (for some longer periods, the observed discharge exceeded the observed precipitation; in addition to this, the discharge values deviated clearly from earlier periods).

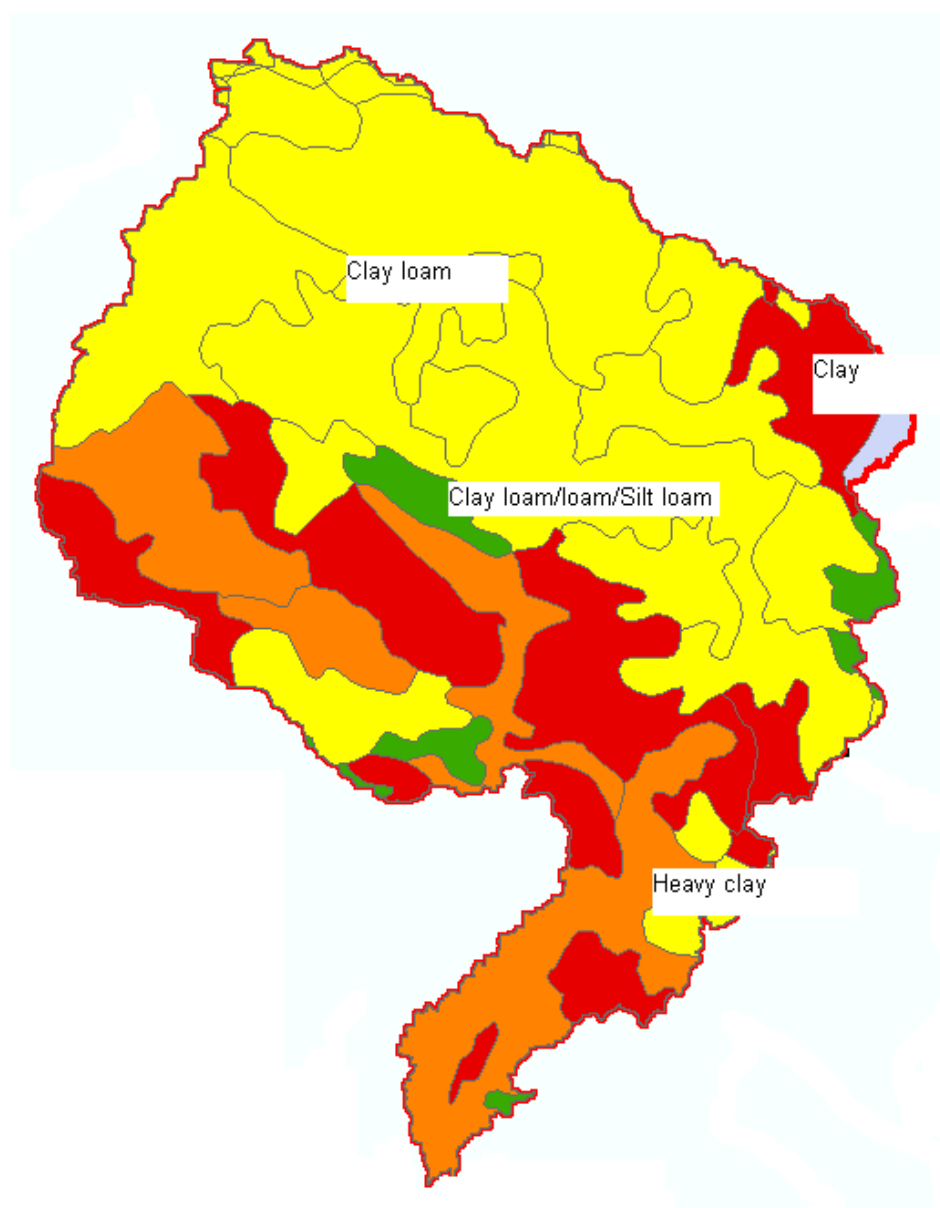
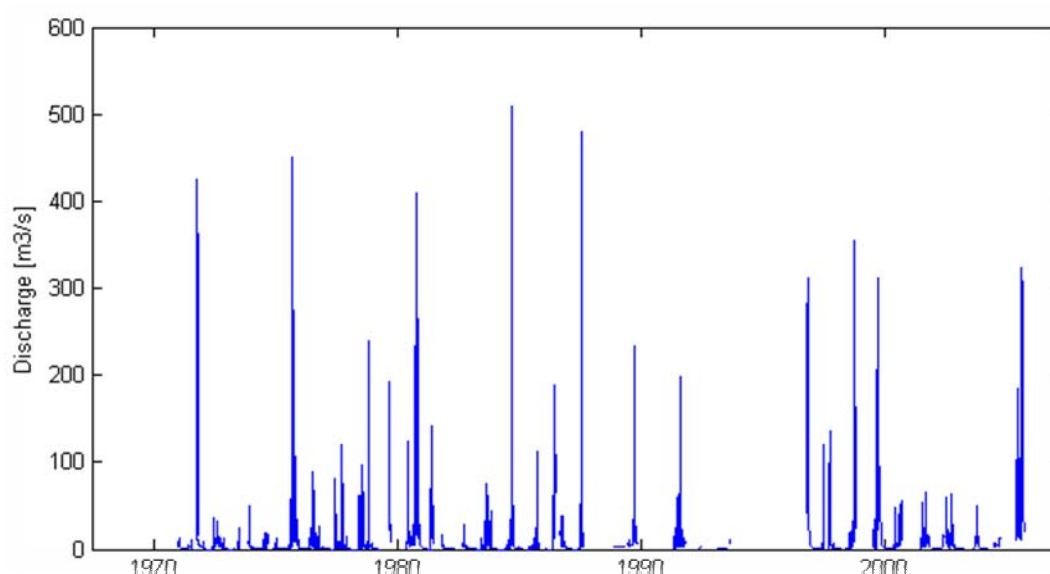


Figure 5.19 Soil types in the Mayales catchment, classification from Mapa Agroecológico 1:50,000, (MAGFOR)

Table 5.2 Soil type parameter values for the soils in the Mayales basin

Parameter	Mannings roughness coefficient	Θ_{wilt}	Porosity (%)	Hydraulic conductivity (cmh^{-1})	Field capacity
Values	0.04-0.05	Clay 0.21-0.23 Clay loam 0.17-0.23 Heavy clay 0.23-0.25	Clay 0.43-0.52 Clay loam 0.41-0.52 Heavy clay 0.47-0.53	Clay 0.03 Clay loam 0.10 Heavy clay 0.001	Clay 0.38-0.39 Clay loam 0.35-0.39 Heavy clay 0.37-0.39
Source	Chow <i>et al.</i> (1988), p35	Grip and Rodhe (1985)	Chow <i>et al.</i> (1988), p35; Grip & Rodhe (1985)	Chow <i>et al.</i> (1988), p35; Grip & Rodhe (1985)	Grip & Rodhe (1985)

**Figure 5.20** Daily (unrevised) discharge data from the Jicaral station in the Mayales catchment

Interception from different land uses was not modelled as there were no appropriate land use data for the calibration period available at the start of the simulations. However, this is not likely to have a large effect on the simulated results as interception storage is small compared to the high amounts of daily precipitation in the catchment. In the model, the groundwater is modelled as a linear reservoir. An analysis of the recession curves of the daily discharge data were made, in order to determine an approximate value for the groundwater recession parameter. An exponential curve (see recession equation for a linear reservoir below) was fitted to the recession periods of the observed discharge datasets, and a value of around 20 to 40 for the k parameter was obtained.

$$Q = Q_0 e^{-\frac{1}{k}t}$$

where: k is the recession parameter (1/day), Q is discharge (mm/day) and t is time (day).

5.6 Calibration and validation

5.6.1 Water balance modelling: Filling of shorter gaps in the time series

A cross-validation was performed to evaluate the performance of the two methods for gap-filling in precipitation data at all stations with daily data during the periods 1970-1995 and 1996-2005 (Table 5.3).

The CCWM method performed better than IDW for all evaluation criteria. A clear increase in the coefficient of determination can be observed for the monthly scale compared to the daily scale – this is not surprising as correlation between stations is much higher on a monthly scale than on a daily scale (Figure 5.8). The observed and filled data series showed good correlation on a monthly time scale, and the smoothing effect of the interpolation process is apparent in the lower interpolated than observed peak values (Figure 5.21).

Based on the former results, it was decided to use the CCWM method for the filling of shorter data gaps. The conversion of daily precipitation data to monthly data were done requiring complete data for the entire month. The gap-filled dataset contained 644 additional monthly data values, compared to the original monthly dataset based on the non-filled daily time series. The mean gap length filled with the CCWM-method was 5.5 days. A comparison of the chronogram of the monthly data before and after the gap filling shows the clear increase in the number of months with data (Figures 5.22 and 5.23).

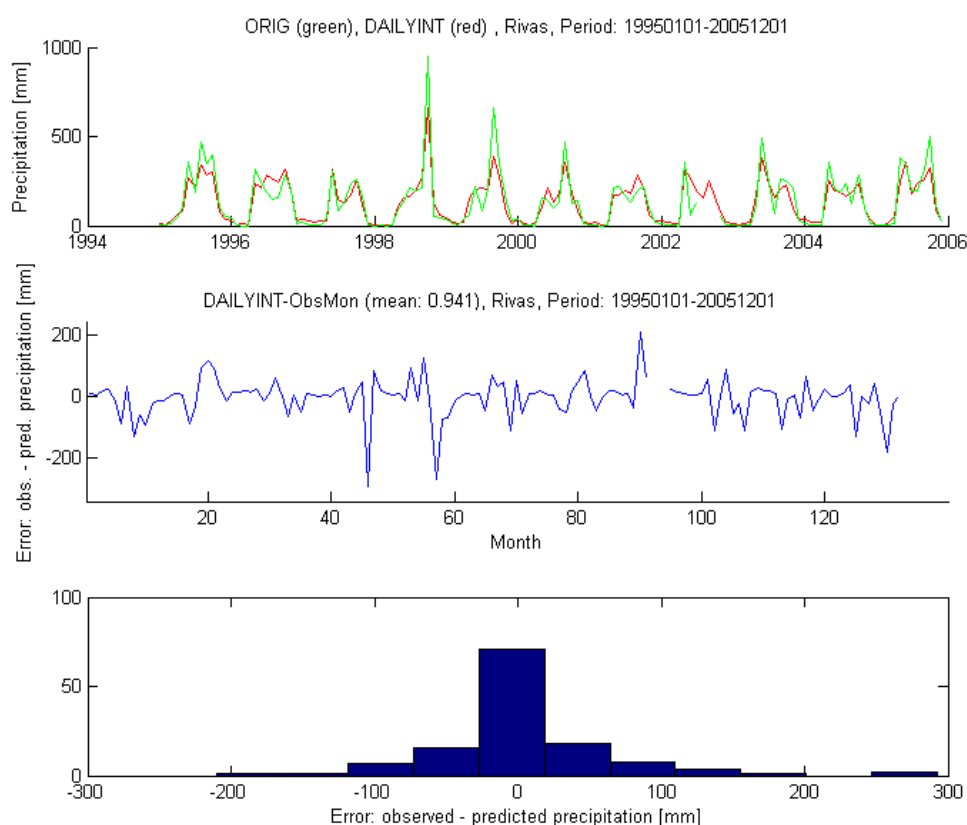


Figure 5.21 Results of the CCWM gap filling method at the station Rivas for the period 1995-2005, observed and filled in values have been converted to monthly values.

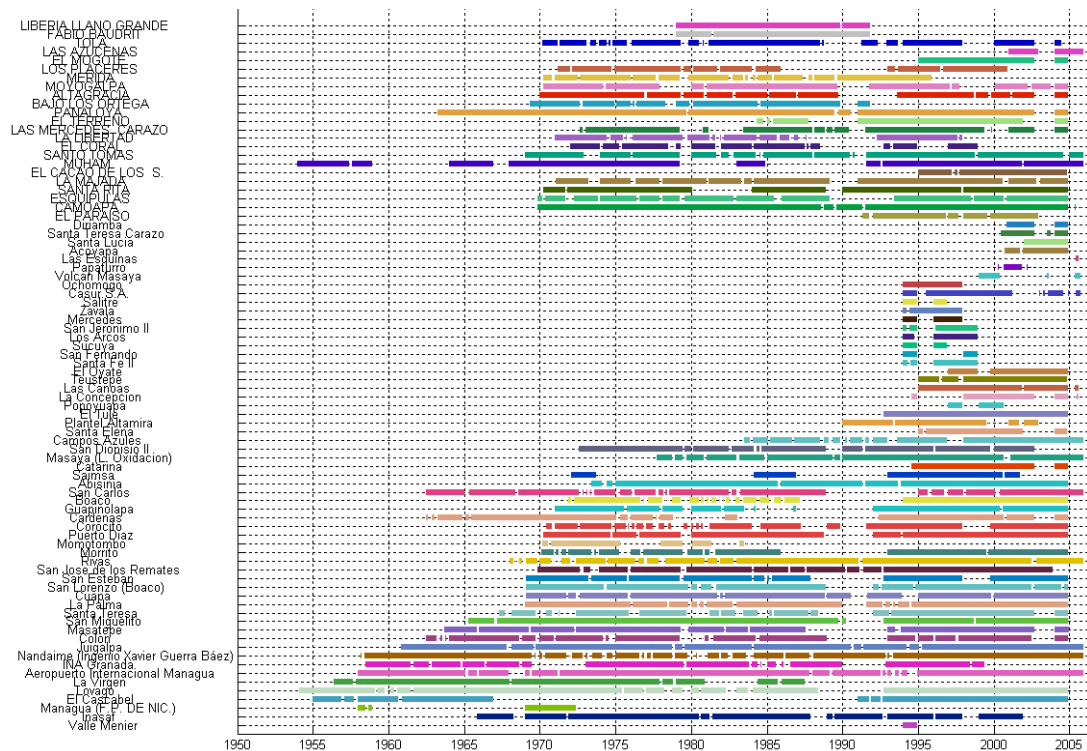


Figure 5.22 Chronogram of original daily data converted to monthly data

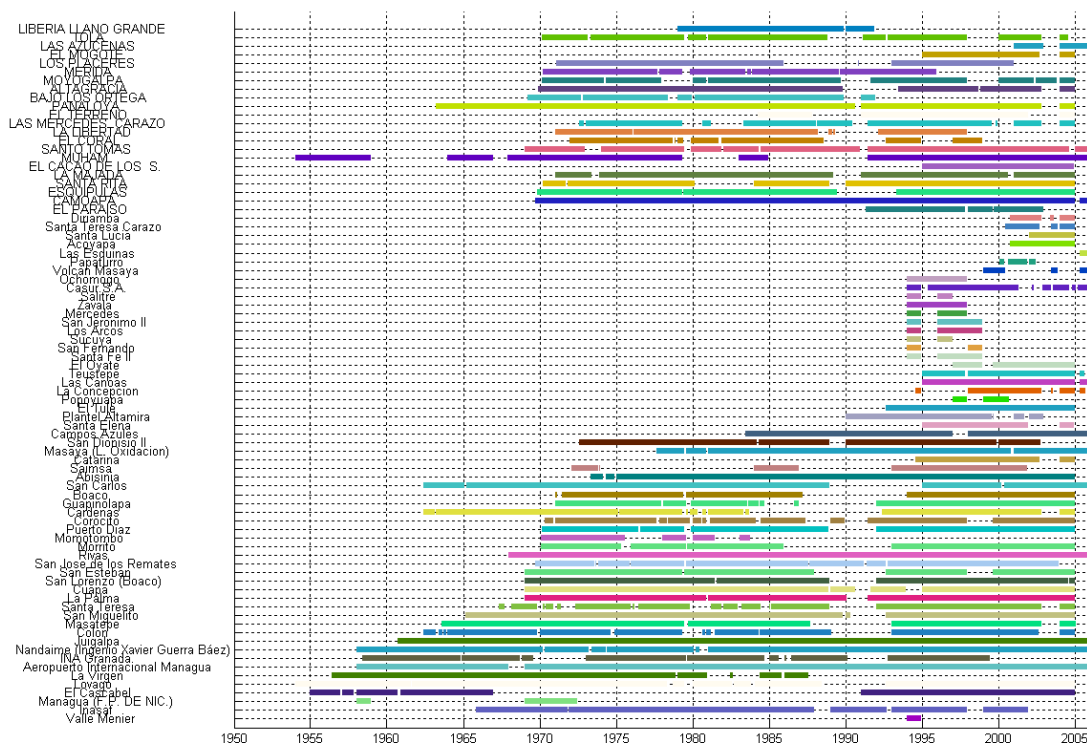


Figure 5.23 Chronogram of monthly data after gap-filling with the CCWM method

Table 5.3 Mean error measures at all stations for the evaluation of gap-filling methods

	1970-1995		1996-2005	
	IDW	CCWM	IDW	CCWM
R^2_{daily}	0.23	0.32	0.24	0.30
R^2_{monthly}	0.71	0.78	0.69	0.74
MAE_{daily} (mm)	4.66	4.18	4.96	4.57
MAE_{monthly} (mm)	55.90	44.30	60.32	50.75
MRE_{daily} (%)	2.93	2.59	2.71	2.60
MRE_{monthly} (%)	2.57	1.63	2.49	1.78
$RMSE_{\text{daily}}$ (mm)	9.73	9.25	10.70	9.84
$RMSE_{\text{monthly}}$ (mm)	77.99	65.36	88.64	76.72

5.6.2 Water balance modelling: Interpolation of precipitation

Spatial characteristics of rainfall and mean annual precipitation distribution

The degree of spatial autocorrelation between the station precipitation data are described by the semi-variogram, estimated from the data during the kriging interpolation. If the spatial autocorrelation is high, data from stations close to each other are more similar than data from stations far apart. In the semi-variogram for mean annual precipitation 1995-99, calculated on stations with more than 50% data in that period (there were no stations in the Costa Rican part of the basin) it can be seen that the averaged squared difference between the pairs of the stations (the semi-variance) increases with distance between the stations and the spatial autocorrelation is thus rather high (Figure 5.24).

The spatial autocorrelation in the Nicaraguan part of the basin was however different from that of the Costa Rican (southern) part; the sample semi-variograms for mean annual precipitation for the 1975-85 period (when there were many stations operational throughout the basin), show that at short distances the semi-variance was much higher in the Costa Rican part; an anisotropic (different in different directions) semi-variogram can be used to address this situation (Figure 5.25).

There was not a clear increase in precipitation with elevation in the Costa Rican part of the basin, and this could probably be explained by rain shadow effects in the mountains (Figure 5.7). A comparison of different interpolation methods (Universal Kriging, Ordinary Kriging, Inverse Distance Weighting and Co-Kriging with elevation as the second variable) for mean annual precipitation was made for the years 1975-1994 when there were stations with data in the southern part of the basin (Figure 5.26).

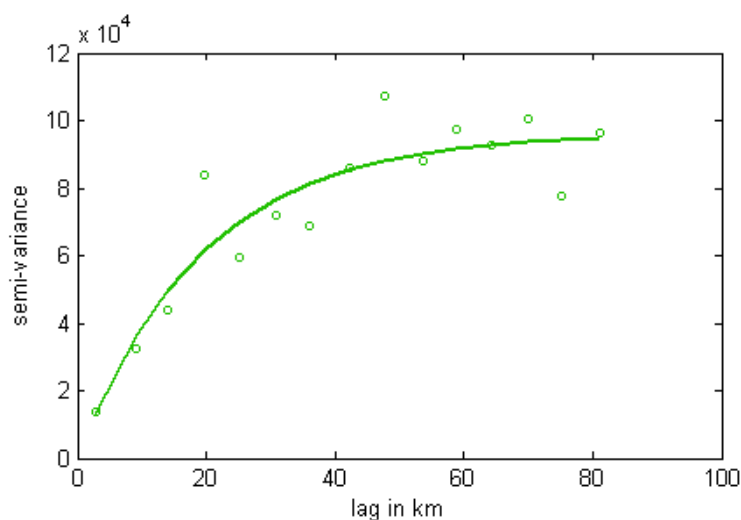


Figure 5.24 Sample semi-variogram for mean annual precipitation 1995-99, calculated on stations with more than 50% data in that period

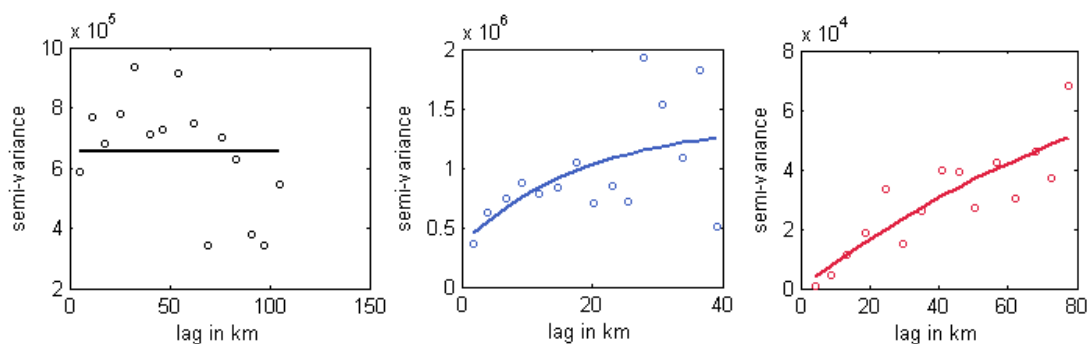


Figure 5.25 Sample semi-variogram for mean annual precipitation 1975-85, calculated on stations with more than 70% data in that period, for the whole basin (left), Costa Rican part (middle) and Nicaraguan part (right).

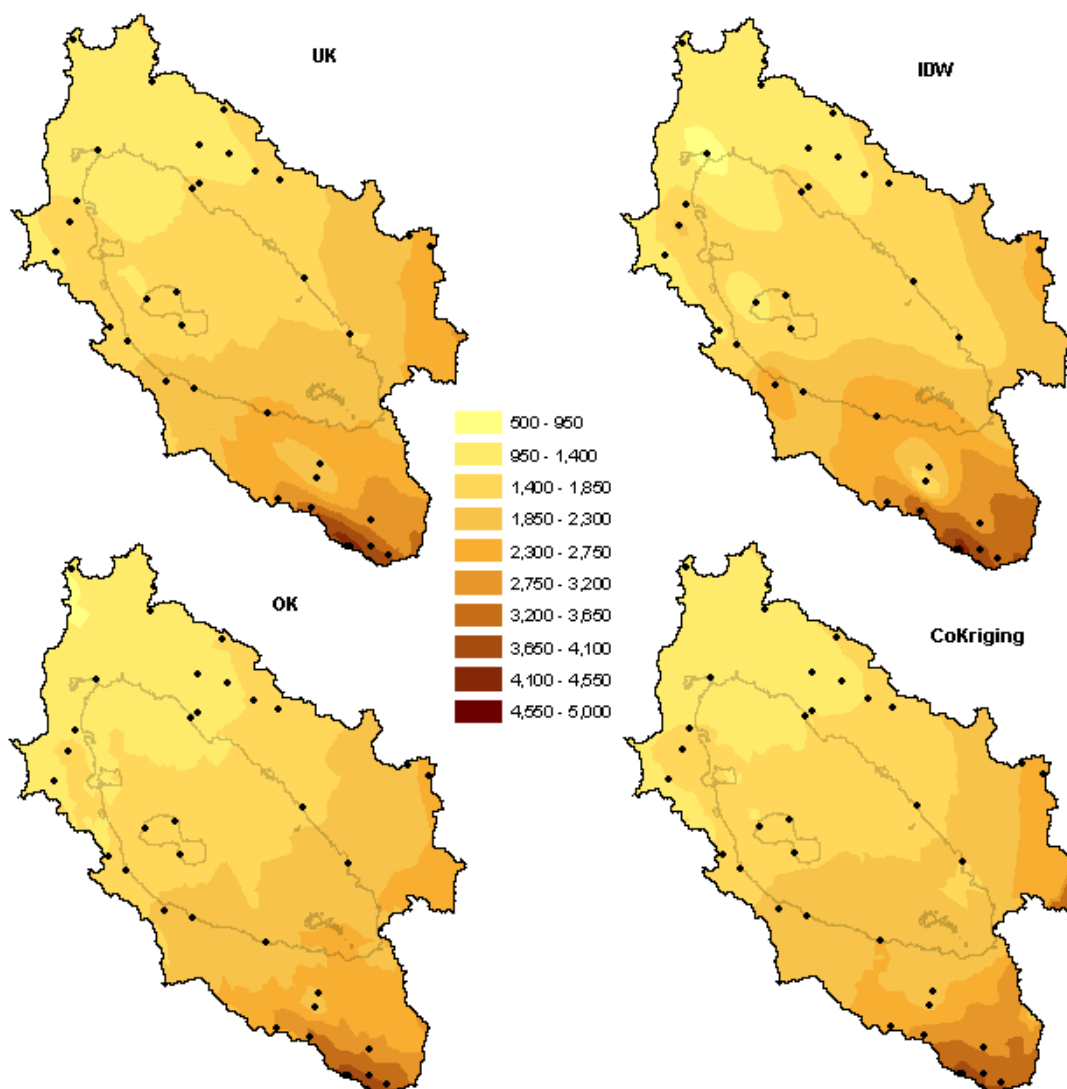


Figure 5.26 Comparison of methods for mean yearly precipitation in 1975-1994 calculated on stations with more than 30% complete years of monthly precipitation; stations within the basin are shown as black dots.

Universal Kriging with a first-order trend gave the lowest RMSE which appears reasonable as there was a trend with higher precipitation values in the south-east. The UK-method was used for the calculation of mean annual precipitation for the simple water balance model as it showed the best accuracy (Table 5.4) in this period and also in the period 2000-2005 (not shown). Co-kriging was performed with elevation as the second variable but did not yield a very good estimate as there was not a clear altitudinal variation in precipitation due to e.g. rain shadow effects.

Table 5.4 Cross-validation errors for interpolation of mean annual precipitation data in the whole basin 1975-1994.

	Ordinary Kriging (OK)	Universal Kriging (UK)	IDW	Co- Kriging
Mean error (mm)	-16	26	24	-24
RMSE (mm)	479	430	488	504

Mean monthly precipitation regime

The range of monthly precipitation in the basin for the 20-year period 1975-1994 was calculated on the stations with more than 50% complete years of monthly precipitation (Figure 5.27). The start of the rainy season was well defined at all stations and for most stations the midsummer drought was clearly seen, appearing in general later for stations with high precipitation compared to those with the lowest precipitation amounts.

These data were also used for interpolation of monthly precipitation distributions in the basin (Figures 5.28 and 5.29) with IDW. The strengthening of the easterly trade winds in July-August and the associated increased precipitation on the Caribbean Coast of Nicaragua are apparent as well as the NW-SE gradient. Note the different scales for each monthly map.

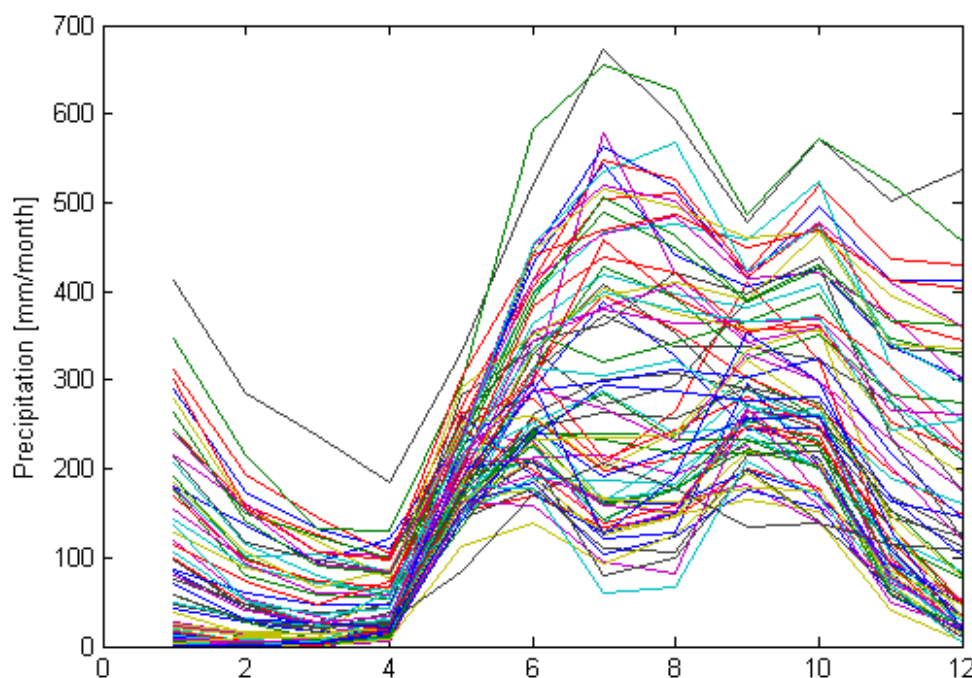


Figure 5.27 The range of monthly precipitation in the basin for the 20-year period 1975-1994 was calculated on the stations with more than 50% complete years of monthly precipitation.

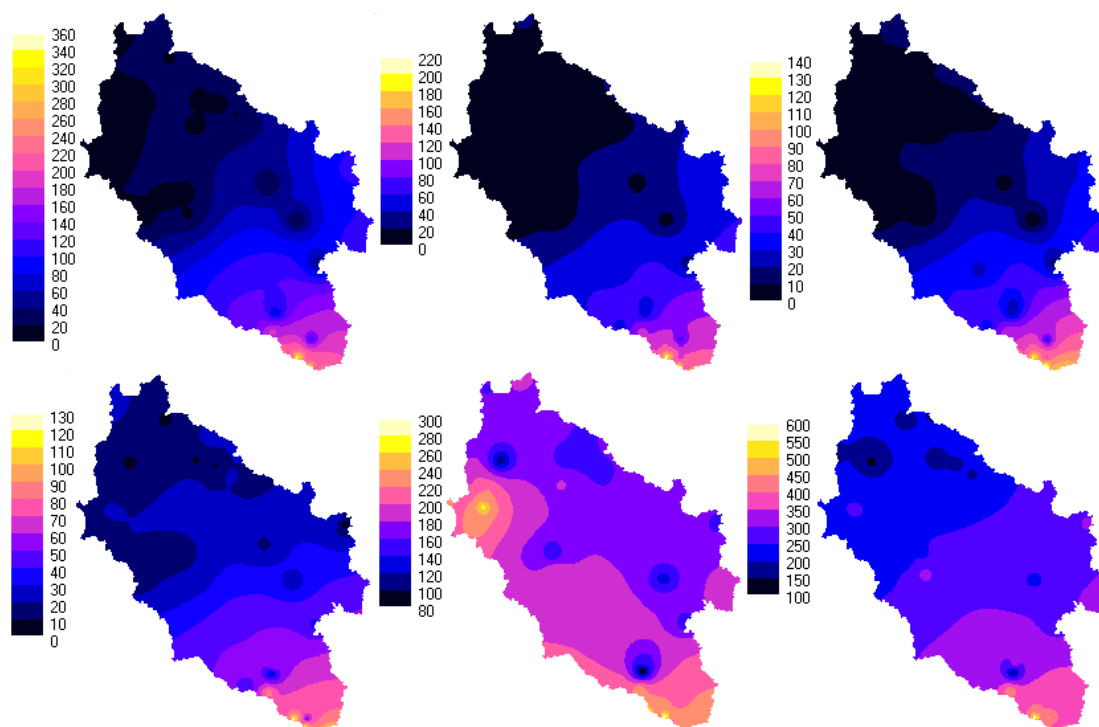


Figure 5.28 Mean monthly precipitation for the 20-year period 1975-1994 was calculated on stations with more than 50% complete years of monthly precipitation. January through March is shown in the upper row (left to right) and April through June in the lower row (left to right).

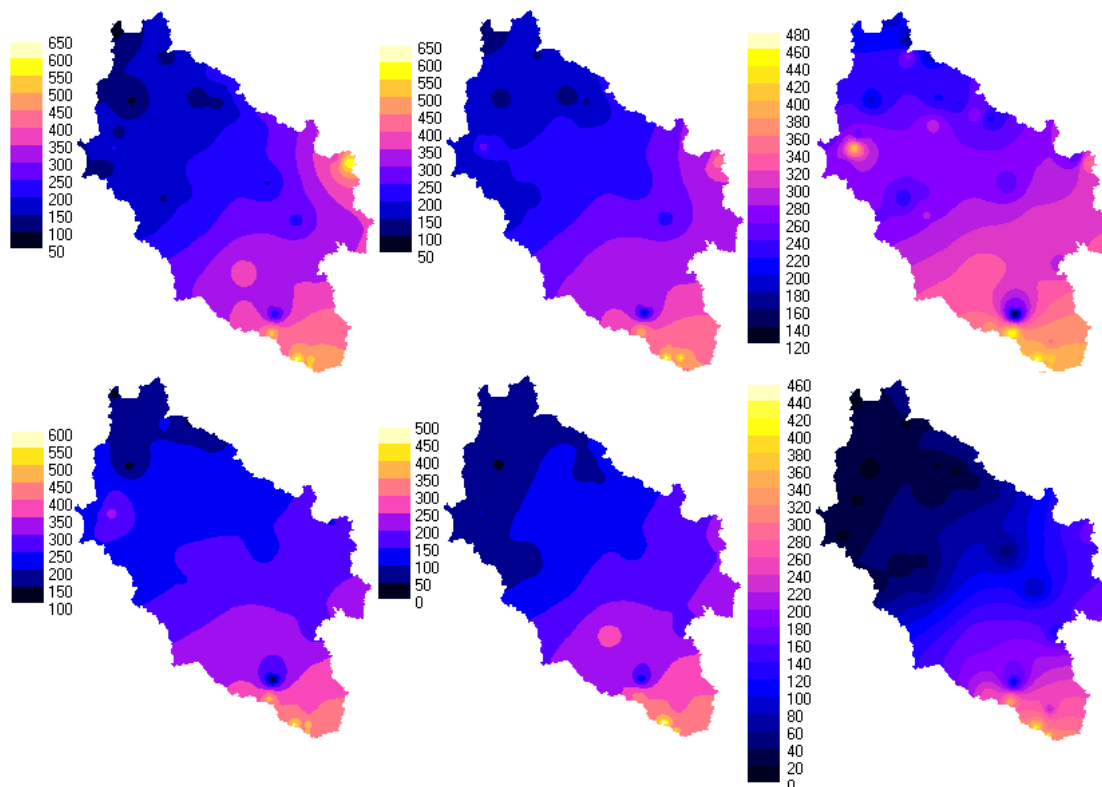


Figure 5.29 Mean monthly precipitation for the 20-year period 1975-1994 was calculated on stations with more than 50% complete years of monthly precipitation. July through September is shown in the upper row (left to right) and October through December in the lower row (left to right).

The greater influences from the Pacific Ocean in May-June and September-October can be seen in the mountains in the westernmost part of the basin, as well as the pronounced dry season in the north-western parts. In the eastern parts close to the Caribbean coast there were high precipitation amounts in July-August and November. Interpolated mean monthly areal precipitation amounts were lowest in March and highest in September (Table 5.5).

Table 5.5 Mean areal monthly precipitation amounts

	Jan	Feb	Mar	Apr	May	Jun	Jul	Aug	Sep	Oct	Nov	Dec
Precipitation (mm/month)	63	35	23	32	182	266	258	258	284	267	157	103

Interpolation of monthly time series data

The monthly gap-filled precipitation was interpolated (Figure 5.30) for the whole basin for the period 1965 to 2005, the IDW and UK provided the best results during the cross-validation (Table 5.6 and 5.7).

IDW and UK gave the best results for the monthly interpolation (Table 5.6). The spatial variability was greater on a monthly scale and only one semi-variogram in all directions was used in the automatic semi-variogram estimation, which might explain why the IDW-method gave better results in the cross-validation than the kriging methods. There was not a very clear relation with elevation in the Costa Rican part and the Kriging with external drift (KED) therefore gave rather low cross-validation results.

In conclusion, the UK-method can be recommended for interpolation of mean annual precipitation in the basin and IDW for automated interpolation of time series data. The complex topography, rain shadow effects, lack of measurements over the lake and data availability problems limits the estimation of the precipitation regime.

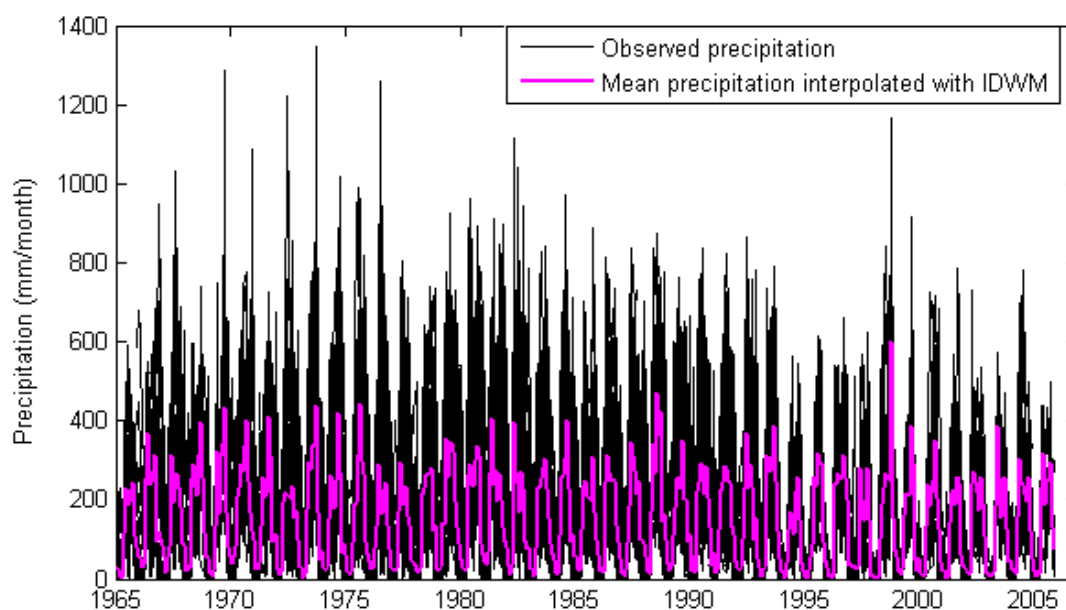


Figure 5.30 Gap-filled monthly precipitation for all stations and mean areal precipitation interpolated with the IDW-method.

Table 5.6 Cross-validation errors for interpolation of monthly precipitation data in the whole basin 1965-2005. Errors are given as observed minus interpolated.

	OK	UK	IDW	KED
Correlation coefficient	0.36	0.57	0.59	0.40
Mean error (mm)	-0.67	-1.07	-3.88	-1.08
Max. pos. error (mm)	286	254	242	284
Max. neg. error (mm)	-143	-171	-176	-193
Mean abs. error (mm)	67	56	53	66
Mean relative error (%)	4.28	2.08	1.85	3.22
RMSE (mm)	88	77	74	89

Table 5.7 Cross-validation mean statistics of monthly data for different interpolation methods and observed data 1965-2005

Statistics for 1965-2005	OK	UK	IDW	KED	Observed
Minimum (mm)	113	59	74	98	28
Maximum (mm)	271	304	336	390	479
Mean (mm)	168	168	171	168	167
Median (mm)	159	170	159	150	141
Standard deviation (mm)	35	67	68	56	102

5.6.3 Water balance modelling: Calculation and analysis of evapotranspiration

Potential evapotranspiration was calculated with the Full Penman-Monteith equation (ET_{FPM}) at five meteorological stations having sufficient data for the period 2000-2005. ET_{FPM} was compared to FAO56 Penman-Monteith calculated from the same data (ET_{FAO}) and measured PanA evapotranspiration as well as evapotranspiration from the MODIS-project (Table 5.8).

Full Penman-Monteith data were converted to 8 day-values for comparison with MODIS-data (Figures 5.31 and 5.32). MODIS-data were lower than Full Penman-Monteith and the difference was greatest in the north-west, driest part of the basin (Aeropuerto Internacional Managua) compared to the wetter areas in the south-east part (San Carlos).

Table 5.8 Comparison of mean evapotranspiration values (mm) for 2000-2005

Station	Missing days in calculation with FPM and FAO56	Full Penman-Monteith (ET_{FPM})	FAO56 (ET_{FAO})	PanA	MODIS project
Aeropuerto Internacional Managua	34	1351	1810	2656	336
Juigalpa	165	1255	1584	2246	446
Nandaime	3	1315	1840	2632	607
Rivas	63	1235	1566	1876	576
San Carlos	136	1130	1287	1095	785

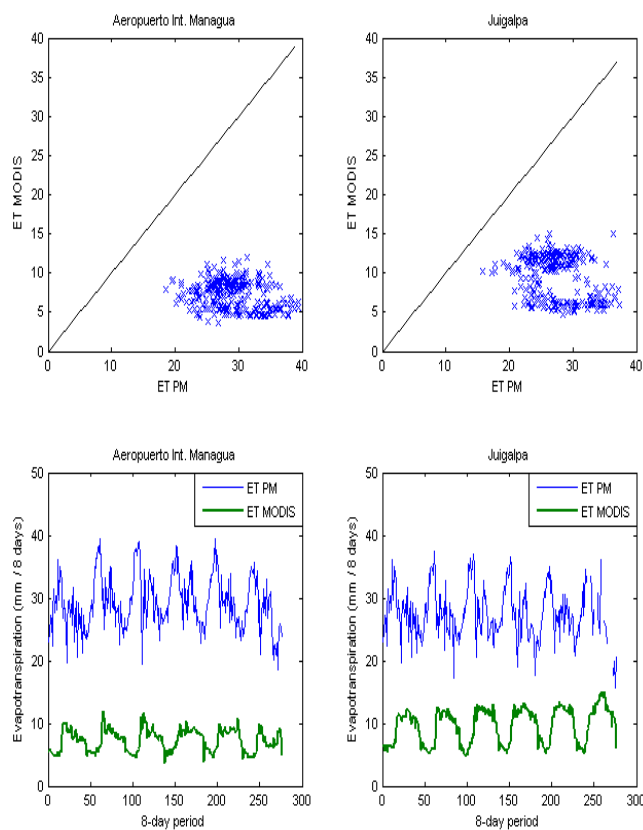


Figure 5.31 Comparison of 8-day evapotranspiration calculated with the Full Penman-Monteith equation and from the MODIS project.

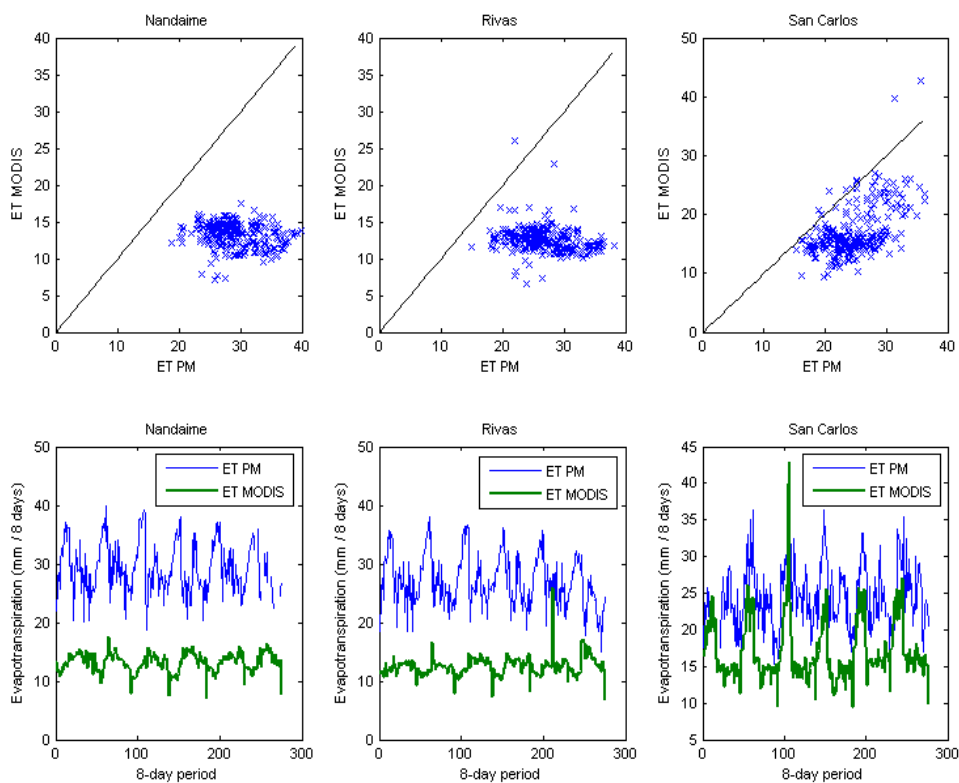


Figure 5.32 Comparison of 8-day evapotranspiration calculated with the Full Penman-Monteith equation and from the MODIS project.

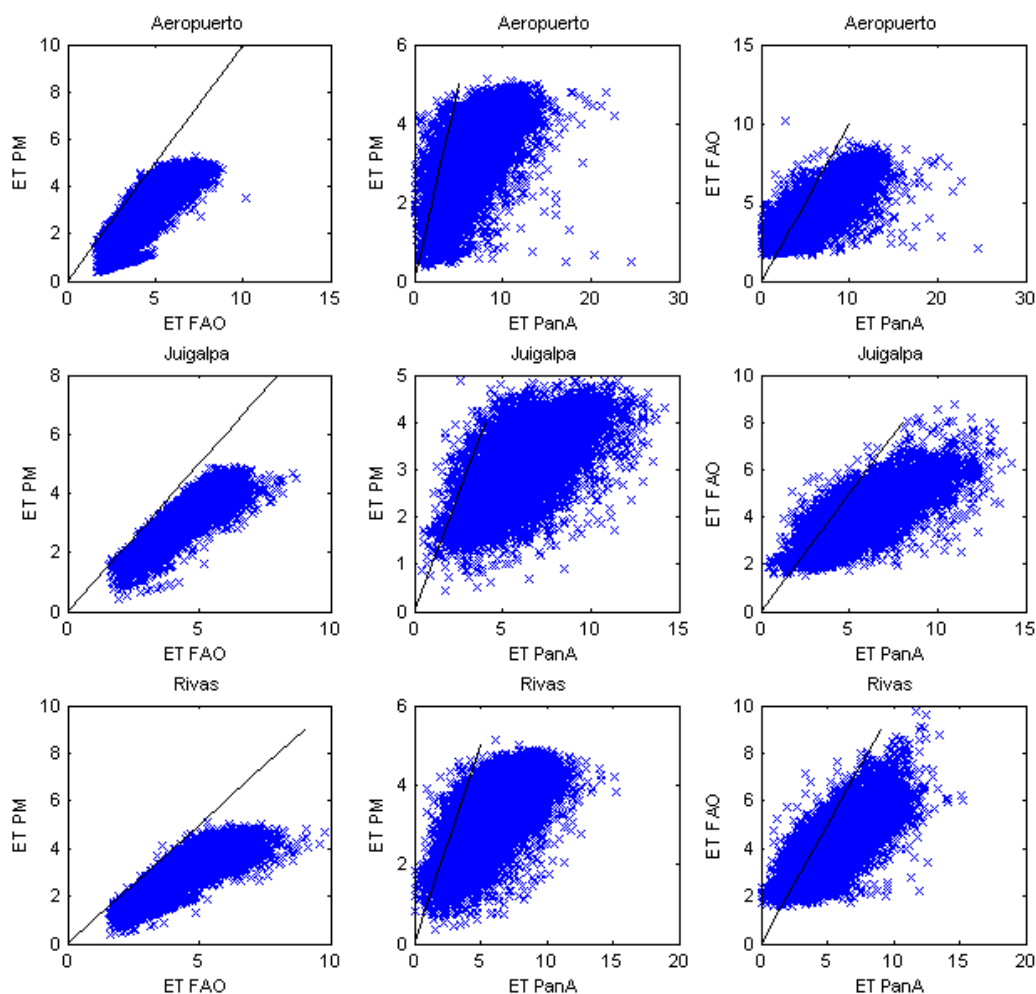


Figure 5.33 Cross-comparison of evapotranspiration calculations and PanA evapotranspiration at Aeropuerto Internacional Managua, Juigalpa and Rivas stations

FAO56 gave 28% higher annual mean potential evapotranspiration for the years 2000-2005 than Full Penman-Monteith which was attributed to the simplified and less dynamic formulation of the aerodynamic resistance term in FAO56. Overestimation of potential evapotranspiration by FAO56 compared to Full Penman-Monteith has been reported in several studies where the performance of the two formulations has been compared with lysimeter data for grass and crops. The overestimation was also seen on a daily scale comparing calculated Full Penman-Monteith and FAO56 data, which were also compared to measured PanA evapotranspiration for three stations (Figure 5.33).

MODIS-calculated evapotranspiration was only 25-70% of the 2000-2005 annual mean potential evapotranspiration calculated with the Full Penman-Monteith formulation. The main difference is that the formulation of the Penman-Monteith used here assumes that there is no limitation of the water supply and that no additional resistances to water-vapour transfer have been taken into account. The basis of the MODIS algorithm is the Penman-Monteith equation which has been extended with surface resistance formulations based on the derivation of large-scale parameters from the MODIS sensor as LAI and α . There are also several constraints on e.g. vapour pressure deficit and temperature on the surface resistance formulations used in the MODIS project. To account more correctly for the different types of moisture releasing surfaces the MODIS algorithm also uses a separate formulation for soil evaporation.

MODIS data mirror the precipitation regime with lower values in the north-west part of the basin and higher in the south-east (Figure 5.34), which in part reflect the importance of water availability for actual evapotranspiration, especially in the dry season.

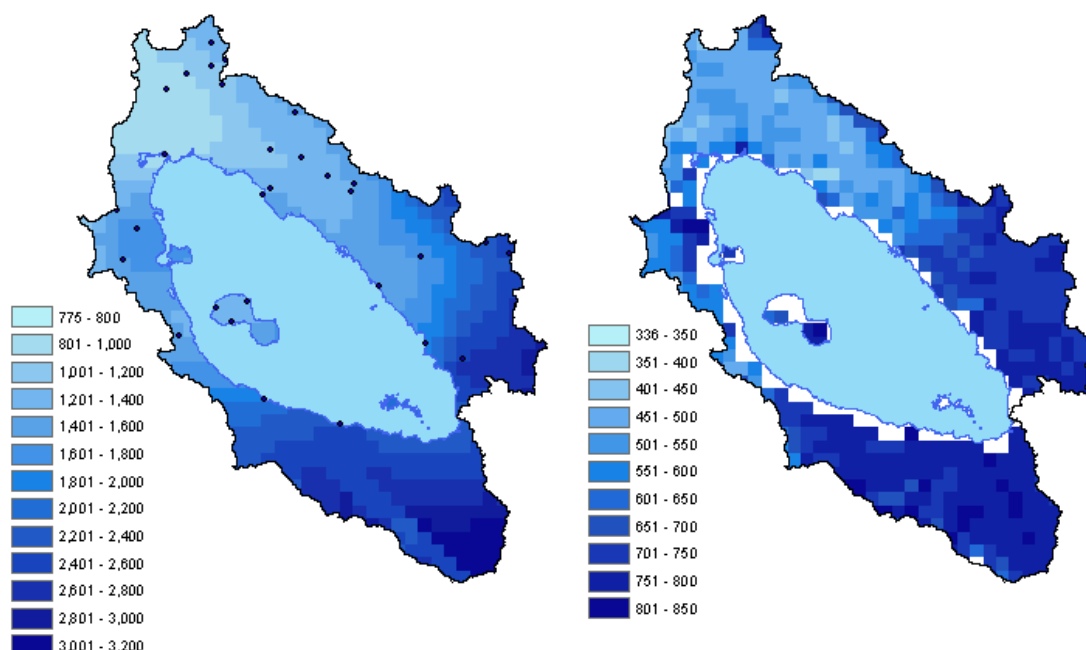


Figure 5.34 Mean annual precipitation (left) and actual evapotranspiration from the MODIS project (right) for the years 2000-2005. In the precipitation map the location of the precipitation stations are included as dots. The interpolation of precipitation cannot be considered valid in the Costa Rican part of the basin.

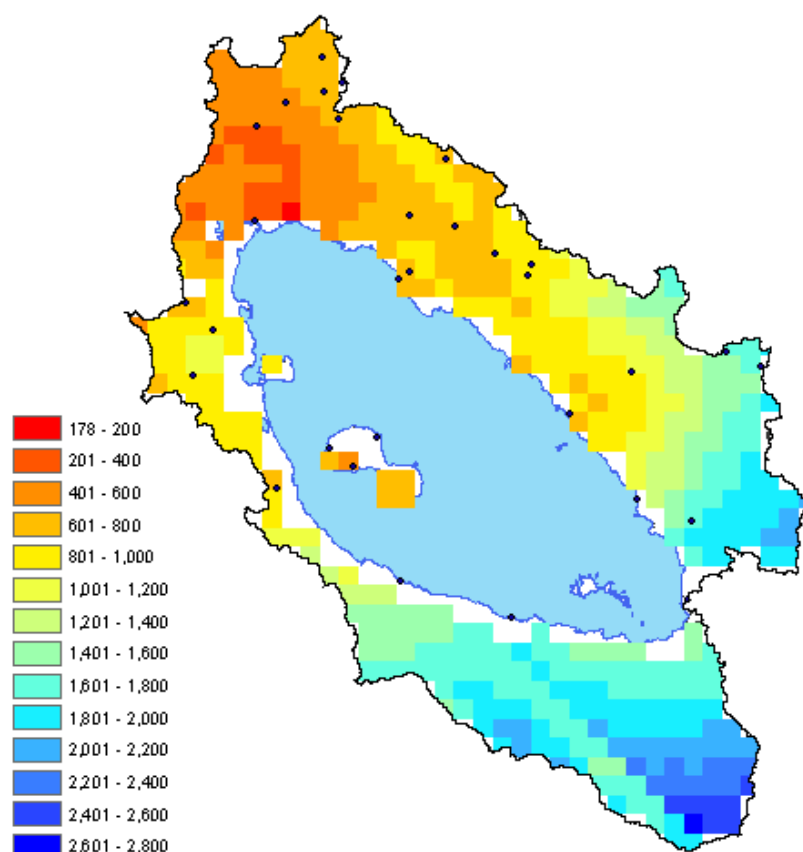


Figure 5.35 Mean annual run-off 2000-2005 calculated with the simple water balance model. The dots represent the precipitation stations in the basin where there were at least three years of complete data in this period; they were used for the interpolation of precipitation. The water balance cannot be considered valid in the Costa Rican part of the basin as there were no precipitation stations there during this period, and the interpolation of precipitation there is thus very uncertain.

5.6.4 Water balance modelling: Simple water balance model

MODIS evapotranspiration data were available for the period 2000-2005, but unfortunately there were no precipitation data in the southern (Costa Rican) part of the basin then, which did not make it possible to estimate the water balance of the complete basin. Mean annual available water resources were calculated as precipitation minus evapotranspiration (Figure 5.34). The results cannot be considered valid in the Costa Rican part of the basin due to the lack of precipitation data, and it can be seen that the available water resources follow the north-west to south-east gradient in precipitation (Figure 5.35).

There were no complete yearly discharges to compare the water balance with for the period 2000-2005 but a comparison to modelled discharge in the Mayales basin was made (section 5.6.5). Precipitation data for 1975-1994 when there were data in the Costa Rican part of the basin are presented in Figure 5.36 to enable a qualitative comparison with the evapotranspiration data for 2000-2005. If the evapotranspiration was approximately the same in this period, there would be around 2000-3500 mm of mean annual water resources in the south-easternmost part of the watershed.

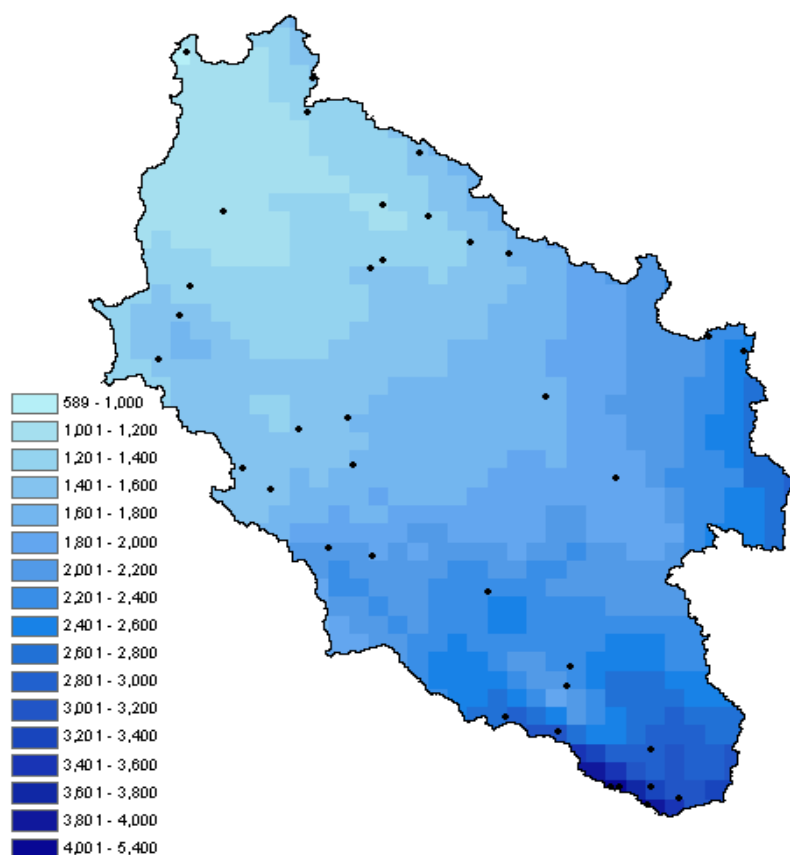


Figure 5.36 Precipitation interpolated with Universal Kriging for the period 1975-1994, stations having more than 30% complete yearly data in that period were used for the interpolation and those stations located within the watershed boundary are shown as black dots. The precipitation is considerably higher in the Costa Rican part of the basin.

5.6.5 Modelling of the Mayales sub-basin: Monthly water balance modelling

The cross-validation of the precipitation interpolation with the IDW method gave a mean error for the entire interpolation period of 0.24 mm/month and a mean error for each month that varied between -40 to 30 mm/month. The monthly water balance was calibrated for the years 1970 to 1990 and validated for the years 1991-2005 and vice versa (i.e. a differential split-sample test). Calibration and validation was performed for two different evaluation criteria, the standard Nash-Sutcliffe (Nash & Sutcliffe, 1970) and limits of acceptability around observed discharge (Beven, 2006).

Observed discharge data had several inconsistencies compared to precipitation data both on a daily, monthly and yearly time scale (e.g. there were several occasions when observed monthly discharge was higher than monthly precipitation). A visual inspection of the discharge data showed that it is likely that the rating curves have been changed from year to year; more frequent changes could however be necessary as cross-section geometry change after peak flow events because of erosion of the channel bed. It is also very probable that there exist few measurements at high flows in the data used for deriving the rating curves, as floods pass rapidly and there are technical difficulties in measuring at very high flows. Discharge data at high flows should thus be considered as very uncertain, the accepted error percentage for the maximum discharge was set to 60% in the calculation of the limits of acceptability (Figure 5.37).

The behavioural thresholds were set to 0.5 for the R_{eff} criterion and 75% of the time for the R_{LA} criterion. This resulted in 7920 parameter sets acceptable in both the calibration and the validation period for the R_{eff} criterion and 10446 for the R_{LA} criterion out of the 200,000 model runs. The uncertainty bound should ideally encompass the observed data in both the calibration and validation period. The results for the calibration (Figure 5.38) and validation period (Figures 5.39 and 5.40) show that the observed discharges were within the uncertainty bounds most of the time but that there were times when the peak flows were underestimated.

There were several high flow occasions where the model results given by both criteria underestimate observed discharge. This suggests errors in precipitation data and/or it is because the model was mainly calibrated for low and medium flows as there were not that many high flows in the observed records (but this should not be as important for R_{eff} for which high-flows are given a large weight as squared errors are used).

For both of the split-sample tests, the highest value of the R_{eff} criterion was found in the period 1970 to 1990, with lower values in 1991-2005. The highest value of the limits-of-acceptability criterion stayed the same (within the limits of acceptability around 88% of the time). The values achieved with the evaluation criteria were rather low (Table 5.9).

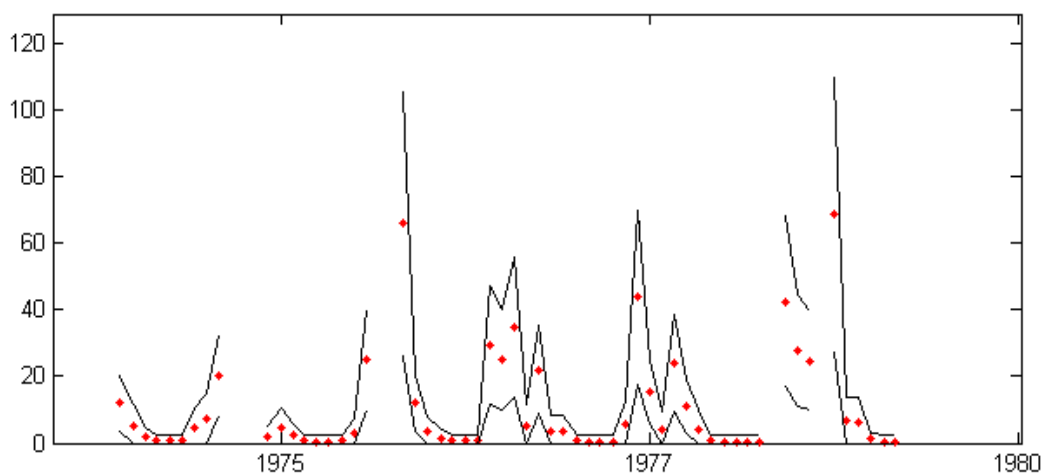


Figure 5.37 Limits of acceptability around the observed monthly discharge (mm) in the Mayales catchment.

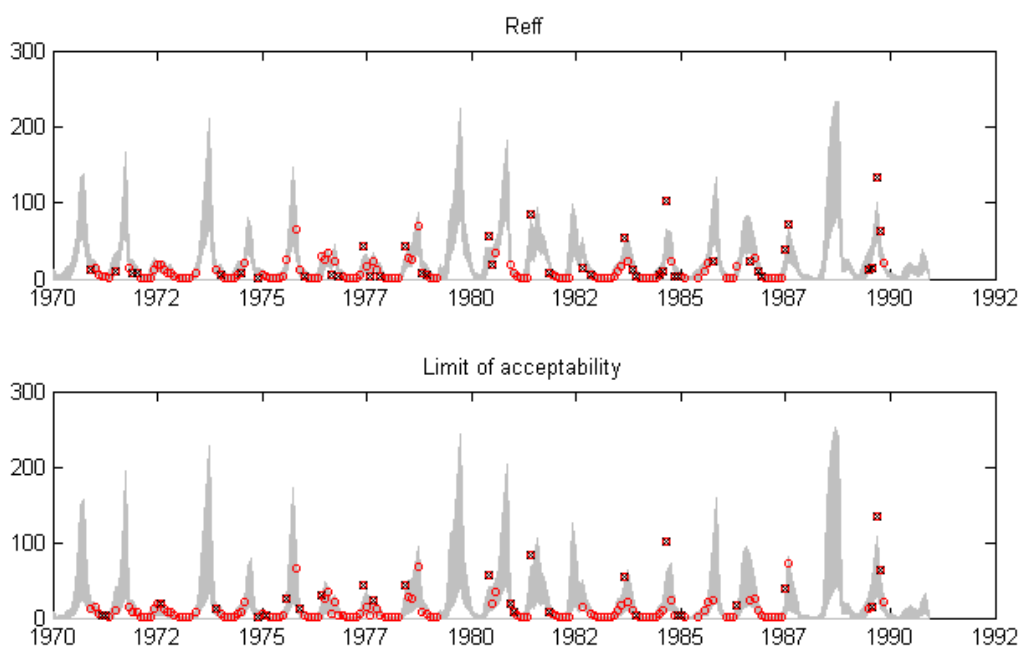


Figure 5.38 Discharge in mm for the *calibration* of WASMOD in the period 1970-1990, the top graph shows the simulated uncertainty bound for the Reff-criterion and the bottom graph the uncertainty bound for the limit of acceptability criterion. Most of the observed data (red rings) were within the uncertainty bounds. The red rings with a black cross mark months where the model fails and the observations fall outside the limits of acceptability, this occurs less frequently for the low flows for the limit of acceptability criterion.

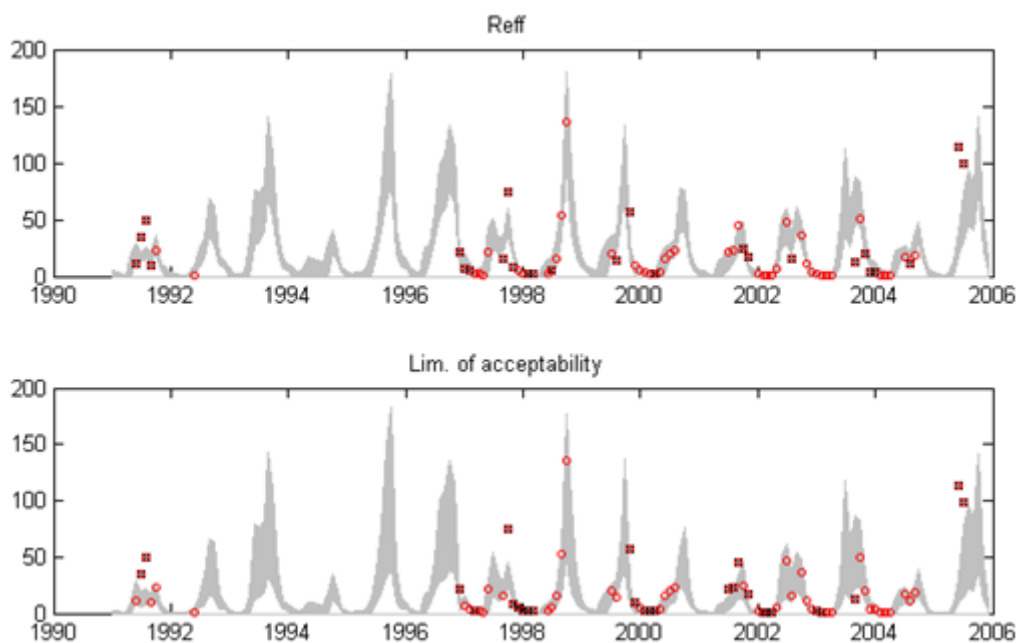


Figure 5.39 Discharge in mm for the *validation* of WASMOD in the period 1991-2005, the top graph shows the simulated uncertainty bound for the Reff-criterion and the bottom graph the uncertainty bound for the limit of acceptability criterion. Observed discharge within the uncertainty bounds are shown as red rings and those outside as a ring with a cross in it.

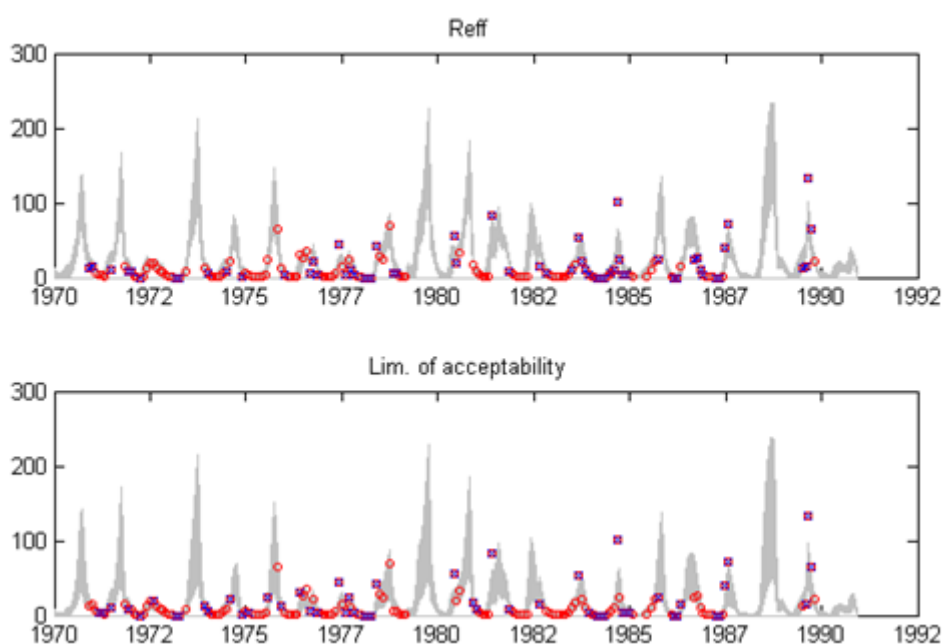


Figure 5.40 Discharge in mm for the *validation* of WASMOD in the period 1970-1990, the top graph shows the simulated uncertainty bound for the R_{eff} -criterion and the bottom graph the uncertainty bound for the limit of acceptability criterion. Observed discharge within the uncertainty bounds are shown as red rings and those outside as a ring with a cross in it.

Table 5.9 Model validation results

	Number of observed data	Highest value of R_{eff}	Highest value of R_{LA}	Percentage of observed data outside the uncertainty bounds
1970-1990	154	0.65	0.87	39% (R_{eff}), 34% (R_{LA})
1991-2005	69	0.60	0.88	37% (R_{eff}), 39% (R_{LA})

Predicted uncertainties in yearly discharge for the validation periods were high and reflect the high uncertainty in observed discharge and low model performance. The only years with complete observed discharge were in the period 1970-1990 and these data were within the predicted range during all years for the limits-of-acceptability criterion but not for the R_{eff} -criterion, all years with complete data were low-flow years (Figures 5.41 and 5.42).

5.6.6 Modelling of the Mayales sub-basin: Distributed daily modelling

The coefficients used to define the limits-of-acceptability criterion were the same as on the monthly scale and the behavioural threshold was set to 90% of the time. 2000 model runs were made and each run took a few minutes, there were 1303 acceptable parameter sets. The highest value of the limit of acceptability criterion was 0.96, the highest R_{eff} was calculated for comparison and was 0.5. The magnitude of the observed data were represented by the uncertainty bounds, but the observed data were often outside the uncertainty bound (Figures 5.43 and 5.44).

Accumulated groundwater flow in the flow-network during a precipitation event in the calibration period is shown in Figure 5.45.

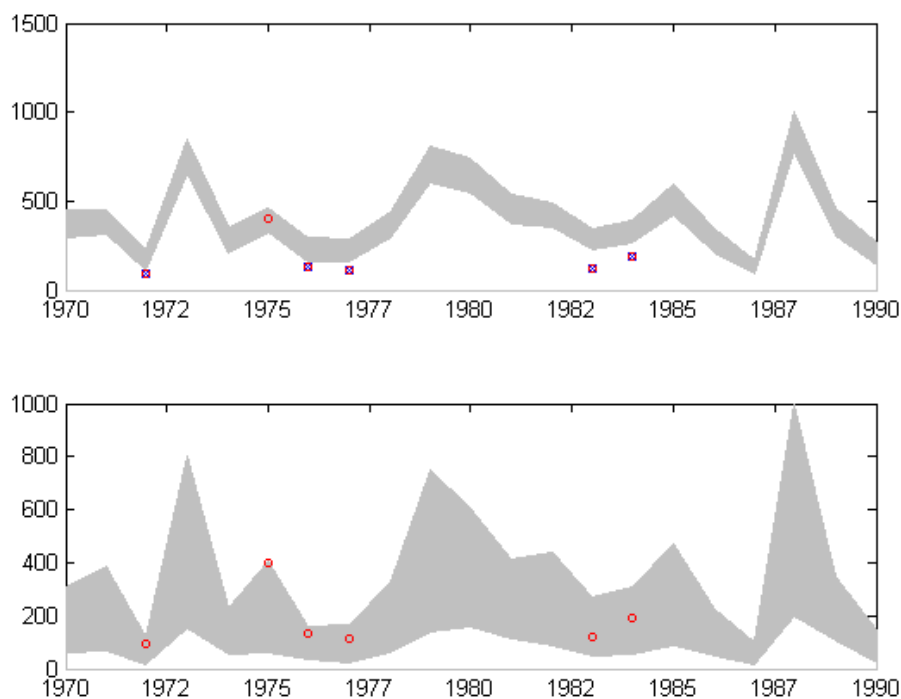


Figure 5.41 Uncertainty in predicted yearly discharge (mm) 1970-1990 in the Mayales catchment for the R_{eff} (top) and the limit of acceptability criterion (bottom). Red rings are observed yearly discharge.

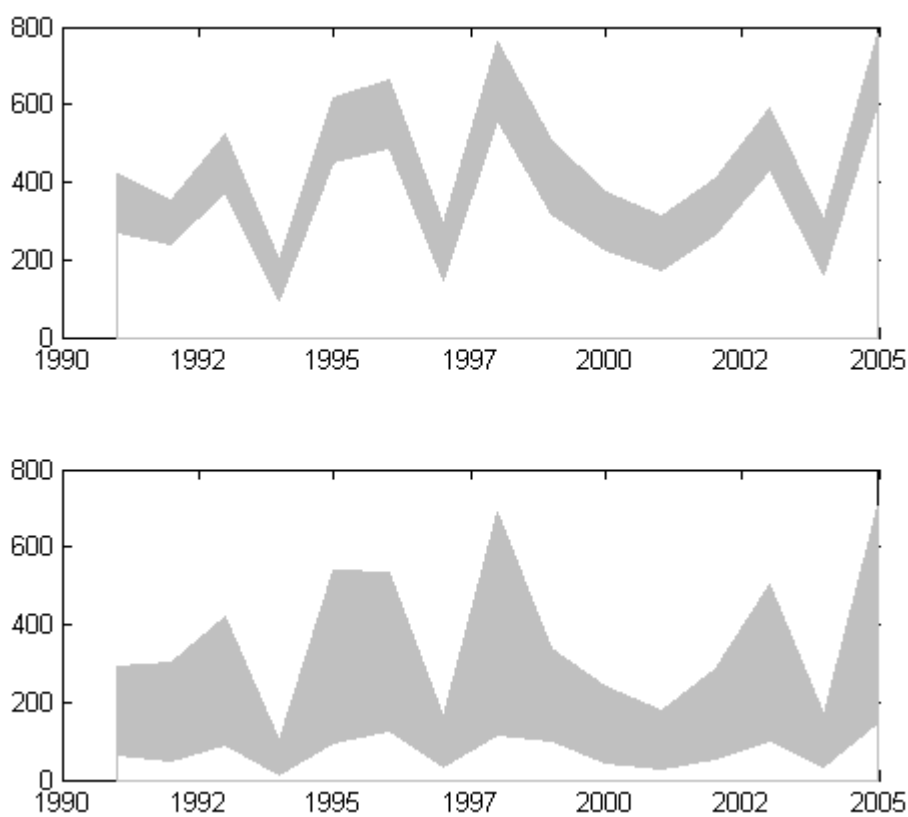


Figure 5.42 Uncertainty in predicted yearly discharge (mm) 1991-2005 in the Mayales catchment for the R_{eff} (top) and the limit of acceptability criterion (bottom).

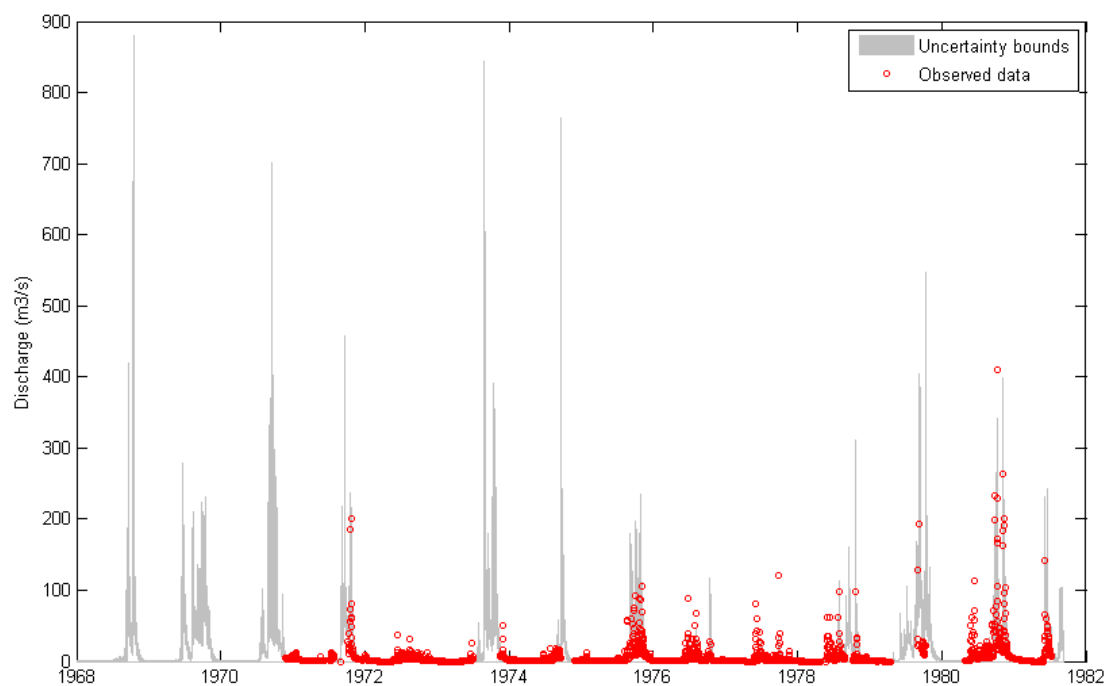


Figure 5.43 Calibration results from 1968 to 1982 for the PCRaster model application in the Mayales sub-catchment.

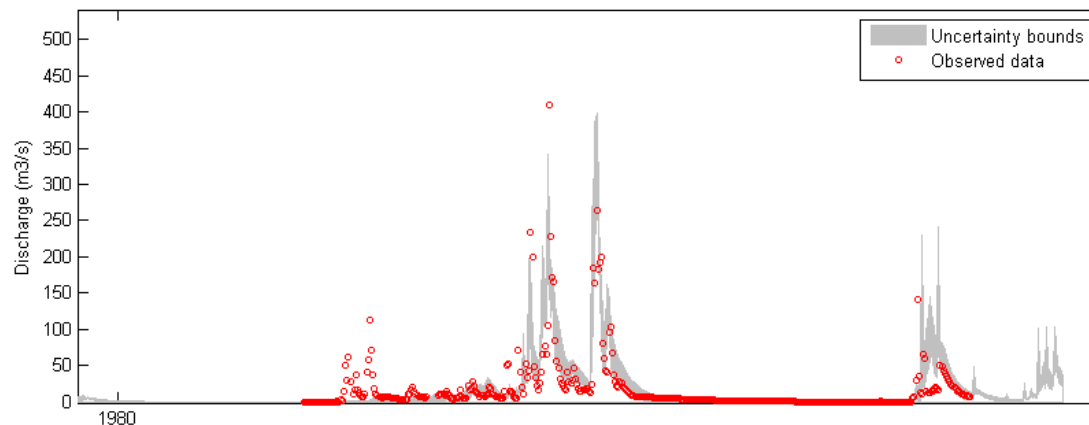


Figure 5.44 Calibration results for 1980-1981 for the PCRaster model application in the Mayales sub-catchment. The simulated discharge data do not match the observed discharge in the start of the rainy season during 1980 where there are no peaks in the simulated discharge, but model performance is acceptable around the peak flows.

There were better performances for linear reservoir coefficients that were lower (around 5-10) than the 20-40 given by the recession analysis. Given the low calibration results only the 90 best parameter sets were used for validation. Out of these parameter sets, 88 gave a limits-of-acceptability criterion higher than 90%, suggesting that the parameter sets which gave reasonable results in the calibration period also did so in the validation period (Figure 5.46).

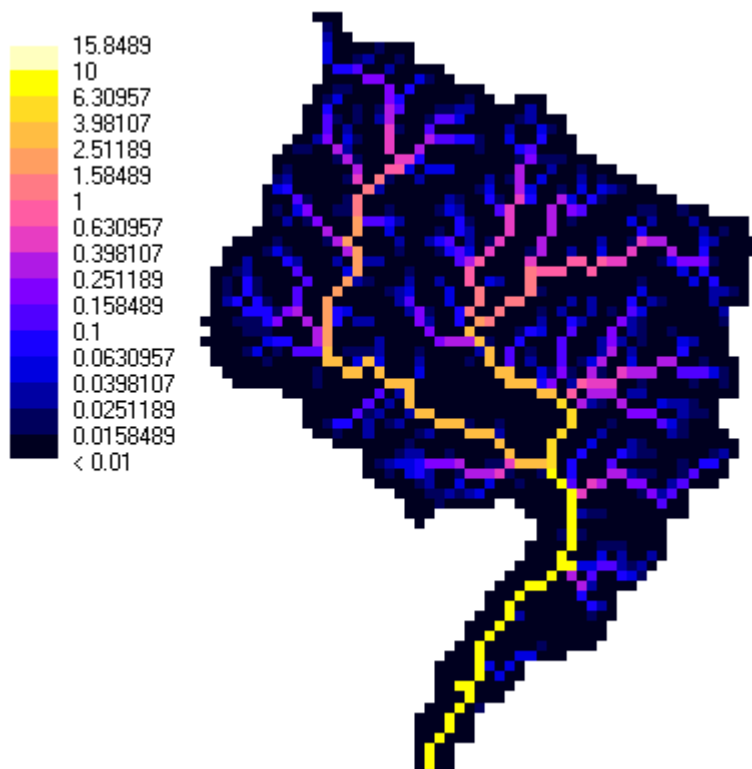


Figure 5.45 Accumulated groundwater flow (m³/s) simulated in the model during a precipitation event.

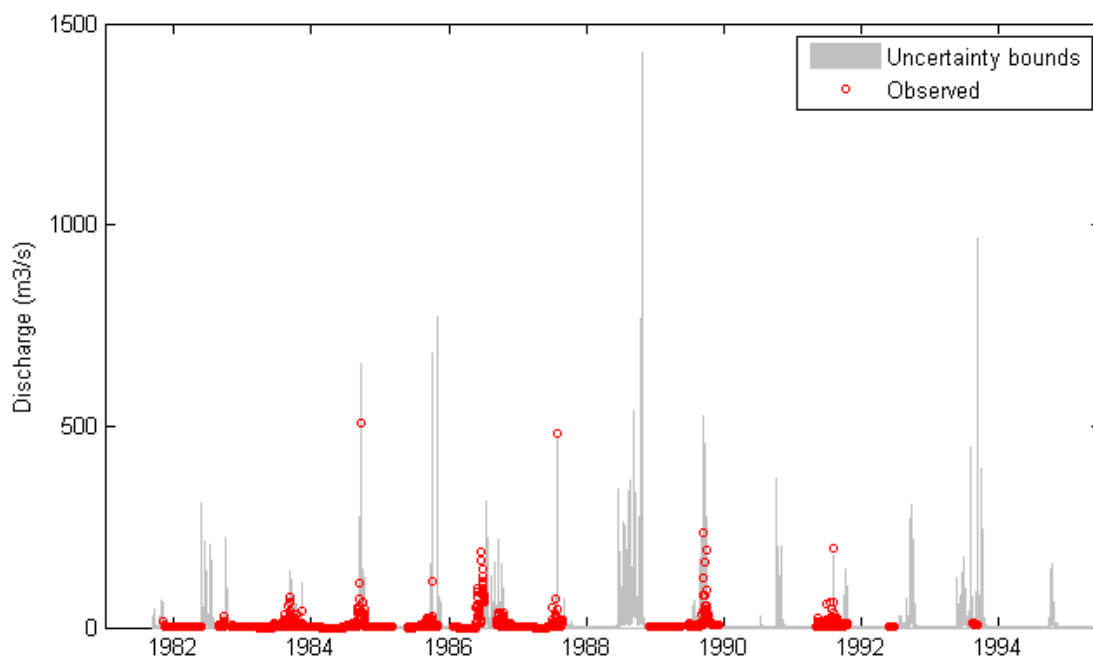


Figure 5.46 Validation results from 1982 to 1994 for the PCRaster model application in the Mayales sub-catchment

There were some periods in the validation period when the simulated discharges did not correspond to the observed discharges and where the observed discharge did not seem to be in proportion to the observed precipitation (Figure 5.47). This could result from errors in the response of the model, the discharge data or the precipitation data.

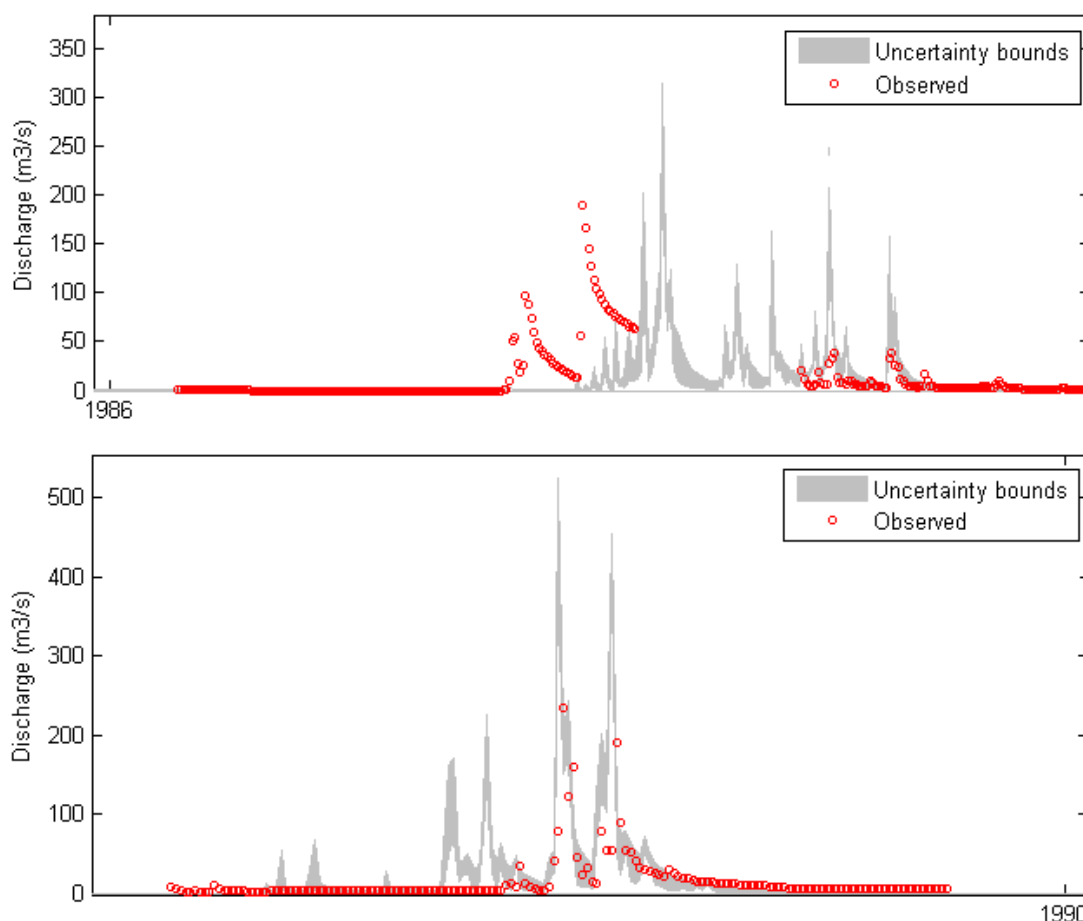


Figure 5.47 Validation results from 1986 (top) and 1989 (bottom) for the PCRaster model application in the Mayales sub-catchment. In 1986 the first observed discharge peaks are not matched by the model which might be because of errors in the response of the model, discharge or precipitation. In 1989 there were peaks in the modelled discharge, which were not in the observed data. This suggests a too-fast response in the model, errors in discharge data or that the registered precipitation events were local and not representative of the basin as a whole.

5.7 Evaluation of hydrological modelling (D3.2)

5.7.1 Gap-filling and interpolation of precipitation

The CCWM method for gap-filling is a relatively simple method that gave better results compared to the IDW method. For the purposes of spatial interpolation of precipitation it is recommended to only fill gaps shorter than a month in the time series and let the longer gaps be handled by the spatial interpolation. The method is more accurate when filled values are aggregated to a monthly time scale compared to the filled daily values.

The availability of precipitation data in the Costa Rican part of the basin is important for the description of the precipitation regime in the basin as the spatial variability in this area is different from the rest of the basin. Universal kriging with anisotropic semi-variogram estimation can be

recommended for interpolation of mean annual precipitation in the basin and IDW for automated interpolation of time series data. Station density varies in the basin and over time and so also the accuracy of the interpolated field. Complex topography, rain shadow effects, lack of measurements over the lake and data availability problems all complicate the estimation of the precipitation regime. Estimated precipitation over the actual lake is highly uncertain because of the few stations and large surface area of the lake. Also, such a large lake can influence the climate over the lake itself. The program with the CCWM method for filling gaps and the interpolation tools in ArcGIS Geostatistical Analyst were demonstrated at a workshop in Managua in 2008, and can in the future be used at INETER.

The mean monthly precipitation regime clearly showed the effects of the location of the watershed across the climatic divide between the precipitation regimes of the Caribbean and Pacific coast, and additionally the mountain climate in the Costa Rican part of the basin. The climatic divide is most apparent during July-August when there is a rainfall maxima on the Caribbean coast (the south-eastern part of the basin) and a relative minimum of precipitation, the midsummer drought, on the Pacific coast (the north-western part of the basin).

5.7.2 Calculation of actual evapotranspiration

The advantage of using MODIS data for water balance modelling is that they reflect the actual evapotranspiration and that the spatial coverage, which will be approximately 1x1 km in the final product, is fine enough to make them useful for water balance modelling also at small scales. The limitation is that the temporal resolution is eight days (many small-scale hydrological models use a time-step of one day or less). Another limitation is that the MODIS data do not extend back to before 2000 when the first instrument became operational. The advantage of using Penman-Monteith is that it is a robust formulation and that it is readily applicable everywhere to calculate potential evapotranspiration as long as the necessary input data are available. Taking the MODIS data as a reference, the Full Penman-Monteith formulation performs better than the FAO56 version, in accordance with other studies.

5.7.3 Simple water balance method

The spatial pattern of calculated mean annual runoff shows a clear relation with the precipitation distribution; there are higher values in the south-east part of the catchment compared to the north-west. In the future it would be important to assess the water balance at sub-annual (e.g. mean seasonal) scales too, but some idea can be given by the interpolated mean monthly precipitation. Water resources are especially scarce in the north-western part of the basin during the dry season (Dec–April). There were no complete years of discharge records during the period 2000-2005 for evaluation of the simple water balance method but in the cross-comparison in section 5.7.6, a comparison to modelled discharge in the Mayales catchment is made. The MODIS project data will be made globally available in the near future and can then be used for water balance calculations in other parts of Nicaragua by INETER.

5.7.4 Monthly water balance modelling in the Mayales sub-basin

The low values of the evaluation criteria for the monthly water balance modelling indicate that there are high uncertainties in the input and/or validation data. The WASMOD model has few parameters and has been shown to give good results in catchments in similar climate conditions where observed data have been of good quality, for example in Honduras and Costa Rica. The model parameters are usually well identified i.e. the best results are found in a small parameter interval and model performance decrease rapidly outside this interval. In this case the evaporation and fast-flow parameters were well identified but the slow-flow parameter was not clearly identifiable. The slow-flow parameter is however less important in catchments such as this one with a fast response to rainfall. The percentage of observed data outside the uncertainty bounds was relatively high in both validation periods. It might be that changing of rating curves in combination with few high flow measurements (which could alter the form of the rating curve a lot) could make it appear as if the rainfall-runoff relationship changes abruptly from year to year even if change is occurring more

frequently at high flow events throughout the rainy season. In combination with precipitation data uncertainty this could be a reason for the difficulty in identifying parameter sets providing good simulations for the entire period.

It can be concluded that errors in data are large (there were months with higher discharge than precipitation) and that a limits-of-acceptability approach could be a good way to account for uncertainties in discharge data. In hindsight the limits of acceptability should have been wider as the errors in the modelling process were greater than the estimated limits of acceptability allowed for. It could also be estimated how much the limits need to be expanded to achieve an acceptable percentage of simulated results at the data points that are inside the limits (e.g. 95%). There are only complete yearly discharge data for low flow years. The limits-of-acceptability criterion as defined in this application will however tend to over condition on the most frequently occurring type of flow in the observed records, in this case low and medium flows. To achieve better results for higher flows a weighting of the limits-of-acceptability performance by the flow could be used. Given the better prediction results for low flow years, the limits-of-acceptability criterion could be useful for assessing water scarcity scenarios. On a yearly time scale the observed discharges were inside the prediction bounds for all years (sometimes by a small margin) for the limits-of-acceptability criterion. For the R_{eff} criterion, which is more focused on high-flow accuracy, predicted discharge was overestimated during low flow years

5.7.5 Distributed daily modelling in the Mayales sub-basin

Data limitations and high spatio-temporal variability make daily-scale hydrologic modelling problematic. The model gave higher discharge during recession periods than measured data in the calibration period; this could suggest that evapotranspiration was underestimated or that there is seepage from the groundwater directly to the lake, a process that was not included in the model. It is problematic that complete discharge data are only available for low flow years in the Mayales basin as this makes it hard to evaluate the hydrological characteristics of the basin. In the validation period there were some periods where the observed discharges seemed erroneous in comparison to observed precipitation and modelled discharge, but this could also be the result of precipitation data errors. When potential evapotranspiration is given as input, the dependence on land use lies only in the interception parameter; interception was not used in this application because of lack of suitable land use data covering the modelling period. However, the inclusion of interception would not have greatly affected the results as rains are most often heavy. More important could be the calculation of potential evapotranspiration which might be underestimated, especially in areas with bushy vegetation, with the FAO56 Penman-Monteith method. In future applications the model could be developed to include the calculation of evapotranspiration with the Full Penman-Monteith equation with the meteorological parameters as input, and the land use parameters (such as surface roughness) derived from land use data. Given the large uncertainties in the simulations, modelling of ungauged catchments and scenario modelling on a daily time scale do not appear feasible. Modelling results from daily-scale modelling could be a useful tool for quality control of discharge data as the modelling application also serves as an evaluation of the coherence and quality of the hydrometeorological data.

5.7.6 Cross-comparison of water balance modelling and uncertainties

Mean annual runoff from the simple water balance modelling in the Mayales sub-basin was around 700 mm in 2000-2005. The results from the monthly-scale water balance model gave uncertainty bounds roughly around 150-400 mm which was considerably lower. Possible explanations could be that there is deep seepage from the groundwater directly to the lake in the Mayales sub-basin (the modelled is calibrated on the river discharge) or that the MODIS evapotranspiration is underestimated. It could also be that the monthly water balance model gives too-low results for high flow years as it is predominantly calibrated with low and medium size flows.

5.8 Summary and recommendations

Daily scale hydrometeorological analysis using interpolated precipitation is not recommended (if the density of precipitation stations is not very high); given the spatiotemporal correlation structure a 4–5 day timescale would be the shortest possible for meaningful interpolation of precipitation. Larger data availability on a monthly time scale favours monthly or yearly analysis; also on a monthly or yearly scale variability is lower and data more representative. A thorough revision of discharge data should be carried out to remove outliers, and rating curve data should be analysed to assess the uncertainties in the discharge data. In this process it would be important to establish the highest measured discharges included in the rating curve to know which discharge data are based on the extrapolated parts of the rating curves. Such an analysis can be used to set better limits of acceptability in future modelling efforts. If possible, more high flow measurements should be made to reduce uncertainty in peak flows. Frequent rating measurements can also make it possible to change rating curves more often and improve the calculation of discharge from gauge height. Scenario modelling of land use change effects could not be recommended with the present data quality problems. Land use change effects can be expected to be seen in the dynamics of the peak flows; given the high climate variability and the high uncertainty in peak discharges such effects would be hard to detect in the data. It is highly recommended to use uncertainty estimation in future modelling studies in the basin.

Used in a hydrological model, with surface resistance formulations with constraints on soil water supply, vapour pressure deficit and temperature, the Full Penman-Monteith can be applied to calculate actual evapotranspiration in any region. The limitation is the availability of meteorological input data which might not reflect local conditions if the nearest meteorological station is located far away. This can to some extent be solved by utilising downscaling techniques for meteorological variables, or if fields of re-analysis data are used as input to the Penman-Monteith. Another approach to study climate variability impacts on the water balance at the regional or local scale is to use a Regional Climate Model (RCM). A RCM is typically run with boundary condition from a GCM but the resolution is much higher, around 40-50 km. The high resolution local climate scenarios can be used in impact, vulnerability and adaptation studies. In the future use of MODIS project evapotranspiration data in Nicaragua, possible underestimation as compared to modelled discharges should be kept in mind. Further comparisons with modelled and/or measured discharges should also be made to analyse this.

6. Quaraí River Basin (Brazil)

6.1 Description of basin

The Cuareim River is a tributary of the Uruguay River on its left margin, which is a part of the La Plata basin, the second largest in South America. The Cuareim basin is located between Brazil and Uruguay. The Brazilian part of the basin is placed at the extreme south of the Federative Republic of Brazil, and the river is known in Portuguese as Quaraí. The Uruguayan part is somewhat larger and is placed to the north of the Oriental Republic of Uruguay. Some important tributaries are: Tres Cruces Creek, Cuaró Creek and Yucutiá Creek, on the Uruguayan (left) side of the main stream, and the Espinilho Creek, the Sarandi Creek, the Quaraí-Mirim Creek and the Garupá Creek, on the Brazilian (right) side. Artigas (Uruguay) and Quaraí (Brazil) are the most important cities in the basin.

Most of the basin's upper parts have shallow soils (depth up to 0.5 m) which determine low soil water-storage capacity, which consequently generates fast-response runoff that may cause flooding in the cities of Artigas and Quaraí, and very low flows during droughts.

Statistical analysis of streamflow recorded at Concordia Bridge between Artigas and Quaraí, shows a maximum flow of $4.813 \text{ m}^3 \text{ s}^{-1}$, a minimum flow of zero, and an average flow of $95.6 \text{ m}^3 \text{ s}^{-1}$. Most of the streamflow occurs during and shortly after the rainfall events.

There are several interests concerning water resources in this basin. Flooding of the city of Artigas, in Uruguay, is one of the most important issues and this problem was preliminary addressed by a pilot project supported by WMO (2003). During the TWINLATIN project, however, problems related to water demand and availability, and to water quality, were raised repeatedly by the participants of the general public, local stakeholders and local government during activities of WP4 and WP5. Therefore, in the context of TWINLATIN, the main interest in hydrological modelling in the Quaraí basin was water resources in general, with emphasis on water availability related to the widespread use for irrigation of rice fields.

The whole basin area down to the confluence with the Uruguay river was modelled, and special attention was given to the influence of the small reservoirs and rice fields on the hydrologic behaviour of the basin.

6.2 Choice of model

The hydrological model chosen to be applied in the Quaraí river basin is the large-scale distributed MGB-IPH model.

MGB-IPH is a large-scale distributed hydrological model that was developed to be applied in large South American basins, and having in mind situations of low spatial and temporal data availability typical to this region. It can be classified as a Hydrology Response Unit model, according to the classification proposed by Beven (2001). The model structure benefits from facilities provided by Geographical Information Systems, taking into account basin characteristics such as land use, topography, vegetation cover and soil types, which guide the calibration of parameter values. The MGB-IPH model was initially based on the LARSIM (Bremicker, 1998) and VIC (Liang *et al.*, 1994; Nijsssem *et al.*, 1997) models, with some changes in the evapotranspiration, percolation and river propagation modules.

The MGB-IPH model is composed of modules for calculation of soil water budget, evapotranspiration, flow propagation within a catchment, and flow routing through the drainage network. The drainage basin is divided into elements of area (normally square grids) connected by channels, with vegetation and land use within each element categorised into one or more classes, the number of vegetation and land use types being at the choice of the user. The Grouped Response Unit (GRU) (Kouwen *et al.*,

1993) approach is used for hydrological classification of all areas with a similar combination of soil and land cover without consideration of their location inside the catchment. A catchment contains a limited number of distinct GRUs. The soil water budget is computed for each GRU, and runoff generated from the different GRUs in the catchment is then summed and routed through the river network. This approach has been used by several large scale hydrological models, such as VIC (Wood *et al.*, 1992; Liang *et al.*, 1994; Nijssen *et al.*, 1997) and WATFLOOD (Soulis *et al.*, 2004).

Soil water balance is computed independently for each GRU of each catchment. The model has components representing canopy interception, evapotranspiration, infiltration, surface runoff, sub-surface flow, baseflow and soil water storage. Rainfall values are interpolated spatially and at each time step, to give an estimate at the centre of each catchment, using the inverse-distance-squared interpolation method. Flow generated within each catchment is routed to the stream network using three linear reservoirs (baseflow, sub-surface flow and surface flow). Streamflow is propagated through the river network using the Muskingum–Cunge method. More comprehensive descriptions of the model, including proxy-basin tests, are given by Collischonn & Tucci (2001) and Collischonn *et al.* (2007a) and further applications are presented by Tucci *et al.* (2003) and Allasia *et al.* (2005).

Water quality modelling capabilities were also added to the MGB-IPH model recently, including calculation of both point and diffuse sources of pollution, advection and change of concentration along the rivers and reservoirs (Larentis *et al.*, 2008).

The MGB-IPH model was chosen because it is a hydrological model that can be applied to large basins, taking into account the spatial variability in precipitation, land use, vegetation, soil types and relief. Another important reason for choosing this model is the large experience the Brazilian TWINLATIN members of the project have in applying this model in South America (Allasia *et al.*, 2005).

The MGB-IPH model offers the opportunity to take into account spatial variability of rainfall and physical characteristics of the basin. Different soils and vegetation types can be also represented by this model, although with considerable uncertainty. Tests in other parts of the Uruguay basin, of which the Quaraí/Cuareim river is a tributary, have shown that the MGB-IPH model can be applied to estimate streamflow in ungauged basins if its parameters can be calibrated in a nearby catchment with similar characteristics (Collischonn *et al.*, 2007a).

Another important reason for choosing MGB-IPH model is the possibility of including the hundreds of small reservoirs and rice fields explicitly in the simulation, by programming special modules to represent both types of hydrological elements. This development was done in the context of the TWINLATIN project because of the unique aspects of the Quaraí basin hydrology and due to the lack of information on the actual water use in rice fields in this region.

6.3 Data requirements

Data requirements of the MGB-IPH hydrological model are: digital elevation model (DEM); land use; vegetation classes; soil types; river cross-sections; reservoir characteristics; rainfall; streamflow; water quality data; temperature; humidity; atmospheric pressure; radiation; and wind velocity.

In the case of the MGB-IPH model, due to the large scale of the applications, globally available datasets are used as much as possible. Digital elevation models (DEMs) are now obtained from the Shuttle Radar Topography Mission (SRTM). This is a DEM with a nearly 90 m resolution which have shown to be satisfactory in the region.

The model was initially applied using a square cell discretisation. A first stage of the model application in square cells is the pre-processing of data, including the step of attributing flow directions for each of the square cells (Davies & Bell, 2008). In the Quaraí basin, a modified version of the COTAT algorithm by Reed (2003) was used to generate low resolution drainage networks from high resolution DEMs (Paz *et al.*, 2006). A new technique was recently developed to obtain river reach length and slope automatically for each cell of the model while conserving the whole river network length of the basin (Paz & Collischonn, 2007).

In a second application, the MGB-IPH model was adapted to be applied using a catchment subdivision of the basin, using the same type of discretisation used in ArcHydro data structure. The basin discretisation followed the method first used in the application of the MGB-IPH model to the Cai river basin, located in South Brazil, as described by Collischonn *et al.* (2007b). In this case, pre-processing of data for the application of the model was based on tools provided by ArcHydro, which is a general use data structure and set of tools, and GeoHMS, which is a set of tools to prepare data for the HEC HMS hydrological model, based on the ArcHydro data structure.

Rainfall data are collected by several different institutions in Brazil, but most of the data are collected and finally based on the data bank of the National Water Agency - ANA (Agencia Nacional de Água). Rainfall time series of a specific raingauge can be downloaded free from www.ana.gov.br.

In Uruguay, the responsibility of collecting rainfall data are from the DNH (Dirección Nacional de Hidrografía), the Uruguayan hydrography department, which is one of the partners of the TWINLATIN project.

Streamflow is measured by the same institutions in Brazil and Uruguay but streamflow gauges are rather sparse. Two streamflow gauging stations with data were found in the basin. One, controlling one third of the basin area, located close to the bridge connecting the two most important cities in the basin, Artigas (Uruguay) and Quaraí (Brazil). The other, with a very short streamflow record, located on the river Tres Cruces, a tributary of the South margin of the river Quaraí, which basin is entirely in Uruguayan territory.

Land use and vegetation types can be derived from satellite images and LANDSAT images have been obtained for the entire region and were classified. Classification is being improved by local inspection and comparison with high resolution images which can be examined freely through GoogleEarth.

To classify areas of rice fields, a new satellite image data source was used, obtained from the CBERS program. CBERS stands for China-Brazil Earth Resources Satellite and was born from a partnership between Brazil and China. It has three sensor types and images can be free downloaded from www.cbears.inpe.br. CBERS images were used because of free availability for several different dates in this region.

Soil types were obtained from different sources in the two countries. In Brazil, a 1:1,000,000 map of soil types is available for the whole country and the part concerning the Quaraí/Cuareim river basin was digitised for the purposes of the TWINLATIN project. Soils are classified according to different methods in both sides of the basin, so a reclassification was needed, considering the most important characteristics of soils for hydrology and runoff generation.

River cross-sections for the main river were obtained during the WMO project. First inspection of the data shows that cross sections are relatively far from each other and visible errors were found in the lower parts of the river, close to its mouth. Due to these errors, cross-sections for the last 60 km of the river probably have to be surveyed again.

Reservoirs influence river flows and reservoir characteristics, at least its volume, should be known in order to simulate the basin's hydrology. There are several hundreds of small reservoirs distributed in the Quaraí/Cuareim river basin, on both sides of the country border. Since the basin streamflow is very flashy and baseflow is low, the reservoirs are needed to guarantee water during the rice growing season (summer). Most of these reservoirs are small and entirely built and contained within individual land properties, and some of them were constructed along ephemeral or first-order streams. Local inspection during the start of the TWINLATIN project revealed that many of the reservoirs do not have any hydraulic structure to maintain minimal flows in the streams.

Due to differences in law and law enforcement, information availability about the reservoirs is more easily available in Uruguay than in Brazil. For each reservoir in Uruguay, DNH has information about inundated area; dam height; reservoir volume; and estimated area planted with rice each year. In Brazil, there are only a few reservoirs that are regulated, in the sense that all information and licences needed by law are fulfilled. This is a problem for hydrological modelling activities, because volumes of the vast majority of the reservoirs in Brazil are not known.

A solution to this problem was found by obtaining a relation between inundated area and volume based on data of those reservoirs for which both information items are available. This relation is further explained in section 6.5.1, where the model development is more deeply described.

Water quality data are scarce in the Quaraí/Cuareim river basin. Unlike other rivers in the Brazilian southernmost state of Rio Grande do Sul, the Quaraí is not monitored by the state environmental institution (FEPAM). In Uruguay the agency responsible for the environmental monitoring of river is DINASA, which also has very limited information on water quality of the river Cuareim or its tributaries. Due to this general lack of data on water quality, the monitoring programme during the TWINLATIN project was largely focused on this aspect. Five field campaigns with water quality sampling and streamflow measurement were undertaken during the TWINLATIN project. These campaigns and the results obtained are described in the WP6 report.

6.4 Scenario modelling

Scenario modelling was necessary from the start of the hydrological modelling activities in the Quaraí river basin. This is due to the fact that observed streamflow time series are strongly influenced by the presence of reservoirs and by water abstractions for rice irrigation.

In the first scenario that was simulated, the effort was to represent the actual situation in the basin, with the widespread use of water for irrigation and with the presence of a large number of small reservoirs. This scenario was used to perform the calibration of the model parameters, since observed streamflow data are influenced by the presence of the reservoirs and water uses.

In the second scenario, neither reservoirs nor water abstractions were included in the model. The aim of this scenario was to generate natural streamflow time series.

The third scenario was similar to the second, except for the reservoirs, which were included in the simulations. The aim of this scenario was to generate streamflow time series which could be compared to the ones obtained with the second scenario, so as to allow the analysis of the effect the reservoirs have on the main river streamflow. No water abstractions were included in the third scenario.

The fourth scenario was similar to the third, except for the water abstractions. Water abstractions in the Quaraí river basin are of two types: river abstractions and reservoir abstractions. In the fourth scenario, only water abstractions from the reservoirs were included. The aim of this scenario was to analyse the impact of reservoir water abstractions on streamflow of the main river.

The fifth scenario included reservoirs and both types of water abstractions but did not include the return flow from the irrigated rice fields. The aim of this scenario was to analyse the impact of return flows on streamflows of the main river.

Additional scenarios concerning land use change and climatic change were also simulated and are further described in the WP8 report. Table 6.1 summarises the scenarios that were simulated.

6.5 Model development

6.5.1 The MGB-IPH large-scale distributed model

The MGB-IPH model is composed of modules for calculation of soil water budget; evapotranspiration; flow propagation within a cell, and flow routing through the drainage network. The drainage basin is divided into elements of area connected by channels, with vegetation and land use within each element categorised into one or more classes, the number of vegetation and land use types being at the choice of the user.

The area elements are normally square cells, however for the application described here a more nature like sub-division of the basin was chosen. The Quaraí river basin was divided in catchments generated using the ArcHydro tools. Prior application in another basin showed that the MGB-IPH model has

Table 6.1 Hydrological scenarios analysed in the Quaraí river basin (marked cells refer to aspects that were included in the model during each scenario).

Scenario	Reservoirs	Reservoir water	River water abstractions	Return flow from rice fields	Climatic change	Land use change	Objective
1	X	X	X	X			Model calibration; actual situation
2							Natural situation of the basin
3	X						Analyse effects of reservoirs
4	X	X		X			Analyse effects of reservoirs and reservoir abstractions
5	X	X	X				Analyse effects of return flows
6					X		Analyse effects of climatic change
7						X	Analyse effects of land use change

similar results when the basin is divided in square cells or small sub-basins (Collischonn *et al.*, 2007b). Following the names used within ArcHydro, the whole Quaraí river basin is referred to as the basin. Sub-basins are divisions of the basin defined by the presence of monitoring points, and catchments are the small sub-basins or elements which replace the cells in a more nature like division of the basin.

The Grouped Response Unit (GRU) (Kouwen *et al.*, 1993) approach is used for hydrological classification of all areas with a similar combination of soil and land cover without consideration of its location inside the element (cell or catchment). A cell or catchment contains a limited number of distinct GRUs. The soil water budget is computed for each GRU, and runoff generated from the different GRUs in the cell or catchment is then summed and routed through the river network. This approach has been used by several large scale hydrological models, such as VIC (Wood *et al.*, 1992; Liang *et al.*, 1994; Nijssen *et al.*, 1997) and WATFLOOD (Soulis *et al.*, 2004).

The processes of flow routing and storage that are included in the model are canopy interception, evapotranspiration, infiltration, surface runoff, subsurface flow, baseflow and soil water storage. The soil water balance is computed independently for each GRU of each cell or catchment, considering only one soil layer, according to:

$$W_{i,j}^k = W_{i,j}^{k-1} + (P_{i,j} - E_{i,j} - D_{sup,i,j} - D_{int,i,j} - D_{bas,i,j}) \cdot \Delta t$$

where: k , i , and j are indexes related to time step, catchment and GRU, respectively; Δt is the time step (1 day in most applications); $W_{i,j}^k$ (mm) is the water storage in the soil layer at the end of the k th time step, of the j th GRU of the i th cell or catchment; $W_{i,j}^{k-1}$ (mm) is the same variable at the start of the time step; $P_{i,j}$ (mm/ Δt) is the rainfall that reaches the soil; $E_{i,j}$ (mm/ Δt) is the evapotranspiration; $D_{sup,i,j}$ (mm/ Δt) is the surface runoff, or quick flow; $D_{int,i,j}$ (mm/ Δt) is the subsurface flow; and $D_{bas,i,j}$ (mm/ Δt) is the flow to the groundwater reservoirs.

Variables $W_{i,j}^k$ and $P_{i,j}$ are known in each time step, and $E_{i,j}$, $D_{sup,i,j}$, $D_{int,i,j}$ and $D_{bas,i,j}$ are calculated based on soil water storage at the start of the time step ($W_{i,j}^k$) and on model parameters, according to:

$$D_{sup,i,j} = \Delta t \cdot P_{i,j} - (W_{m_j} - W_{i,j}^{k-1}) \quad \text{when } A \leq 0$$

$$D_{sup,i,j} = \Delta t \cdot P_{i,j} - (W_{m_j} - W_{i,j}^{k-1}) + W_{m_j} \cdot \left[\left(1 - \frac{W_{i,j}^{k-1}}{W_{m_j}} \right)^{\frac{1}{b_j+1}} - \frac{\Delta t \cdot P_{i,j}}{W_{m_j} \cdot (b_j + 1)} \right] \quad \text{when } A > 0$$

$$\text{where: } A = \left[\left(1 - \frac{W_{i,j}^{k-1}}{W_{m,j}} \right)^{\frac{1}{b_j+1}} - \frac{\Delta t \cdot P_{i,j}}{(b_j+1) \cdot W_{m,j}} \right]$$

and where: $W_{m,j}$ (mm) maximum water storage in the upper layer of soil of GRU j (GRU related parameter); and b_j (-) (another GRU related parameter). GRU related parameters are explained below.

The above equation is based on the variable contributing area concept of the PDM (Moore & Clarke, 1981), Arno (Todini, 1996), Xingiang (Zhao *et al.*, 1980), VIC2L and LARSIM models. Parameter b_j (non-dimensional) represents the statistical distribution of water storage capacity of the soil. If b_j is set to zero, then the whole area covered by a particular GRU will have a storage capacity of $W_{m,j}$ (mm) in the upper layer of soil. For positive values of b_j , some portions of the GRU area will have soil storage capacity lower than $W_{m,j}$, thus originating more runoff, even for minor rainfall events. A complete description of this formulation can be found in Todini (1996).

Subsurface flow is obtained by a similar Brooks & Corey non-saturated hydraulic conductivity equation (Rawls *et al.*, 1993):

$$Dint_{i,j} = Kint_j \cdot \left(\frac{W_{i,j} - W_{z,j}}{W_{m,j} - W_{z,j}} \right)^{\left(3 + \frac{2}{\lambda_j} \right)}$$

where: $W_{z,j}$ (mm) is the lower limit below which there is no sub-surface flow; $Kint_j$ (mm/Δt) is a parameter which give the sub-surface drainage of the water from the soil layer, when the soil is saturated; and λ (-) is the soil porosity index.

Percolation from the soil layer to groundwater is calculated according to a linear relation between soil water storage and maximum soil water storage:

$$Dbas_{i,j} = Kbas_j \cdot \frac{(W_{i,j}^{k-1} - W_{c,j})}{(W_{m,j} - W_{c,j})}$$

where: $W_{c,j}$ (mm) is the lower limit below which there is no flow; and $Kbas_j$ (mm/Δt) is a parameter which give percolation to groundwater in the case of saturated soil.

Evapotranspiration from the soil, vegetation and the canopy to the atmosphere is estimated through the Penman–Monteith equation, as described by Wigmosta *et al.* (1994).

The variables $Dsup_{i,j}$, $Dint_{i,j}$ and $Dbas_{i,j}$ are the surface, interflow and groundwater flow, respectively, generated in the soil layer of the GRU. The model uses linear reservoirs to route these flow through the cell or catchment. Outflow from these reservoirs is calculated according to the following:

$$Qsup_i = \frac{1}{TKS_i} \cdot Vsup_i^{k'}$$

$$Qint_i = \frac{1}{TKI_i} \cdot Vint_i^{k'}$$

$$Qbas_i = \frac{1}{TKB_i} \cdot Vbas_i^{k'}$$

where: $Qsup_i$ (m^3s^{-1}) is the outflow of the surface reservoir of catchment i ; $Qint_i$ (m^3s^{-1}) is the outflow of the sub-surface reservoir; $Qbas_i$ (m^3s^{-1}) is the outflow of the groundwater reservoir; $Vsup_i^{k'}$, $Vint_i^{k'}$ and $Vbas_i^{k'}$ (m^3) are the volumes in the surface, subsurface and groundwater reservoirs of catchment i , at the k time step, already updated by the $Dsup_{i,j}$, $Dint_{i,j}$ and $Dbas_{i,j}$ fluxes drained from the soil layer of each GRU; and TKS_i , TKI_i and TKB_i (s) are time parameters.

Streamflow is routed through the river network using the Muskingum–Cunge method with time steps that can be submultiples of Δt , and that are adjusted for accuracy according to the stream reach length and slope.

A relationship between vegetation and soil to Wm is assumed, which means that for the same soil type, Wm values for forest GRUs are higher than for pasture or cropland GRUs. Parameters $Kint$ and $Kbas$ (mm/ Δt) are the drainage rate of the water from the upper soil layer, when the soil is saturated. The parameters are fitted based on recorded hydrographs through trial and error or optimisation technique. Parameters Wc and Wz are fixed as 10% of Wm and are excluded from the calibration procedure.

Following the approach of Bremicker (1998), parameters TKS and TKI are obtained by:

$$TKS_i = C_s \cdot Tind_i$$

$$TKI_i = C_i \cdot Tind_i$$

$$Tind_i = 3600 \cdot \left(0,868 \cdot \frac{L_i^3}{\Delta H_i} \right)^{0,385}$$

where: C_s and C_i are non-dimensional values that correct a first estimate of the retention time of both surface and sub-surface flow obtained by third of the equations above in which ΔH is estimated by the difference in the maximum and minimum high resolution Digital Elevation Model (DEM) altitudes in each catchment, and L is the flow length within a catchment. Each catchment i may have different values for $Tind$, reflecting differences in relief, but the first estimate of the retention time is corrected for surface and sub-surface flow during the fitting phase, multiplying it by the non-dimensional parameters C_s and C_i , respectively. This method for retention time estimates was proposed in the LARSIM model (Bremicker, 1998), and has the advantage of relating these time parameters to relief for each catchment, at the same time it simplifies the calibration. Parameter TKB can be estimated by the recorded hydrograph recession of a long dry period.

For the same GRU, parameter values are the same regardless where in the basin. However, as different catchments across the basin have different fractions of land use and vegetation cover classes (grouped in the GRUs), heterogeneity of the basin runoff generation characteristics can be relatively well represented.

The model is run using rainfall and meteorological data from gauging stations within the basin. Values are spatially interpolated at each time step, to the centre of each grid catchment. Some parameters, such as the Leaf Area Index and the surface or canopy resistance used in the rainfall interception and evapotranspiration calculation, are not used in calibration, but adopted from the literature, considering seasonal variation when necessary.

6.5.2 Basin discretisation

Following the ArcHydro terminology, a basin is divided in sub-basins or watersheds in a first level of division, which has the objective of defining regions of the basin where water flows into a bigger reservoir or that are controlled by gauging stations. A lower level division of the basin are the catchments.

While normally the words basin, watershed and catchment are used to refer to the same thing, in ArcHydro they mean different levels of division of the basin. Figure 6.1 shows the Quaraí river basin divided in three watersheds, according to the presence of streamflow gauges or the confluence with the Uruguay river, and several small catchments (grey polygons). The yellow watershed is the region upstream of the Artigas-Quaraí gauging point. The red watershed is the region upstream of the Tres Cruces river gauging point, called Javier de Viana. The blue region is the rest of the basin, down to the confluence of rivers Quaraí and Uruguay.

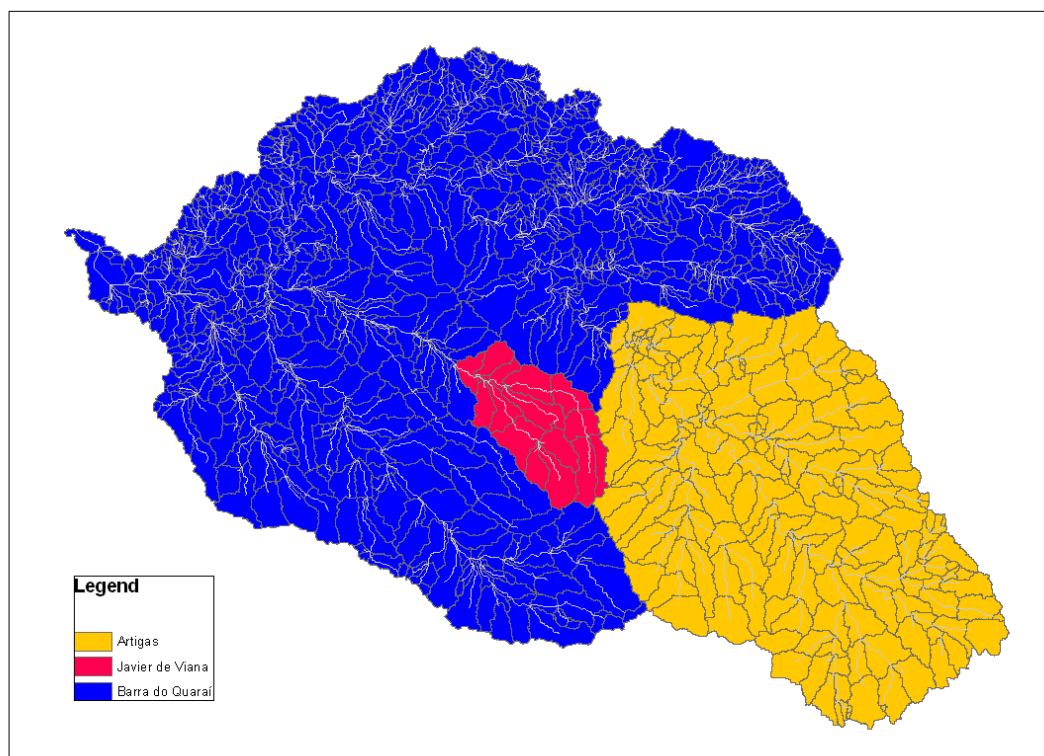


Figure 6.1 Division of the Quaraí river basin in three watersheds according to the availability of data at stream gauges, and in catchments (grey outlined polygons within each watershed).

Within the ArcHydro framework, what defines the existence of a catchment is the junction of two river segments. The existence of a river is normally defined by a threshold in accumulated drainage area. Thresholds can be arbitrarily set when applying ArcHydro tools, and previous studies in Brazil not published yet have shown that rivers can have their upper limit at places with drainage areas from 40 km² to less than 1 km², depending mostly on relief and geological characteristics. In the Quaraí river basin, there is evidence that concentrated flows occur at least temporarily for streams draining less than 1 km².

In the application of the MGB-IPH model to the Quaraí river basin, the area threshold of 24 km², generating 704 catchments, was considered first. Some of the catchments showing more than one reservoir inside were further divided until no catchment could be found with more than one reservoir. The subdivision was also performed to guarantee that reservoirs were close to the catchment's outlet. Very large catchments were also divided in order not to exceed an arbitrarily set threshold of 50 km². After these adjustments, which were performed using the tools available in GeoHMS preprocessing software for HEC HMS, the Quaraí river basin was divided in 1156 catchments.

6.5.3 Land use

Land use maps in the basin were produced through classification of LANDSAT and CBERS satellite images. One of the most important objectives in this land use classification activity was the correct definition of the area used for rice growing. Given the use of water for irrigation in this region, precise estimates of irrigated area are necessary to estimate the water abstractions in every part of the basin.

In the case of regions with widespread rice fields and natural wetlands, the most important difficulty when classifying land use from satellite data are to find differences between the two kinds of land uses or vegetation covers. Due to the high amount of water content in the soil in both types of vegetation, automatic classification using remote sensing normally shows confusion between classes. To

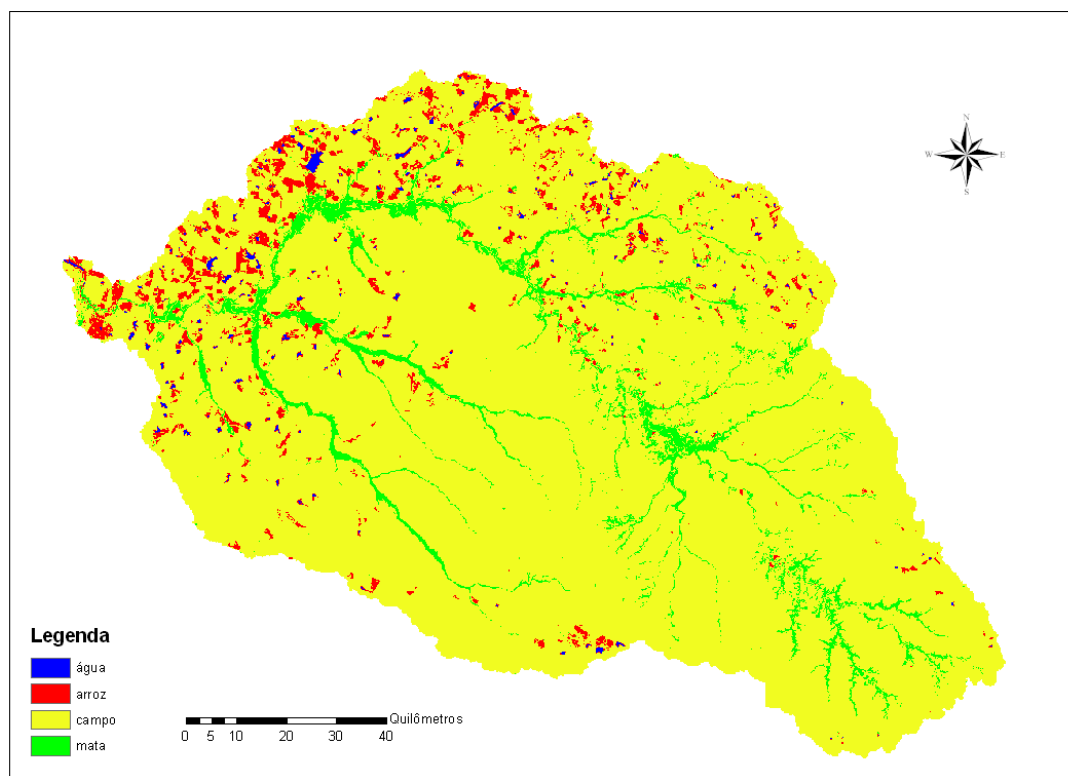


Figure 6.2 Land use map of the Quaraí river basin.

overcome this problem, CBERS satellite images from two dates were used: one from the winter time and another from the summer time. During the winter, rice fields are still being prepared to be inundated, and the soil is exposed. During the summer, rice fields are covered by shallow water and by growing rice plants cover. Three bands of the CBERS image were used for each date, as if they were 6 bands of the same image, and supervised classification procedure was applied to these six bands.

The images were classified in four classes of land use and vegetation: water, pasture, forest and rice fields. The final map generated by this classification is shown in Figure 6.2. Table 6.2 shows the area covered with the different land uses and vegetation types in the Quaraí river basin. Table 6.2 shows that the most widespread land use and vegetation in the basin is pasture, with 90% of the basin area. Forest remains are concentrated along the drainage network, and rice fields are more concentrated to the northwest of the basin. It becomes clear that rice fields are more common in Brazil, which is north of the main river, than in Uruguay.

While only 45% of the basin area is located in Brazil, 67% of the rice field area is concentrated in this country. The most important part of the areas classified as water, which are mostly reservoir surfaces, is also located in Brazil, with 67% of the 117 km². The estimates obtained during this work were compared to other data bases in Brazil, showing a very good agreement.

Table 6.2 Land cover and vegetation areas within the Quaraí river basin.

Land use	Area (km ²)	Area (%)
Water	117.1	1%
Rice	723.4	5%
Pasture	13120.1	90%
Forest	642.7	4%

6.5.4 Simulation of small reservoirs in the MGB-IPH model

One of the most important hydrological characteristics of the Quaraí river basin is the high number of small reservoirs for which the proper data on volume and operation are normally missing.

All reservoirs with surface areas larger than 3 ha were included explicitly in the model, including its connection to the upstream and downstream catchment and river reach and the water abstractions to the nearby rice fields. Each reservoir received an internal identification number, and the total number of reservoirs included in the simulation was 402.

In the MGB-IPH model the small reservoirs were represented using a water continuity equation taken into consideration the main inputs and outputs for each reservoir. The considered water inputs are direct rainfall and input streamflow. The considered outputs are abstractions for irrigation, spills and evaporation. Given the general absence of low flow discharge structures in the basin reservoirs, no discharge outputs were considered except for the spills during high flows.

Figure 6.3 presents the inputs and outputs considered for each reservoir, where Q_i means streamflow entering the reservoir from upstream; E means evaporation; P means direct precipitation over the reservoir surface; Q_v means water spills during high flows and Q_d means water abstractions for rice field irrigation.

For each time step, the water balance equation is applied in order to obtain the reservoir volume at the end of the time step (VR_2) given the reservoir volume at the start of the time step (VR_1) and the inputs and outputs. The equation is applied in daily time steps. A first estimate of the final reservoir volume is obtained by applying the following equation, considering that Q_v is zero:

$$VR_2' = VR_1 + A \cdot (P - E) + (Q_i - Q_d - Q_v) \cdot \Delta t$$

where: VR_2 , VR_1 and VR_2' , are volumes in m^3 ; A is the surface area of the reservoir in m^2 ; P is the rainfall falling over the reservoir surface and given in m; E is the evaporation in m; Q_i is the input streamflow in m^3s^{-1} ; Q_d is the discharge used for irrigation in m^3s^{-1} ; and Δt is the length of the time step in seconds (86400 s).

If VR_2' is more than the reservoir capacity, the water excess has to be spilled, and VR_2 is set to V_{max} (the reservoir capacity). If VR_2' is lower than zero, than the water abstraction is reduced as much as necessary to result in $VR_2' = 0$. If VR_2' is between zero and the reservoir capacity, it is adopted as the volume at the end of the time step ($VR_2 = VR_2'$).

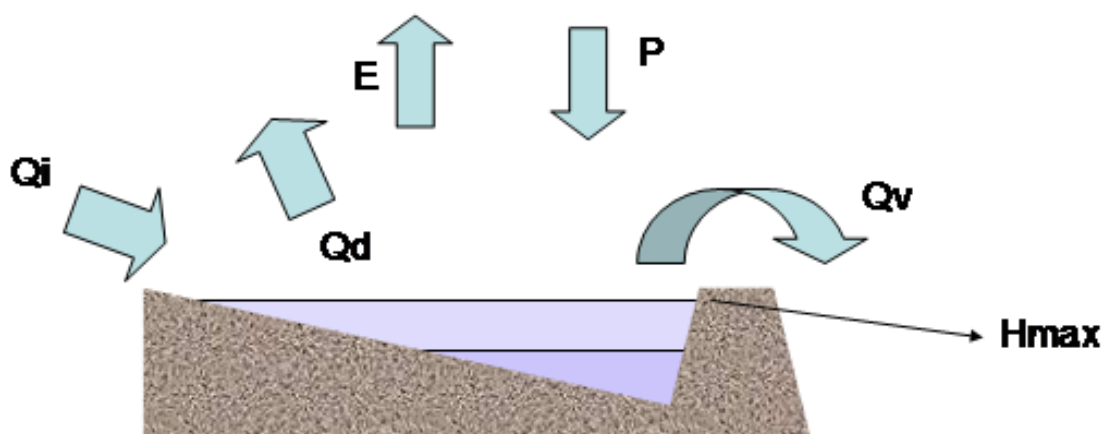


Figure 6.3 Water balance variables considered in the simulation of a reservoir.

These statements mean the same as:

$$VR_2 = VR_2' \quad \text{when} \quad 0 < VR_2' \leq V \max$$

$$VR_2 = V \max \quad \text{when} \quad VR_2' > V \max$$

in this last case, the spilled discharge is calculated as:

$$Qv = \frac{(VR_2' - V \max)}{\Delta t}$$

The surface area of the reservoir is considered to be a linear function of the reservoir volume, according to the following equation:

$$A = A \max \cdot \left(\frac{VR_1}{V \max} \right)$$

where: $A \max$ is the maximum area of the reservoir (obtained from the satellite images for each reservoir) in m^2 ; and $V \max$ is the maximum reservoir volume, or reservoir capacity (m^3).

Reservoir capacity at maximum volume was estimated from databases of reservoirs in Brazil and Uruguay and from a linear regression relating surface area and reservoir capacity. Maximum area of each reservoir was obtained from satellite images. The regression curve relating surface area and reservoir capacity was obtained using data from 93 reservoirs in Uruguay and 15 reservoirs in Brazil for which these data were available. A linear function was adjusted to these data, as can be seen in Figure 6.4.

6.5.5 Simulation of rice fields

For each rice field included in the model a similar approach was applied in the simulation as in the case of reservoirs. Every rice field larger than 10 ha was included explicitly in the simulation. A total number of 477 rice fields were identified after the image classification, filtering and vectorisation of the rice fields. Each field received a identification number.

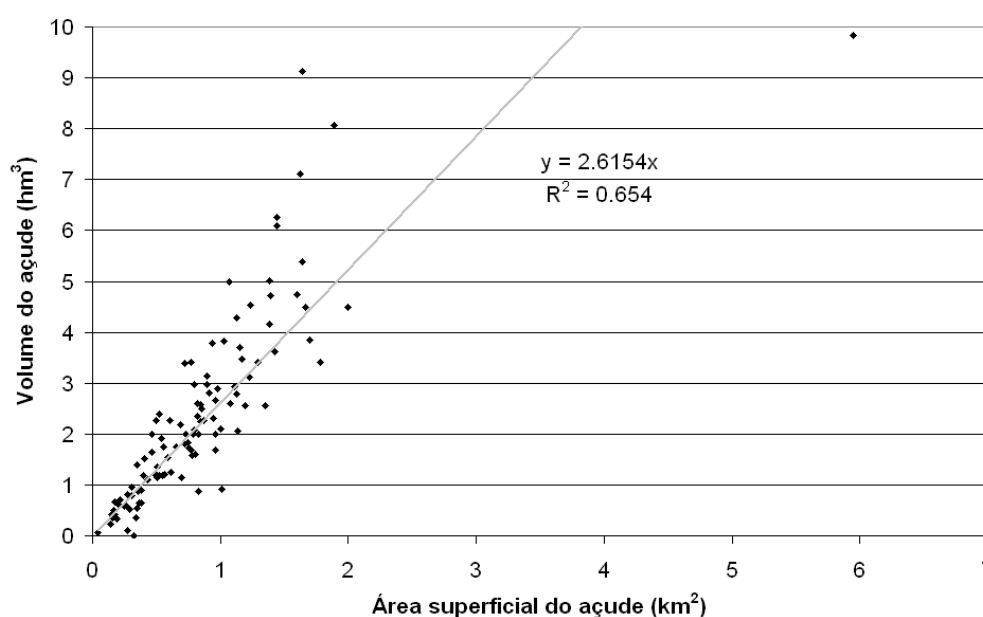


Figure 6.4 Relation between surface area and maximum reservoir volume and linear function adjusted to the data.

Every rice field was connected to a nearby water source (stream or reservoir). These connections were defined based on high resolution satellite images available in GoogleEarth. The relative sizes of rice fields and reservoirs were also considered; the normal relation is 1 ha reservoir for 3 ha rice fields. In several cases, diversion canals and pumping devices could be identified in the high resolution images, however more precise connections should be obtained by field work. It was also considered that a rice field could be connected to more than one water source, as this is often the case in this region, where pumping devices are sometimes moved according to the availability of water.

The rice field water balance equation includes storage of water, input of water from rainfall (P) and irrigation (Irr) and output from evaporation (ET) and losses (Di and Dv). Figure 6.5 illustrates the terms involved in the water budget of a rice field. Irrigation of the rice fields in this region is applied to maintain a minimum depth of water ($Hmin$) while ditches around the rice paddies can hold a maximum amount of water at maximum depth ($Hmax$).

The equation used to simulate the water budget for each rice field is the following:

$$H_2 = H_1 + P - ET + Irr - Di - Dv$$

where: H_2 is the water level inside the rice field at the end of the time step (mm); H_1 is the water level inside the rice field at the start of the time step (mm); P is the rainfall amount falling over the field over the time step (mm); ET is the evapotranspiration over the time step (mm); Irr is the amount of irrigation during the time step (mm); Di is the loss of water due to infiltration into the soil during the time step (mm); and Dv is the loss at the borders of the rice paddies mainly due to overspilling.

The rainfall amount P for each rice field is obtained from the interpolated rainfall data observed at the raingauges. The evapotranspiration ET is obtained by applying the Penman-Monteith equation considering zero surface resistance (which should be a good estimate of water evaporation ET_0). This value is further modified by an equation proposed described by Mota (2000) to include the transpiration of rice plants:

$$ET = 0.91 ET_0 + 1.84$$

where: ET and ET_0 are given in mm/day.

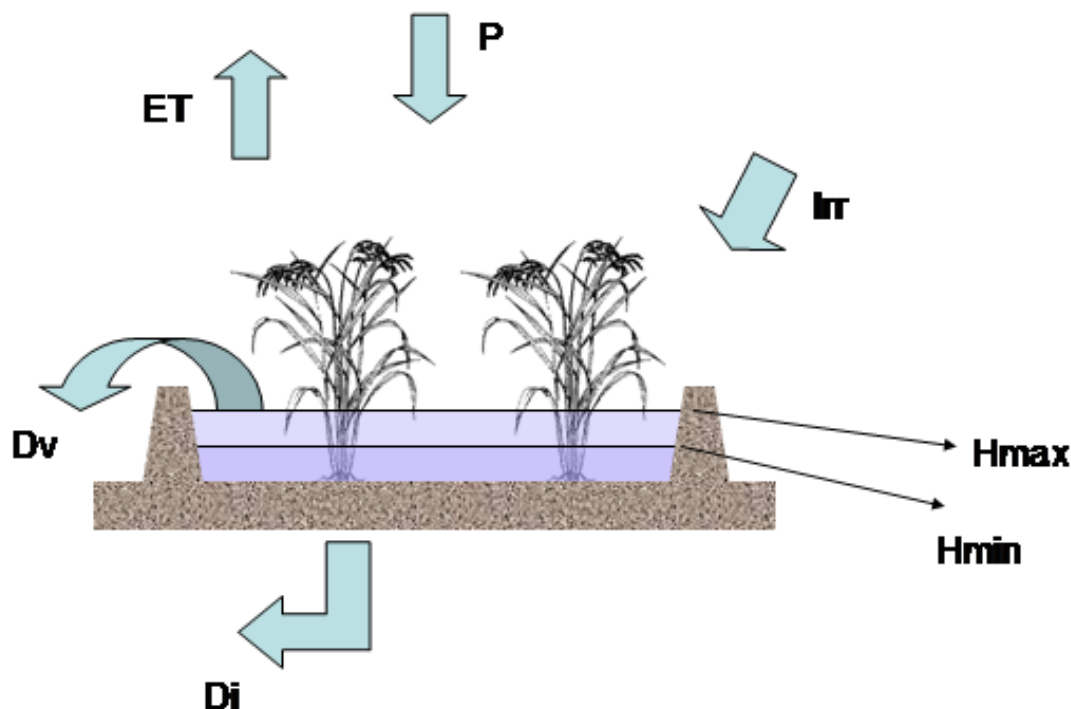


Figure 6.5 Scheme of water fluxes in a rice field: rainfall (P); irrigation (Irr); evapotranspiration (ET); infiltration losses (Di); spilling losses (Dv).

Losses are calculated based on water levels at the start of the time step (H_1), according to the following equations:

$$D_i = \text{PerdMin} \quad \text{when } H_1 \geq H_{\min}$$

$$D_i = \text{PerdMin} \cdot \frac{H_1}{H_{\min}} \quad \text{when } H_1 < H_{\min}$$

and:

$$D_v = (\text{Perd}_{\max} - \text{Perd}_{\min}) \cdot \frac{(H_1 - H_{\min})}{(H_{\max} - H_{\min})} \quad \text{when } H_1 \geq H_{\min}$$

$$D_v = 0 \quad \text{when } H_1 < H_{\min}$$

where: Perd_{\max} and Perd_{\min} are parameters which represent, respectively, the losses occurring when water level is low (H_{\min}) and when water level is maximum (H_{\max}). These values were calibrated in order to result in no overall water use similar to that measured at experimental rice fields in South Brazil. Adopted values of these parameters are shown in Table 6.3.

The simulation is carried out considering that irrigation is applied to supply the water amount needed to end the time step at the minimum water level in the rice field ($H_2 = H_{\min}$). During rainy days, precipitation on the field can partially or totally supply the water needs, and no irrigation is necessary. During dry days, irrigation is needed to balance evapotranspiration and infiltration losses ($\text{Irr} = \text{ET} + D_i$).

The objective of irrigation is to maintain the water level at H_{\min} during the cultivation period. The maximum water level H_{\max} , on the other side, is a threshold which cannot be exceeded. When, at the end of the time step, the water level H_2 is higher than H_{\max} , the value of H_2 is reduced to H_{\max} and the excess water is added to D_v , as additional losses due to spilling.

All the losses due to infiltration and spilling of rice fields are routed to the next downstream reservoir or river reach.

6.5.6 Rice cultivation period

The overall time of rice cultivation in South Brazil is close to 100 days. Irrigation of rice fields starts in October or November. Irrigation in every rice field can start in a different day. To represent this variability in the hydrological model simulations, a probability distribution of the day of irrigation start was created, using a uniform distribution starting at 15 October and ending at 16 November. Every individual rice field starts its irrigation period on one of those days and the irrigation period extend for 100 days. The end of the irrigation period occurs in January or February.

Table 6.3 Values of parameters used in the simulation of rice fields within the MGB-IPH model.

Parameter	Adopted value	Comments
H_{\min}	50 mm	Minimum water level that should be maintained in the rice field
H_{\max}	100 mm	Maximum water level that can occur in the rice field
Perd_{\min}	1 mmday^{-1}	Losses due to infiltration that occur when the water level is between minimum and maximum
Perd_{\max}	45 mmday^{-1}	Losses due to spilling, infiltration of rice paddies walls and break of ditches when water level is at its maximum

6.6 Calibration

Calibration of the MGB-IPH model follows a three-step procedure: firstly, estimating parameter values based on prior applications of the model; secondly, manual adjustments (if necessary); and thirdly, automatic multi-objective calibration.

Based on a parameter sensitivity study that was carried out for a basin with similar climatic characteristics with the Quarai/Cuareim basin, it is known that the most important parameter subject to calibration is Wm , which represents the water holding capacity of the soil. This parameter has a different value for each GRU (combination of soil type and vegetation). Parameter Wm controls the amount of water that is retained in the soil or infiltrated during rainfall events and that is available for posterior evapotranspiration, or that can be percolated to the subsoil; therefore it exerts large influence on calculated streamflow volumes, flood peaks and baseflow.

The other parameters changed during calibration are b ; $Kint$; $Kbas$; Cs and Ci . Parameter b appears in the relation between relative soil moisture and percent saturated area and cannot, in principle, be related to any physical variable. Relatively large values of b result in calculated hydrographs that are very sensitive even to weak rainfall events. Parameters $Kint$ and $Kbas$ have units of hydraulic conductivity and control the outflux from the soil to subsurface flow and baseflow. $Kint$ is normally less important and $Kbas$ is more important to correctly represent low flows and overall volume. Reasonable first estimates of $Kint$ and $Kbas$ should be obtained based on soil types; however, practice shows that these estimates may be far from effective parameter values due to several uncertainties. Parameters Cs and Ci are non-dimensional and are used to adjust first estimates of response times of the linear reservoirs that are based on relief information from the DEM.

After initial tests with a priori defined parameter values and minor manual adjustments, the automatic multi-objective calibration algorithm MOCOM-UA (Multi-Objective Complex Evolution Method; Yapo *et al.*, 1998) is used to calibrate the parameters. MOCOM-UA is a multi-objective optimisation method that combines the evolution of a population of parameter sets that is similar to a genetic algorithm with the simplex of Nelder & Mead method (Press *et al.*, 1995) of downhill search and a Pareto dominance criterion. MOCOM-UA was proposed by Yapo *et al.* (1998).

In the calibration of the MGB-IPH model, the objective functions could be different error statistics for the same gauging station or for different gauging stations. When only one gauging station with data exists the model is usually calibrated considering three objective functions: the Nash-Sutcliffe efficiency NS ; the Nash-Sutcliffe efficiency for logarithms of streamflow NS_{\log} ; and the volume bias ΔV , set out in order below:

$$NS = 1 - \frac{\sum_{t=1}^{nt} (Q_{obs}(t) - Q_{cal}(t))^2}{\sum_{t=1}^{nt} (Q_{obs}(t) - \overline{Q_{obs}})^2}$$

$$NS_{\log} = 1 - \frac{\sum_{t=1}^{nt} (\log(Q_{obs}(t)) - \log(Q_{cal}(t)))^2}{\sum_{t=1}^{nt} (\log(Q_{obs}(t)) - \overline{\log(Q_{obs})})^2}$$

$$\Delta V = \frac{\sum_{t=1}^{nt} (Q_{cal}(t)) - \sum_{t=1}^{nt} (Q_{obs}(t))}{\sum_{t=1}^{nt} (Q_{obs}(t))}$$

where: t is the time step (day); nt is the number of time steps; ΔV is the volume bias; Q_{cal} is calculated streamflow (m^3s^{-1}); Q_{obs} is observed streamflow (m^3s^{-1}); and $\overline{Q_{obs}}$ is the average observed streamflow (m^3s^{-1}).

The calibration of the MGB-IPH model in the Quaraí river basin was based on comparison of calculated and observed flows at Artigas/Quaraí gauging station from 1980 to 2002. Reservoirs and water abstractions were included in the simulation during the calibration period because both were present in the basin for decades.

Calibration results can be seen in the form of streamflow hydrograph comparisons and flow duration curve comparison. Figure 6.6 is a comparison between observed (black) and calculated (red) hydrographs, showing relatively good agreement, however some of the flood peaks are underestimated. Another striking aspect of the hydrographs shown in Figure 6.6 is the very low baseflow.

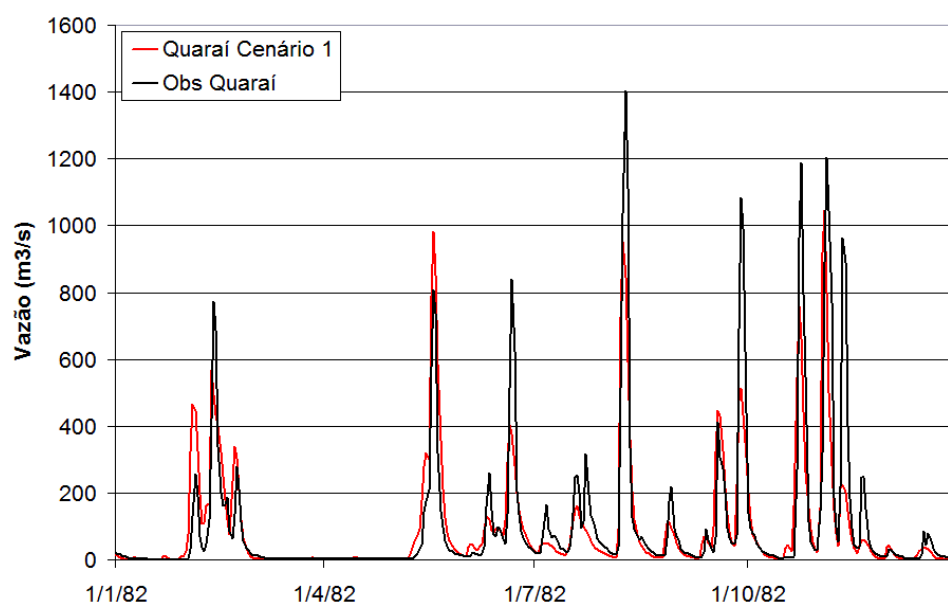


Figure 6.6 Calculated (red) and observed (black) hydrographs of the river Quaraí at Artigas/Quaraí gauging station during part of the calibration period.

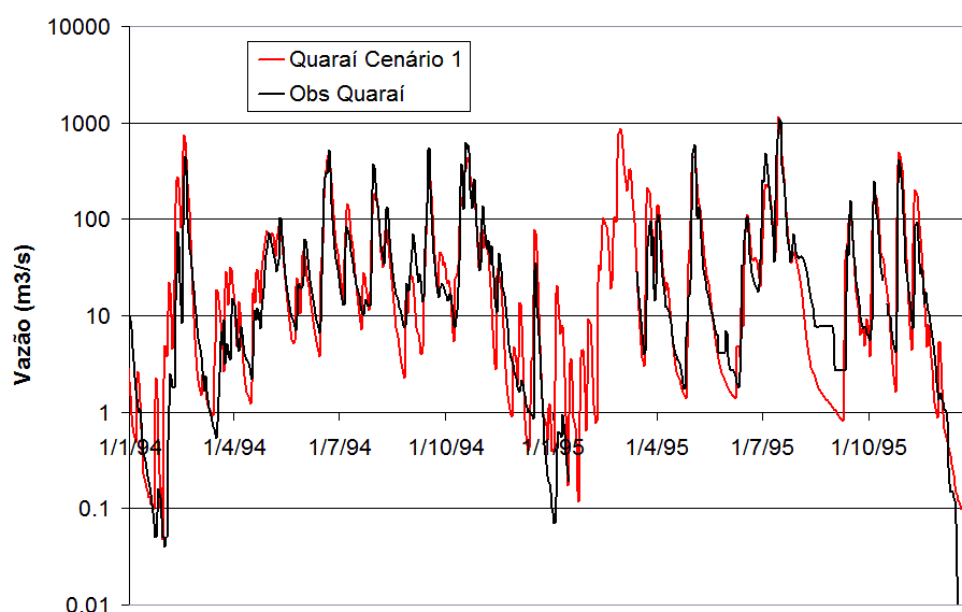


Figure 6.7 Calculated (red) and observed (black) hydrographs of the river Quaraí at Artigas/Quaraí gauging station during part of the calibration period (1994-95 – logc scale to highlight low flows).

Figure 6.7 presents a comparison between observed (black) and calculated (red) hydrographs for two years (94 and 95) where streamflow is depicted in a logarithm axis, giving a better view of the low flow periods. It can be seen that low flows can be close to zero during the summer months, which is probably an effect of both natural conditions and river water abstractions. Adjustment between observed and calculated hydrographs is far from perfect; however, the main aspects, including the intensity of droughts, are relatively well reproduced.

It can be seen in Figure 6.7, that minimum flows during the austral winter are higher than during summer. This difference is a result of the lower evapotranspiration during the winter and of the concentrated river water abstractions during the summer. During the last days of 1995, streamflow decreased to zero.

Flow duration curves base on calculated and observed streamflow time series are presented in Figure 6.8. It can be seen that there is a relatively good overall agreement of these curves, particularly in the range from Q_{50} to Q_{95} . For streamflow values below the Q_{95} there is a tendency of the model to overestimate streamflows.

Observed Q_{90} is $1.3 \text{ m}^3\text{s}^{-1}$ while calculated Q_{90} is $1.2 \text{ m}^3\text{s}^{-1}$. This agreement is very good when considering the uncertainty of both observed and calculated streamflows. The Q_{90} reference flow is frequently used in Brazil as an indication for low flow conditions, and is sometimes used as the basis for water permits analysis; therefore, it is important that the hydrological model is able to generate consistent results in this flow range.

The agreement between observed and calculated flows is also good for the Q_{95} reference flow, with only a slight overestimation: calculated Q_{95} is $0.6 \text{ m}^3\text{s}^{-1}$ and observed Q_{95} is $0.5 \text{ m}^3\text{s}^{-1}$.

Unfortunately there are no other gauging stations with streamflow data on the river Quaraí. Particularly needed would be a gauging station located close to the river confluence with the Uruguay river. It is known, however, that the Uruguay exerts backwater effect on the Quaraí for several kilometres, and this fact should be taken into account when defining a new gauging point.

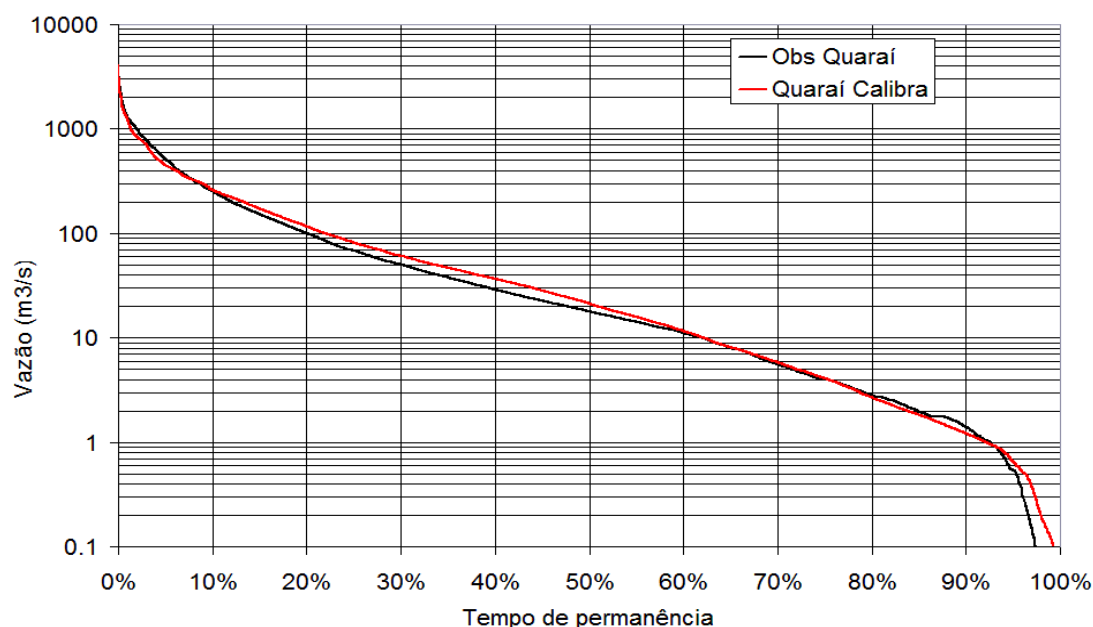


Figure 6.8 Flow duration curves for observed (black) and calculated (red) streamflows at Quaraí/Artigas from 1980 to 2004.

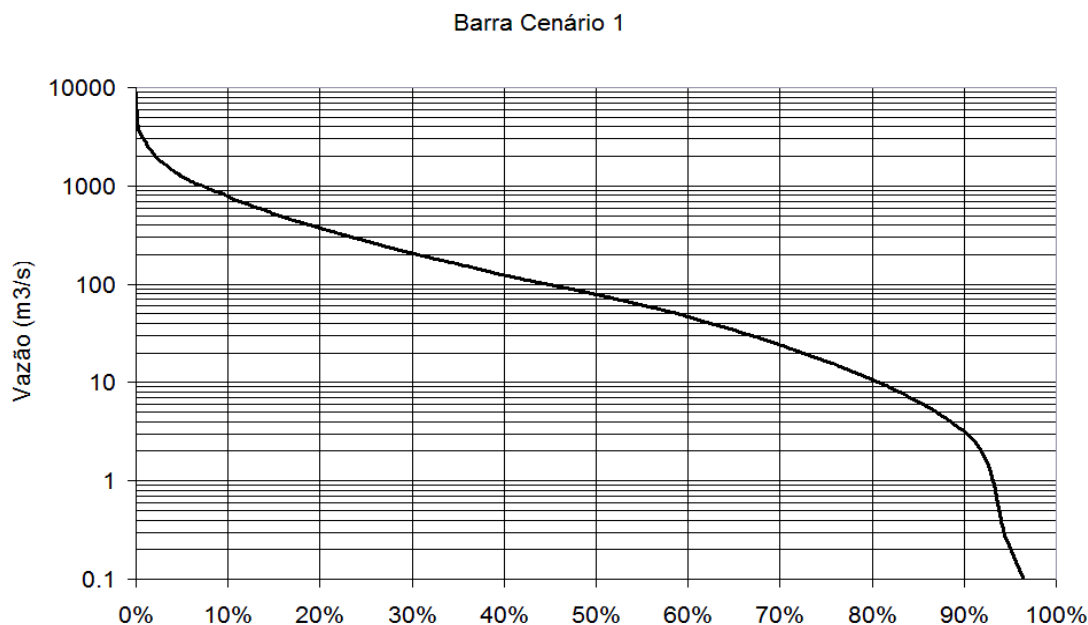


Figure 6.9 Flow duration curve of the river Quarai at its outlet (Barra do Quarai) showing lower values of Q_{95} than further upstream (Artigas/Quarai) due to river water abstractions.

The need for a new gauging station downstream of Quarai/Artigas is because most of the river abstractions are in the lower part of the river. Simulation results show that low flows in at the outlet of the Quarai river are even lower than at the Quarai/Artigas gauging station, due to these increase in water abstractions in the lower reaches. Figure 6.9 presents the flow duration curves at the Quarai river outlet, where it can be seen that calculated Q_{95} is only $0.2 \text{ m}^3\text{s}^{-1}$, which is far less than in Artigas/Quarai ($0.6 \text{ m}^3\text{s}^{-1}$).

6.7 Validation

6.7.1 Validation of hydrological model results

The hydrological model was validated using streamflow data from a gauging station which was not used during the calibration process: the Javier de Viana gauging station on the Tres Cruces river. The Tres Cruces river is one of the most important tributaries of the Quarai, and it flows into the Quarai from the South. Its basin lies completely in Uruguay, and at the point called Javier de Viana its drainage area is 580 km^2 .

Results of streamflow hydrographs of the Tres Cruces river at Javier de Viana gauging station are shown in Figure 6.10, together with observed hydrographs, for year 1995. Flood peaks are somewhat overestimated, but the figure shows a general good agreement between observed and calculated hydrographs

Figure 6.11 shows the hydrographs at the same place using logarithm scale for the streamflow to highlight the low flows. It can be seen that the calculated streamflow is in accordance with the observed flow, both showing the most critical period starting in October.

After the analysis of the results in the Tres Cruces river, it was concluded that the hydrological model is validated and could be used to generate streamflow data at different parts of the basin. It would be very useful, however, to have more gauging stations on the main river and some of its tributaries to improve the calibration.

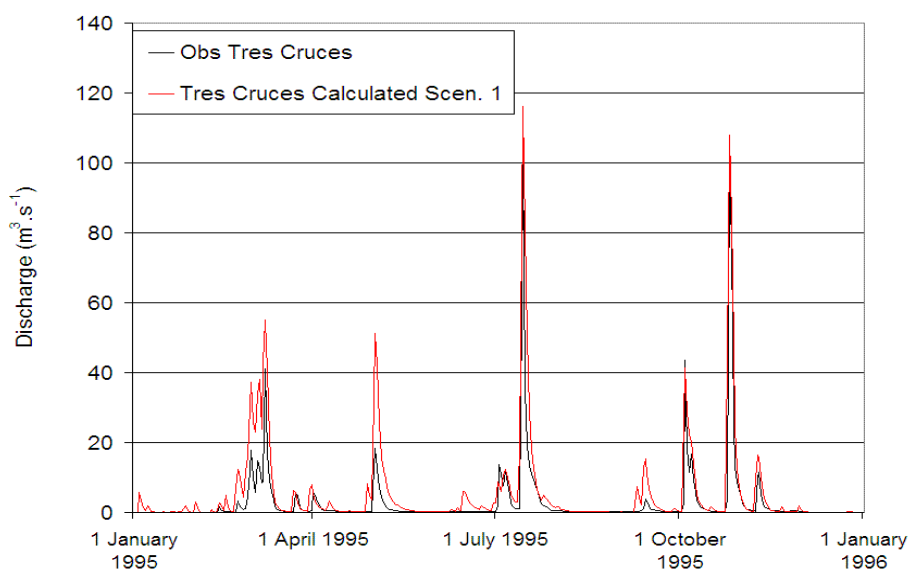


Figure 6.10 Calculated (red) and observed (black) hydrographs of the river Tres Cruces at Javier de Viana gauging station (model validation).

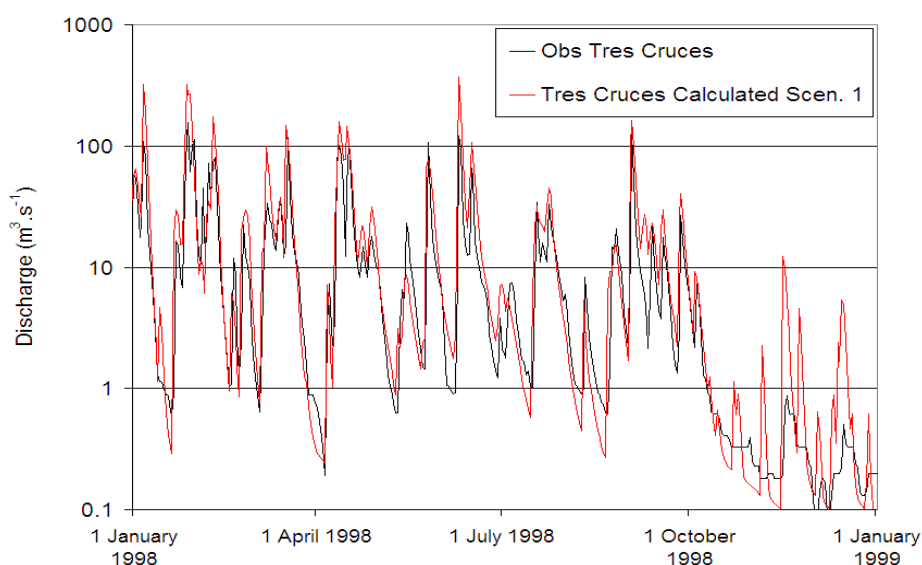


Figure 6.11 Calculated (red) and observed (black) hydrographs of the river Tres Cruces at Javier de Viana gauging station (logarithmic scale to highlight low flows).

6.7.2 Validation of irrigation water use estimates

The amount of water used for irrigation of rice is object of discussion due to the difficulty in measuring the actual water use and differing total use, which is the water abstracted from a river or reservoir, from effective use, which is the amount of water losses due to evapotranspiration. Infiltration losses and leaks at the end of the fields are normally taken as return flows, which may be available for users downstream. The amount of water that infiltrates into the soil depends on soil characteristics, and the amount of leaks at the end of ditches that encircle the fields is normally considered to be proportional to relief variability.

Estimates of total water use for rice irrigation in South Brazil are in the range from $6000 \text{ m}^3\text{ha}^{-1}\text{year}^{-1}$ to $15000 \text{ m}^3\text{ha}^{-1}\text{year}^{-1}$, depending on the region, and depending on the technology used. In the Quaraí river basin, a total water use of nearly $10000 \text{ m}^3\text{ha}^{-1}\text{year}^{-1}$ is used as a reference. It is not clear, however, if this figure considers rainfall or not.

Water use for rice irrigation in the hydrological model varied from year to year, depending on the quantity of rainfall that fell over the field during the summer. As previously explained, irrigation was considered to be the quantity of water necessary to maintain a permanent sheet of water over the soil. Evapotranspiration was estimated using Penman-Monteith's equation and losses due to infiltration and leaks were estimated considering two parameters ($Perd_{Min}$ and $Perd_{Max}$). These parameters were adjusted until the water use for irrigation in the model was close to the estimates normally adopted in the Quaraí river basin.

Figure 6.12 presents the total quantity of water used in each of the cultivation cycles (summer) from 1980 to 2006. The total water use is the sum of irrigation and rainfall. This total varies in the range 10000 to 16000 $m^3ha^{-1}year^{-1}$. Irrigation demand is higher during years with low rainfall and lower during years with high rainfall. The average irrigation demand obtained with the model was close to 8000 $m^3ha^{-1}year^{-1}$.

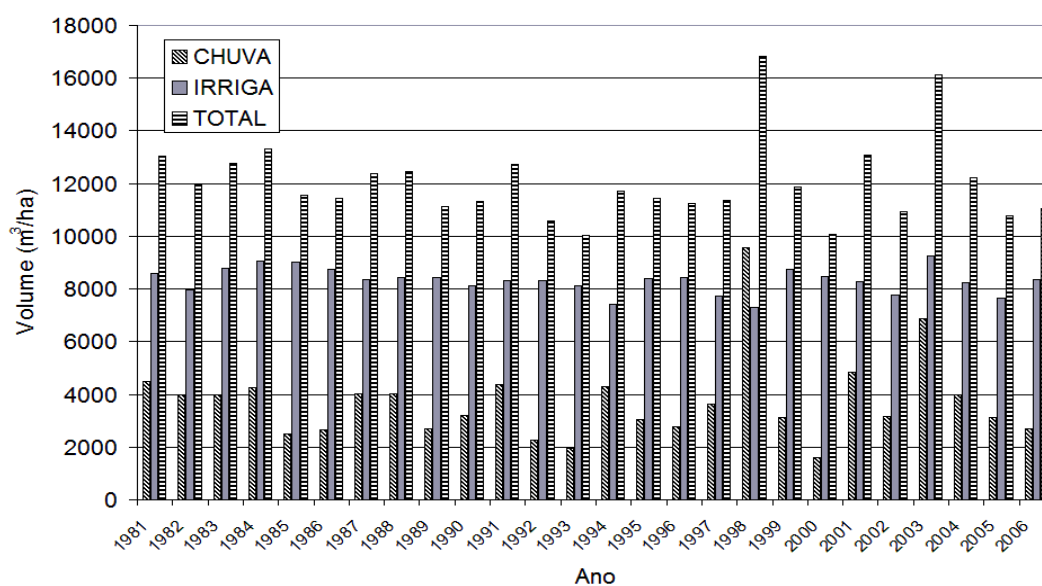


Figure 6.12 Water used in rice irrigation according to the hydrological model results from 1981 to 2006, considering total water use, rainfall and supplemental irrigation.

Given the similarity of the results obtained with the model and the values usually taken as reference in the region, it was considered that the model was validated in terms of water use. This is obviously a very important question, and further work should be carried out to improve the estimates of effective water use. An initiative to do that was taken by the Uruguayan partner of TWINLATIN (DNH).

6.8 Evaluation of hydrological modelling (D3.2)

The hydrological modelling will provide the basis for analysis in several other work packages. Due to the unique characteristics of the Quaraí river basin, particularly the high number of small farm dams and reservoirs, and the intensive use of water for irrigation, it was not a simple application of a hydrological model. It was necessary to adapt a hydrological model to include hundreds of reservoirs and rice fields. Therefore the model that was chosen was the MGB-IPH model, which source code is developed in IPH and can be adapted to handle those characteristics.

Several limitations of the modelling work have been detected during the activities. The first one and probably the most important is the low availability of hydrological data. Rainfall gauging stations are relatively sparse and time series show several periods with data missing. Streamflow is being collected routinely only in one single gauging station. Both Brazil and Uruguay monitor the same point, located close to the bridge between Artigas and Quaraí. At this point the drainage area of the basin is more or less one third of its whole size at the river outlet at Barra do Quaraí.

Streamflow data were found for another location on a tributary of the river Quaraí, the river Tres Cruces, at Javier de Viana. However this gauging station showed only a short period of valid data and could be used only for model validation. Another gauging point is urgently needed in the lower reach of the Quaraí river and at some of its tributaries to permit a clear understanding of the actual effects of water abstractions over the basin.

During the modelling activities several assumptions had to be made concerning the size of reservoirs and the amount of water used for irrigation, because information was not available. A linear regression was used between reservoir surface area and its total volume, since surface area could be easily obtained from satellite images. There is obviously a large uncertainty associated with this assumption. Every one of the more than 400 reservoirs larger than 3 ha found in the basin should have an estimate of volume somewhat better than that obtained by the linear regression function.

Another arbitrary assumption that was made during the modelling work was the definition of connections between rice fields and water sources, which was done based on proximity rather than actual field information. This should be improved for a next phase of hydrological modelling work in the basin.

Water quality data were completely absent in the basin and the first known sampling activities were undertaken during TWINLATIN, and will be discussed in the WP6 report.

Results of the model analysis were already presented to the public, including stakeholders in the basin, and government institutions. The National Water Agency (ANA) is using results of the model to support decisions concerning water permits, and the water authorities in the state Rio Grande do Sul asked for simulations of the effects of large reservoirs in the basin.

6.9 Summary and recommendations

Future hydrological modelling in the basin should be based on better hydrological data. Therefore it is strongly recommended that at least two more flow gauging stations should be established in the Brazilian side of the basin. One should be on the lower reach of the river Quaraí, as close as possible to its mouth, but free of the backwater effects of the river Uruguay. The other should be placed on one of the main tributaries of the Quaraí downstream of the city. This recommendation will be transmitted to the National Water Agency, which is in charge of hydrological measurements in Brazil.

Another recommendation refers to the lack of information that exist concerning the volume and operation rules of the small farm reservoirs. It has been shown during the hydrological modelling work that those reservoirs exert a considerable influence on streamflow. However the real extend of this influence is dependent on the actual size of the reservoirs. The estimates based on the linear regression between area and volume used for this study should be limited to the minority of the reservoirs.

One of the most important obstacles to hydrological modelling in the Quaraí river basin is related to the lack of knowledge of the actual locations where water is being abstracted from the rivers. It is strongly recommended to elaborate an inventory of water users in the basin and to include very detailed information on how much and where water is be taken from the rivers of the basin.

7. Cuareim River Basin (Uruguay)

7.1 Description of basin

7.1.1 Location

The Tres Cruces creek is one of the most important tributaries on Uruguayan territory of the Cuareim River which is a tributary of the Uruguay river, and border between Brazil and Uruguay. The Tres Cruces creek basin has an area of 1.466 km² and is entirely located in the Artigas department (Figures 7.1 and 7.2).



Figure 7.1 Location of the Tres Cruces creek

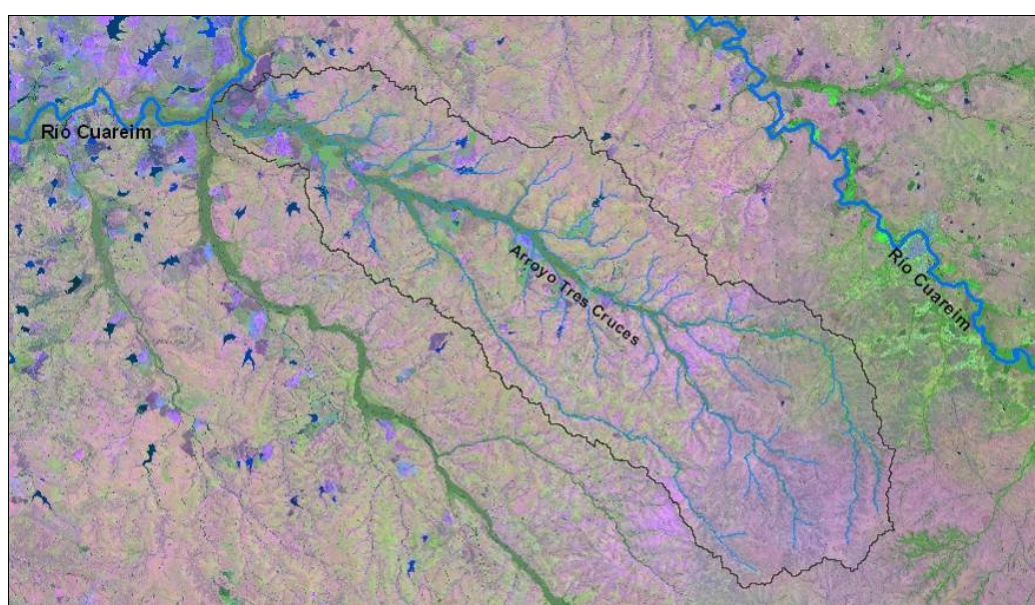


Figure 7.2 Tres Cruces creek basin

7.1.2 Climatology

Uruguay is the only South American country which is entirely in the temperate zone. The absence of major terrain heights contributes to small spatial variations in temperature, precipitation and other parameters. However, it presents a high temporal variability, in particularly interannual one.

Temperature

The average annual temperature for the country is around 17° C while for the department of Artigas is around 19° C, the highest average temperature in Uruguay.

Winds

In Uruguay, the absence of high topography that could act as a barrier, determines very strong and long lasting winds. For the department of Artigas, the average wind intensities are around 4 ms⁻¹.

Precipitation

The Uruguayan climate is characterised by precipitations all year round and a high interannual variability. The average annual rainfall in the country is about 1175 mm while in the department of Artigas it exceeds 1400 mm. The main feature of the precipitation is its extreme irregularity, so there are periods of droughts as well as periods of flooding.

To characterise the precipitation in the Tres Cruces creek basin data recorded by the National Directorate of Meteorology (DNM) were used. The raingauges with influence in the basin which have the largest common registration period (1932 - 2007)³ were chosen. The location of these raingauges is presented in Figure 7.3 and the data record periods in Table 7.1.

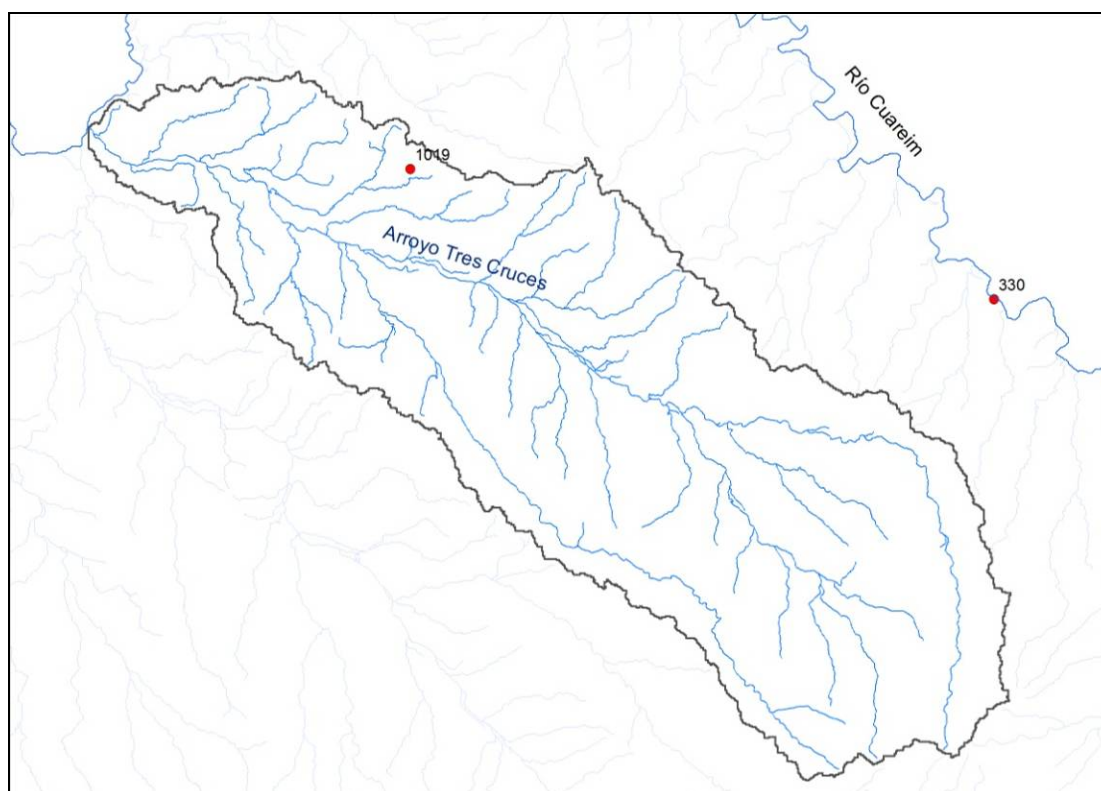


Figure 7.3 Raingauges with influence in the Tres Cruces creek basin

³ Though the raingauges 1021 (El Topador), 1044 (Paso Farías), 1048 (Taruman) and 1082 (Cerro Amarillo) have influence on the Tres Cruces creek basin, their data begin after 1956, or after 1981 in the case of Cerro Amarillo or have missing data as is the case of Paso Farías for 1949-2005 (14% of 95 years).

Table 7.1 Selected raingauges

Code	Name	Longitude (°)	Latitude (°)	Period of registration	
330	Artigas	-56,50	-30,35	April 1931	July 2008
1019	Bernabé Rivera	-56,95	-30,28	January 1914	July 2008

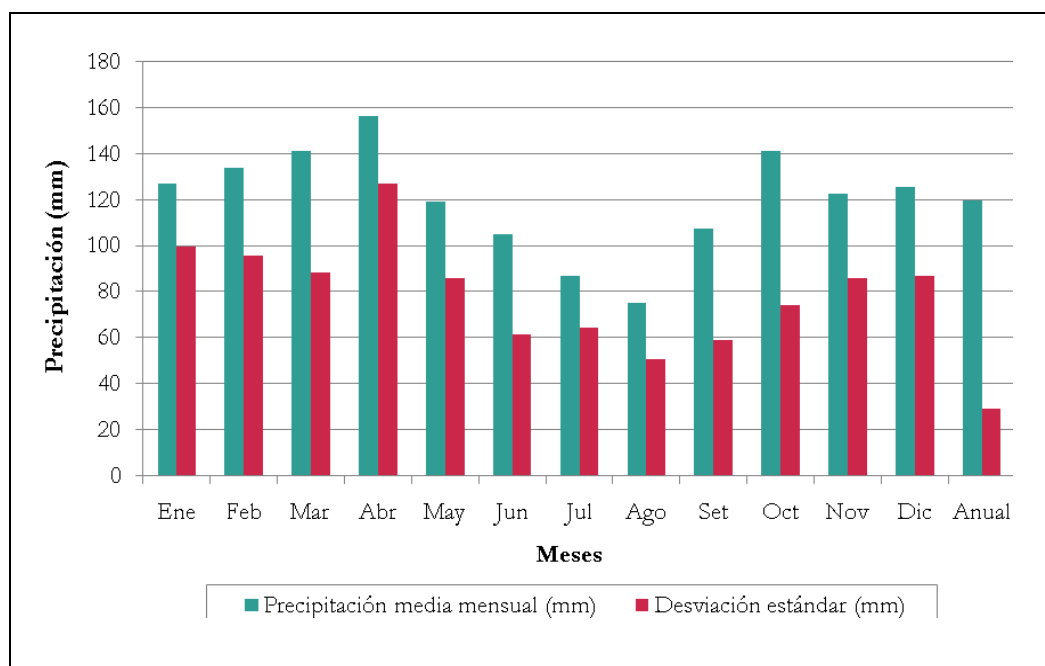


Figure 7.4 Precipitation annual cycle for the 330 rain gauge. Precipitation in mm on the vertical axes and Months from January to December on horizontal axes, being the last one Annual values. The grey bars are the monthly average precipitation and the red bars the standard deviation in mm.

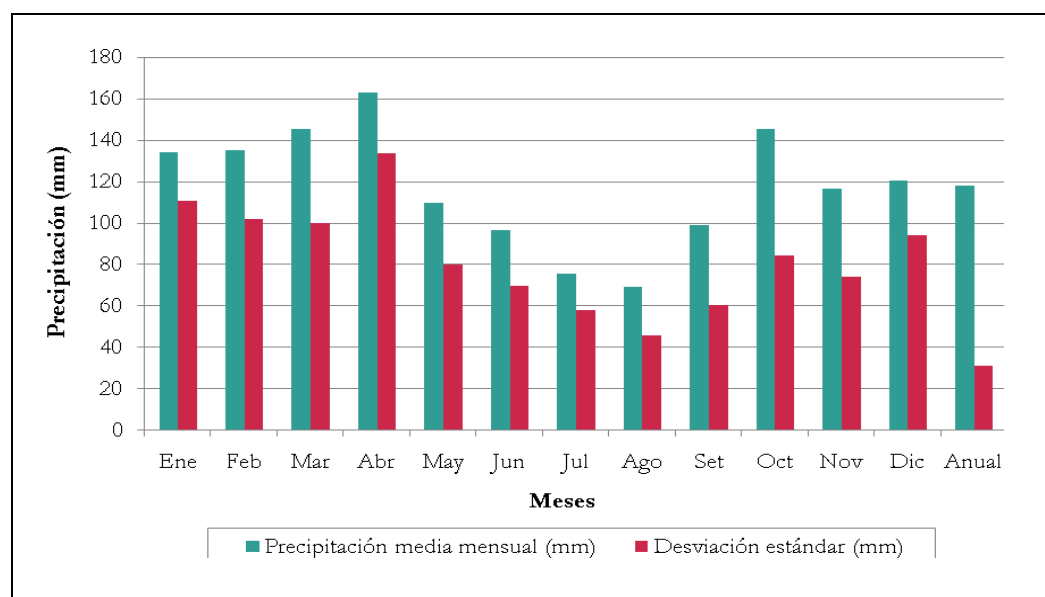


Figure 7.5 Precipitation annual cycle for the 1019 rain gauge. Precipitation in mm on the vertical axes and Months from January to December on horizontal axes, being the last one Annual values. The grey bars are the monthly average precipitation and the red bars the standard deviation in mm.

Figures 7.4 and 7.5 show the annual cycle of the rainfall and standard deviations for the periods 1932 - 2007 for the selected raingauges. They can observe that the standard deviation is about the average monthly rainfall, which translates into a high variability in rainfall month. The monthly rainfall can be extremely variable from zero to more than double the average value.

7.1.3 Geology

Figure 7.6 presents the geology for the Tres Cruces creek basin according to the Geology Map of Uruguay. The lithology is almost uniform, being represented almost entirely by the Arapey formation (integrated by multiple basalt spills with some sheets of sandstones). Also there is the presence of recent sediments (Aluviones).

7.1.4 Soils

Most soils in the Tres Cruces creek basin were developed on basaltic rock (Arapey Formation) and can be categorised based on their depth, in surface soils (less than 40 cm of thickness) and deeper soils (between 40 and 120 cm of thickness). Shallow soils are mainly in the upper basin, area where rooting of pastures is difficult, what makes farming and ranching difficult. Deeper soils are better for the development of pasture and for planting crops including rice.

According to the "Carta de Reconocimiento de Suelos del Uruguay, a escala 1:1.000.000" (Altamirano *et al.*, 1976) which constitutes a morphogenetic classification (cartographic units based associations of soil), the units present in the Tres Cruces creek basin are the ones shown in the Figure 7.7.

Table 7.2 presents the dominant soils, the source material and landscape in the Tres Cruces creek basin. Table 7.3 shows the main characteristics of the profile of the dominant soils of the various soil units.

Another possible soil classification is the productivity index (PI) which is defined in terms of meat and wool (CONEAT groups). It refers to the productive capacity average for the country (100 index). This classification can relate with soil depth associating an IP less than 76 to surface soil and a PI between 109 and 162 to deep soils. Soils with an IP ranging on these values are considered moderately deep (40 to 60 cm of thick). While the surface soil covers a larger area than the deep soils, the deep soils shows a PI average twice as high as the surface ones.

The Tres Cruces creek basin presents IP CONEAT between 26 and 158, having the highest IP on the banks of the creek.

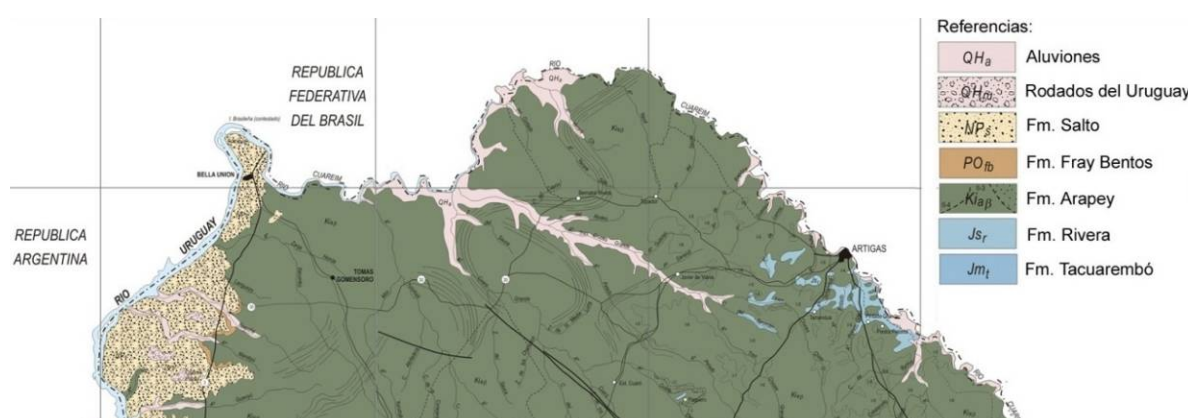


Figure 7.6 Geology of the Tres Cruces creek basin (Source: Geology map of Uruguay)

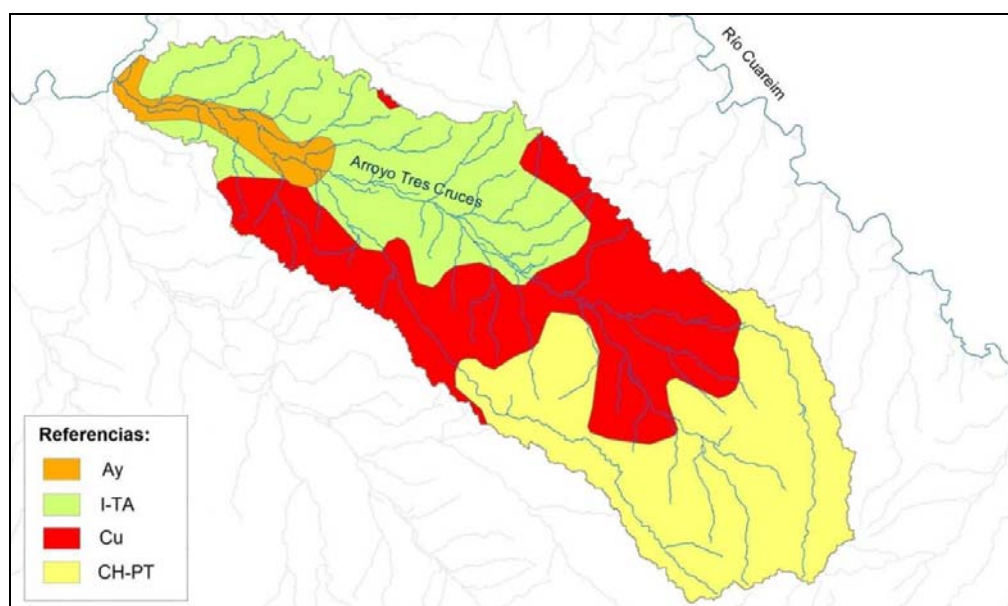


Figure 7.7 Groups of soils in the Tres Cruces creek basin (Source: Altamirano et al., 1976)

Table 7.2 Main features of soils in the Tres Cruces creek basin (Source: Altamirano et al., 1976).

Units	Dominant soils	Source materials	Landscape
CH-PT	Litosoles eútricos/subeutricos melánicos	Basalto y removilizaciones de la Formación Arapey	Sierras rocosas con escarpas y colinas cristalinas algo rocosas
Cu	Litosoles eutricos melánicos Brunosoles eútricos típicos Vertisoles háplicos	Basaltos de la Formación Arapey y recubrimientos limo-arcillosos	Lomadas fuertes y colinas cristalinas algo rocosas con escarpas asociadas
I-TA	Brunosoles eútricos típicos Vertisoles háplicos	Sedimentos limo-arcillosos cuaternarios sobre la Formación Arapey. Algunos suelos se generan directamente sobre basalto y removilizaciones de éste	Lomadas suaves, a veces fuertes, con valles cóncavos y escarpas asociadas
Ay	Vertisoles háplicos	Sedimentos limo-arcillosos holocenos y sedimentos aluviales recientes	Llanuras altas y medias

Table 7.3 Characteristics of the dominant soil profile units present in the Tres Cruces creek basin (Source: Altamirano et al., 1976)

Soil	Horizon	Thickness (cm)	Texture	Color
Litosoles eútricos/subeutricos melánicos	A	3 - 20	Franco limoso/franco arcilloso	Pardo rojizo oscuro/rojo
	R*	-	-	-
Litosoles eútricos melánicos	A	10 - 30	Franco arcillo limoso/franco arcilloso	Negro/pardo muy oscuro/rojo
	R*	-	-	-
Brunosoles eútricos típicos	A	10 - 25	Franco arcillo limoso	Pardo muy oscuro/negro
	Bt	15 - 60	Arcillo limo/arcilloso	Negro/pardo muy oscuro
	Cca	-	Franco arcillo limoso	Pardo
Vertisoles háplicos	A	45 - 120	Arcillo limo/arcilloso	Pardo muy oscuro/negro
	Cca	-	Franco arcillo limoso	Pardo

* Contacto lítico: basaltic rock impenetrable to the roots

Soil aptitude

The Soil and Water Division of MGAP conducted in 2000, a study of " Land Zoning in the Cuareim River Basin " (Molfino *et al.*, 2000), which created a 1:100.000 aptitude soil map for an irrigated rice-pasture system, considering the type of soil, topography and hydrology of the watershed. It was considered as a rice-pasture system a rotation of two years of rice followed by four years of grassland.

Based on these characteristics four kinds of soils were defined according to their degree of aptitude for the proposed system: very apt, apt, moderately apt and not apt. Table 7.4 and Figure 7.8 show the apt area for the rice-pasture system with direct planting and under irrigation in the Tres Cruces creek basin.

In the MGAP work, 30% of the flooded area suitable for preservation of the native forest was not taken into account. However, in this it was decided to deduct the entire area of native forest given its great environmental value. So the suitable area for the rice-pasture system to consider was determined by the MGAP work except the area occupied by native forest. This area of native forest was determined by digitising the limits shown in some satellite images (obtained from the Google Earth). This provides for the Tres Cruces creek basin 39.303 ha of apt area. Considering the apt area for rice-pasture system and considering the rotation system proposed in the MGAP work, the suitable area for growing rice was estimated as a third of the area suitable for the system, 13.101 ha in the Tres Cruces creek basin.

Table 7.4 Areas apt for rice-pasture system in the Tres Cruces creek basin
(Source: Molfino *et al.*, 2000).

Aptitude of soil	area (ha)
Very apt	14.285
Apt	28.285
Moderately apt	1.003
Total	43.573

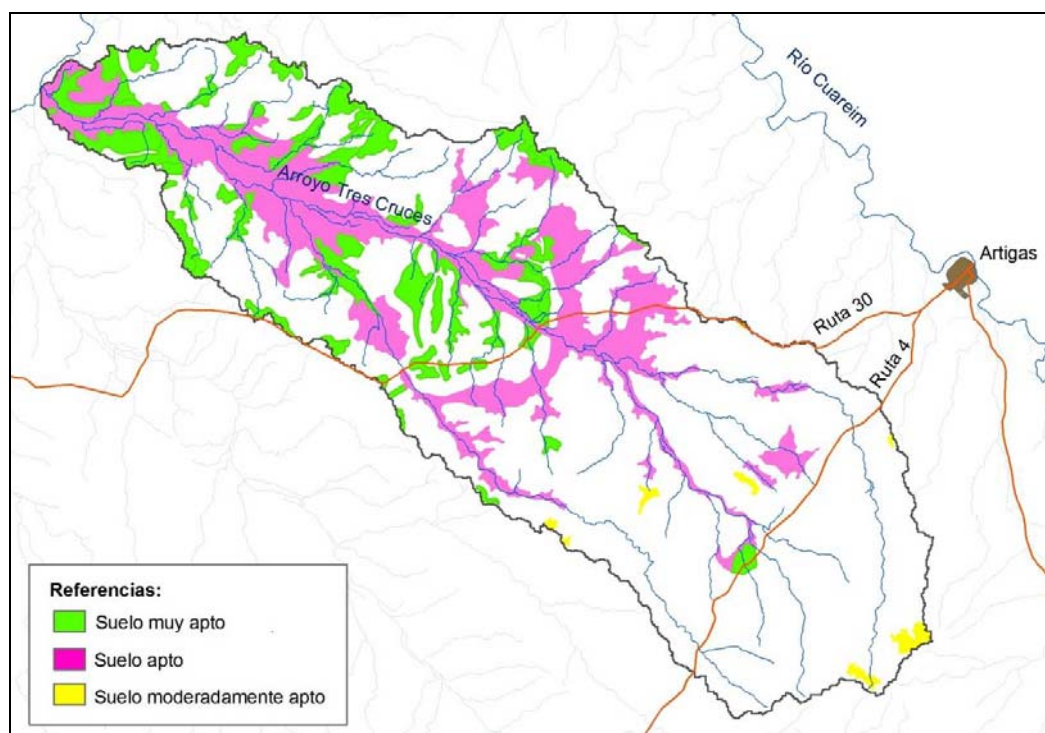


Figure 7.8 Apt areas for rice-pasture system in the Tres Cruces creek basin (In green soil very apt, in pink soil apt, in yellow soil moderately apt)

7.1.5 Topography

The main channel length of the Tres Cruces creek is 75 km and the difference in heights between its source and mouth at the Cuareim River is 100 m, with an average slope of 1.3 m km^{-1} .

In this study it was the Digital Elevation Model (DEM) from the National Aeronautics and Space Administration (NASA) which consists of a digital representation of elevations in a raster format. This is the only DEM available for the whole basin. The elevation data of this model were obtained with the SRTM (Shuttle Radar Topographic Mission) and they can be accessed free of charge. This information is distributed by the United States Geological Survey (USGS) and can be downloaded from the internet page <http://srtm.csi.cgiar.org>. Figure 7.9 shows the topography of the Tres Cruces river basin, given by the DEM of the NASA.

Digital Elevation Model

A Digital Terrain Models (DTM) is a numerical data structure that represents the spatial distribution of a quantitative and continuous variable, such as temperature, altitude or atmospheric pressure. These models are widely used in sciences for mapping and geographic information systems (GIS). In particular, when the variable of the DTM was represents levels or heights of land, it is called digital elevation models or DEM.

There are several ways of representing these elevation models, based on the structure and organisation of the data, being two of the most common: vector representation (based on geometric objects defined by the coordinates of their nodes and vertices) and rasters (based on locations defined by a regular grid). The DEM with a raster structure is the result of a grid overlay on the ground and extracting the average height of each cell or associating a height value to the centre of the cell.

This work used the “agreedem” created in WP2, using the DEM downloaded from Hydrosheds (<https://hydrosheds.cr.usgs.gov>) and processed with ArcHydro Tools. Figure 7.10 shows a 3D image of the DEM in the Cuareim River Basin.

The DEM data format is raster. The elevation is in metres and are referenced to WGS84 EGM96 geoid. It is in geographic (latitude, longitude) coordinates and referenced to WGS84 horizontal datum. The resolution is approximately 90 m and there is a vertical error of approximately 16 m.

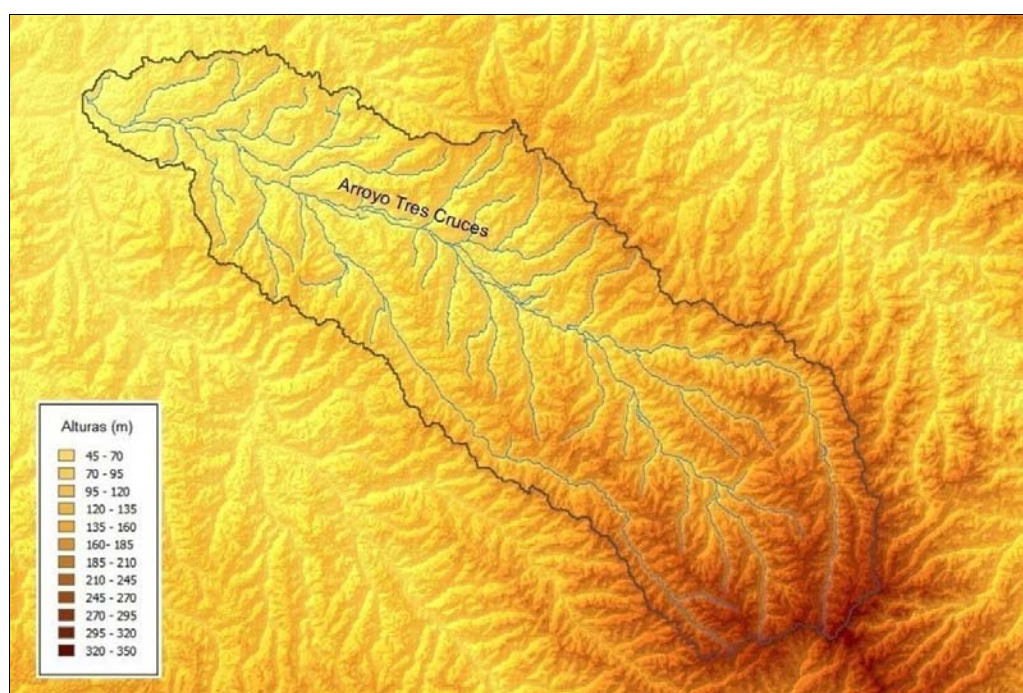


Figure 7.9 Tres Cruces creek basin's topography. Heights in m. (Note: The reference zero for the heights is 21.2 m below the official zero, see section 7.1.5).

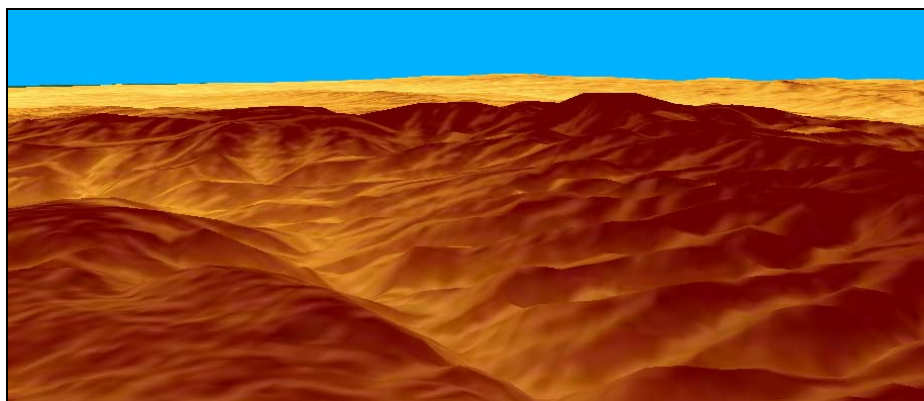


Figure 7.10 3D representation of the DEM in an area of the Cuareim River basin

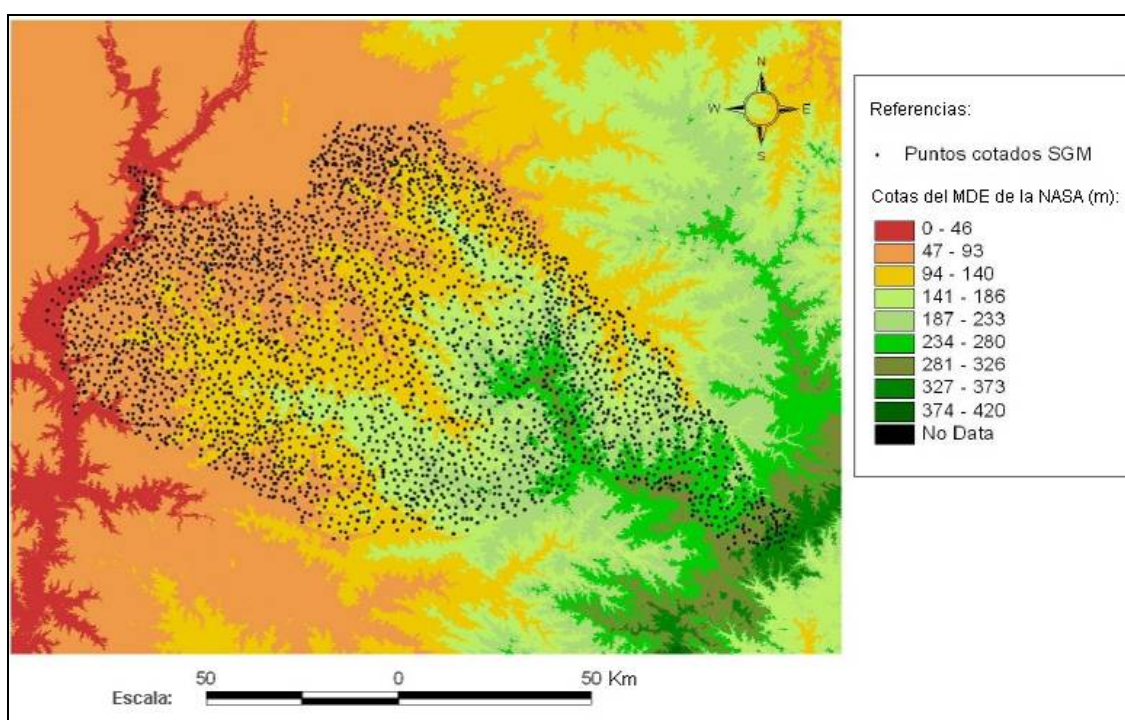


Figure 7.11 Measured points of SGM and heights of the NASA MDE (Source: “Proyecto Piloto de Gestión Integrada de Crecidas en la Cuenca del Río Cuareim/Quaraí – Uruguay/Brasil”, 2005)

Validation of the NASA DEM for the Cuareim River basin

In order to homogenise the heights of the NASA DEM with the heights of the Servicio Geográfico Militar (SGM) in the Cuareim River basin, there was a correlation done between the two heights under the framework of the project “Proyecto Piloto de Gestión Integrada de Crecidas en la Cuenca del Río Cuareim/Quaraí – Uruguay/Brasil” (“Validación del modelo numérico del terreno del USGS (STRM) para la cuenca del Cuareim - Quaraí utilizando los puntos cotados del SGM de Uruguay”). Data from the SGM are in projected coordinates (Kruger Gauss-projection, earth model: spheroid international 1924, horizontal datum Yacaré), geoidal heights, expressed in metres and referred to the official zero.

To do this correlation, 3218 SGM levelled points in the department of Artigas were used (see Figure 7.11), and were compared with the heights of the NASA DEM. Figure 7.12 shows the linear adjustment between the two systems.

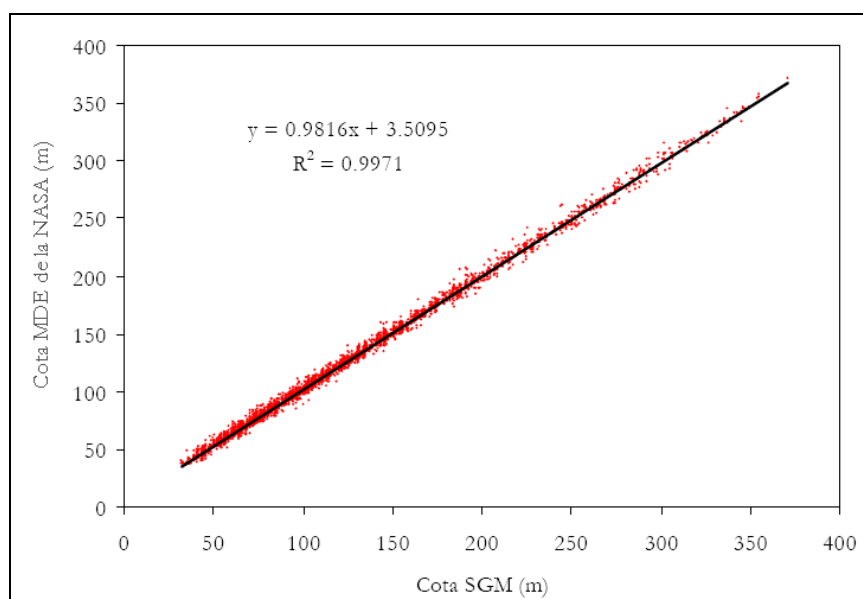


Figure 7.12 Correlation between SGM and NASA DEM levels (Source: “Proyecto Piloto de Gestión Integrada de Crecidas en la Cuenca del Río Cuareim/Quaraí – Uruguay/Brasil”, 2005)

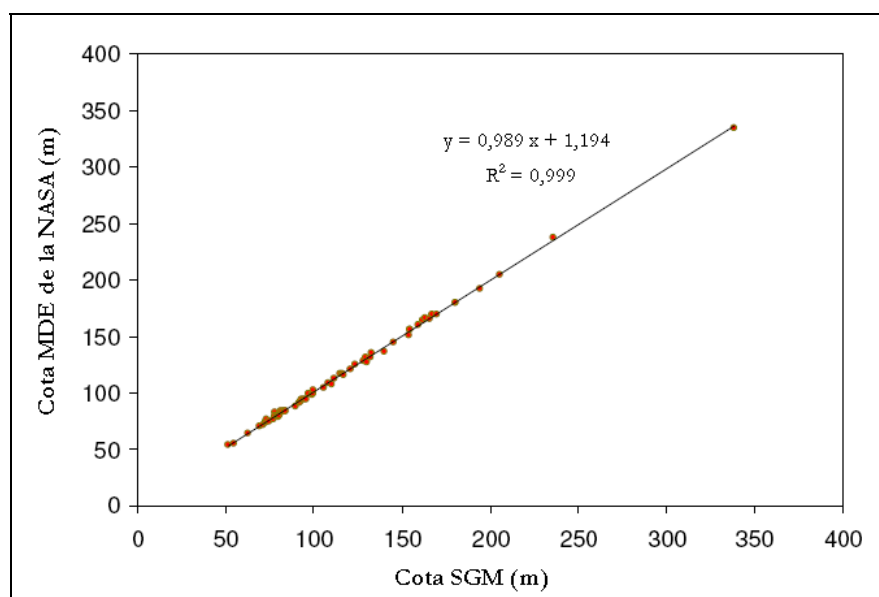


Figure 7.13 Correlation between the 60 geodetic vertices of the SGM and the NASA DEM (Source: “Proyecto Piloto de Gestión Integrada de Crecidas en la Cuenca del Río Cuareim/Quaraí – Uruguay/Brasil”, 2005)

Figure 7.12 shows that there is a good correlation between the levels of the NASA DEM and those of the SGM, as the correlation coefficient is close to the unit. However, it shows a clear shift in the heights, maintaining an altitude difference of about 3.5 m.

As a second step, of the 3218 points only the 60 geodetic vertices were chosen. Figure 7.13 shows the new linear adjustment. There is now an even better correlation and the shift from the heights of DEM compared with those of the SGM is reduced to 1.19 m.

It can be concluded that there is a good correlation between levels of the NASA DEM and the SGM, existing a shift of 1.19 m. The zero reference level of the NASA DEM is 1.19 m below the official zero. To work with the NASA DEM it had to be reconditioned and not to get negative elevations it was raised 20 vertical units, obtaining the agreedem. Therefore, the agreedem is 21.19 m above the SGM. This study will work with zero reference levels located 21.2 m below the official zero.

7.1.6 Runoff

As a result of the low storage capacity of the soils of the Tres Cruces creek basin, high discharges occur after precipitation events, with a rapid decline in the runoff afterwards. This determines flood peaks and rapid decline and in a few days the return to the base flows, which are generally low.

Figures 7.14 and 7.15 show the Tres Cruces creek in the proximity of Route 30, downstream of it. The Tres Cruces creek has a gauging station (155) located at its junction with Route 30 (Table 7.5), near Javier de Viana town. Figure 7.16 shows the location of it, Figure 7.17 the same and the scale with which the levels are read.

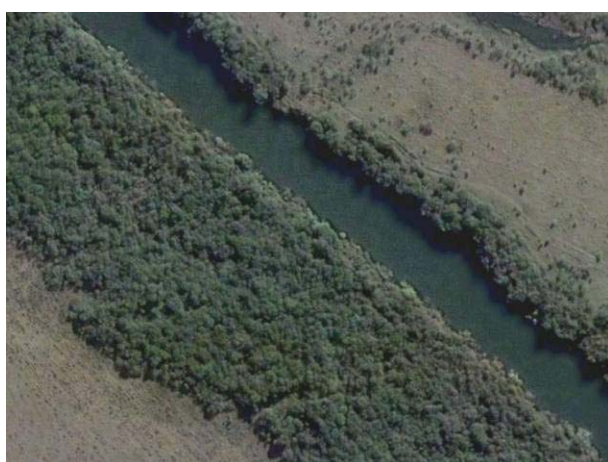


Figure 7.14 Aerial photo of the Tres Cruces creek
(Source: Google Earth)



Figure 7.15 Photographic view of the Tres Cruces creek



Figure 7.17 Scale at the 155 gauging station

Table 7.5 Gauging station details

Code	Name	Area (km ²)	Longitude (°)	Latitude (°)	Period of registration
155.0	Javier de Viana	573	-56 47	-30 26	August 1982 June 2008

Based on the recorded data at the 155 gauging station in the 1982-2006 period, it can be obtained the annual flow cycle of the Tres Cruces creek (Figure 7.18). The large standard deviations in Figure 7.18 show a high interannual runoff variability (mostly in the summer months), which may be explained by the high variability of monthly rainfall and runoff amplification due to soils with low water storage capacity (runoff coefficient is high, approximately 0.45). Figure 7.19 shows the flow permanence curve for 155 gauging station.

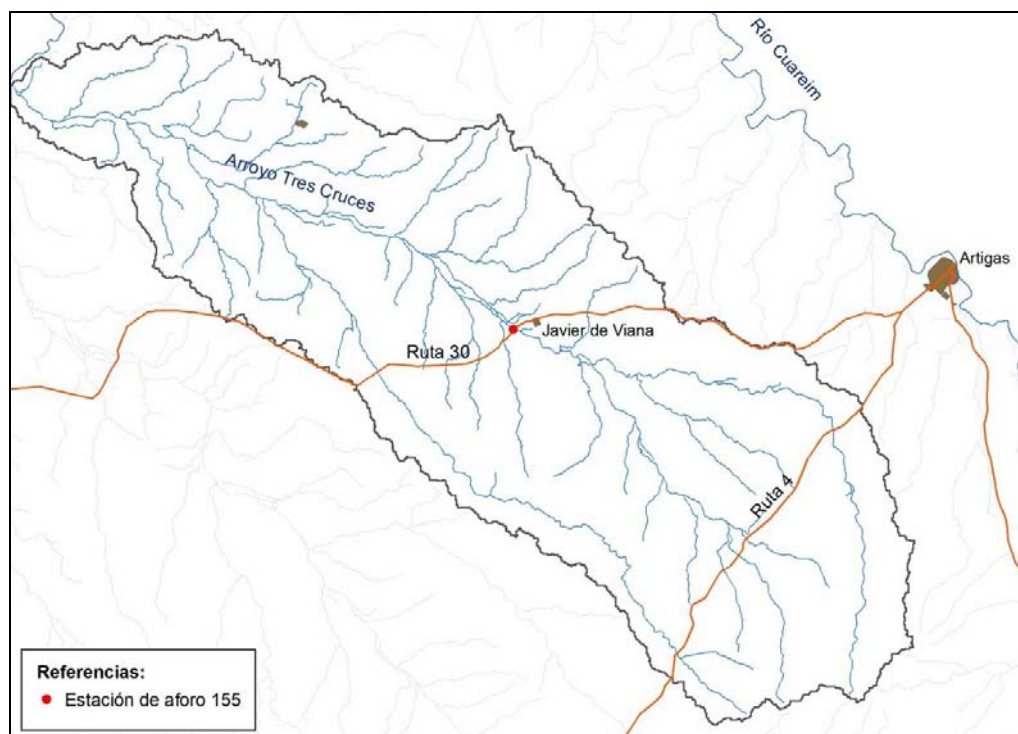


Figure 7.16 Location of 155 gauging station (red dot)

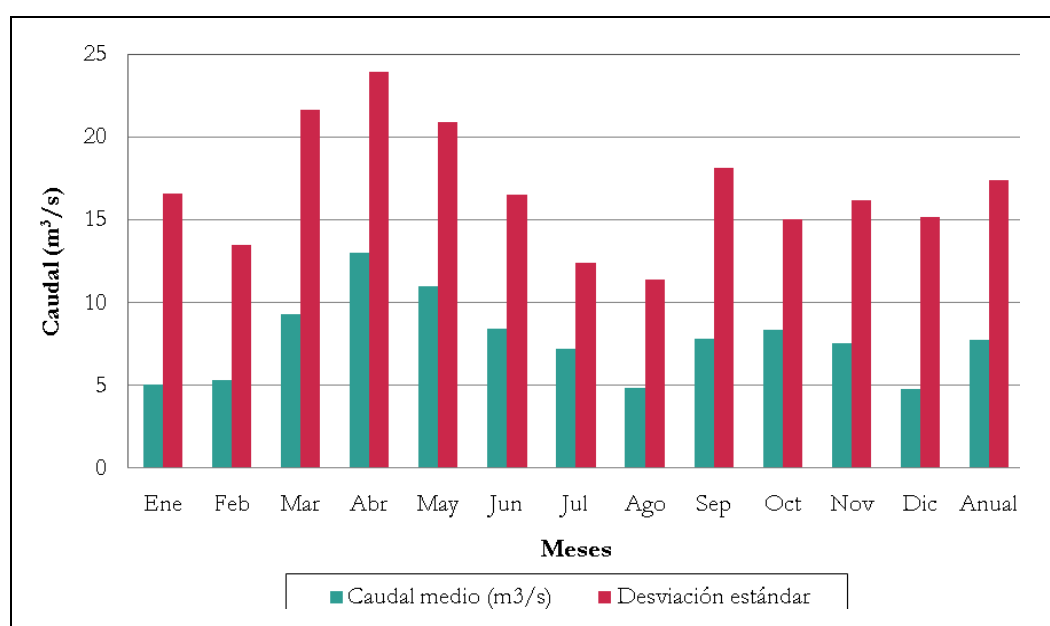


Figure 7.18 Annual flow cycle of the Tres Cruces creek at the 155 gauging station. In vertical axis Flow m^3s^{-1} , in horizontal axis Months from January to December, and the last two bars correspond to the whole year. Bars in blue are average flow in m^3s^{-1} while bars in red are standard deviation.

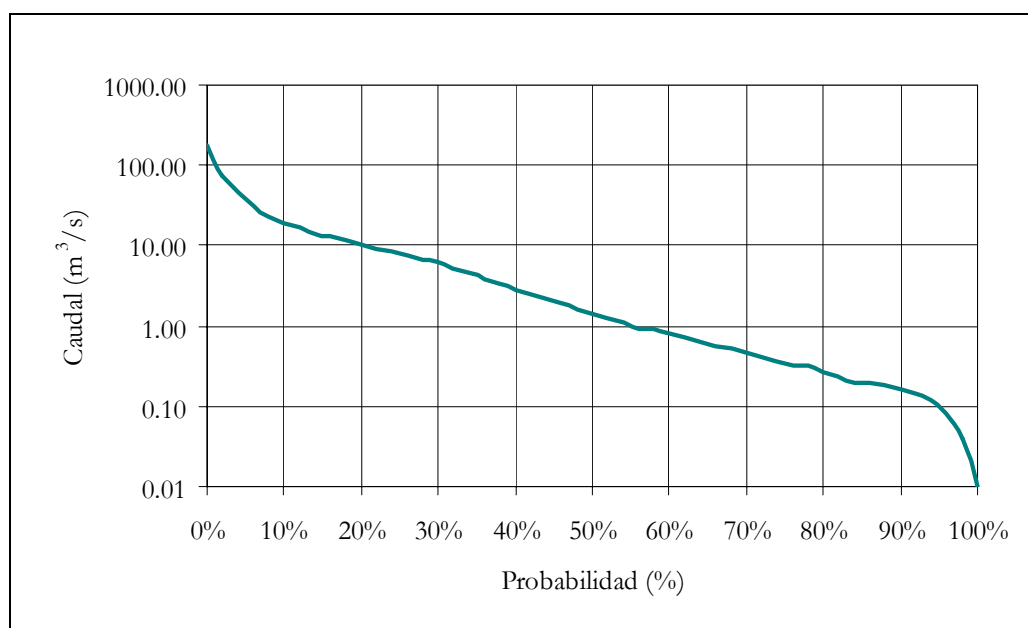


Figure 7.19 Permanence curve of 155 gauging station. Vertical axis is Flow m^3s^{-1} and horizontal axis is Probability.

7.2 Choice of model

The main objective of this work is to take a first step in managing the granting of water rights considering the global system in the Tres Cruces creek basin. The outlet of the basin is where the Tres Cruces creek reaches the Cuareim River. The purpose of the study specifically includes:

- To implement, calibrate and validate a distributed daily-step hydrologic model that will quantify the water resources (SWAT);
- To implement a generic simulation model of operations of a hydraulic system, as a decision tool to be used for the hydrological simulation of irrigation network systems (MODSIM);
- To evaluate and make recommendations on how to manage water resources and grant water rights.

7.2.1 Current administration

Currently DNH grants water rights for direct intakes, reservoirs and small reservoirs.

Direct intakes

An extraction of $0.2 \text{ ls}^{-1}\text{km}^{-2}$ of the contributing basin area at the offtake location, without affecting previously authorised water rights, is authorised. For the basin at Javier of Viana (gauging station 155; 570.8 km^2), there is a potential extraction flow of 114 ls^{-1} which, based on the permanence curve (Figure 7.19), would have a 1% probability of occurrence. Likewise, at Paso del Cerro (1241 km^2) there are 249 ls^{-1} . To estimate the area of rice that it is possible to irrigate, it is considered that the volume of water is used for a 90-day irrigation period; the total volume is divided by an assumed needed $14,000 \text{ m}^3$ per hectare to get the irrigation area.

Reservoirs

To authorise the construction of a reservoir, the project has to be accompanied by an irrigation project, that has to be approved the MGAP. The maximum reservoir storage volume is determined by multiplying the annual runoff in mm by the area of the basin. That runoff is obtained with the following expression:

$$E_{\text{annual}} = \frac{(P - 0,25)^2}{P + 0,85} = 568,5 \text{ mm}$$

where: S is a parameter in mm, that is considered to be 1000 mm, P is the annual average precipitation in mm, that is considered to be 1290 mm.

Once the volume is granted (that will be equal or smaller than the maximum permitted), the remaining available volume of water upstream of the reservoir, that is calculated as the difference between the maximum volume and the granted volume, is recorded for future reference.

Small reservoirs

Small reservoirs have to be registered only when the water stored is utilised for irrigation. It is observed that very little volume can be granted to direct intakes, with the construction of dams the surest way to have large quantities of water.

7.2.2 Reservoirs and direct intakes

Figure 7.20 shows the existing dams and direct intakes in the Tres Cruces creek basin and Tables 7.6 and 7.7 show their main features.

Although the water production in the Tres Cruces creek basin is enough to increase the number of dams in the basin (as discussed in section 7.4.1) it is not the case for the direct intakes. The Tres Cruces creek may have flow discontinuities in times of drought because of the low water storage capacity of the basin.

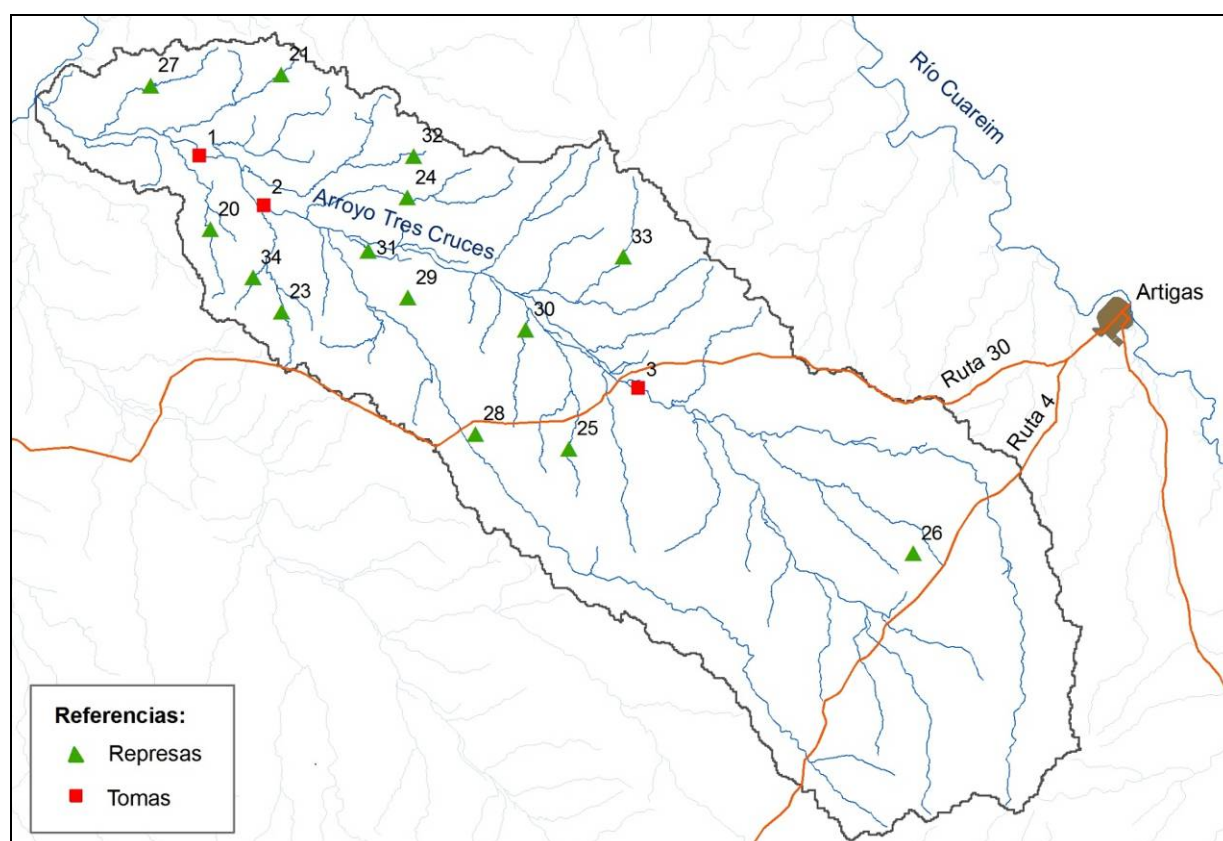


Figure 7.20 Existing dams and direct intakes in the Tres Cruces creek basin (red squares are direct intakes and green triangles are reservoirs)

Table 7.6 Main features of existing dams in the basin

Nº	Basin area (ha)	Lake area (ha)	Dam height (m)	Maximum volume (thousands of m ³)
27	1430	263.0	11.4	9132
34	480	61.0	10.4	2256
21	340	46.8	9.9	1650
30	1700	135.0	7.2	2557
33	1990	112.3	12.9	4282
26	130	15.9	7.5	447
20	1750	116.0	9.4	3473
32	615	99.7	9.0	2453
28	115	20.4	8.2	628
24	2150	128.3	10.2	4317
23	1050	81.8	11.1	2605
31	415	101.0	4.2	906
29	600	115.5	9.5	3704
25	867	94.0	13.3	3790

Table 7.7 Main features of existing direct intakes in the basin

Nº	Maximum flow (ls ⁻¹)	Maximum annual volume (thousand of m ³)
1	332	2540
2	51	390
3	85	650

7.2.3 Water uses

The current demand of water is estimated based on the annual sworn declarations of those who have the rights granted by DNH. This information was acquired at the DNH office in Artigas during the field visit to the basin (Table 7.8 and Figure 7.21). In the 2004-2005 rice season there were insufficient data. Table 7.9 shows the average planted area in the sworn declarations.

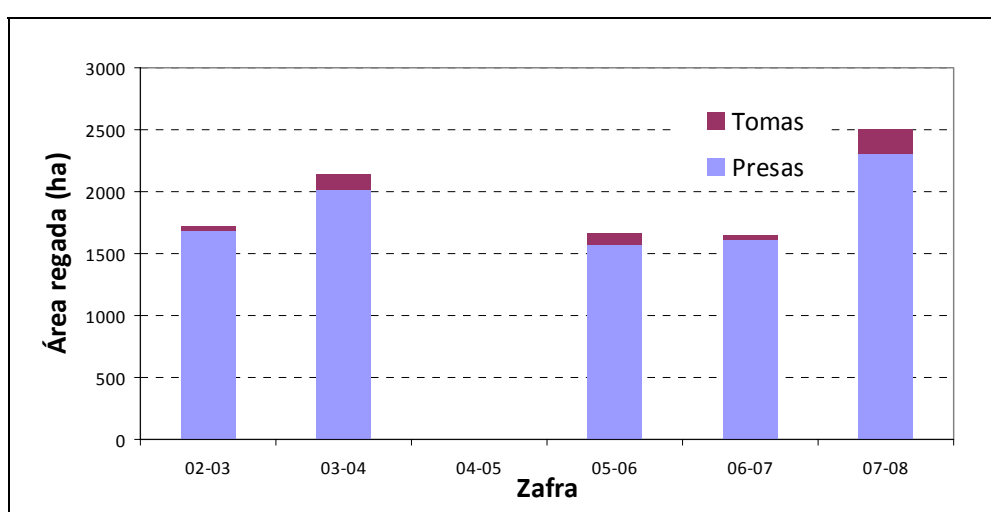


Figure 7.21 Planted rice area per rice season. On vertical axis, irrigated area in hectares. On horizontal axis, rice season. On blue, reservoirs. On red, direct intakes.

Table 7.8 Irrigated areas based on annual sworn declaration

N°	2002-2003	2003-2004	2005-2006	2006-2007	2007-2008
Dams					
20	120	248	245	167	265
21	-	180	170	160	150
23	220	230	100	100	150
24	200	-	-	100	-
25	-	240	-	118	-
26	-	-	-	-	-
27	-	-	500	290	805
28	-	-	-	-	-
29	200	200	200	-	150
30	161	-	-	-	-
31	-	-	-	-	50
32	150	230	190	180	200
33	470	500	-	450	430
34	160	180	160	55	100
Direct intakes					
1	-	100	100	-	150
2	35	35	-	30	-
3	-	-	-	-	50
Total	1.716	2.143	1.665	1.650	2.500

Table 7.9 Average planted area in the sworn declarations

N°	Average planted area (ha)
20	161
21	165
23	169
24	150
25	138
26	-
27	628
28	40
29	188
30	161
31	50
32	190
33	455
34	136
Total	2.479

7.3 Data requirements

This section presents the available data needed for the development of the models. The results obtained from WP2 “Quantification of the return of water to the river from the rice irrigated fields” was included in the modelling of the distribution of water to meet the demands of the system, using MODSIM.

7.3.1 Raingauges and meteorological data

Figure 7.22 and Table 7.10 show the location and the available periods of information of the raingauges, and Table 7.11 the parameters measured at the meteorological station of Artigas (E. M. Artigas), all belonging to the network of the National Directorate of Meteorology (DNM).

Table 7.10 Raingauges

Code	Name	Period of Observation	Years	CordX	CordY	Miss data
330	E.M.Artigas	01-Abr-31 31-Jul-08	78	546425	6636791	0%
1001	Paso de Leon	01-Ene-56 31-Jul-08	53	492293	6667915	0%
1013	E.M. Bella Union	01-Feb-25 31-Jul-08	84	443855	6658909	5%
1016	Paso de la Cruz	01-Abr-82 31-Jul-08	27	471147	6650150	0%
1019	Bernabe Rivera	01-Ene-14 31-Jul-08	95	504808	6647970	3%
1021	El Topador	01-Ene-56 31-Jul-08	53	514423	6647962	0%
1035	Colonia Rivera	01-Ene-56 31-Jul-08	53	540345	6636815	0%
1040	Tomas Gomensoro	01-Jun-09 31-Jul-08	100	455169	6636798	4%
1044	Paso Farias	01-Ene-14 31-Jul-08	95	489442	6628020	14%
1047	Javier de Viana	01-Ago-12 30-Jun-08	97	522082	6631327	0%
1048	Taruman	01-Ene-58 31-Jul-08	51	531674	6627979	0%
1054	Colonia Palma	01-Ene-56 31-Jul-08	53	434476	6617853	2%
1062	Cuaró	01-Nov-25 31-Jul-08	84	511506	6616937	0%
1066	Colonia Pintado	01-May-31 31-Jul-08	78	549890	6623477	0%
1077	Col Gral Artigas	01-Mar-65 31-Jul-08	44	494412	6613806	0%
1082	Cerro Amarillo	01-Mar-81 31-Jul-08	28	535462	6612452	2%
1092	Baltazar Brum	01-Ene-14 31-Jul-08	95	469682	6599912	4%

Table 7.11 Measured parameters at the meteorological station in Artigas

Variable	Series
Monthly average temperature	1991-2005
Absolute monthly maximum temperature	1991-2005
Absolute monthly minimum temperature	1991-2005
Maximum monthly average temperature	1991-2005
Minimum monthly average temperature	1991-2005
Monthly average relative humidity	1991-2005
Monthly average atmospheric pressure	1991-2005
Monthly average of the monthly accumulated direct insolation time	1991-2005
Monthly average vapor pressure	1991-2005
Monthly average wind velocity	1991-2005

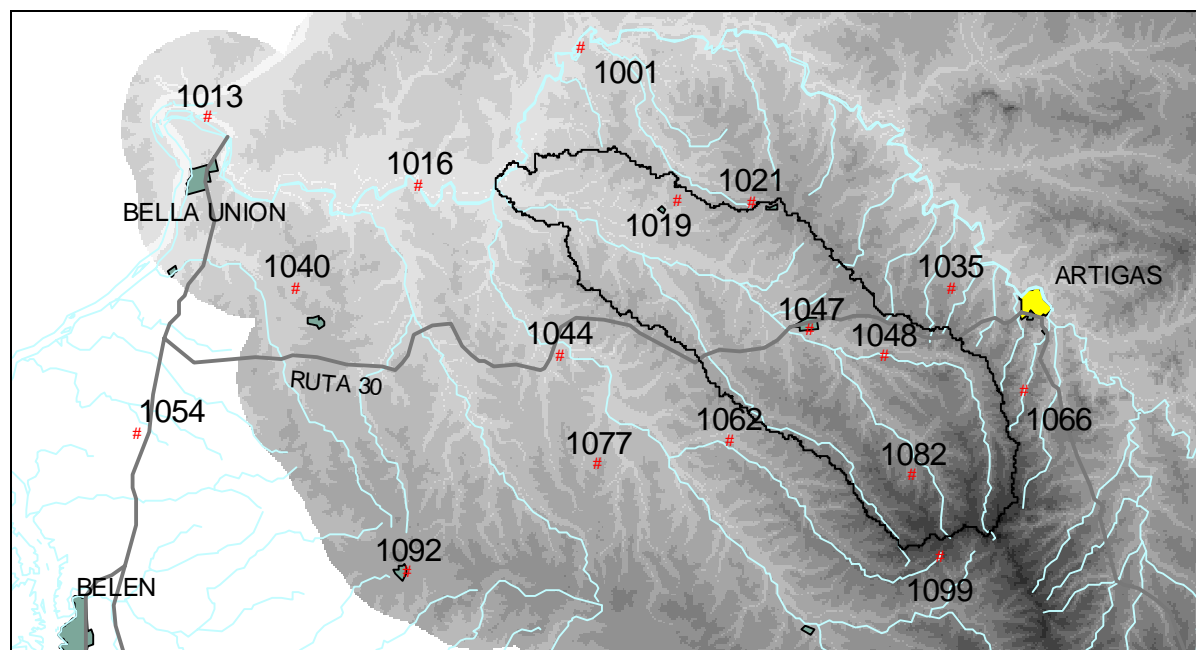


Figure 7.22 Raingauges (red) and meteorological station (yellow)

7.3.2 Flows

The Tres Cruces creek basin has a hydrometric station with flow measuring in Javier de Viana (N° 155) and flow measurements at three other locations (Figure 7.23). The monitoring period at 155.0 Javier de Viana station is 1982-2008. Table 7.12 shows the basin areas and Table 7.13 the TWINLATIN flow measurements.

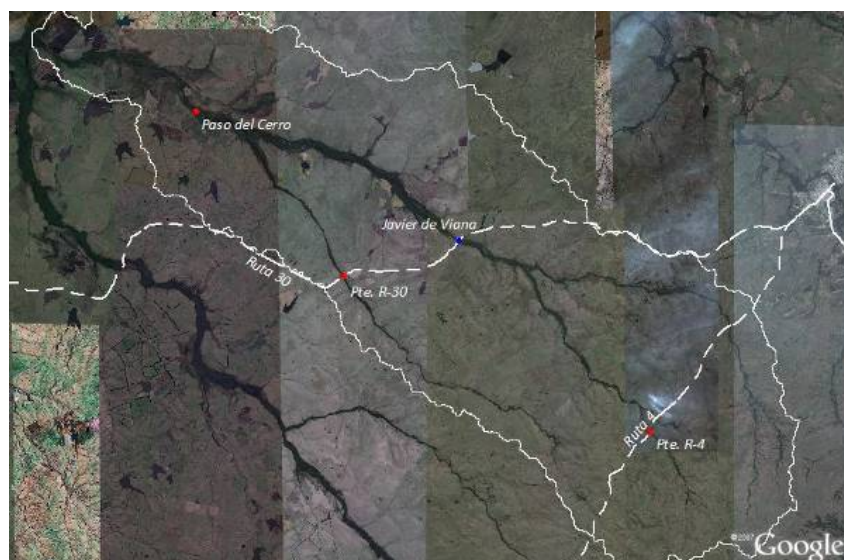


Figure 7.23 Flow measurements at Tres Cruces creek basin

Table 7.12 Contributing areas at flow measuring points

Point	Name	Area (km ²)
1	Javier de Viana (N° 155)	570,8
2	Puente R-4 – A° Tres Cruces	52,3
3	Puente R-30 A° Pelado	174,7
4	Paso del Cerro	1.243

Table 7.13 Flow measurements

Gauge Station	Date	Flow (m ³ s ⁻¹)
Javier de Viana	30-Jul-08	42.301
	31-Jul-08	16.749
	01-Ago-08	12.957
	20-Dic-07	0.043
	11-Dic-07	0.261
	07-Nov-07	3.191
	02-Oct-07	2.244
	07-Sep-07	1.457
	09-Ago-07	0.277
	20-Jul-07	0.878
	13-Jun-07	0.319
	16-May-07	0.841
	11-Abr-07	1.721
	31-Ene-07	0.043
	24-Ene-07	0.116
	20-Dic-06	13.170
13-Dic-06	0.170	
06-Dic-06	0.268	
Pte. R-4	30-Jul-08	3.868
	31-Jul-08	2.131
	01-Ago-08	1.413
Paso del Cerro	30-Jul-08	99.933
	31-Jul-08	36.066
	01-Ago-08	20.784
Pte. R-30	30-Jul-08	18.932
	31-Jul-08	5.263
	01-Ago-08	3.680

7.4 Scenario modelling

Below is presented an analysis of the potential water availability in the Tres Cruces creek basin. Firstly, the potential production of water is analysed, using the Temez model at the outlet of the basin, obtaining monthly runoffs. Then follows a brief analysis of the obtained monthly runoffs to determine the water available for irrigation. Finally, assuming different production system scenarios, the histograms of the areas that could be irrigated with the available water are found.

7.4.1 Water availability: Tres Cruces creek basin

To characterise the potential water production of the Tres Cruces creek basin, a monthly water balance for the period 1932-2007 was done, using the monthly-step precipitation-runoff Temez model. This model calculates the runoff of the basin from monthly precipitation data, the available water in the soils and it has four parameters.

Runoff

Figures 7.24 and 7.25 show the runoff and the annual runoff cycle of the Tres Cruces creek (1932-2007 period) at a point located immediately upstream of the mouth of the Tres Cruces creek in the Cuareim River. The average monthly runoff volume is approximately 50,000 m³. The annual runoff cycle shows large inter-annual variability, with similar behaviour to the annual rainfall cycle.

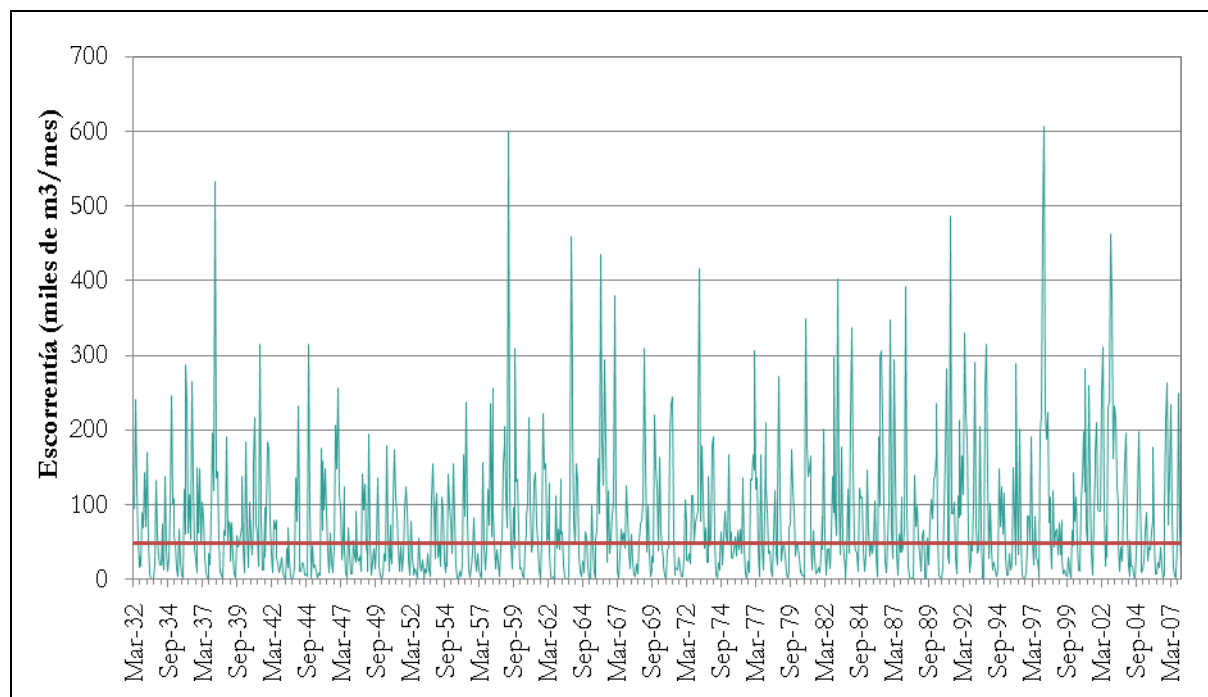


Figure 7.24 Runoff in the 1932-2007 period, in the Tres Cruces creek basin (Vertical axis, runoff in thousands of m^3 per month, horizontal axis, month and year)

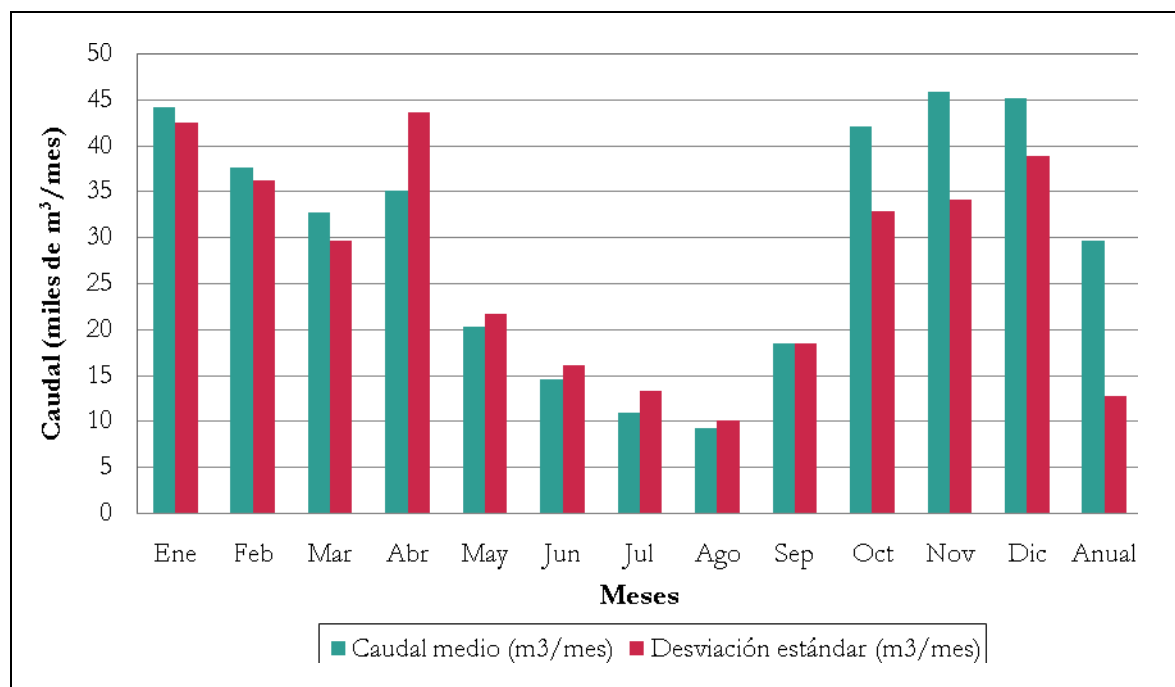


Figure 7.25 Annual runoff cycle in Tres Cruces creek basin (Vertical axis, flow in thousands or m^3 per month). Horizontal axis, Month from January to December and at the end Annual. Green bars are average flow in m^3 per month, and red bars are standard deviations in m^3 per month)

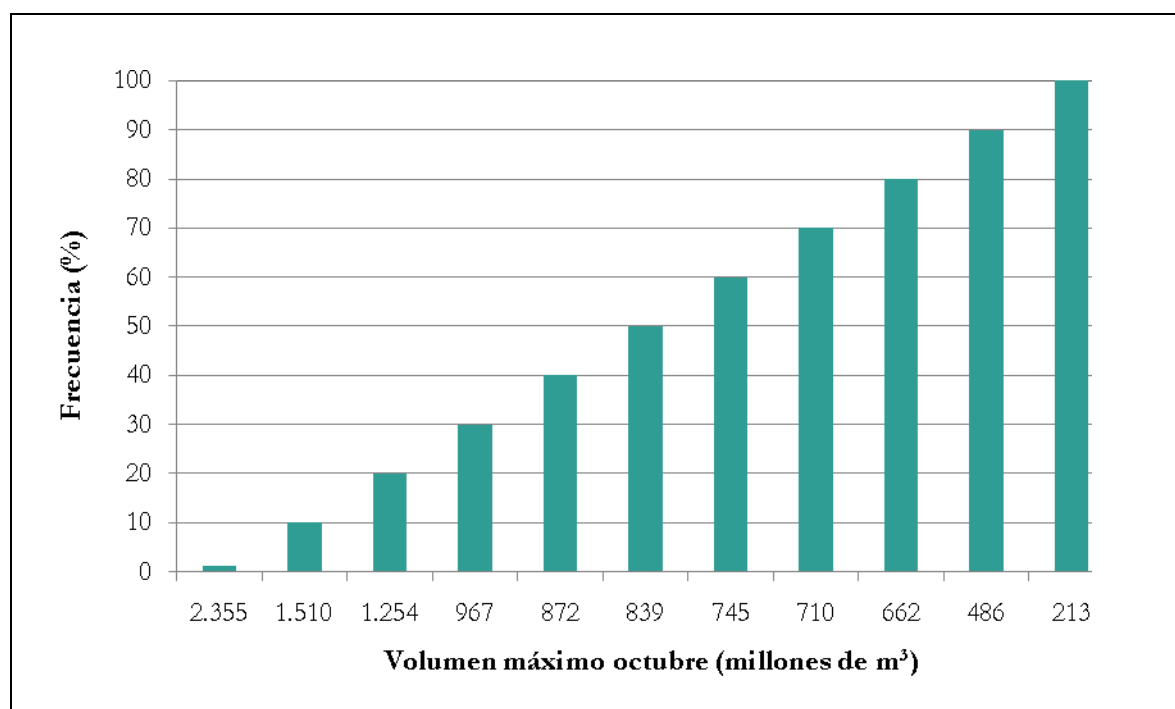


Figure 7.26 Histogram of the stored volume in October at an infinite reservoir located at the outlet of the Tres Cruces creek basin (1932-2007). Vertical axis: frequency, Horizontal axis: Maximum volume in October (millions of m³)

Potential volume

To do a first estimation of the potential available water in the Tres Cruces creek basin, it was assumed an infinite reservoir located at the outlet. A monthly water balance was made for the 1932-2007 period using the Temez monthly-step rainfall-runoff model. To do the water balance the following hypothesis were considered:

- The filling time of the reservoir corresponds to the non-calendar year November- October. This is because the rice season begins on average in November.
- The rainfall and evaporation in the lake of the reservoir are not considered in the water balance because it was assumed that the loss through evaporation is the same as the rainfall in the lake.
- Infiltration losses into the soil are not considered.

This produces a series of volumes at the beginning of the rice season (October). Figure 7.26 shows the volume stored in October histogram in an assumed infinite reservoir located at the outlet of the Tres Cruces creek basin for the 1932-2007 period. The estimated volume aims to evaluate the potential water in the basin and does not represent a real available volume (whether for physical limitations due to the large size of the reservoir or due to limitations that may arise in the water distribution throughout the basin).

7.4.2 Water availability: contributing areas to existing reservoirs

To calculate the water availability in each of the existing reservoirs a simulation was done with the model MODSIM (see section 7.6) for the period 1960-2007. The simulation used the runoff of each basin, determined with the Temez model. The remaining input parameters are presented in section 7.6, with the difference that in this case the reservoirs are considered infinite. Table 7.14 and Figure 5.27 present, for each basin, the maximum volumes that would be reached in October with a frequency of 100%, 90% and 80%, respectively. These percentages are considered representative of the water production of the basin, from the point of view of storing water, as they correspond to, say, that in 10 years of operation of a reservoir of 80% volume, it would reach the maximum volume 8 out of 10 years and the 90% and 100% volumes the remaining 2 years, respectively.

Table 7.14 Maximum volume in October that is reached with 100%, 90% and 80% frequency

Basin	100% volume (thousands of m ³)	90% volume (thousands of m ³)	80% volume (thousands of m ³)
27	2441	3423	4009
34	1182	1463	1734
21	603	845	990
30	4394	5700	7095
33	5341	6776	8383
26	399	581	752
20	3568	4522	5574
32	1097	1519	1788
28	460	569	674
24	4405	6178	7233
23	3225	3990	4732
31	949	1325	1554
29	737	1033	1211
25	2530	3131	3711
Total	31331	41055	49440

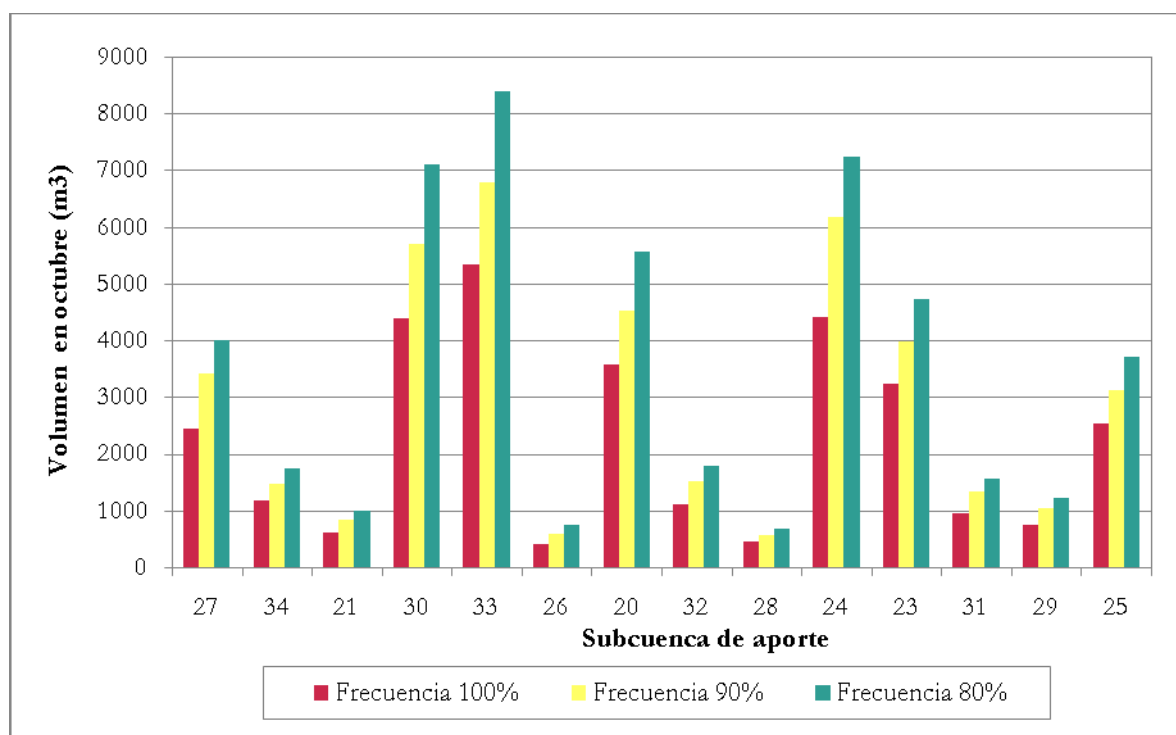


Figure 7.27 Maximum volume in October that is reached with 100%, 90% y 80% frequency. Vertical axis: volume in October. Horizontal axis: basin. Red bar, 100% frequency, yellow bar 90%, and green 80%.

Table 7.15 presents a comparison between the 80% volume just calculated and the maximum volume of the existing reservoirs in the Tres Cruces creek basin, as well as the difference between both. This difference, in the case of being positive, is the available volume of water in the basin (based on the selected criterion) that is not currently stored. Negative values (indicated with a dash) correspond to reservoirs that have a filling frequency less than 80%.

Many of the contributing basins have an available volume of water that currently is not stored, based on the selected criterion (80% volume), while others do not have remaining available volume and in addition they get to their maximum volume with a frequency lower than 80%. Table 7.16 calls to attention the low frequency at which some of the reservoirs reach their maximum volume.

Table 7.15 80% Volume vs volume of existing reservoirs

Basin	80% vol (thousands of m³)	Max vol (thousands of m³)	Available vol (thousands of m³)
27	4009	9132	-
34	1734	2256	-
21	990	1651	-
30	7095	2556	4539
33	8383	4282	4101
26	752	447	305
20	5574	3472	2102
32	1788	2453	-
28	674	628	46
24	7233	4317	2916
23	4732	2605	2127
31	1554	906	648
29	1211	3704	-
25	3711	3790	-
Total	49440	42199	16784

Table 7.16 Frequency with which the current reservoirs reach their maximum volume

Dam	Max vol (thousands of m³)	Max vol Frequency (%)
27	9132	23
34	2256	53
21	1651	45
30	2556	100
33	4282	100
26	447	98
20	3472	100
32	2453	64
28	628	81
24	4317	100
23	2605	100
31	906	100
29	3704	17
25	3790	79

7.4.3 Potential demand: Tres Cruces creek basin

At present the demand for water in the Tres Cruces creek basin is entirely for rice irrigation. Hence, to estimate the potential demand that could be met with the water available in the basin, the maximum area of rice that could be irrigated with the assumed reservoir (located at the outlet of the basin) was determined. To do that it was assumed that rice needs $14,000 \text{ m}^3$ per hectare. This value was obtained from interviews with professionals related to rice production in Artigas.

Figure 7.28 shows the maximum rice area histogram that could be irrigated for the 1932-2007 period. Recalling that the area apt for rice in the basin is 13101 hectares, Figure 7.28 shows that with the assumed reservoir it would be possible to irrigate the whole apt area 100% of years.

While at present the available water is used only for rice irrigation, the high prices of cattle and the increasing climate variability that translates into extreme droughts and forage crises, it is reasonable to consider the irrigation of pastures. That point of view is supported by producers in the area, who have expressed their intention to irrigate pastures, but for that there is a need of an efficient irrigation system in the country.

Figure 7.29 shows the histogram of the maximum area of rice that would be possible to irrigate considering pasture irrigation in rotation with rice, for the 1932-2007 period. The assumed pasture-irrigation demand is 3000 m^3 per hectare during summer (at the same time rice is irrigated). Again, the area apt for planting rice in the basin is 13101 hectares, and with the assumed reservoir, 98% of the years the whole apt area would be possible to irrigate.

Lastly, due to the increased prices of grains (sorghum, soybeans, corn), it is also reasonable to consider to irrigate them during the summer months, as they can start to compete with rice. Assuming an irrigation demand of 4000 m^3 per hectare for them and considering that the suitable area for planting them is the same as for rice, it is easily observed that the entire planted area with grains could be irrigated.

All the results reveal the great potential of the Tres Cruces creek basin to produce water.

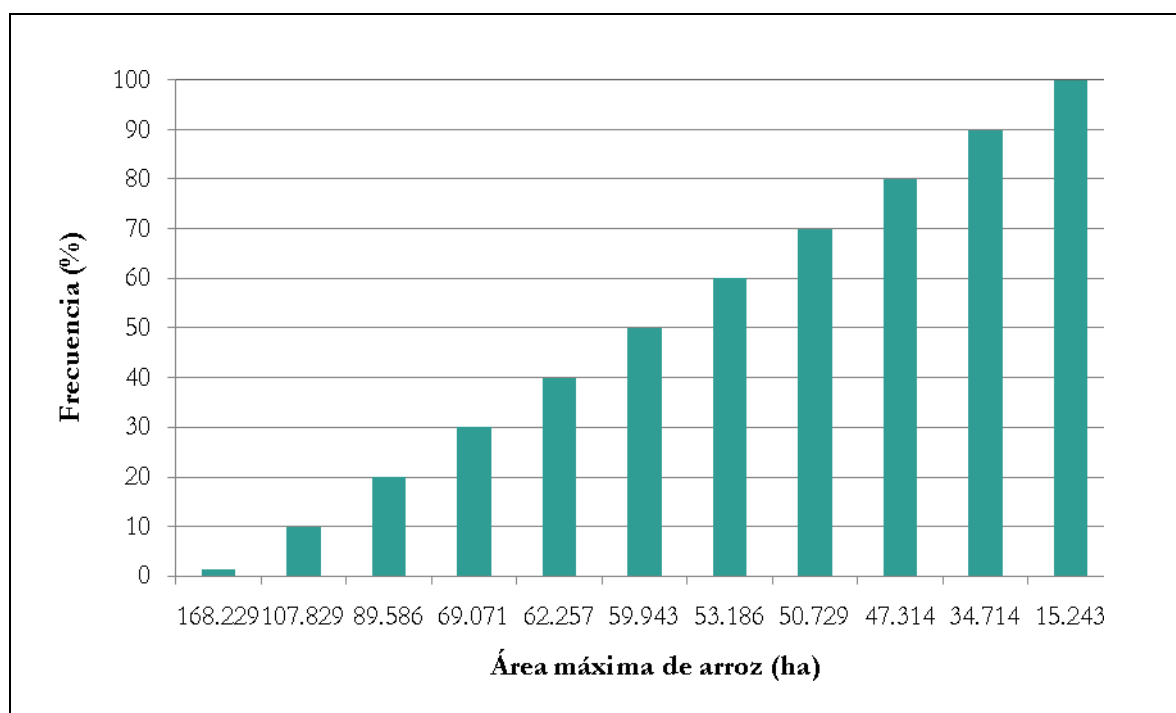


Figure 7.28 Histogram of the maximum area of rice that could be irrigated, considering that only rice is irrigated. Vertical axis: Frequency. Horizontal axis: Maximum area of rice.

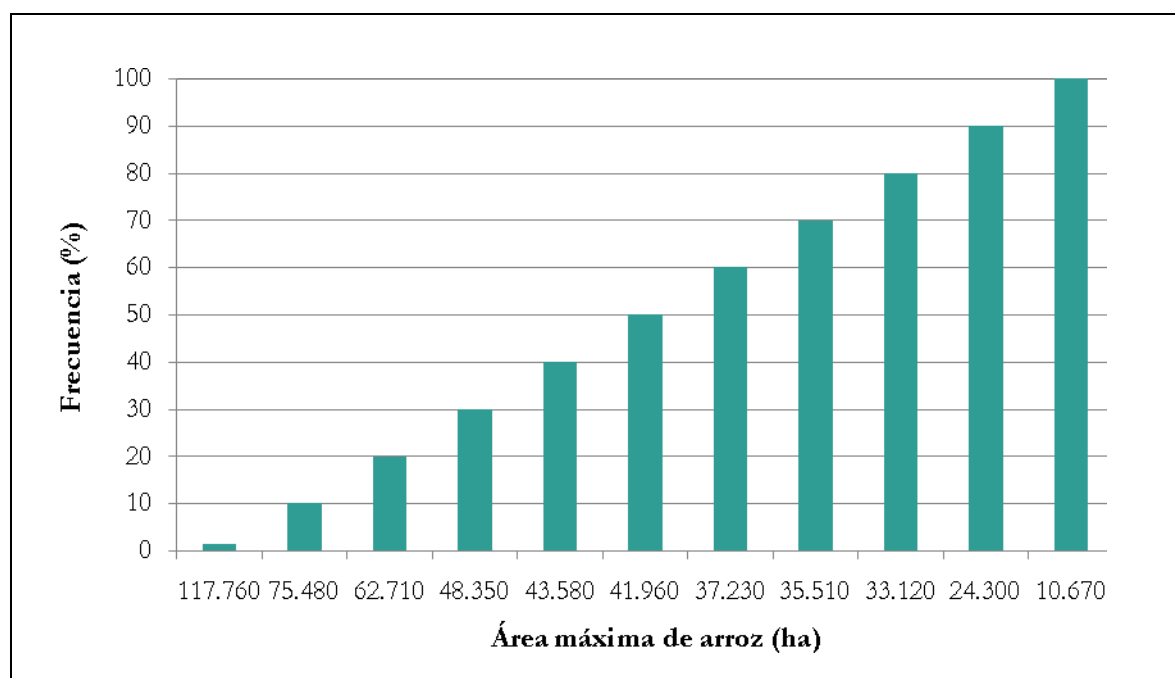


Figure 7.29 Histogram of the maximum area of rice that could be irrigated, considering that rice and pastures are irrigated. Vertical axis: Frequency. Horizontal axis: Maximum area of rice.

7.4.4 Potential demand: contributing areas to existing reservoirs

In Tables 7.17 and 7.18, and Figures 7.30 and 7.31, for each contributing area of each existing reservoir, the maximum area of rice that would be possible to irrigate with a frequency of 100%, 90% and 80% is presented, considering the irrigation of only rice and of both rice and pastures.

In Table 7.19, a comparison of the 80% area of rice recently calculated and the area of rice that is possible to irrigate with the maximum volume of the existing reservoirs in the Tres Cruces creek basin, as well as the difference between them, for each scenario is presented. That difference corresponds, in the case it is positive, to the surface of rice that could be irrigated with the available water in the basin (based on the chosen criterion), that is not currently being stored.

Table 7.17 Maximum area of rice that would be possible to irrigate with a frequency of 100%, 90% and 80%, considering only the irrigation of rice

Basin	Area of rice 100% (ha)	Area of rice 90% (ha)	Area of rice 80% (ha)
27	174	245	286
34	84	105	124
21	43	60	71
30	314	407	507
33	382	484	599
26	29	42	54
20	255	323	398
32	78	109	128
28	33	41	48
24	315	441	517
23	230	285	338
31	68	95	111
29	53	74	87
25	181	224	265
Total	2238	2933	3531

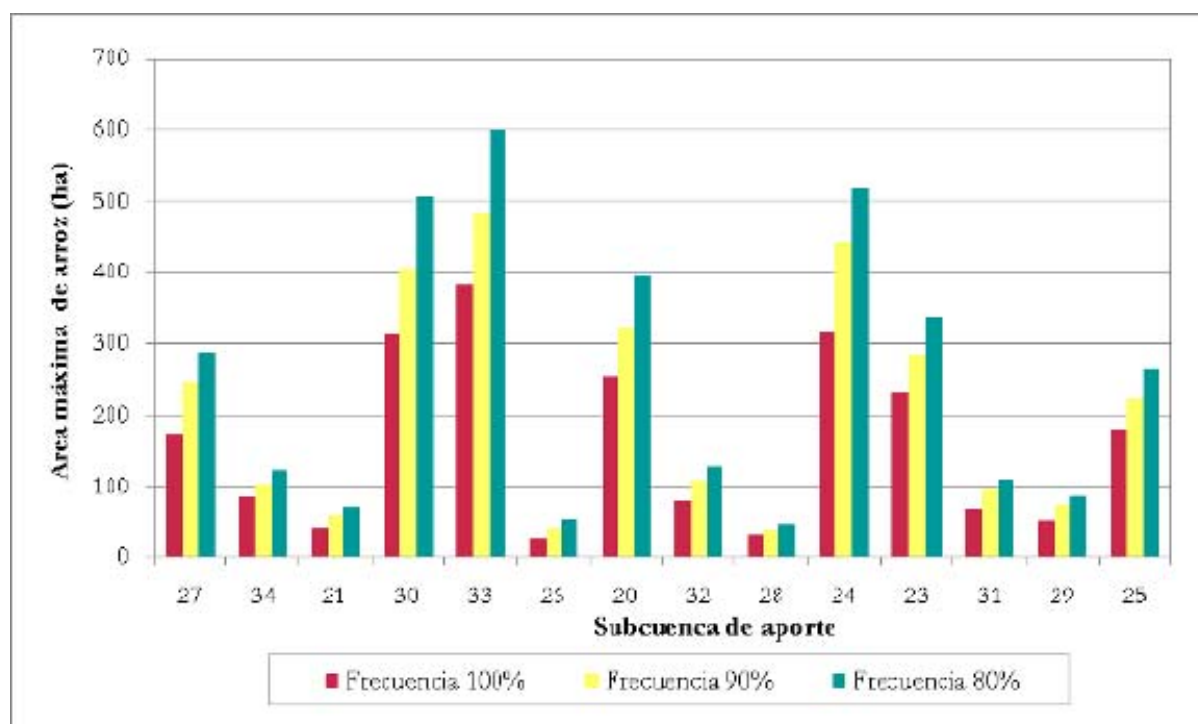


Figure 7.30 Maximum area of rice that would be possible to irrigate with a frequency of 100%, 90% and 80%, considering only the irrigation of rice. Vertical axis: Maximum area of rice. Horizontal axis: Contributing basin. Red bar: 100% Frequency. Yellow bar: 90% Frequency. Blue bar: 80% Frequency.

Table 7.18 Maximum area of rice that would be possible to irrigate with a frequency of 100%, 90% and 80%, considering only the irrigation of both rice and pasture

Basin	Area of rice 100% (ha)	Area of rice 90% (ha)	Area of rice 80% (ha)
27	122	171	200
34	59	73	87
21	30	42	50
30	220	285	355
33	267	339	419
26	20	29	38
20	178	226	279
32	55	76	89
28	23	28	34
24	220	309	362
23	161	200	237
31	47	66	78
29	37	52	61
25	127	157	186
Total	1567	2053	2472

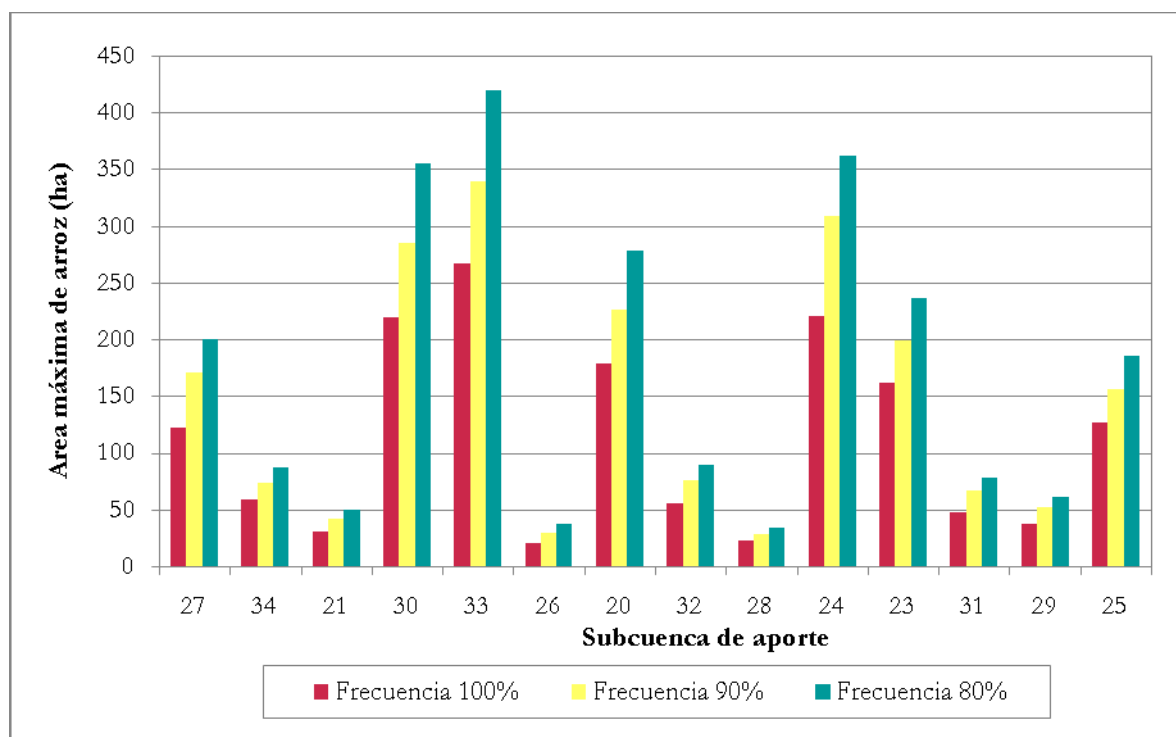


Figure 7.31 Maximum area of rice that would be possible to irrigate with a frequency of 100%, 90% and 80%, considering the irrigation of both rice and pastures. Vertical axis: Maximum area of rice. Horizontal axis: Contributing basin. Red bar: 100% Frequency. Yellow bar: 90% Frequency. Blue bar: 80% Frequency.

Table 7.19 Area of rice 80% vs area of rice that is possible to water with the maximum volume of the existing dams

Basin	Rice irrigation			Rice and pasture irrigation		
	Rice 80% (ha)	Max Rice - current reservoir (ha)	Dif. rice (ha)	Rice 80% (ha)	Max Rice - current reservoir (ha)	Dif. rice (ha)
27	286	652	-	200	457	-
34	124	161	-	87	113	-
21	71	118	-	50	83	-
30	507	183	324	355	128	227
33	599	306	293	419	214	205
26	54	32	22	38	22	15
20	398	248	150	279	174	105
32	128	175	-	89	123	-
28	48	45	3	34	31	2
24	517	308	208	362	216	146
23	338	186	152	237	130	106
31	111	65	46	78	45	32
29	87	265	-	61	185	-
25	265	271	-	186	190	-
Total	3531	3014	1199	2472	2110	839

7.5 Model development: SWAT

This section presents the implementation, calibration and validation of the SWAT daily hydrologic model that permits calculation of the quantity of available water resources.

The projected coordinate system chosen for TWINLATIN was the Universal Transverse Mercator (UTM) 21 S, datum WGS 84, in which:

Central meridian =	-57
Reference latitude =	0
Scale factor =	0.9996
False east =	500,000
False north =	10,000,000

In this coordinate system, the position of the Tres Cruces creek basin outlet is 481203, 6650966 (-30.2728 Lat, -57.1954 Long). In this study the threshold for river generation was 300 hectares. Within the Tres Cruces creek basin, three sub-basins were studied (Figure 7.32), with the locations of their outlets as follows:

- Point 1: 518949; 6632523 (-30,4393 Lat; -56,8027 Long)
- Point 2: 535892; 6615537 (-30,5922 Lat; -56,6256 Long)
- Point 3: 508663; 6629356 (-30,4680 Lat; -56,9098 Long)

The land uses were identified from a satellite image of the 2005/06 rice season. In this image it was possible to distinguish the following land uses in the Tres Cruces creek basin: Water (WATR), Pasture (PAST), Native forest (FRDS) and Rice (RICE) (Figure 7.33). The parameters for each land use are presented in Table 7.20.

The soils map at scale 1:1,000,000 in the Tres Cruces stream basin shows four dominant soils: Arapey, Itapeby, Cuchilla de Haedo y Curtina (Figure 7.34). The soil parameters are shown in Table 7.21. The option of multiple hydrologic responses 0% soil-land use was chosen.

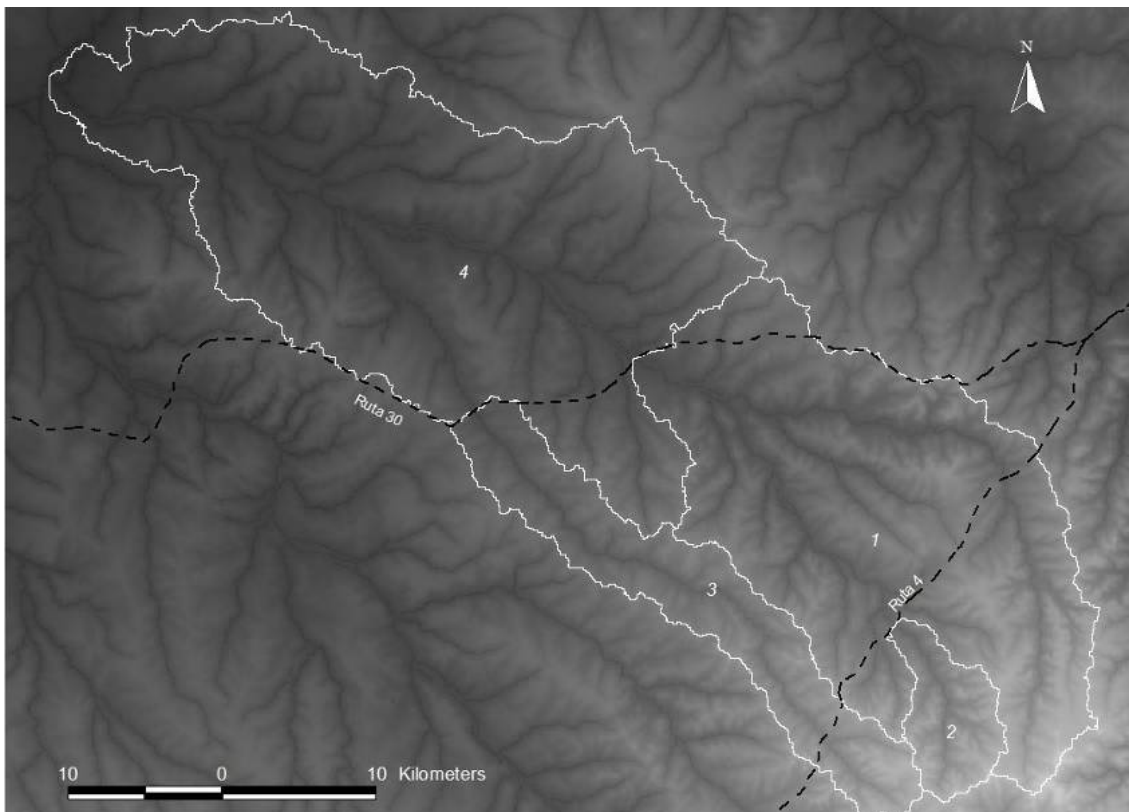


Figure 7.32 Studied sub-basins

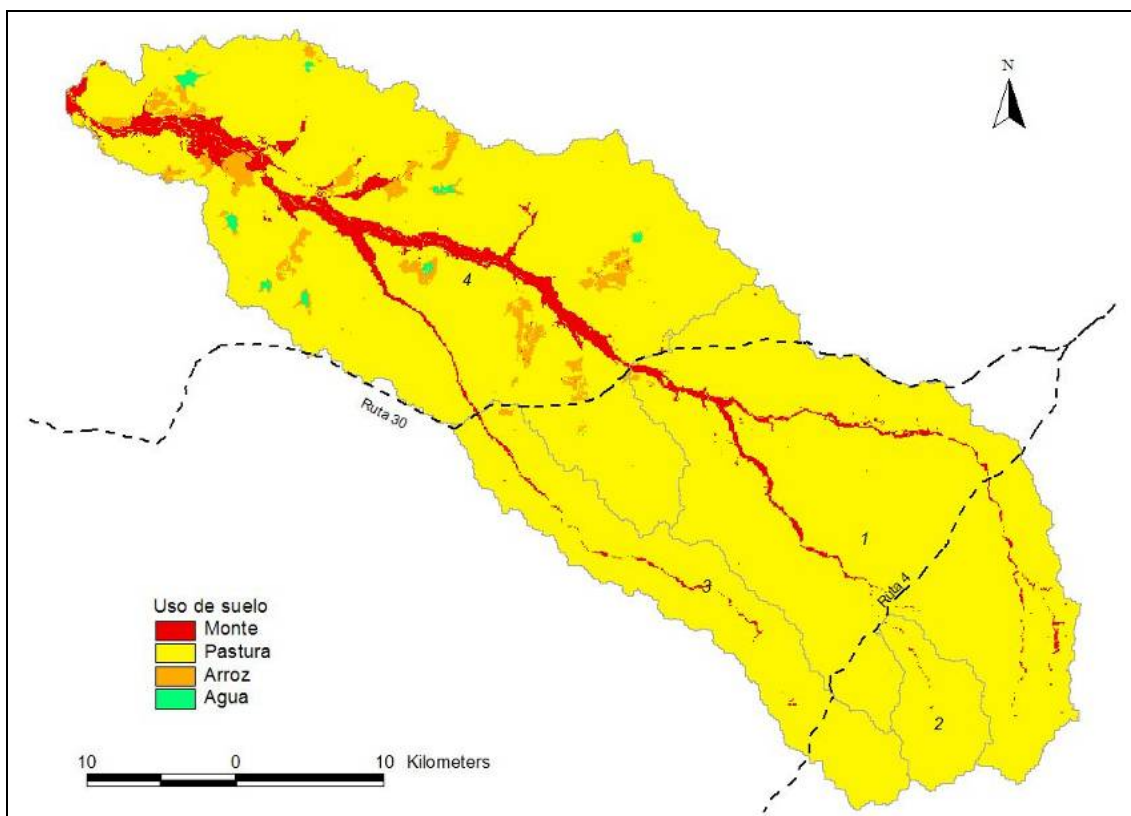


Figure 7.33 Current land uses (Red: Native Forest, Yellow: Pasture, Orange: Rice, Green: Water)

Table 7.20 Land use parameters

Parameter	Water (WATR)	Pasture (PAST)	Rice (RICE)	Native forest (FRSD)
CPNM	WATR	PAST	RICE	FRSD
IDC	Perennial	Perennial	Warm season annual	Trees
BIO_E	0.00	35.00	22.00	15.00
HVSTI	0.00	0.90	0.50	0.76
BLAI	0.00	4.00	5.00	5.00
FRGRW1	0.00	0.05	0.30	0.05
LAIMX1	0.00	0.05	0.01	0.05
FRGRW2	0.00	0.49	0.70	0.40
LAIMX2	0.00	0.95	0.95	0.95
DLAI	0.00	0.99	0.80	0.99
CHTMX	0.00	0.50	0.80	6.00
RDMX	0.00	2.00	0.90	3.50
T_OPT	0.00	25.00	25.00	30.00
T_BASE	0.00	12.00	10.00	10.00
CNYLD	0.0000	0.0234	0.0136	0.0015
CPYLD	0.0000	0.0033	0.0013	0.0003
BN1	0.0000	0.0600	0.0500	0.0060
BN2	0.0000	0.0231	0.0200	0.0020
BN3	0.0000	0.0134	0.0100	0.0015
BP1	0.0000	0.0084	0.0060	0.0007
BP2	0.0000	0.0032	0.0030	0.0004
BP3	0.0000	0.0019	0.0018	0.0003
WSYF	0.000	0.900	0.250	0.010
USLE_C	0.000	0.003	0.030	0.001
GSI	0.000	0.005	0.008	0.002
VPDFR	0.000	4.000	4.000	4.000
FRGMAX	0.000	0.750	0.750	0.750
WAVP	0.000	10.000	5.000	8.000
CO2HI	0.000	660.000	660.000	660.000
BIOEHI	0.000	36.000	31.000	16.000
RSDCO_PL	0.000	0.050	0.050	0.050
OV_N	0.01	0.15	0.14	0.10
CN2A	92.00	49.00	62.00	45.00
CN2B	92.00	69.00	73.00	66.00
CN2C	92.00	79.00	81.00	77.00
CN2D	92.00	84.00	84.00	83.00

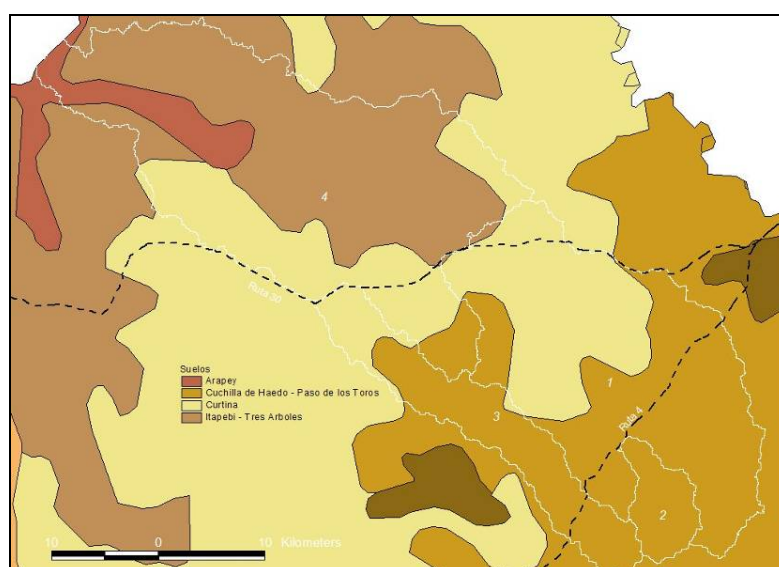


Figure 7.34 Soils in the basin
Table 7.21 Soil parameters

Parameter	Arapey	ItapebiTresArb	Curtina	CuchAhePToros
SNAM				
NLAYERS	4	4	1	1
HYDGRP	D	D	D	D
SOL_ZMX	300	190	120	50
ANION_EXCL	-	-	-	-
SOL_CRK	-	-	-	-
TEXTURE				
SOL_Z	300	190	120	50
SOL_BD	1.20	1.10	0.84	1.01
SOL_AWC	0.18	0.23	0.26	0.26
SOL_K	2.0	2.0	2.0	2.0
SOL_CBN	3.02	3.99	6.63	5.2
CLAY	48	40.6	44	29
SILT	25	46.3	42	32
SAND	27	13.1	14	39
ROCK	-	-	-	-
SOL_ALB	-	-	-	-
USLE_K	-	-	-	-
SOL_EC	-	-	-	-
NUMLAYER	1	1	1	1
SOL_Z	600	510		
SOL_BD	1.36	1.29		
SOL_AWC	0.09	0.19		
SOL_K	1.5	1.5		
SOL_CBN	0.91	1.81		
CLAY	59	65.2		
SILT	36	27.4		
SAND	5	7.4		
ROCK	-	-		
SOL_ALB	-	-		
USLE_K	-	-		
SOL_EC	-	-		
NUMLAYER	2	2		
SOL_Z	1100	780		
SOL_BD	1.38	1.36		
SOL_AWC	0.07	0.14		
SOL_K	1.5	1.5		
SOL_CBN	0.74	1.01		
CLAY	62	64.5		
SILT	31	28.4		
SAND	7	7.1		
ROCK	-	-		
SOL_ALB	-	-		
USLE_K	-	-		
SOL_EC	-	-		
NUMLAYER	3	3		
SOL_Z	1200	920		
SOL_BD	1.43	1.40		
SOL_AWC	0.05	0.11		
SOL_K	1.5	1.5		
SOL_CBN	0.26	0.59		
CLAY	63	61.1		
SILT	30	28.1		
SAND	7	10.8		
ROCK	-	-		
SOL_ALB	-	-		
USLE_K	-	-		
SOL_EC	-	-		
NUMLAYER	4	4		

All the data needed for the weather generation station (Table 7.22) were taken from the meteorological station E. M. Artigas except for precipitation data. After studying the available precipitation data, the 1048-Taruman and the 1082-Cerro Amarillo raingauges were chosen. Using Thiessen polygons, the precipitation time series were defined for the period 1981-2008. The Taruman raingauge has 53% of the basin area with outlet at Javier de Viana (N°. 155) hydrometric station, while the Cerro Amarillo raingauge has the remaining 47%. If there were missing data in one of the two raingauges, the value that was adopted was the one of the gauge with data.

The Basin Input File parameters are shown in Table 7.23.

7.6 Model development: MODSIM

This section describes the implementation of the MODSIM generic model of simulation of operations of a system and corresponding management.

MODSIM is a generic operations simulation model for a hydraulic system developed as decision support and used to simulate hydrological networks systems in a basin. It has the capacity to incorporate simultaneously the hydrologic, physical complexities and the administrative and institutional aspects of the management of a basin, including the water rights. Initially developed by the Dr. John Labadie of the University of Red State (CSU) in the middle 1970s, it has been used in many parts of the world.

The components of the system are represented as a network of nodes: storage nodes (reservoirs, ground basins, etc.) and non-storage nodes (confluences of rivers, points of divergent points, demands, etc.) and segments or arches (channels, pipes, etc.) connecting the nodes.

Table 7.22 Weather generation station parameters for Artigas station

TITLE	Artigas											
WLATITUDE	30.4											
WLONGITUDE	56.51											
WELEV	120.88											
RAIN_YRS	70											
	Jan	Feb	Mar	Apr	May	Jun	Jul	Aug	Sep	Oct	Nov	Dec
TMPMX	37.83	35.93	34.62	31.97	28.74	27.06	27.45	30.58	31.63	32.88	35.00	36.67
TMPMN	12.96	12.13	10.50	5.24	2.59	-0.69	-1.43	0.05	1.68	5.10	7.39	10.55
TMPSTDMX	1.35	1.52	1.85	2.37	1.76	1.30	1.76	2.43	2.33	1.42	1.67	2.30
TMPSTDMN	2.45	2.18	1.82	1.57	1.77	2.08	1.39	2.38	1.37	2.12	2.40	1.81
PCPMM	131.03	134.35	143.68	160.53	114.07	99.89	80.76	73.01	102.96	143.98	119.39	124.78
PCPSTD	11.97	12.97	13.00	15.60	11.76	9.48	7.44	7.02	9.57	12.07	12.07	11.98
PCPSKW	4.51	4.86	4.82	5.23	5.16	4.67	4.72	4.48	4.49	3.82	5.84	4.87
PR_W(1,mes)	0.14	0.16	0.14	0.16	0.14	0.16	0.14	0.13	0.16	0.15	0.12	0.10
PR_W(2,mes)	0.45	0.46	0.43	0.43	0.39	0.46	0.41	0.38	0.43	0.46	0.40	0.39
PCPD	4.20	4.58	4.46	4.84	4.42	4.91	4.43	4.01	4.82	4.75	3.50	3.21
RAINHHMX	45.51	45.51	45.51	45.51	45.51	45.51	45.51	45.51	45.51	45.51	45.51	45.51
SOLARAV	22.46	20.78	17.61	13.01	10.66	8.46	9.82	12.84	15.95	19.03	23.19	24.38
DEWPT	17.67	18.02	17.35	14.77	11.91	10.48	8.59	9.37	10.33	13.53	14.40	16.02
WNDVAV	22.13	21.73	19.97	19.89	19.17	20.00	22.79	23.59	27.82	26.53	24.85	23.79

Table 7.23 Basin parameters

Water balance	
SFTMP	-
SMTMP	-
SMFMX	-
SMFMN	-
TIMP	-
SNOCOVMX	-
SNO50COV	-
IPET	0
ESCO	0.950
EPCO	1.000
EVLAI	3.000
FFCB	0.000
Runoff	
IEVENT	0
ICRK	0
SURLAG	4.000
ADJ_PKR	1.0000
PRF	1.0000
SPCON	0.0001
SPEXP	1.0000
Nutrient cycle	
RCN	-
CMN	-
CDN	-
N_UPDIS	-
P_UPDIS	-
NPERCO	-
PPERCO	-
PHOSKD	-
RSDCO	-
Pesticide cycle	
PERCOP	-
Algae/CBOD/Dissolved oxygen	
ISUBWQ	0
Bacteria	
WDPQ	-
WGPQ	-
WDLPQ	-
WGLPQ	-
WDPS	-
WGPS	-
WDLPS	-
WGLPS	-
BACTKDQ	-
THBACT	-
WOF_P	-
WOF_LP	-
WDPF	-
WGPF	-
WDLPF	-
WGLPF	-
Model options: streams	
IRTE	0
IDEG	0
MSK_CO1	0.000
MSK_CO2	3.500
MSK_X	0.200
TRNSRCH	0.000
EVRCH	1.000
IWQ	0

The components used to represent the Tres Cruces creek basin are shown below and the configuration of the hydrologic system for MODSIM is presented in Figure 7.35.

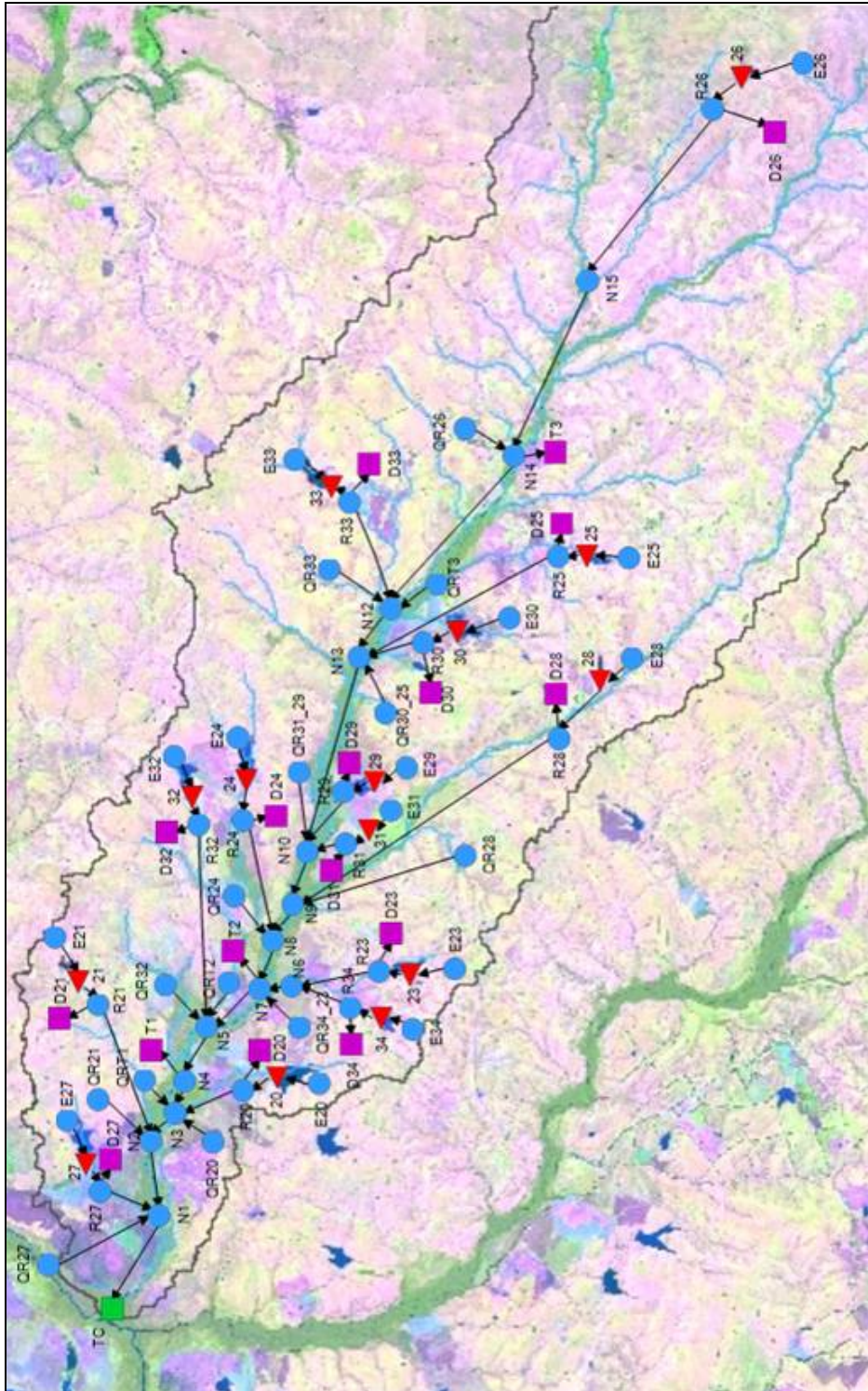


Figure 7.35 Hydrologic configuration system for the Tres Cruces creek basin in MODSIM

The input data to the model correspond to the period January 1932–December 2007, as it is the period with data for both raingauges with influence in the basin. The simulation was carried out for the period November 1960–October 2007, the non-calendar year in which it is assumed that the reservoirs get filled out for the irrigation of rice and because the period 1960-2007 is considered to be long enough to run the model. A monthly-step was chosen because of the climate available information.

7.6.1 Reservoirs

The 14 existing reservoirs in the basin were represented in the model. The information input in MODSIM is described below.

Maximum volume

The maximum volume of each reservoir was obtained from the publication "Aprovechamiento de los recursos hídricos superficiales – Inventario Nacional " of the DNH (2006).

Minimum volume

The minimum volume (dead volume) of each reservoir was calculated as 10% greater than the volume of sediment accumulation in 10 years, considering that one to be $200 \text{ m}^3 \text{ km}^{-2}$ of the basin per year.

Initial volume

The initial volume of the reservoirs was considered to be equal to the minimum volume.

Area – volume – height curves

These curves were obtained from the available documentation of the reservoirs in the DNH's office in Artigas. For those reservoirs without this information, it was assumed the following:

$$A = a \cdot h^b \quad \text{Integrating} \quad V = a \cdot \frac{h^{(b+1)}}{(b+1)}$$

Where: a and b are two coefficients that were determined using both equations and the volume, area and maximum height of the dams (obtained from the publication "Aprovechamiento de los recursos hídricos superficiales – Inventario Nacional " of the DNH (2006)).

Priority number

A priority number is assigned to each dam. It goes between 1 and 5000, the smaller the number, the higher the priority. If in one sub-basin, the water available is not enough to meet all the demands, MODSIM needs a priority order, because if all the components have the same priority, the results given by the model are not consistent.

For the Tres Cruces creek sub-basin, as currently all reservoirs have an independent contributing area, the same priority was given to all.

Water level objective

The water level objective of the reservoir represents the maximum active volume of the reservoir. In all cases and for all the time, it was considered to be the difference between the maximum volume and the minimum volume ("useful" volume).

Net evaporation

The net evaporation of each reservoir is defined as the rate of evaporation minus the precipitation rate (a negative value means that the rate of precipitation exceeds the rate of evaporation for that period).

7.6.2 Demands

Two types of demands were considered: reservoir demands and direct intake demands.

Reservoir demands

It was assumed that each reservoir has an associated demand that withdraws a volume equal to the useful volume of the reservoir in the month of October, every year of calculation. This assumes that the water that runs during the rice season (November–February) is not used for the irrigation of that season, but it is stored for the next one, because the decision on how much area to plant is made October based on the available volume of water in the reservoir.

Direct intake demands

Currently there are three direct intakes that withdraw water from the same node. It was assumed that their annual volume is withdrawn in equal parts during the four months of irrigation (November–February). Just like for the dams, the demands also have an associated priority number. Zero priority was assigned to all. This number has to be lower than the priority number for the reservoirs.

7.6.3 Nodes

The nodes E_i , N_i and QR_i are used to input the runoff data.

The E_i nodes are located upstream of each dam and add the monthly runoff of the area contributing to the reservoir. The runoff was obtained with Temez model.

The N_i nodes add the runoff of the remaining sub-basins. Those runoffs were obtained with Temez model.

The QR_i nodes add the return flows to the stream back from the irrigation of rice. The monitoring of the amount of water returning to the creek from the irrigated rice fields was a result of TWINLATIN WP2. It was assumed to be 10% of the total volume of irrigation and it was distributed in equal parts during the four months of the rice season (November–February).

In addition, the R_i nodes downstream of each dam, where the demand is extracted, are utilised only for the transfer of water from the reservoir to the demand.

Figure 7.36 shows the basins contributing to the reservoirs and Figure 7.37 the remaining basins.

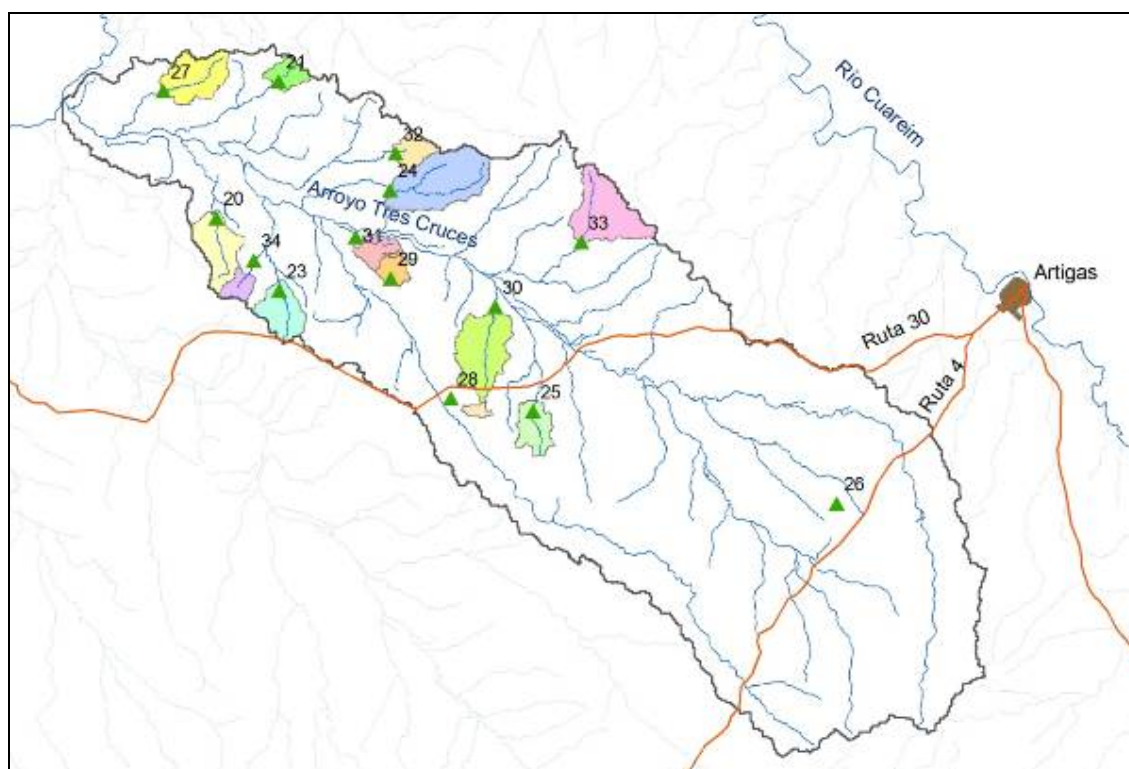


Figure 7.36 Basins that contribute to the existing reservoirs in the Tres Cruces creek basin

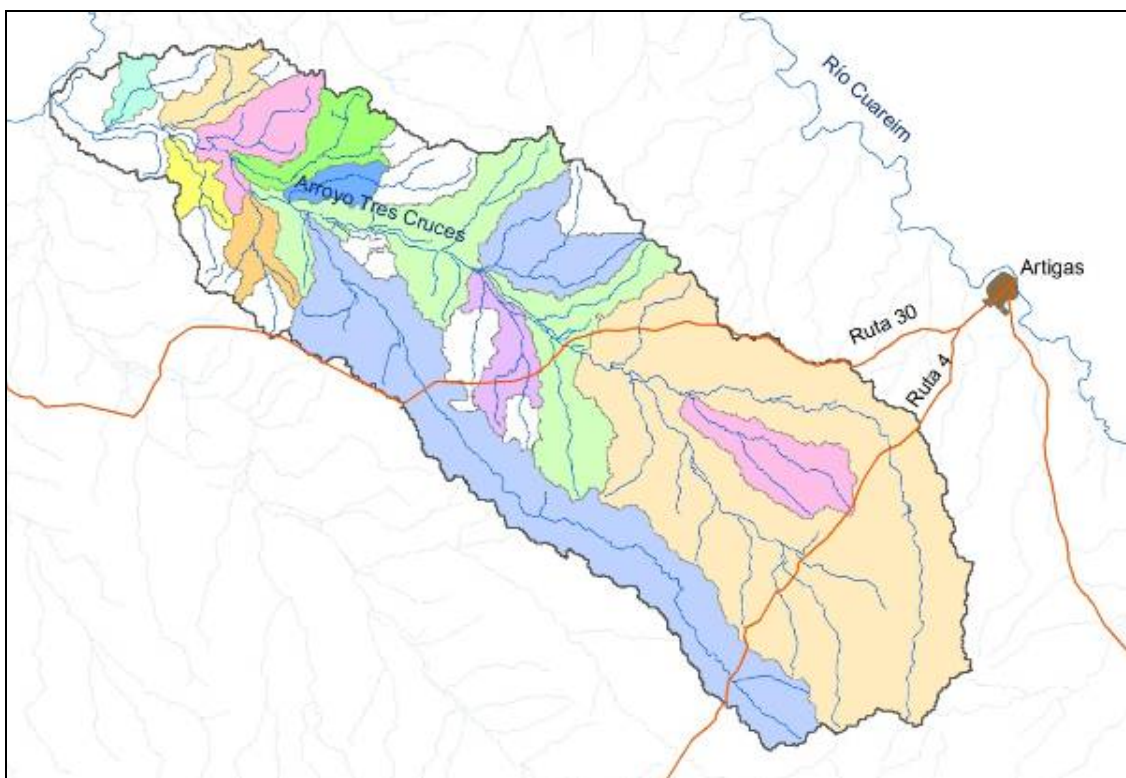


Figure 7.37 Remaining basins

7.6.4 Results

The MODSIM outputs are in graph and table formats. Some of the outputs are presented in Figures 7.38 to 7.41.

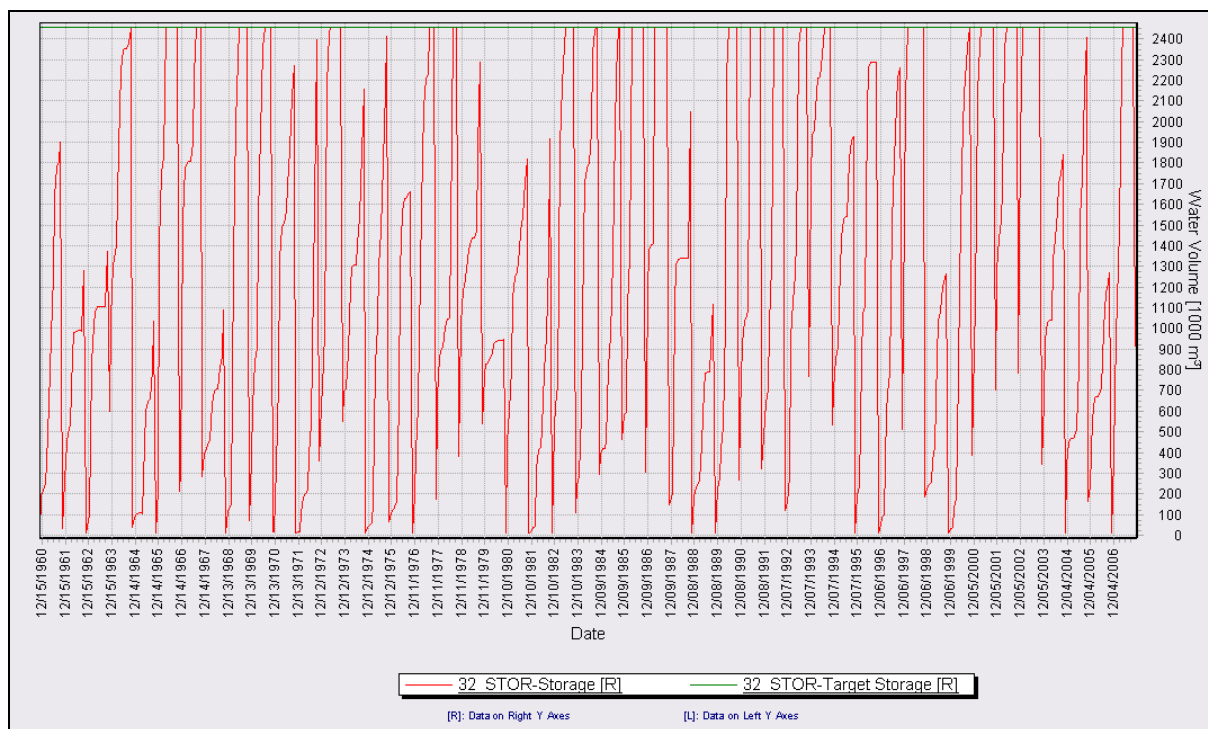


Figure 7.38 Volume of water in the reservoir 32

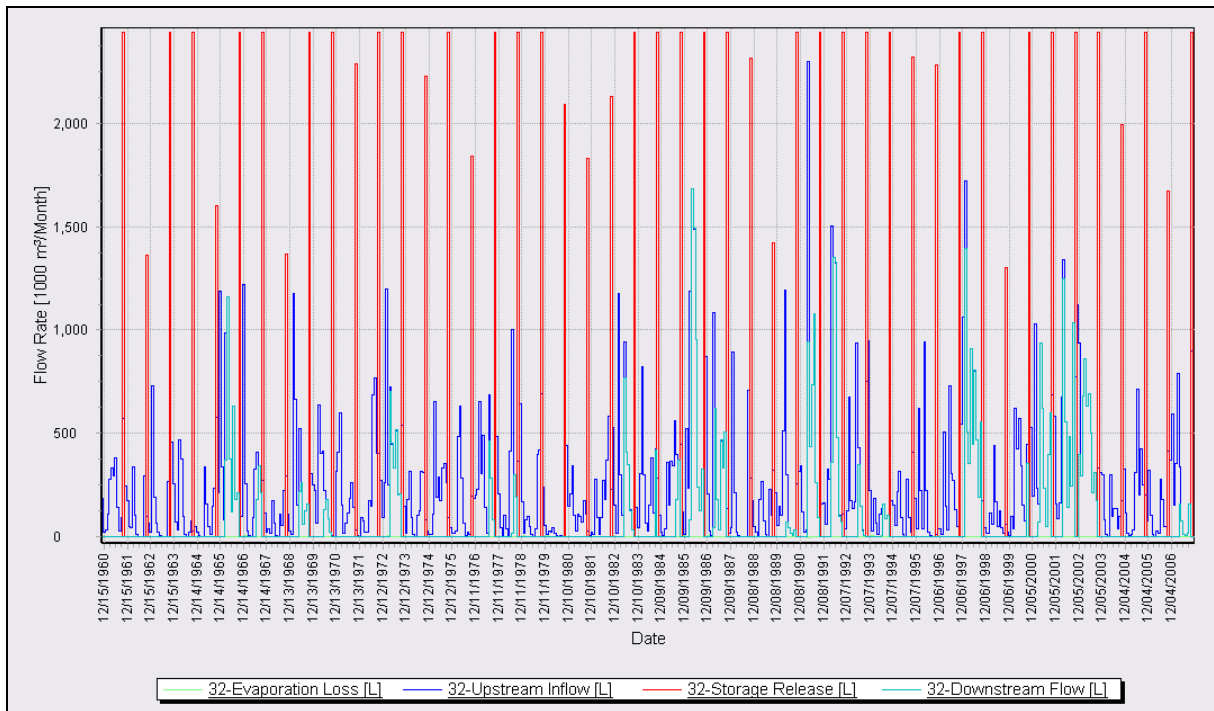


Figure 7.39 Runoff, evaporation and volume of water in October – reservoir 32



Figure 7.40 Demand for reservoir 25

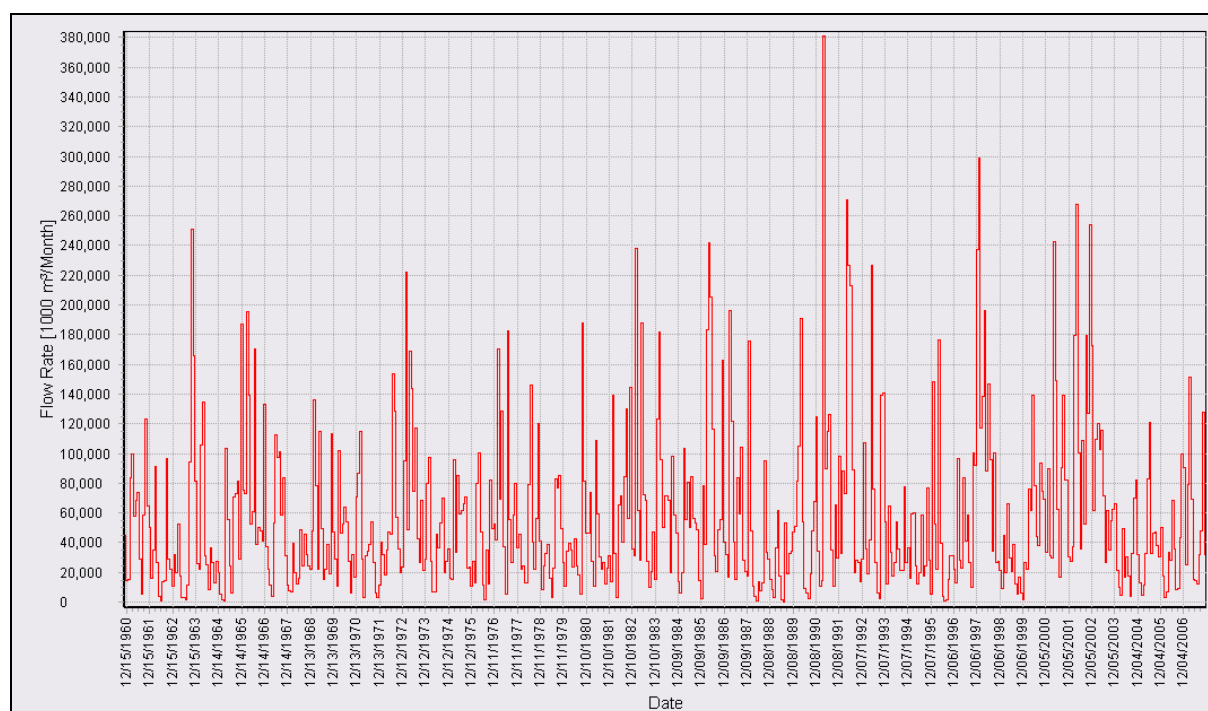


Figure 7.41 Monthly runoff in link N8_N7

7.6.5 Evaluation of the model and its implementation

MODSIM can incorporate more detailed information about the characteristics of the basin, for example, infiltration in the irrigated surface, as well as in channels and reservoirs. This type of information was not input into the model due to the lack of data.

On the other hand, it would be important to have consistent information about the level of water in the reservoirs before, during and at the end of the irrigation period, as well as the surface of rice planted and harvested by each producer.

With respect to the model, it is important to mention the special attention that has to be paid when assigning priorities. When flows are higher than the normal ones in the basin, all the demands are generally met while, when the flows are less than normal, severe deficits may occur. The way MODSIM is set, it distributes the available water satisfying first those with higher priority. If the administrative goal is an equal distribution of the water in drought periods, assigning the same priority to all the uses in the basin, that does not necessarily mean an equal distribution for MODSIM. If no priorities are set, MODSIM outputs inconsistent results and random distribution of the water available.

7.7 Calibration of SWAT

The 27 parameters of calibration of the SWAT model are:

rchrq_dp	CN2	GWQMN	GW_REVAP	SOL_AWC	ESCO	sol_z	sol_k	canmx
GW_DELAY	REVAPMN	ALPHA_BF	BIOMIX	epco	CH_K2	surlag	sol_alb	SLOPE
SLSUBBSN	ch_n	SFTMP	SMFMX	SMFMN	TLAPS	SMTMP	TIMP	blai

For the calibration a sensitivity analysis of the different parameters was done so to detect the most relevant ones. The work was carried out with the module AVSWATX Sens-Car- Unc⁴ of SWAT. It put the parameters in order from the most to the least sensitive one and in this manner it was possible to define the process of calibration. Figure 7.42 shows the result of the analysis of sensitivity⁵. The parameters that do not appear in the figure have a relative sensitivity equal to zero.

Table 7.24 shows in green the parameters whose values are known. Therefore, there remain 10 parameters to be calibrated. Those parameters with relative sensitivity lower than 0.4 were ruled out. The Nash-Sutcliffe efficiency function and R^2 were used as objective functions. Figure 7.43 shows the flow chart used to carry out the calibration.

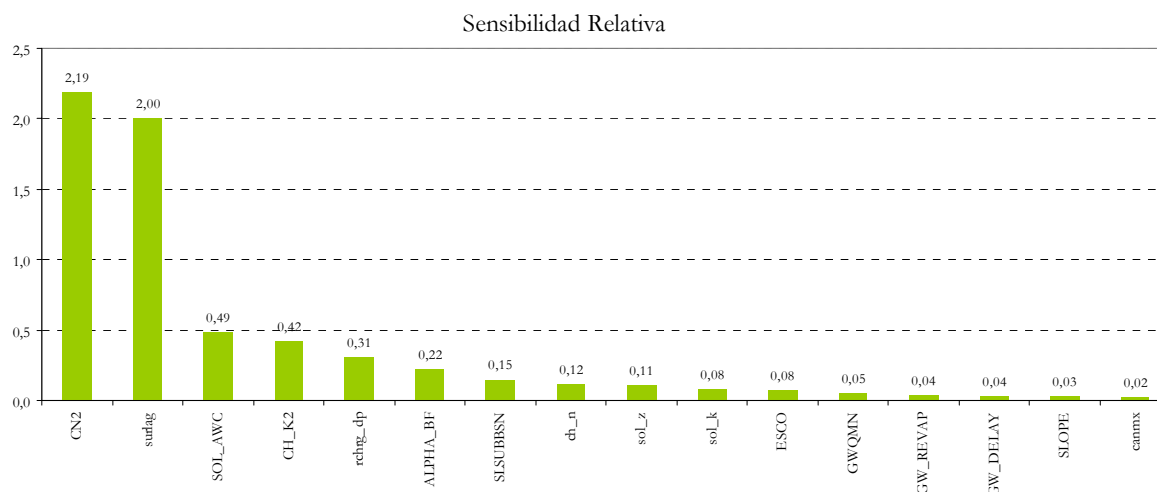


Figure 7.42 Daily runoff for Javier de Viana in 2005. Vertical axis: relative sensitivity. Horizontal axis: SWAT parameters

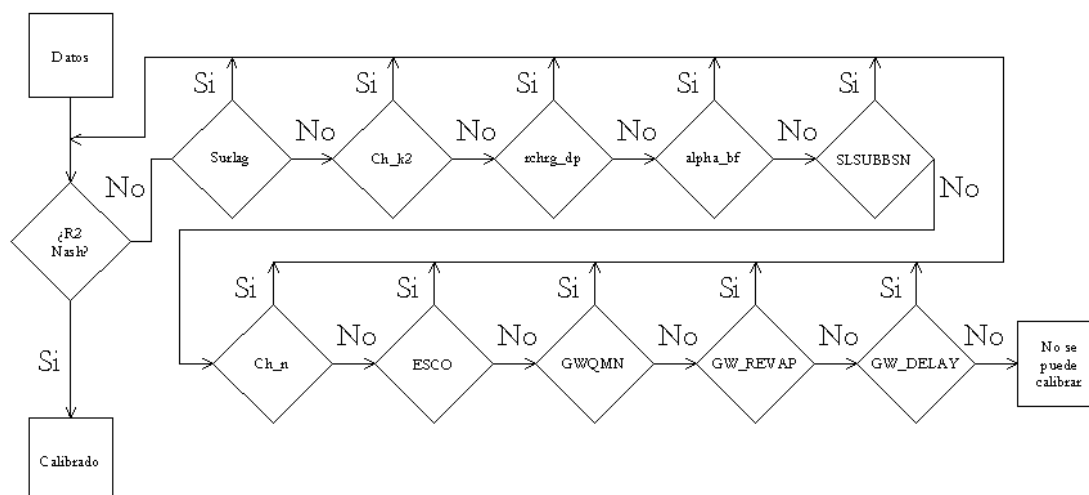


Figure 7.43 Flow chart for calibration

⁴ Sensitivity Analysis-Autocalibration-Uncertainty tools for SWAT2003 and AVSWATX MDL Wed Mar 02 17

⁵ "Sensitivity, auto-calibration, uncertainty and model evaluation in SWAT2005", Ann van Griensven, a.vangriensven@unesco-ihc.org

The whole time series data (1982-2008) of the gauge station 155 was intended to be used to calibrate and validate the model. The calibration period chosen was 01/07/2004 to 30/06/2006. Figures 7.44 and 7.45 show the daily runoff at Javier de Viana (gauge station 155) that resulted from running SWAT for the period 01/07/2004-30/06/2006 and the value of rain of the representative raingauge. Table 7.25 presents the values of the calibrated parameters. Table 7.26 shows the values of the Nash-Sutcliffe efficiency function and R^2 .

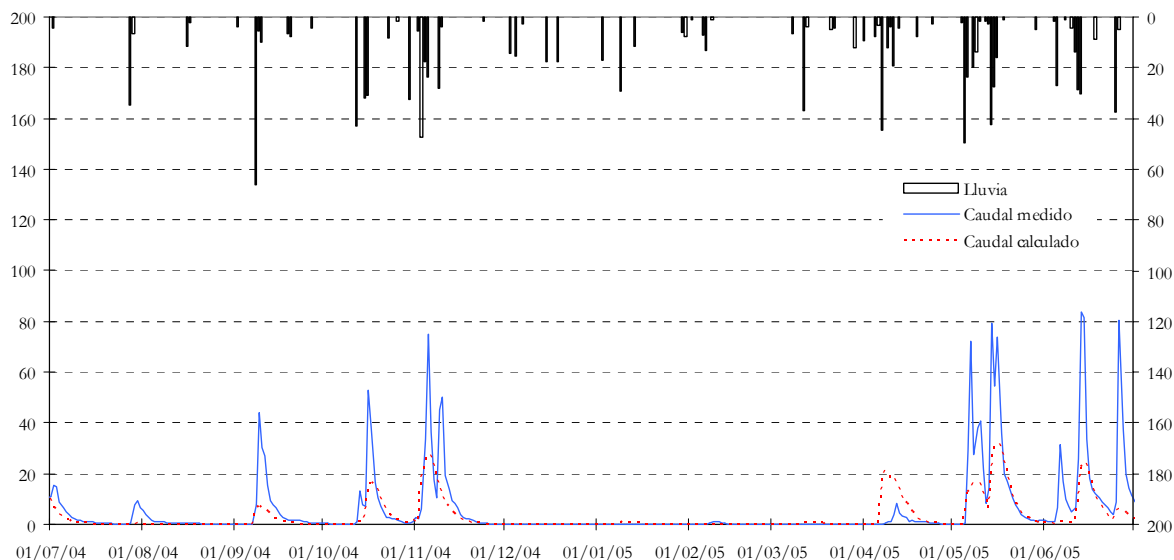


Figure 7.44 Daily runoff for the period 01/07/2004 - 30/06/2005 at Javier de Viana. Blue graph: measured flow. Red graph: calculated flow. Black graph: precipitation.

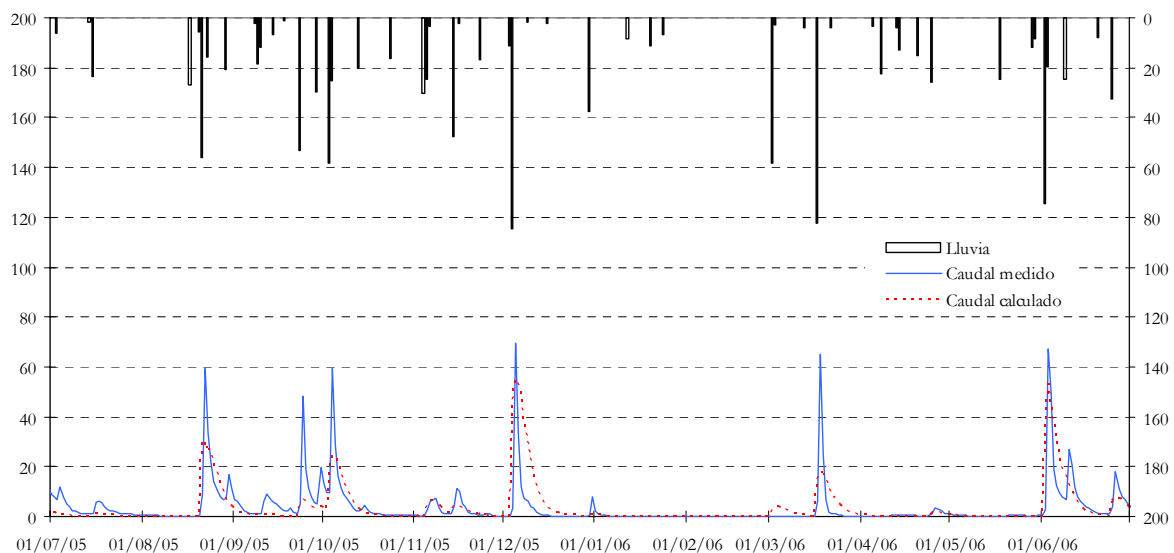


Figure 7.45 Daily runoff for the period 01/07/2005 - 30/06/2006 at Javier de Viana. Blue graph: measured flow. Red graph: calculated flow. Black graph: precipitation.

Table 7.24 Basin parameters

CN2	2.19	ch_n	0.12
Surlag	2.00	sol_z	0.11
SOL_AWC	0.49	sol_k	0.08
CH_K2	0.42	ESCO	0.08
rchrq_dp	0.31	GWQMN	0.05
ALPHA_BF	0.22	GW_REVAP	0.04
SLSUBBSN	0.15	GW_DELAY	0.04

Table 7.25 Values of the calibrated parameters in the basin

surlag	4.106
CH_K2	100
rchrq_dp	0.50
ALPHA_BF	0.4956
SLSUBBSN	91.463
ch_n	0.082
ESCO	0.800
GWQMN	3132.2
GW_REVAP	0.0792
GW_DELAY	31

Table 7.26 Values of the objective function for the calibration period

Nash	0.4362
R ²	0.4521

Table 7.27 Values of the objective function for the validation period

Nash	0.4270
R ²	0.4472

7.8 Validation of SWAT

The calibration period chosen was 01/07/2006 to 30/06/2008. Figures 7.46 and 7.47 show the daily runoff at Javier de Viana (gauge station 155) that resulted from running SWAT for the period 01/07/2006-30/06/2008 and the value of rain of the representative raingauge. Table 7.27 shows the values of the Nash-Sutcliffe efficiency function and R².

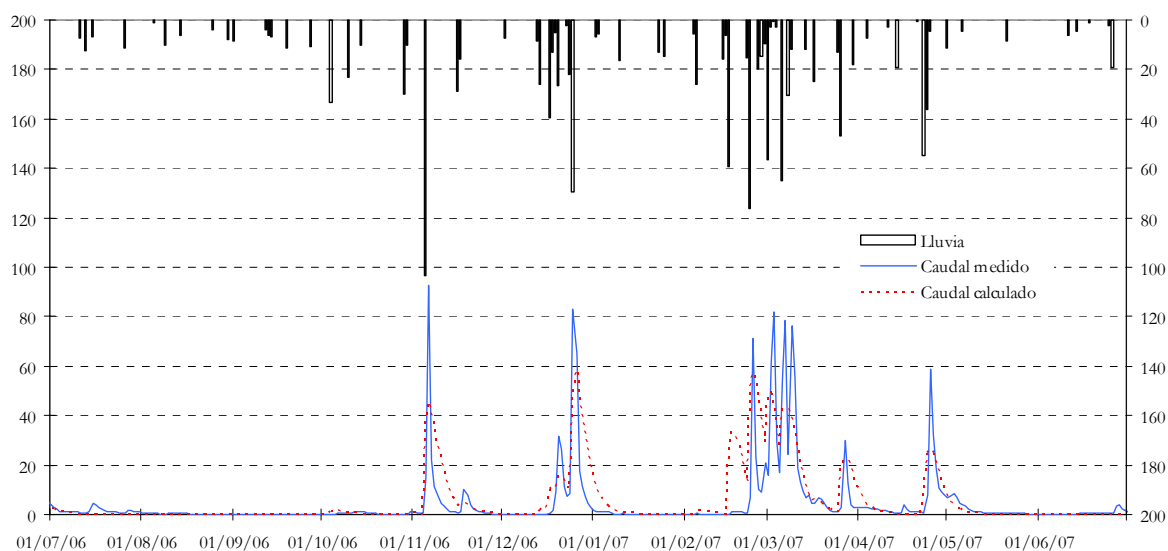


Figure 7.46 Daily runoff for period 01/07/2006 - 30/06/2007 at Javier de Viana. Blue graph: measured flow. Red graph: calculated flow. Black graph: precipitation.

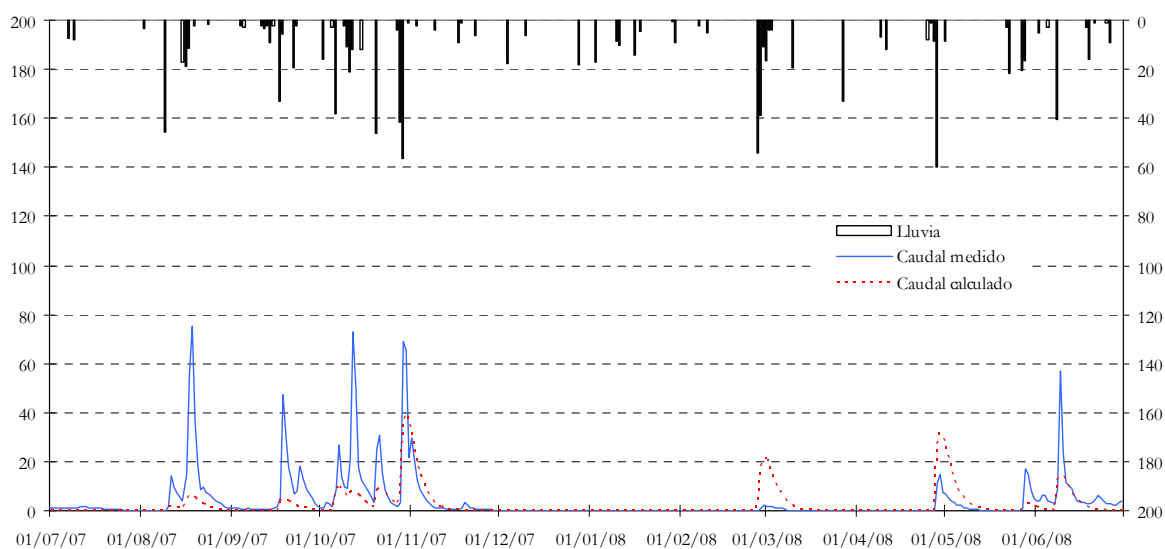


Figure 7.47 Daily runoff in period 01/07/2007 - 30/06/2008 for Javier de Viana

7.9 Evaluation of hydrological modelling (D3.2)

7.9.1 Evaluation of SWAT daily hydrological model

The daily hydrologic model SWAT was implemented, calibrated and validated in the Tres Cruces creek basin. The calibration and validation that were carried out are not very encouraging (Nash-Sutcliffe efficiency 0.43 and R^2 0.45), attributing those results to the quality of the information used. Likewise, the flow data have a runoff coefficient of 0.29, much lower than the calculated with the monthly-step Temez model (0.45), which would indicate that the flow is being underestimated, because it is a basin with a concentration time less than 24 hours with only three daily measurements.

The advantages of the SWAT model are:

- It models the hydrologic cycle with daily step.
- Many researchers have evaluated the model and their applications publishing a great number of articles.
- It helps to validate flow and precipitation daily data
- It has a GIS friendly interface and good documentation.
- It is a physically-based model .
- It is programmed in Fortran and it permits the experienced user to modify the code.
- It is a good tool to study erosion as well as water quality.

On the other hand, it presents some disadvantages:

- It does not simulate events of less than one day steps like, for example, a storm.
- It is not easy to calibrate.
- It does not have a friendly post-process interface.
- It is very sensitive to the quality of the input data.

Based on the advantages and disadvantages, it is recommended to use it as a tool to validate daily data of precipitation and flow, and to model erosion and water quality in a basin with diffuse source pollution.

To assess the amount of water there is in the basin it is recommended to use the monthly-step Temez model (with four parameters against the 27 in SWAT).

7.9.2 Evaluation of climate change scenarios

A runoff elasticity study was carried out to evaluate climate change. Small changes to the input data were made and changes in runoff were calculated. Figures 7.48 and 7.49 present the curves that show the variation of the average, percentiles and permanence curves.

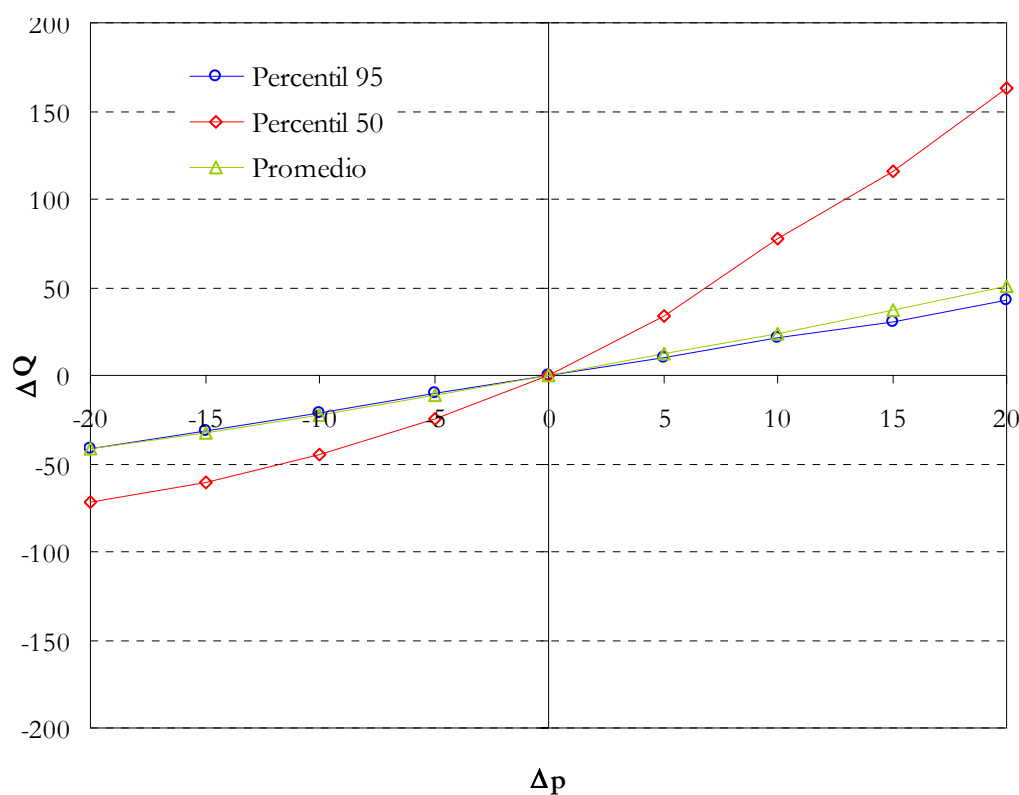


Figure 7.48 Relationship between a variation in precipitation and the corresponding variation in runoff. Green: Average. Red: Percentile 50. Blue : Percentile 95

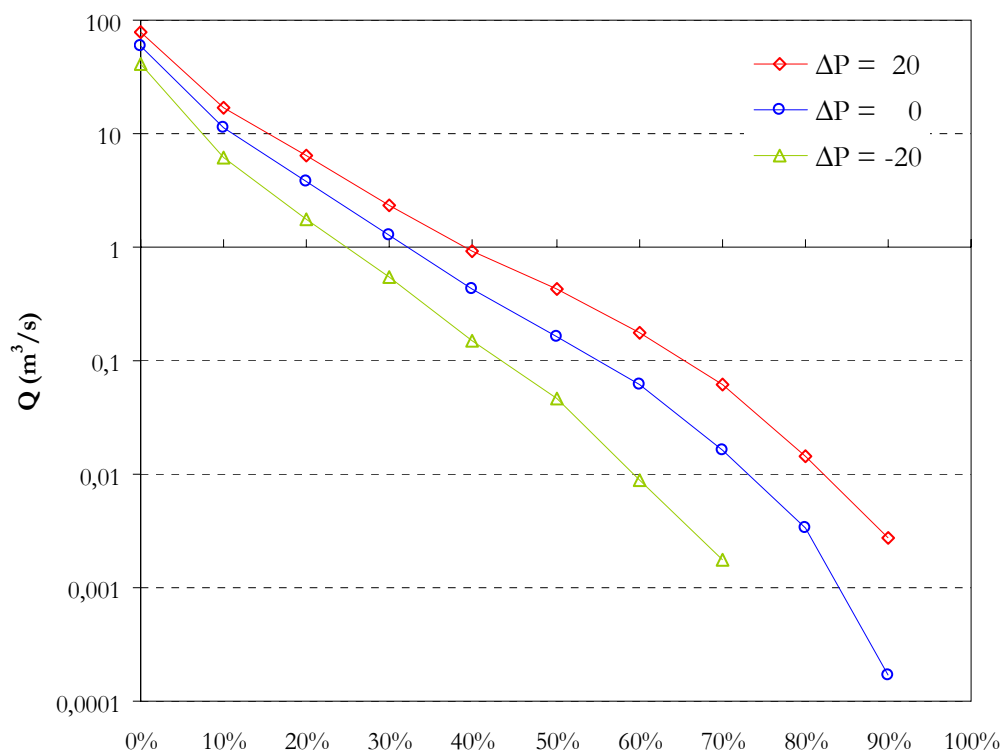


Figure 7.49 Permanence curves

7.9.3 Evaluation of MODSIM water resource management model

MODSIM was implemented as a generic model of simulation of operations of a system, to support decisions to manage it. It is a simple model and after being implemented in the basin it is easy to use. Therefore it is recommended for the management of the water resources.

It was estimated that five times more water could be used in the basin compared with what it is currently used, but for this it is necessary to store water. Because of this, it is proposed to do a multisite analysis to choose the best locations to build the necessary reservoirs.

Likewise it is recommended to use the tools presented in this work for the management of water resources. To analyse the criterion with which DNH determines the maximum volume to be stored, the annual runoff that DNH uses is compared with the average annual runoff determined with Temez model for all the contributing areas for all the existing reservoirs, for the period 1932–2007. Figure 7.50 and Table 7.28 show the results. Figure 7.50 shows that the runoff used by DNH is slightly higher (12 mm) than the average of the annual average runoffs of the considered sub-basins. Table 7.28 shows for each sub-basin, the volume determined by DNH and the frequency with which that volume is reached. Only for subbasin 26 the volume determined by DNH is acceptable for the construction of a reservoir.

Another common way of expressing DNH's criterion is to transform the annual runoff to a relationship between the area of rice that is possible to irrigate with a basin and the area of the basin. Assuming that rice needs 14000 m³ per hectare, to consider an annual runoff of 668.5 mm is equivalent to say that to irrigate 1 hectare of rice, a contributing area of 2.5 hectares is needed.

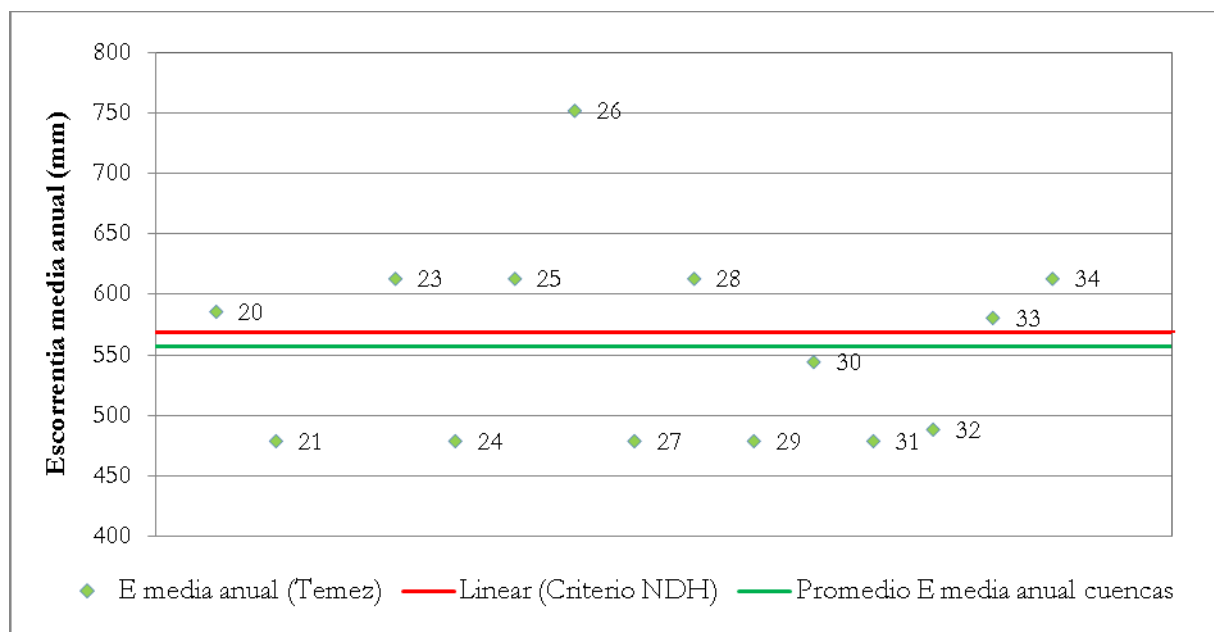


Figure 7.50 Annual runoff used by DNH vs annual average runoff for the subbasins (Temez). Vertical axis: Annual average runoff (mm). Green dots: Annual average runoff (Temez). Red line: Criterion DNH. Green line: Average annual average runoff.

Table 7.28 Volume calculated by DNH and frequency of occurrence for the contributing areas to the existing reservoirs

Basin	DNH volume (thousands of m ³)	Frequency
27	7.828	28
34	2.217	53
21	1.933	28
30	10.676	45
33	11.278	51
26	739	81
20	7.401	51
32	3.357	30
28	861	53
24	14.121	28
23	6.043	53
31	3.047	28
29	2.365	28
25	4.738	53

However, to leave upstream of a reservoir a volume of available water equal to the difference between the annual volume determined by DNH and the maximum volume of the reservoir, can have a negative impact. For instance, considering dam 20, based on the results obtained with MOSDIM for the period 1960–2007, the existing reservoir reaches its maximum volume with a frequency of 100% i.e. it fills 100% of years, so demand is always met. A new reservoir is assumed to be constructed upstream of dam 20 with a volume equal to the available volume based on DNH calculations. Figure 7.51 shows the basins for both reservoirs and MODSIM scheme. The demand is assumed to be equal to the

“useful” volume of the reservoir and is withdrawn in the month of October every year of the simulation. Figures 7.52 to 7.54 show MODSIM outputs of demands for the current scenario and the assumed one. It can be observed that after incorporating the new reservoir, the new one can meet its demands most years while dam 20 does it few years. Therefore, it is recommended to have a more conservative criterion to manage water resources, for example, to consider that the maximum volume to store be reached with a frequency of 80%. Likewise, it is important to say that each basin has its own particular behaviour so it is important to do the approach case by case.

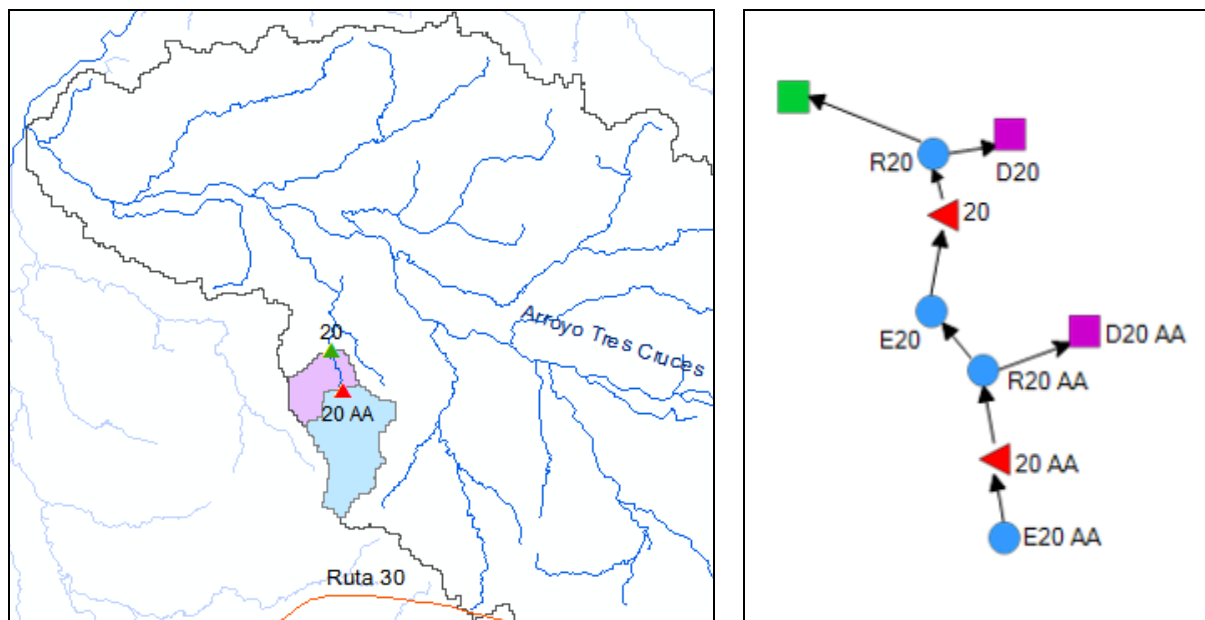


Figure 7.51 Sub-basins for the two reservoirs and MODSIM scheme

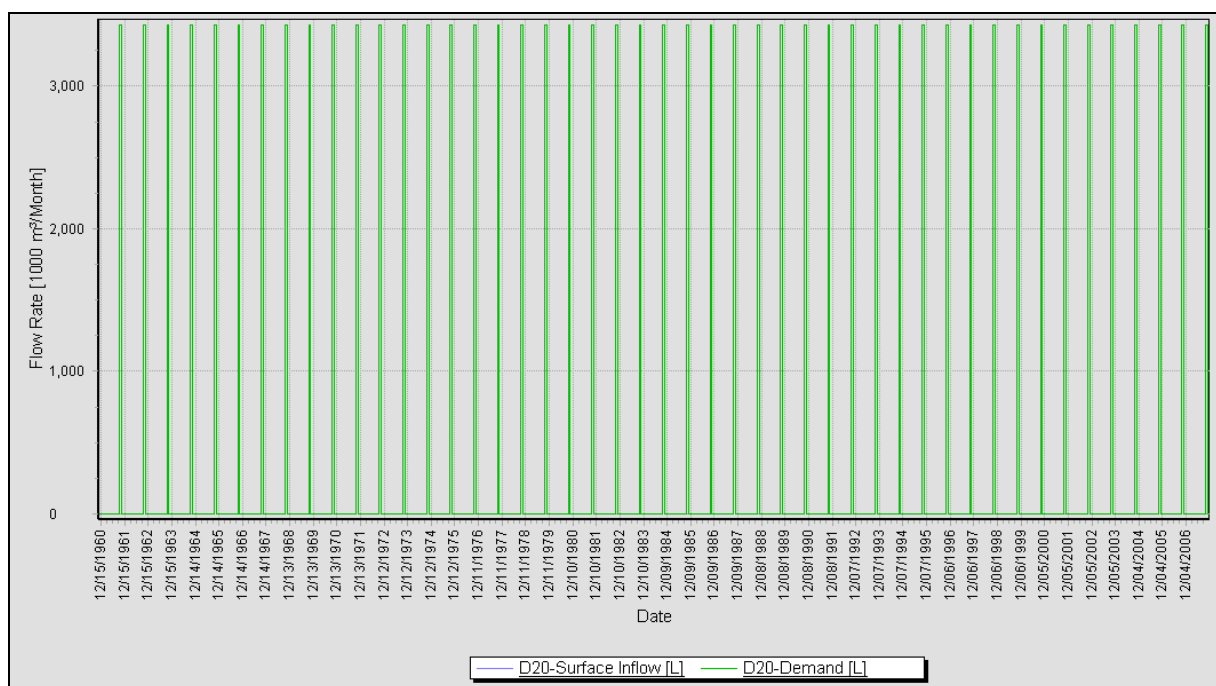


Figure 7.52 MODSIM output: dam 20's demand, current scenario

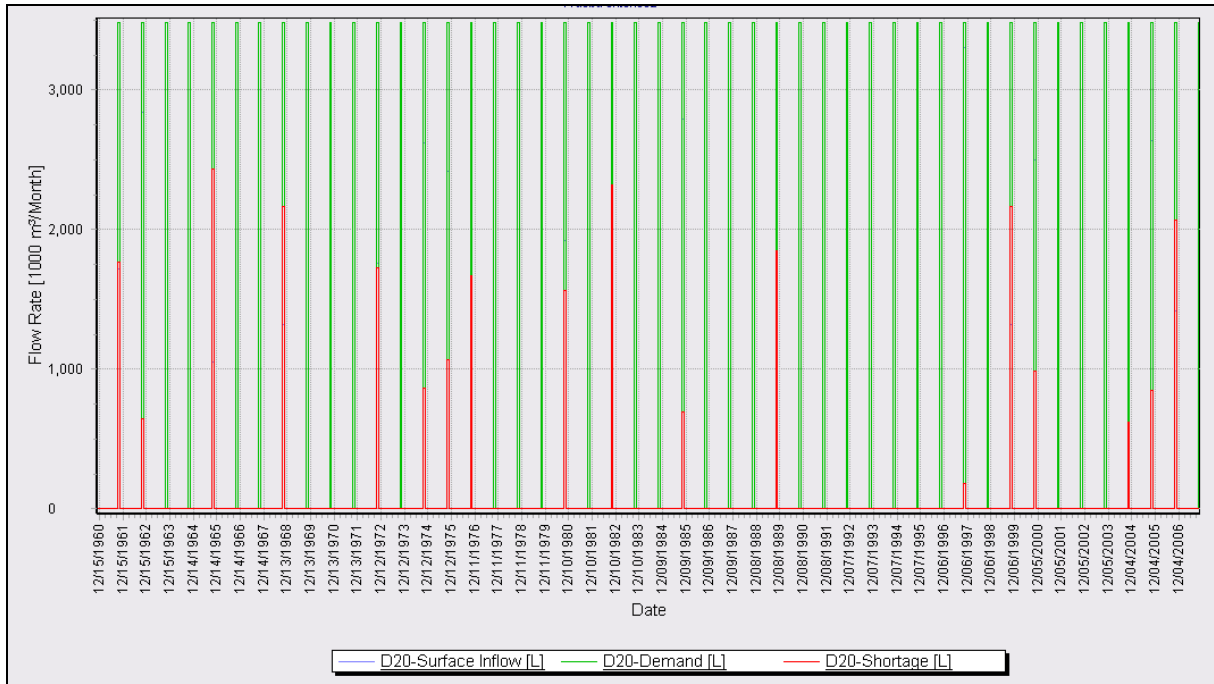


Figure 7.53 MODSIM output: dam 20's demand, assumed scenario

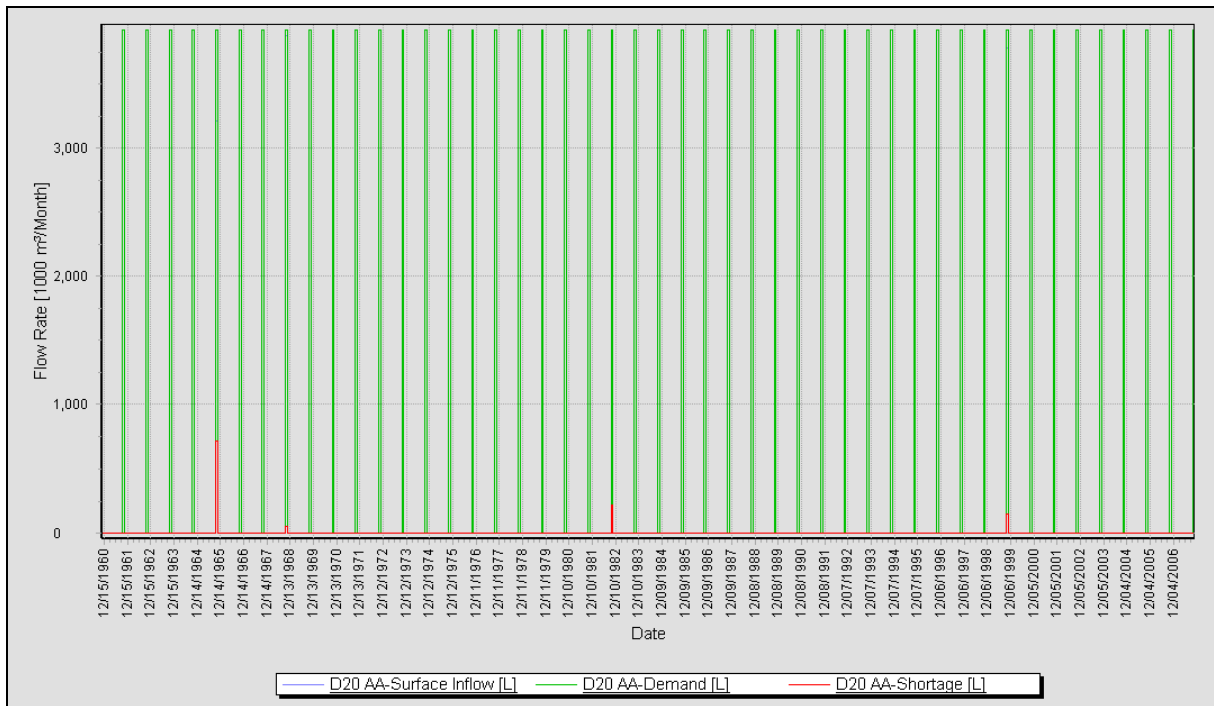


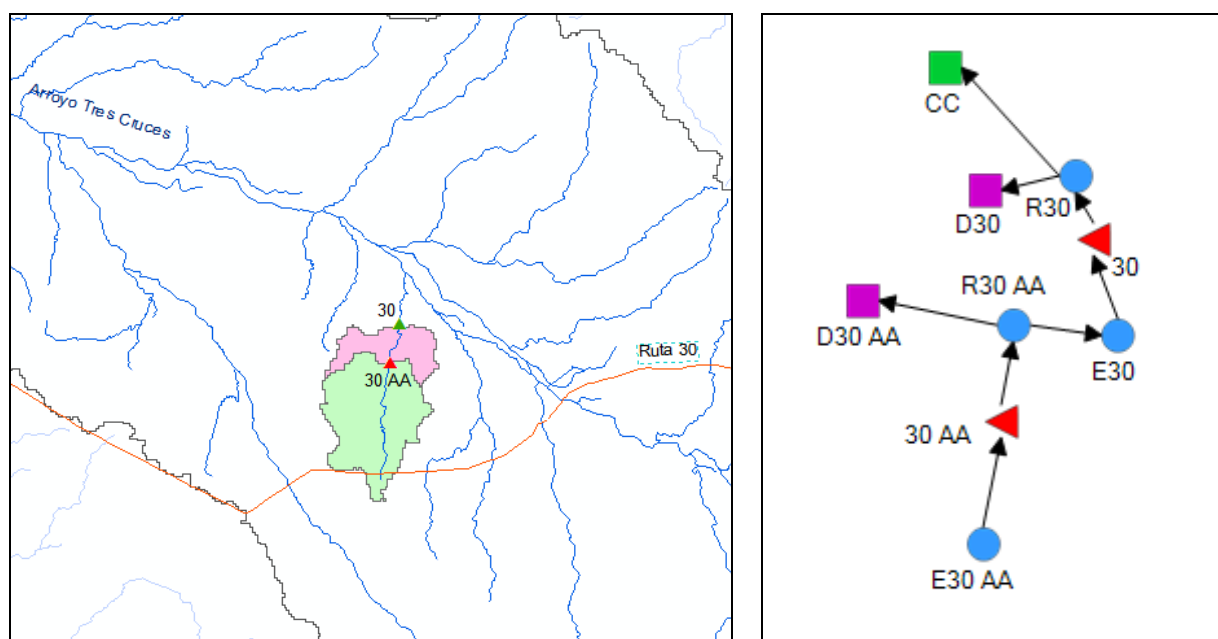
Figure 7.54 MODSIM output: dams 20AA's demand, assumed scenario

Table 7.29 Area of the basin/Area of rice for volumes of 80% and 100% frequency

Basin	Área of basin (ha)	Volume 80% (thousands of m ³)	Abasin/ARice	Volume 100% (thousands of m ³)	Abasin/ARice
27	1377	4009	4.8	3000	6.4
34	390	1734	3.1	1313	4.2
21	340	990	4.8	741	6.4
30	1878	7095	3.7	5289	5.0
33	1984	8383	3.3	6214	4.5
26	130	752	2.4	487	3.7
20	1302	5574	3.3	4116	4.4
32	590.5	1788	4.6	1348	6.1
28	151.5	674	3.1	511	4.2
24	2484	7233	4.8	5414	6.4
23	1063	4732	3.1	3583	4.2
31	536	1554	4.8	1164	6.4
29	416	1211	4.8	906	6.4
25	833.5	3711	3.1	2810	4.2

Table 7.29 presents the relationship Area of the basin/Area of rice for the contributing areas for the existing reservoirs, for volumes that are reached with 80% and 100% frequency. Table 9.2 shows that for the studied sub-basins, the relationship Area of the basin/Area of rice must be, on average, higher than 3.8, to comply with the assumed criterion.

Regarding the available water DNH maintains upstream of a certain reservoir, that same criterion could be used for the whole basin. In other words, if the existing reservoir has a maximum volume smaller than the annual volume that the basin produces with a frequency of 80%, there will remain upstream a volume equal to the difference of the latter and the maximum volume of the reservoir. The impact on demands is illustrated with the example set out in Figure 7.55.

**Figure 7.55** Basins of the reservoirs and MODSIM scheme

The MODSIM outputs of the demands for the current and assumed scenarios are presented in Figures 7.56 and 7.57. It is important to say that a higher priority was assigned to the demand of reservoir 30 as it was the existing reservoir. That means that if one year the demand is not met with the water of the reservoir 30, the reservoir 30AA covers that difference. This is another issue to have into consideration when managing the system. It is observed from Figure 7.56 that, currently, reservoir 30 fills out 100% of the years, and therefore the demand is always met. Figure 7.57 shows that the demand of reservoir 30AA is not met during only three years of the simulation.

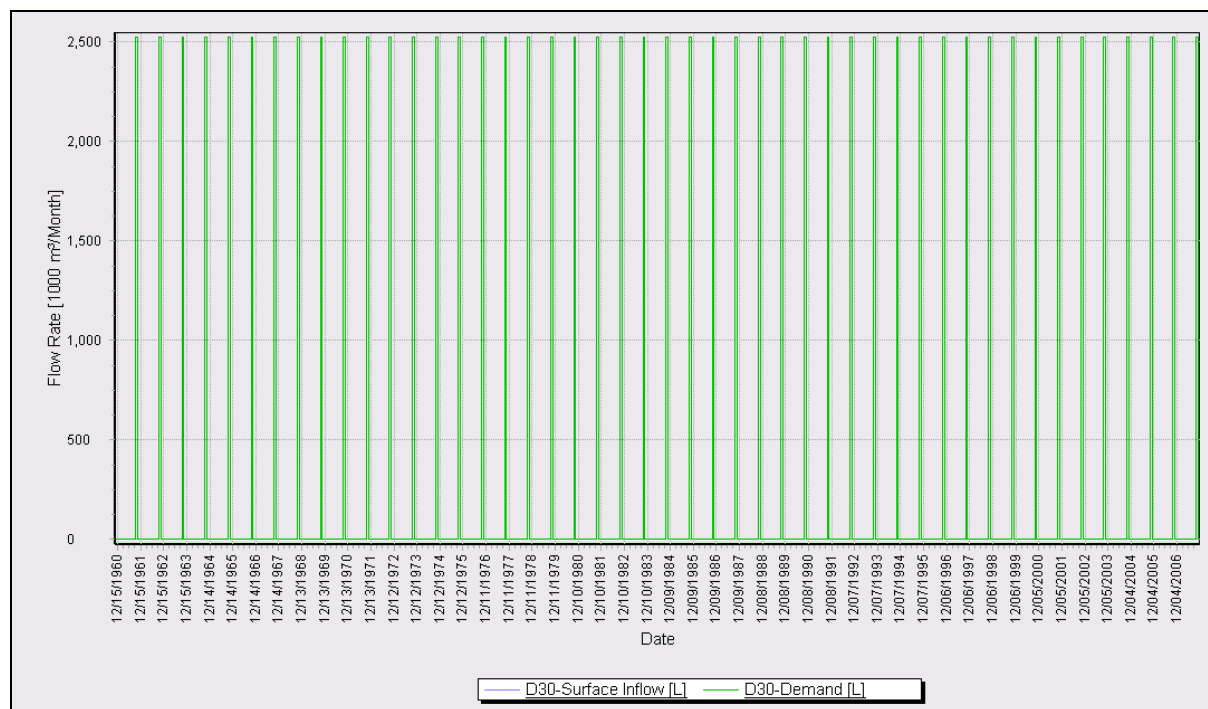


Figure 7.56 MODSIM output: reservoir 30's demand, current and assumed scenarios.

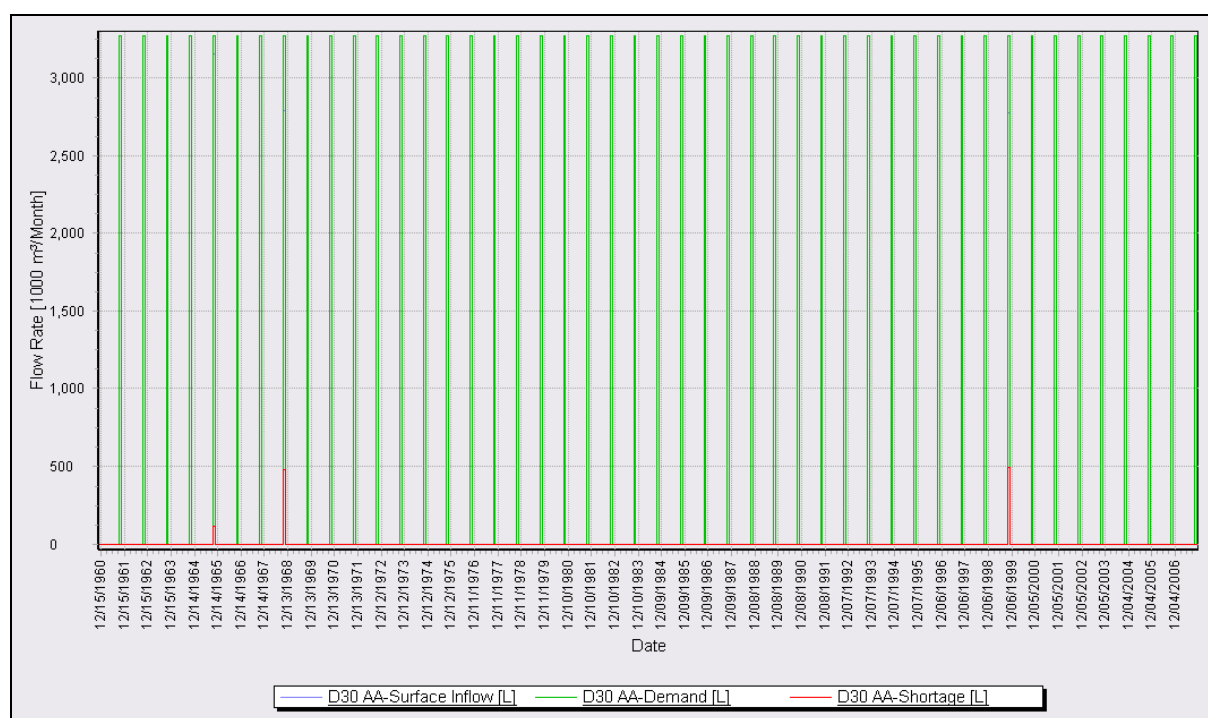


Figure 7.57 MODSIM output: reservoir 30AA's demand, assumed scenario

7.10 Summary and recommendations

7.10.1 SWAT daily hydrological model

Based on the advantages and disadvantages presented before about the SWAT model, it is recommended to use it as a tool to validate daily data of precipitation and flow, and to model erosion and water quality in a basin with diffuse source pollution.

To assess the amount of water there is in the basin it is recommended to use the monthly-step Temez model (with 4 parameters against the 27 in SWAT).

7.10.2 MODSIM water resource management model

MODISM was implemented as a generic model of simulation of operations of a system, to support decisions to manage it. It is a simple model and after being implemented in the basin it is easy to use. Therefore it is recommended for the management of the water resources.

8. Norrström

8.1 Description of basin

In the TWINLATIN project only the closest area around the Lake Mälaren has been modelled, the contributing watersheds to Lake Mälaren have already been modelled in the TWINBAS project. Figure 8.1 shows the area that has been modelled and the meteorological stations that were used.

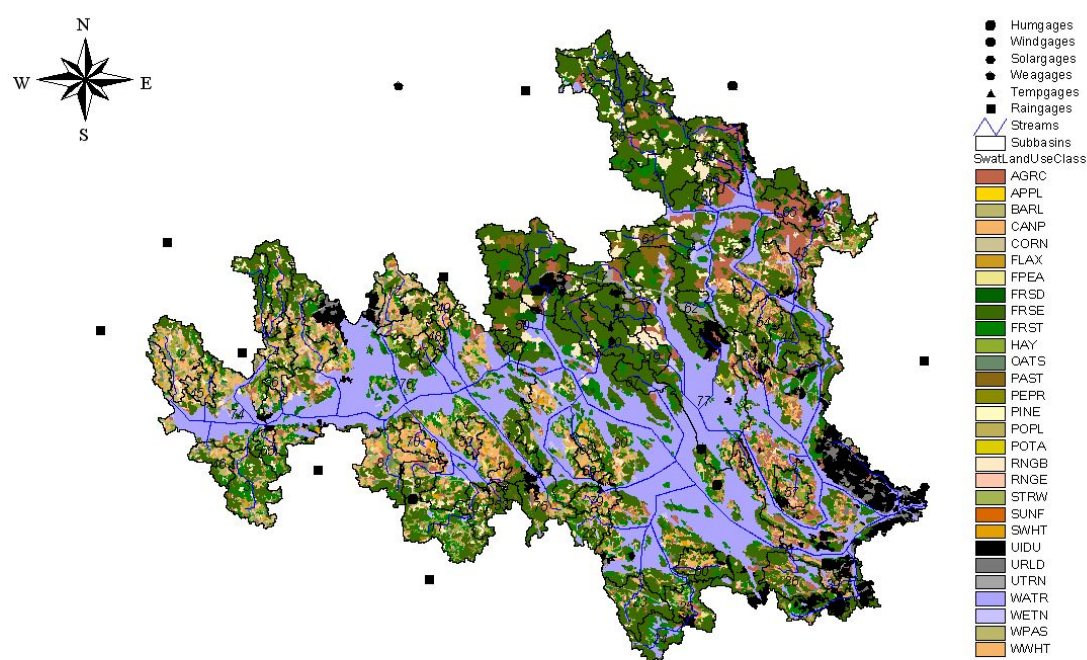


Figure 8.1 The Lake Mälaren and its surrounding land use

8.1.1 Natural Setting

The Norrström River Basin covers an area of 22.600 km², which corresponds to about 5% of the area of Sweden. The basin includes two of Sweden's largest lakes: Mälaren, which has an area of 1000 km², and Hjälmaren, which covers approximately 500 km². The number of people living in the area is approximately 1, 2 million. In the Norrström Basin, forests and mires dominate the landscape and cover about 70% of the surface area.

Norrström river basin is one of the most studied areas in Sweden, much because of its location in a densely populated area with its outlet to the Baltic Sea in Stockholm. The basin is commonly divided into 12 tributaries, all with outlets in Lake Mälaren. Administratively, the Norrström basin belongs to 31 municipalities, and is a part of six different counties. The closest area around Lake Mälaren covers 4900 km² and is dominated by forest.

8.1.2 Hydrology

Agricultural areas occupy an additional 20%, while lakes cover around 10 % of the Norrström basin (Wallin et al., 2000). The Mälaren and Hjälmaren lakes are connected through the Eskilstunaån River. The outlet of Lake Mälaren to the Baltic Sea is situated in the centre of Stockholm. Figure 8.2 shows the percentages of the different land uses of the modelled area close to Lake Mälaren. The Lake Mälaren has 10 major tributaries (Arbogaån, Kolbäcksån, Hedströmmen, Köpingsån, Svartån, Sagån, Örsundaån, Fyrisån, Råckstaån and Eskilstunaån), which together contribute approximately 80 % of the total inflow. Lake Mälaren consists of several bays and islands and has been divided into six well-defined basins. The westernmost basin, Galten, receives 46 % of the total inflow, while the other sub-basins receive between 11 and 24 %. During the last 30 years the water flow at Norrström has been 164 m³/s in average. The precipitation shows greater variation than the water flow, which shows regular variations. Average annual precipitation for period 1961 to 1990 was 618 mm in Västerås and 541 mm in Uppsala. The monitoring of Lake Mälaren started in the mid 1960's. During the late 1960's and early 1970's there were large improvements in chemical composition and biological status.

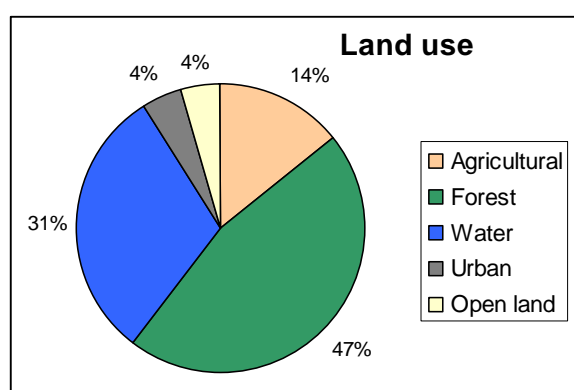


Figure 8.2 land use percentage of the modelled area

8.1.3 Water Resources

Mälaren provides drinking water to 1, 5 million people and is also the recipient of the wastewater from the surrounding cities and industries. Advanced sewage treatment and continuous monitoring of water quality is thus of utmost importance.

Lake Mälaren is both an important transport route for oil and chemical products and an appreciated recreational resource. Both lake itself and its tributaries have been stepwise dammed since 1943. For instance, 24 hydropower stations are situated on Svartån, Arbogaån, Kolbäcksån and Hedströmmen and many more dams and ponds control water flow in Norrström basin.

The major problem is nutrient transport, causing eutrophication both in smaller rivers and lakes as well as in Lake Mälaren and in the Baltic Sea. The contribution of agricultural land to the net load on Lake Mälaren is significant since large agricultural areas are located in the nearby area, with direct drainage to the lake and with very little retention. This has a large impact on the total nutrient transport to the lake. However few studies have been conducted on the importance of the area close to Lake Mälaren, so far most studies have been focused on the surrounding tributaries. The area near Lake Mälaren is 4900 km², i.e. about 20% of the total Norrström river basin, of which 2416 km² is open land and 1338 km² forest and wetlands. According to recent data, the total load from agriculture could be as high as 280 ton phosphorus and 3400 ton nitrogen from the whole basin. The measurements are however scarce and the real figures could be both higher and lower.

8.2 Norrström collection of source data

8.2.1 Data storage

The hydrological modelling in Norrström requires high storage capabilities for both tabular data and geographical data. Several data sets are needed to set up the SWAT 2005 model. The Norrström area is one of the most studied areas in Sweden, which means there is a lot of data of varying quality, collected for different purposes. In the TWINBAS project an ArcSDE database was created to allow easy data access for the group involved in modelling the different tributaries, this database were also used in TWINLATIN. ArcSDE enables multi-user read and write access to geodatabases. ArcSDE can support large geodatabases and any number of users. The ArcSDE database for the Norrström river basin is supported by an SQL server. In this database both geographical data (vector/raster) and tabular data can be stored. The emission data has been stored in a separate SQL server database. The emission data combined with the AVSWAT modelling results provide information for making calculations of source distributions.

8.2.2 Geographical input data

Generally, the geographical data is owned by and purchased from the Swedish Land Survey, however, for special thematic areas several other public authorities own parts of the data.

Watercourses and topographical pre-processing

The Swedish Meteorological and Hydrological Institute (SMHI) has created a connected watercourse layer. All watercourses are given a direction (Westman and Gyllander, 2005). This is a basic need to be able to perform hydrological modelling. The scale of this data is 1:250 000, and contains all rivers longer than 15 km. Water courses from 1:5000 digital map data is available in the database developed, but these water courses are not always connected, e.g. at locations where the stream runs in pipes. To connect them would be associated with a substantial amount of manual work, and therefore only the streams from map data at the scale of 1:250 000 were used. This was found adequate for the size of subcatchments that was defined in SWAT.

The Digital Elevation Model (DEM) of the Norrström river basin has a resolution of 50 x 50 metres. The elevation data has a maximum deviation of four metres from the actual state. This means that the data is not accurate enough to use without some pre-processing. The DEM was modified by imposing the watercourse onto the DEM (burning). The pre-processed DEM was then used for automatic delineation of the subbasins into smaller sub-catchments. The produced sub-catchment distribution was compared to an already existing division of Swedish watersheds provided by SMHI.

Land use, Crop Management and Soil Type

Since the land use data is very important for the AVSWAT modelling it deserves extra attention. For land use data, several different data layers have been acquired and added to the database. For the AVSWAT modelling it was decided to use the European Environmental Agencies database from the Corine programme. Corine is a land cover database consistent and comparable across Europe, using 44 classes to describe different land use types. This database was chosen because it contains detailed nomenclature and recent data (2000). Because the agricultural land is of specific importance the Corine Land Cover 2000 database was combined with crop distribution data IAKS (Integrerat Administrativt Kontroll System) from the Swedish Board of Agriculture. The IAKS crop data has high spatial resolution (crop and areal statistics per property submitted by the property owner) on and valuable attribute data because it is legally binding to maintain the most current information and the information is handed in by the farmers themselves in order to get governmental economical support. However, the IAKS data is limited to crop land uses only. The spatial fit was not exact when these various data sets with different resolutions were put together. Small gaps and overlaps existed. To clean the layers, a program in MatLab was built. This program sorted all of the agricultural land that was not included in the data from the Swedish Board of Agriculture and converted it to the class with

which it shared the longest border. Combining the data resulted in a new layer containing the information of both crops and other land uses in the Norrström river basin.

Data concerning crop description and management were collected from various sources such as Statistics Sweden (SCB), Swedish Board of Agriculture and various literature sources (Blombäck, 1998, Alavi 1999, Johnsson and Mårtensson, 2002). The nutrient content in crops was changed to Swedish conditions, where Statistics Sweden (www.scb.se) and the Swedish Board of Agriculture (www.sjv.se) were the main sources. Information on leaf area index and maximum root depth were gathered from earlier studies concerning the SOIL model (Blombäck, 1998, Alavi 1999).

The Swedish soil type survey has inventoried all of the Swedish soils. Soil type maps at 1:50 000 do however not exist for the entire country. In some areas, for example in a small part of the northern sub catchment in Norrström, only data in a scale of 1:1 million were available.

To further improve the data, soil samples taken on agricultural land by the Swedish Board of Agriculture were used. These samples are point data taken on agricultural land containing percentages of sand, clay, silt, etc. In the Norrström river basin there are 448 sample points according to this database which is about 2 samples per 100 km². This data was interpolated using an inverse distance weighted method. The percentage of sand, which is the soil particle with the weakest influence on soil properties, was adjusted to bring the total up to 100 %. The distribution was then used to classify the data into different texture classes according to the USDA classification system. The SWAT 2005 soil database for description of soil parameters was also adjusted to Swedish data and conditions.

Monitoring data

SMHI is the major owner of meteorological and hydrological data in Sweden. For acquisition of data there are special rules that apply to projects that have a research background and these rules serve to make required data for these projects less expensive. This made it possible to buy long time-series of data of up to 30 years with high resolution for Norrström, which was needed for the AVSWAT modelling (Table 8.1).

Table 8.1. Input data to the AVSWAT model and its resolution.

Classification	Type of data	Resolution
Meteorological	Precipitation	Daily
Meteorological	Min & max temperature	Daily
Meteorological	Air humidity	Daily
Meteorological	Wind speed & solar radiation	Daily
Stream flow	m ³ /s	Daily

There are several different monitoring programs in the Norrström river basin regarding water quality. The Swedish University of Agricultural Sciences (SLU) is data host for the national monitoring program initiated by the Swedish EPA. This data has high quality and accuracy and was therefore used in the modelling.

8.3. Development of the new Watshman modelling system

A new version of the Watshman modelling system (Zakrisson *et al.*, 2004), based on the ArcHydro database was developed at IVL. The ArcHydro framework is a standard database for water-resources management that is used in several advanced hydrological models such as SWAT (Arnold *et al.*, 1998). Watshman was developed for presentation and analysis of monitoring data and modelling results, as well as modelling of nitrogen and phosphorous losses. Source apportionment calculations from different leakage sources, such as diffuse leakage from different land-use classes as well as emissions from point sources, are also included. Except for presentation of modelling results from models such as SWAT (a model which has been integrated with ArcHydro in the newest ArcSWAT version) a simpler hydrological modelling module based on the SCS curve-number method and a degree-day snow routine, as well as a module for leakage calculations from diffuse and point sources is included in the modelling system. Retention in water bodies and streams can also be calculated to obtain the net load. The approach in developing the modelling modules of Watshman was to make a simple and transparent modelling based on readily available GIS-data, such as digital elevation models (DEMs), soil-type and land-use data. Land-use and soil-type data were combined into hydrological response units (HRUs), the smallest spatial unit in the modelling. HRUs are derived for each sub-watershed in the geoprocessing module during the model setup and run-off is computed for each HRU with the SCS curve-number method and a degree-day snow routine. With the aim of using the advantages of spatially distributed modelling in a GIS, Watshman was developed as an extension to ArcGIS and consists of six modules; Point Source Analysis, Geo-Processing, Hydro Modelling, Leakage Modelling, Scenario analysis and Presentation of data and results. The modelling is performed step-wise so that the result from the runoff calculation is used as input to the leakage modelling with model calibrations performed between each step. The Point Source Data Analysis (including monitoring data) and the presentation modules can be used independently of each other and the modelling modules.

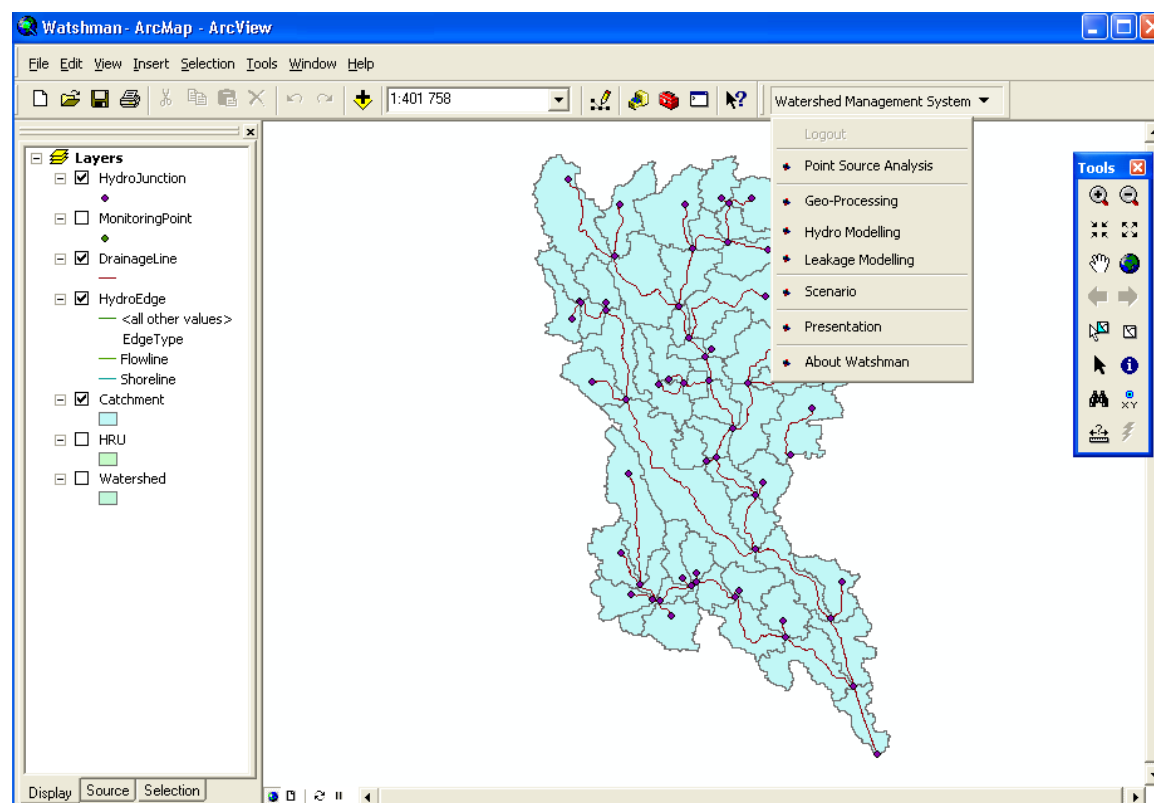


Figure 8.3 The user interface of the Watshman extension to ArcMap

8.3.1 Input data

All spatial and tabular data are stored in the ArcHydro database. The built-in hydrological modelling requires daily data of temperature and precipitation as input to the model and daily or monthly discharge data for calibration and model evaluation. Monthly or daily data of nitrogen and phosphorous leakage (if available) is used for model calibration and evaluation and this modelling is based on leakage coefficients. Data of emissions from nitrogen and phosphorous emissions from point sources can be included in the database. GIS-data needed for modelling and database setup include; a DEM, stream network, lakes, land use, soil type and locations of monitoring stations.

8.3.2 Database design

The Watshman database was based on the ArcHydro data model and was extended with objects needed in Watshman. The ArcHydro Data Model can be defined as a geographic database containing a GIS representation of a hydrological information system under a case-specific database design which is extensible, flexible, and adaptable to the user requirements. The ArcHydro data model takes advantage of the next generation of spatial data in Relational Database Management Systems. This concept has been developed by ESRI (www.esri.com) and is called GEO-database. Conceptually, it is a combination of GIS objects enhanced with the capabilities of a relational database to allow for relationships, topologies, and geometric networks. GIS-experts from all over the world have taken part in developing the ArcHydro framework into a standard for water resources management.

There are several advantages in developing Watshman based on the ArcHydro structure:

- Cheaper and faster to develop a database based on an existing structure
- Better transparency and quality control if the database is open and standardised
- Many calculation models like SWAT can easily connect to the ArcHydro database. The new ArcSWAT-model is fully integrated in ArcGIS.
- Communication of data within the GIS community is simplified by using a well known structure
- Further development of ArcHydro tools and structure in the future by researchers all over the world can benefit functionality in Watshman.

The Watshman database is implemented in the form of an ESRI personal GEO-database, which basically is a Microsoft Access database with the capability of storing spatial features. Using an Access database has several advantages. Access is an easy to use database, which is inexpensive and widely used. A personal GEO-database has however one important limitation. It is not built to handle more than 2 Gb of data (raster layers not included). If there is a need for more data storage Watshman can be migrated to an enterprise GEO-database (ArcSDE). In order to run Watshman and access spatial features in a GEO-database the users have to have an ArcGIS 9 installation on their client computers, since Watshman is implemented as an ArcMap extension. ArcGIS from ESRI is a family of products consisting of ArcView, ArcEdit and ArcInfo as the top version. In order to use the full functionality of Watshman at least ArcView with the extension Spatial Analyst is needed but ArcInfo is preferred.

8.3.3 Watshman system architecture

The system architecture is shown in Figure 8.4, including how results from SWAT can be imported into the database instead of using the simpler SCS-model included in Watshman. A GIS/Web-

application (ArcIMS /.NET) can also be included to make it possible to publish data and maps from the database on Internet.

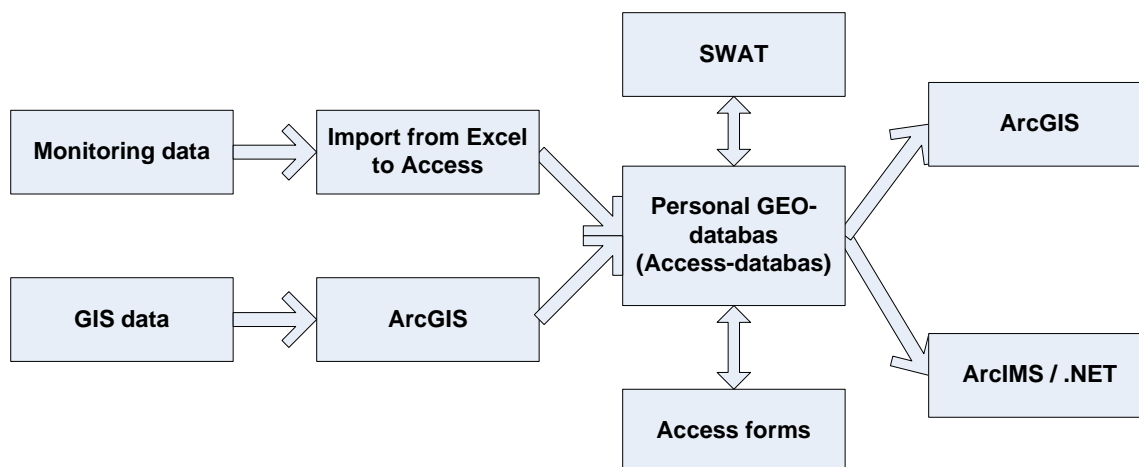


Figure 8.4 Watshman system architecture and data flow

Watshman is a module built system and not all modules are needed in order to get benefit out of the system.

8.3.4 Point Source Data Analysis

The interface of the Point Source Data Analysis module for point source and monitoring data analysis is presented in Figure 8.5 below, in which the data for different measured variables can be summarised, analysed and appended to the map for a spatial analysis of the data. The module is built with wizards guiding the user through the process of displaying and analysing data.

Figure 8.5 Interface of a step in the Point Source Data Analysis wizard

8.3.5 Geo-processing

In the geo-processing step the land use and soil type data are combined with the GIS-data of the watersheds to derive the HRUs (Figure 8.6) and the Watshman database is set up based on an existing ArcHydro database.

Figure 8.6 The first step of the Geo-processing wizard.

8.3.6 Hydrological modelling

The built in run-off model in Watshman is based on the SCS Curve Number (CN) method and a degree-day snow routine. The run-off is calculated on a daily basis, using daily data of temperature and precipitation. Land-use and soil-type data are used as input data and combined for each catchment into HRUs. In order to make the application easy to use, the Watshman interface is built with wizards guiding the user through the process of running and calibrating the model.

Figure 8.7 The interface of the hydrological modelling module.

8.3.6 Leakage modelling, scenario analysis and data presentation

The gross load modelling uses typical mean concentrations of leakage of nutrients from different land-uses, point source loads and the modelled monthly water flow as input to the calculations. It is also possible to insert monthly water flow from other models or measured flow into the database as input to the leakage modelling. The leakage calculations can be made more complex if detailed nutrient loading data for atmospheric deposition and agricultural areas are available. The output from this modelling is the gross load from each HRU and catchment (including load from point sources). The net load modelling uses the gross load modelling result as input together with information about retention in water bodies and streams based on water surface area and stream width. The results from each calculation can be analysed in time series plots or be appended to maps for spatial analysis. In the scenario analysis the effect of changes of e.g. land use can be analysed. In the data presentation, e.g. source apportionment calculations and other results can be appended to a map and displayed.

8. 4. Hydrological modelling in Norrström subbasins

The Norrström river basin is divided into 12 different tributaries (subbasins) of which Hedströmmen, Köpingsån, Sagån, Svartån, and Örsundaån have been hydrologically modelled within the TWINBAS project. The subbasin Lake Mälaren has been modelled within the TWINLATIN project. Considering the best available data regarding land use, water flow and nutrient measurements, the modelling period for the different subbasins in the Norrström basin was set to 1996-2001. This period was then divided into two periods, calibration year 1996 –1998, and validation year 1999 – 2001. The first six months of each period was used as a “warm up” period to avoid errors related to initial conditions. By running the model for six months the model is more likely to better represent the area than it would be from the start when it comes to initial parameters for variables like soil water content, infiltration rate and soil chemistry. The agrohydrological year (July to June) was used in order to encompass both main water flow episodes and important agricultural management operations.

The initial soil water content was assumed to be at field capacity, since model runs started on 1st of January when soil moisture is usually rather high. Model performance was measured by three statistical indicators: coefficient of determination (R^2), deviation of water flow volume (D_v), and Nash-Sutcliffe model efficiency (R_{eff}) (Equation 8.1).

$$D_v = \frac{\sum(Q_{obs} - Q_{sim})}{\sum Q_{obs}}$$

$$R_{eff} = 1 - \frac{\sum(Q_{obs} - Q_{sim})^2}{\sum(Q_{obs} - \overline{Q_{obs}})^2}$$

Where D_v is the deviation of water flow volume, R_{eff} is the Nash & Sutcliffe’s model efficiency, Q_{obs} is observed water flow (m^3sec^{-1}), and Q_{sim} is the simulated water flow (m^3sec^{-1}).

Equation 8.1. Nash & Sutcliffe model efficiency and deviation of water flow volume

8.4.1 Results of hydrological modelling in Norrström subbasins

Calibration results from Lake Mälaren

The subbasin of Lake Mälaren has been modelled for water flow. The subbasin of Lake Mälaren has three locations where daily measurements of water flow were available, which increased the accuracy in the calibration. Unfortunately these locations were not optimal from a calibration point of view since they were not evenly distributed in the subbasin. Figure 8.8 shows the location of the measurement station in the subbasin of Lake Mälaren. The station near Stockholm was not used due to difficulties in modelling the water flow from Lake Mälaren. The statistical values for Lake Mälaren are shown in Table. The calibration period was set to July 1996- June 1998 and climate data set including point sources was created for the period 1 January 1996 to 31 December 1998. The simulation period lasted three years but the first six months were used as a “warm-up” period to avoid initial errors related to initial conditions.

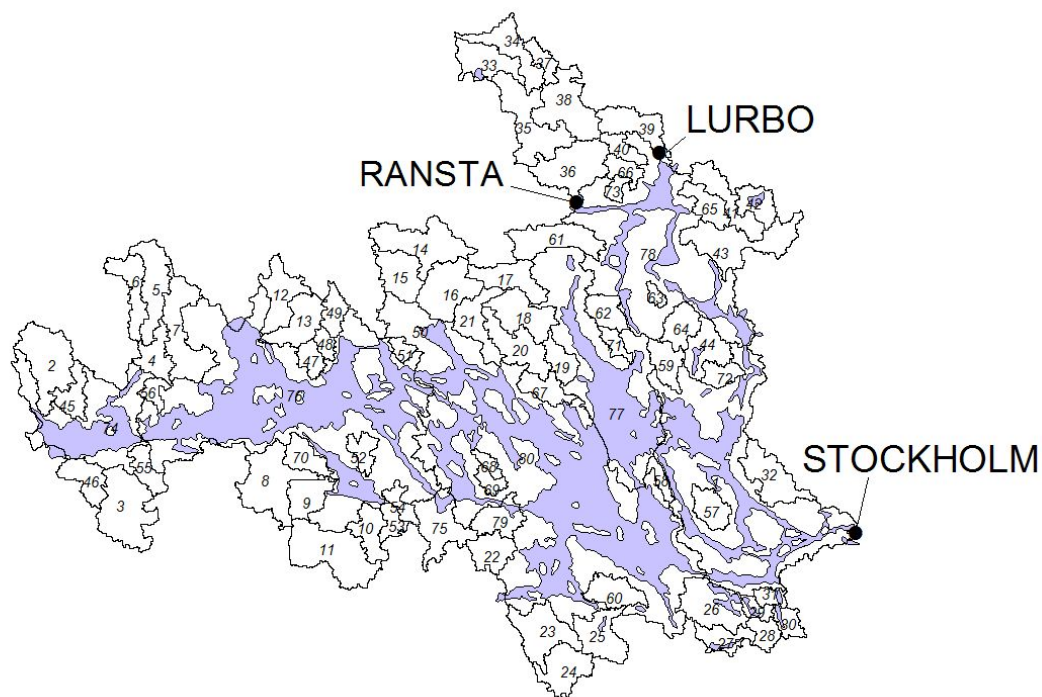


Figure 8.8 Measuring stations used in the modelling.

The Figure 8.9 shows the dynamics of the model for the measuring station Ransta for the whole period 1996-2001. The results show good adjustment to dynamics but some problems due to snow melting parameters.

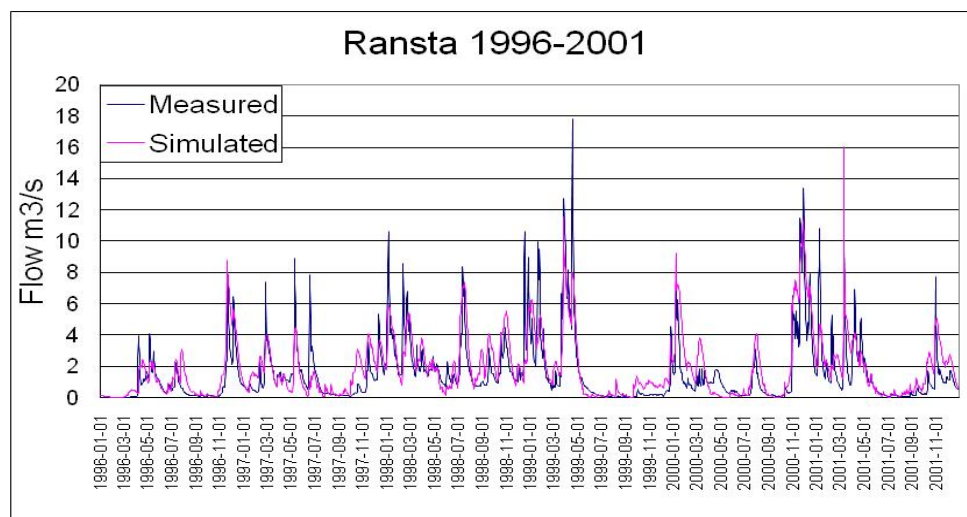


Figure 8.9 Measured and modelled water flow at Ransta measuring station 1996-2001

Table 8.2 Hydrological results for Lake Mälaren.

		Lake Mälaren	
Calibration		Ransta 1996-1998	Lurbo 1996-1998
	Coefficient of determination (R^2)	0,56	0,59
	Nash-Sutcliffe model efficiency (Reff)	0,49	0,54
	Deviation of water flow volume (D_v)	0,16	0,21
Validation		Ransta 1999-2001	Lurbo 1999-2001
	Coefficient of determination (R^2)	0,74	0,68
	Nash-Sutcliffe model efficiency (Reff)	0,6	0,65
	Deviation of water flow volume (D_v)	0,35	0,21

Validation

Validation of the SWAT model was done by applying exactly the same parameter values for different basins as those used for the calibration period. New climate data and point sources data set for the validation period 1 January 1999 to 31 December 2001 was applied. The simulation period lasted three years but the first six months were used as a “warm-up” period to avoid initial errors related to initial conditions. The statistical indicators in Table 8.2 were therefore calculated only for the agro-hydrological year 1 July 1999-30 June 2001.

A good correspondence between the measured and simulated water flow is necessary to model the water quality. If there is too large of differences between the model results and the measured results the pressure modelling will suffer in reliability, since much of the phosphorus leakage is influenced by intensive precipitation and water flow.

Although calibration is a time consuming task and sometimes very difficult depending on the accuracy of input data such as soil types and amount of calibration points, it is preferable to use “nested watershed” approach, which is associated with calibration at several stations whenever possible. The results are thereby improved and uncertainties reduced. In Lake Mälaren this was however not possible, this made the calibration more difficult.

8. 5 Results from flow proportional measurements conducted by IVL

To further improve the pressure modelling two flow proportional measurement stations have been set up in the surrounding area of Lake Mälaren. The geographical locations of the two stations are shown in Figure 8.10. Measurements were only being conducted during one year, between 2007 and 2008. This makes it hard to calibrate and validate the water flow for the stations, especially since the two stations are located on different places than the Stabby and Ransta which both are located in the

northeast. On the other hand the different geographical location constitutes a good test for the earlier water flow model settings. The results from the flow proportional measurements helps also to get a better understanding of the nutrient loading from the agricultural areas around Lake Mälaren.

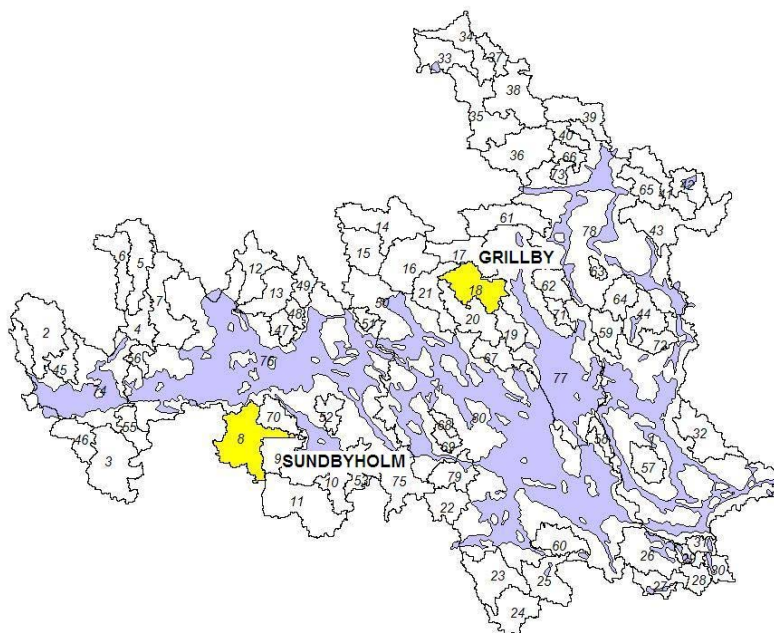


Figure 8.10 Lake Mälaren catchment as represented in the SWAT-model. Sub-basin division coincides with the Swedish national division system. The catchments where the flow-driven sampling stations are located are indicated with yellow.

The hydrological result for the Ransta subbasin for the period 2007-2008 was satisfying, and validates the result for the earlier model parameters for the calibration and validation period. The prerequisites for the flow proportional measurements are different, where both Ransta and Lurbo receives water flow from upwards located subbasins, Sundbyholm and Grillby are the sole subbasin for the water flow.

Even though the prerequisites for the two subbasins for flow proportional measurements, differs from the location for the flow measurements stations used during calibration and validation period, the hydrological results were satisfying for the Grillby and Sundbyholm station after some minor calibration. The result for the calibration year is shown in Table 8.3 below and Figure 8.11.

Table 8.3 Results for flow proportional measurements and Ransta

		Lake Mälaren		
Results	2007-2008	Grillby	Sundbyholm	Ransta
	Coefficient of determination (R^2)	0.61	0.59	0.66
	Nash-Sutcliffe model efficiency (R_{eff})	0.48	0.55	0.60
	Deviation of water volume (D_v)	-0.17	0.01	-0.20

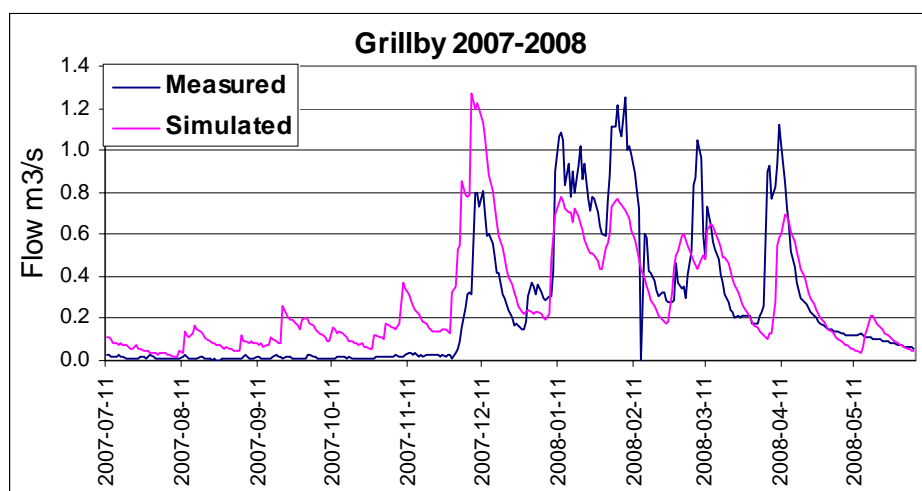


Figure 8.11 Hydrological results for Grillby

Limitations

Modelling should give feedback to existing monitoring programs, data collection and database development.

1. Predefined delineation

In areas where watershed delineation into sub-catchments already exists it would be preferable to use predefined watershed delineation. This is now available in a later version of the SWAT model, this version was however not available when the project started.

2. Application of SCS CN method in Sweden

In Sweden the use of SCS Curve Number (CN) method for runoff calibration is limited and national or regional databases relating a Curve Number to local land use and/or soil types are not always available. Surface runoff seldom occurs in Sweden's flat landscape (Grip & Rodhe, 1991). In Sweden, surface runoff is more often the cause of saturated soils or freezing processes that lowers the soil conductivity, than a result of intense precipitation. Hence the recommended CN value is something that must be revised when calibrating the model, since they often result in too high simulated values for surface runoff.

3. Soil maps

Existing soil maps are of rather low resolution. Additionally, data and soil types from Swedish Geological Investigation are rather poorly described regarding texture and soil physical properties. Combination of this data with data from Eriksson et al. (1997) and Wiklert et al. (1983) study is an improvement but further efforts and mapping of Swedish soils are needed to facilitate model applications at the watershed scale.

4. Lake Modelling

The SWAT model build to model watersheds and nutrients and not to model lakes as first priority, therefore the lake modelling within SWAT is not its biggest strength. When modelling areas with a large proportion of lakes it can therefore be hard to calibrate the water flow from the lakes.

5. Tile drainage

Data regarding distribution of tile-drained fields in a GIS format is not available. One third of Swedish arable land is assumed to be drained, but the drainage that the farmers usually have is not digitised and information is lacking on higher scales such as municipality or regional levels.

6. Physical characteristics of water bodies.

Data concerning physical characteristics of streams and lakes is scarce. This made it very hard to model the area of interest since the Lake Mälaren constitutes such a big fraction of the total area. The knowledge of the fluctuations of water level in Lake Mälaren is also scarce.

7. Water flow monitoring

As concluded above, more than one point where water flow is being measured considerably improves the accuracy of the results. The use of “nested watershed” gives better model results and a lower amount of uncertainties. In the modelled area this was not possible and due to the geographical locations of water flow measurements.

8.5.1 Discussion of hydrological modelling results

The hydrological results were satisfying; the major difference between the calibration and validation period was that the validation had a higher correspondence. This is explained by the difference in precipitation between the two periods. The validation period therefore has higher statistical results, which shows that the model is not incorrectly calculated. In all subbasins there are some peaks that are missed. This may be attributed to many reasons such as a low resolution of precipitation, lacking information of drainage, scarce measurements, and information concerning the soils hydraulic conductivity. In the beginning of each period there was a low response that can be explained by the lack of knowledge of the initial soil and climate parameters of each model run. This also motivates the use of the agro-hydrological year and thereby letting the model run for six months before comparing the results.

An important precondition for pressure modelling is satisfactory modelling results of water flow and dynamics. Considering the coarse resolution of some input data layers, specifically soil profile data, and the low amount of monitoring stations for water flow, the achieved results regarding water flow were of sufficient quality to proceed with the nutrient modelling. The conclusions that can be drawn from this work package regarding the hydrological modelling are that it is possible with available data to get a good overview of the situation and produce reliable data.

9. South America continental modelling

9.1 Description of basin

South America has a total land area of 17.8 million km². The continent extends across some 67 degrees latitude from tropical, sub-tropical and temperate climates. It is characterised by diverse landscapes and habitats of the Amazonian rainforest, the Pantanal wetland and the Andean mountain chain that runs almost the entire length of the continent. The Andes are important in regulating the eastward movement of moisture onto the continent from the Pacific giving rise to the arid Patagonian steppe, as well as the presence of glaciers and icefields. The water balance of this continent is of special importance to the global hydrology as well as to the 346 million inhabitants (FAOSTAT) and reported to account for 28% of the total world freshwater resource (FAO, 2003).

Development of water resources is variable throughout the continent. Argentina and Brazil have reasonably well-developed water resources infrastructure with reservoirs for water supply and hydropower generation. The most notable scheme is the Itaipu Hydropower plant on the border of Paraguay and Brazil which, in 2007, provided an estimated 91% of total energy needs of Paraguay and 19% of the Brazilian electricity demand (source: Itaipu Binational <http://www.itaipu.gov.br>).

Each of the TWINLATIN study basins varies dramatically in terms of climate, geography, hydrological response and the issues faced by the inhabitants e.g. flooding, water quality, sustainable water resources, soil erosion and development to name but a few. Basin-scale modelling ambitions focus on specific localised issues. However, it is hoped that, from a water quantity perspective, a continental approach will provide a wider regional context for some of the problems faced, in particular droughts and water resources. It will also provide an opportunity for climate change impacts to be examined and compared at the continental, regional and basin scales.

9.2 Choice of model

The choice of the model should be determined by the questions to be answered, but it must also consider the availability of data and, perhaps, who are going to be the users of the results. Macro-scale hydrological models are typically simple conceptual models but applied in a semi-distributed manner such that the land surface is discretised into regular grid cells. Modelling hydrology on a continental scale requires a somewhat different approach to that of basin or sub-basin modelling and has the following implications:

- Small catchment-scale problems may not be resolved within the model resolution;
- Main data inputs, such as soil texture, which are often produced nationally should be standardised across the region of interest;
- Ground truth data for validating remote sensing data should be standardised across the region e.g. land cover;
- Driving climate data requires a great deal of quality control and interpolation;
- Care should be taken to ensure the observed streamflow data used to calibrate the model should cover all hydrological regimes in time and space and, yet, the stations selected are located on the main river in line with the gridded river network.

Although the data demands to set up such model are apparently very large, there are a number of publicly available global datasets which can be used. There is, however, a trade-off between the model cell resolution and amount of data processing and the errors that may be introduced when it is necessary to upscale or downscale particular information. In terms of understanding water resources issues, monthly timescales are sufficient and this means that sub-monthly processes need not be explicitly modelled.

The aim of applying a global-scale model in TWINLATIN is to provide a broader regional picture of hydrology and spatial extents of water scarcity. The Global Water AVailability Assessment (GWAVA) model (Meigh *et al.*, 1998; Meigh *et al.*, 1999) enables water use to be superimposed on top of the water supply (runoff), thus enabling water scarcity and/or abundance to be examined.

The GWAVA model comprises two main components: the rainfall-runoff model and the demand estimation model. The model is calibrated over a baseline period and then used to examine impacts of change either in climate or in water demand. Through a series of water stress and river flow indicators calculated cell by cell it should be possible to identify regions that are experiencing or are predicted to experience water stress.

The core rainfall-runoff model in GWAVA, the PDM (Moore, 1985), operates on a daily timestep. However the demand calculations and model outputs are performed on a monthly basis which is more than sufficient to understand the seasonal variation of water supply and demands across the region.

The model is, of course, limited in the approximations made by discretising the land surface into 0.5 degree cells and this will impact most greatly on the small catchments (those occurring on the western Andes). The continent-wide approach does, however, mean a consistent methodology can be applied across four of the subject basins in the TWINLATIN project (Baker, Catamayo-Chira, Cauca and Quarái/Cuareim) as well as the regions in between. Particular advantages will be apparent when examining changes in climate through the application of Global Circulation Model (GCM) outputs as well as examining demographic changes which also impact at the national level.

9.3 Data requirements

GWAVA requires wide ranging inputs of data both to drive the rainfall-runoff model and in order to estimate the anthropogenic water demands at the scale of the grid cell. The data are largely derived from existing global datasets and a number of methodologies have been developed to incorporate these. The data and sources are summarised in Table 9.1 and a more detailed explanation of their use follows. The data sources are divided into two classes: those needed to inform the hydrological model and those to derive monthly water demands per cell.

9.3.1 Physical parameters

The gridded river network is defined by the direction in which flow may leave a cell which may be in one of eight directions or denoted as zero for no net direction. There are a number of methods for defining the gridded river network with much documentation devoted to deriving an upscaled river network from fine scale digital elevation data such as Hydro1K (USGS). There is considerable work required in deriving upscaled river networks, and it was opted to use the existing DDM30 network derived by Doll & Lehner (2002). A stream order is then assigned to each cell. In Figure 8.1, higher stream orders are denoted by light blue/white small stream orders by dark blue. The area of each cell was computed using the latitude and longitude coordinates of the cell and assuming the Earth's radius of 6371 km.

Soil textures are derived from the Digital Soil Map of the World (FAO, 1995) in which the soil legend is resampled to seven main soil texture types: sand, sandy loam, silt loam, clay loam, clay, lithosol and organic, with the dominant texture assigned per 0.5 degree cell.

The Global Land Cover Characteristics (GLCC) dataset is derived from remote sensing at 1km resolution and sampled using the IGBP classification (Belward, 1996). The data which provide a fraction of cover per pixel are extracted for South America, reclassified from 17 to six land cover types, and resampled from 0.042 degrees to 0.5 degrees. The raw Advanced Very High Resolution Radiometer (AVHRR) data used in this product span the 12-month period from April 1992 to March 1993, which is very close to the end of the proposed 'baseline' period 1961 to 1990 for which the model will be run. It should be noted that the algorithm for obtaining the data moves to the lower left hand coordinates of the cell but samples at 55 x 55 pixels in the cell, so that in the southernmost reaches of the continents there may be some errors in the sampling may occur.

Table 9.1 Summary of data requirements and sources for GWAVA

Parameter	Source name	Resolution	Source reference
Physical parameters for runoff estimation			
Monthly precipitation, temperature gridded data 1901 – 1994	Climate Research Unit (CRU) TS2.1	0.5 degrees monthly	Mitchell & Jones, (2005)
Soil Texture	Digital Soil Map of the World and Derived Soil Properties		FAO (1995)
Land Cover	Global Land Cover Characteristics (GLCC) Database	0.042 degrees	USGS (2005)
Routing network	Based on DDM30	0.5 degrees	Döll & Lehner (2002)
Elevation	Hydro1k DEM	1km	USGS (2000)
Glacier location, percentage ice	Digital Chart of the World	coverage	ESRI (1993)
Lakes, wetlands and reservoir	Global, Lakes and Wetlands Database (GLWD)	Coverage	Lehner & Döll (2004)
Demands			
Human populations	Gridded Population of the World	2.5 arc minutes	CIESIN <i>et al.</i> (2000)
Urban fraction	Global Rural-Urban Mapping Project (GRUMP)	5 minutes	CIESIN <i>et al.</i> (2004)
Livestock populations	Gridded Livestock of the World	5 minutes	FAO (2007)
Irrigation - cropping locations, areas, calendars & crop types	FAOSTAT Global Map of Irrigation Areas - version 4.0.1	national	Siebert <i>et al.</i> (2007)
Data to validate water withdrawals	FAO-AQUASTAT	5 minutes	
	FAO-AQUASTAT	national	
Data for scenarios			
Climate change data from GCMs/RCMs	Various GCM/RCM outputs available from IPCC-DDC.org	Various	
Population	World Population prospects	national	

The four land cover classes of tree, grass (which includes croplands), shrub, and bare soil distributions look reasonable (Figure 9.2). However, some discrepancies were observed when comparing the ice and wetland extents to other data sources. The GLCC dataset were found to be missing the glaciers in Chile in comparison to the Digital Chart of the World so additional glacier locations were incorporated from the latter dataset.

A comparison of the distribution of wetlands (see Figure 9.3) derived from GLCC the Global Lakes and Wetlands Database (GLWD) (Lehner & Döll, 2004) seemed to show differences with, for example, quite high fractions of wetland (up to 0.5) in the headwaters of the Parana river system and yet low fractions in the Pantanal itself. It was, therefore, decided to use the wetland locations from the GWLD dataset rather than the GLCC dataset, with some redistribution of the four vegetation classes required to maintain unity in each cell. The water fraction obtained from the GLCC dataset does however, correspond very well with the location of reservoirs in the GLWD and thus the fraction is unchanged. The physical characteristics of the reservoirs i.e. surface area and capacity, are taken from the GLWD. Where reservoirs extend across more than one cell the reservoir parameters are input at the outlet cell only.

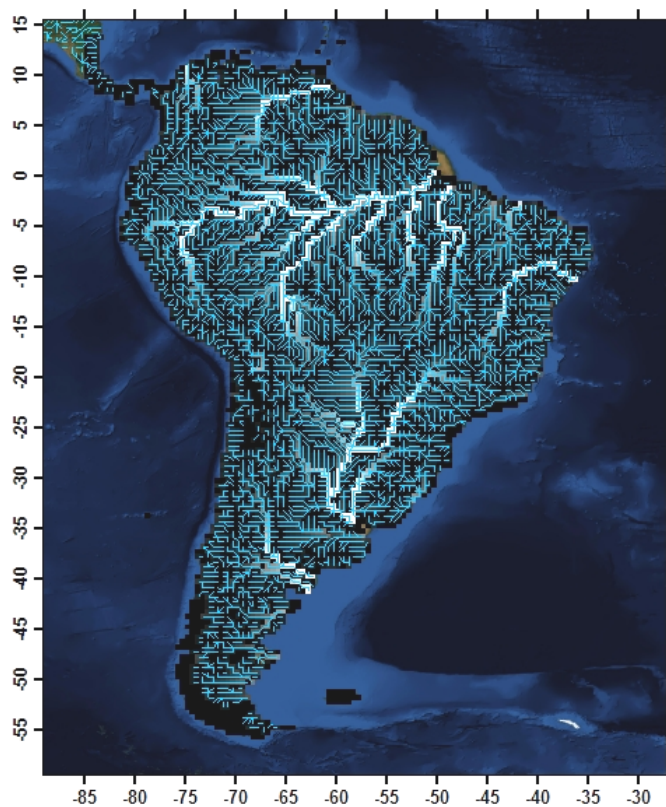


Figure 9.1 Illustration of the gridded river (thin line) and accumulated flow (thick line) networks

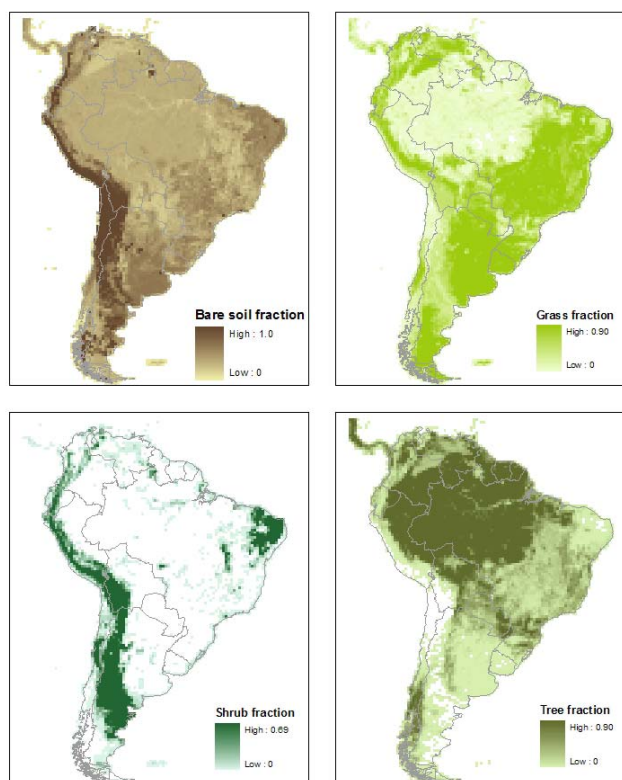


Figure 9.2 Derived landcover for four indicative vegetation classes

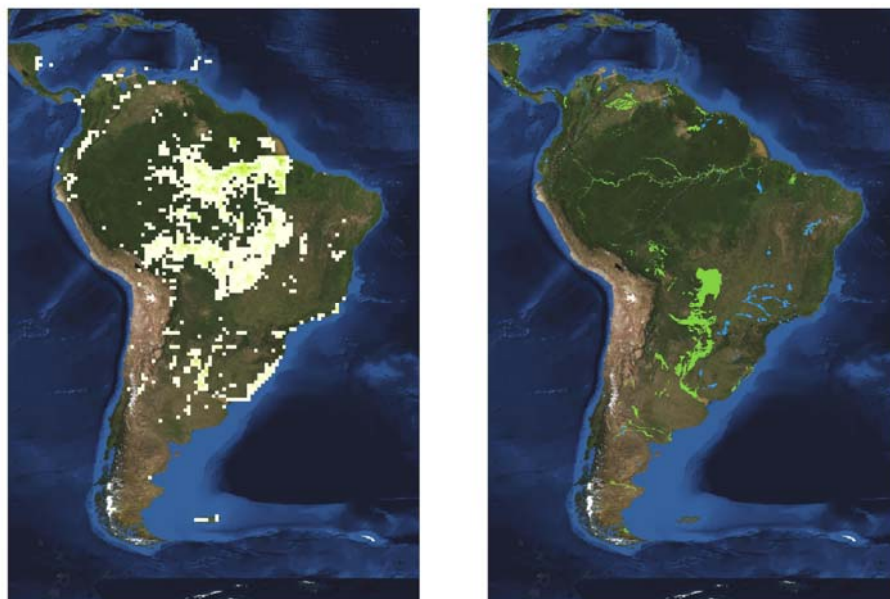


Figure 9.3 Comparison of wetland coverage for two datasets: left, GLCC/IGBP classification and right, GLWD (Lehner & Doll, 2004) denoted by green areas

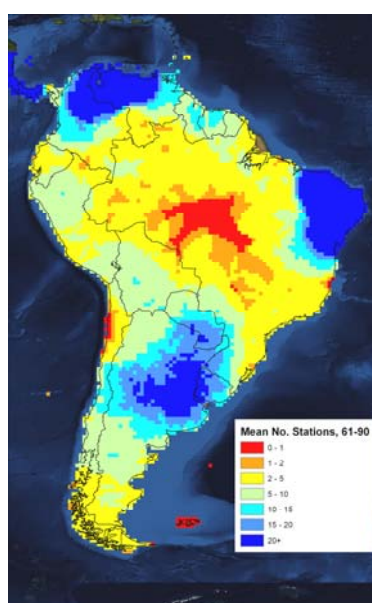


Figure 9.4 Mean number of climate stations used in the derivation of the CRU dataset for the period 1961 - 1990.

9.3.2 Climate data

The Climatic Research Unit (CRU) TS2.1 dataset are used as input driving data for GWAVA. Gridded climatic inputs of monthly precipitation, raindays, temperature, vapour pressure and cloud cover were obtained along with monthly windspeed mean (as a 1961-1990 average). Short reference crop evapotranspiration is computed using the America Society of Civil Engineers (ASCE) Standardised Reference Evapotranspiration Equation (ASCE, 2005). Net radiation is computed assuming a constant albedo of 0.23.

Mean monthly raindays are also provided in this dataset and are used in disaggregating monthly precipitation to daily. Data are input as baseline means and a time series of anomalies. Figure 9.4 shows the distribution of rainfall gauges used to derive the gridded rainfall inputs for South America over the baseline period 1961 to 1990 highlighting, in particular, the lack of information available in the Amazon region and generally low levels of climate data used in deriving the model inputs.

9.3.3 Demands data: domestic water supply

Domestic water demands cover water use for washing, cleaning and cooking plus small scale industrial use. Data on actual domestic water supply are not readily available so one element of the demand module is to estimate the annual water withdrawal based upon the urban and rural population per cell an urban/rural water consumption rates and assumptions about return flows and percentage network losses.

To estimate the total and urban populations for each cell a number of datasets are required. Spatial datasets such as the Gridded Population of the World (CIESIN *et al.*, 2005) provide total populations on a fine scale, while the urban extents dataset (CIESIN *et al.*, 2004) indicates cell that have been identified as urban based on remote sensing of night-time light distribution as well as population density estimates. Urban populations are allocated to pixels which are identified as urban whilst the remaining population is allocated to the rural cells maintaining the total population distribution. Figures are also scaled to 1990 figures using national figures (FAOSTAT). Finally the total and urban data are aggregated to the model resolution of 0.5 degrees.

9.3.4 Demands data: agricultural water supply

Water demand for crop irrigation makes agriculture the largest consumer of water of all major sectors both by country and continent as shown in Figure 9.5. Irrigation water demand is also strongly seasonal and can vary considerably from year to year.

Actual water demand is dependent on the type of crop grown, cropping area, location and local climate. Water demand for irrigation is estimated in GWAVA using the FAO crop water requirement calculations (Doorenbos & Pruitt, 1977) and is based on established crop coefficients. The required model inputs in addition to temperature and precipitation are crop type, cropping area and planting month. Up to eight crops or multiple cropping patterns can be specified per cell. Information on major crops, cropping calendars and planting areas are available on a national basis from the FAO AQUASTAT (see, for example, Table 9.2). More difficult to obtain are detailed information on the location of schemes, types of crops, number of seasons and planting dates. Some indication of when a scheme was implemented is also important if this happened during the modelling period.

Overall, rice and sugarcane are the most widely grown crop by area accounting for 50% of the total land area equipped for irrigation across South America followed by fruits, vegetables and maize (Figure 9.6).

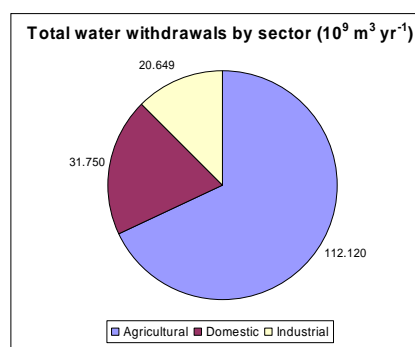


Figure 9.5 Summary of water withdrawals by sector for South America

Table 9.2 An example of a cropping calendar for Argentina showing crop area as percentage of the total area equipped for irrigation by month (Source: FAO AQUASTAT)

Argentina	Irrigated area (1000 ha)	J	F	M	A	M	J	J	A	S	O	N	D
Rice	97	6	6	6								6	6
Maize	171	11	11	11								11	11
Potatoes	163	11	11	11								11	11
Sugarcane	240	15	15	15	15	15	15	15	15	15	15	15	15
Vegetables	262	17	17	17								17	17
Citrus	25	2	2	2	2	2	2	2	2	2	2	2	2
Fruits	471	30	30	30	30	30	30	30	30	30	30	30	30
Cotton	121	8	8	8	8						8	8	8
All irrigated crops	1550	100	100	100	55	47	47	47	47	47	55	100	100

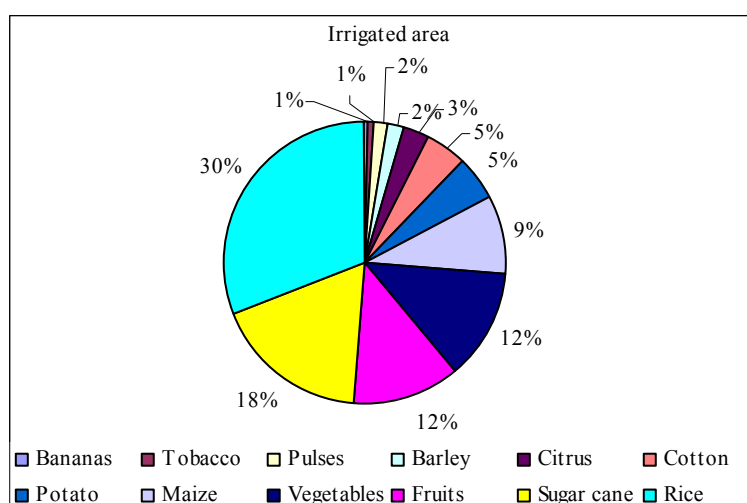


Figure 9.6 Percentage of crop type by area that are irrigated across South America (source: FAO-AQUASTAT)

The Center for Sustainability and the Global Environment (SAGE) Major Crops dataset (Leff *et al.*, 2004) characterises the distribution of major crops across the globe. The dataset indicates the probability of locating one of 18 major crop types in a particular location. It does not, however, whether the crops are irrigated and so this dataset is used in conjunction with the Global Map of Irrigation areas version 4.0.1 (Siebert *et al.*, 2007). Factoring of areas is carried out to match FAO figures at a national level.

Other agricultural demands are linked to water requirements for livestock watering and are estimated for cattle, sheep and goat production. Fine resolution data are available from the Gridded Livestock of the World dataset (FAO, 2007) for cattle, pigs, sheep, goat and poultry based on national census data. These data were obtained for cattle, sheep and goats and provide the number of animal per 5 minute pixel, subsequently aggregated to provide animal populations per 0.5 degree grid cell.

9.3.5 Demands data: industrial water supply

Water demands for industrial use refer to large-scale industrial water users which are not included in the rural or urban water supply and include water for cooling, mixing and diluting, and as a raw material for industries as diverse as mining, chemical processing, processing of raw materials and food, and the production of energy. There are insufficient data available to make a detailed analysis of

water use by industry even at the national level. The industrial water demand in GWAVA is simply specified, where known, as an annual average volume per cell.

9.3.6 Other data requirements

Data for calibration is discussed in the section on calibration (section 9.5). Data requirements to carry out scenario modelling are discussed briefly in section 9.4 and in greater detail in the WB8 report.

9.4 Scenario modelling

As with all hydrological models, one important objective of applying a model is to use the model to then try and understand how the catchment will behave under different conditions. The GWAVA model was developed to enable various type of scenarios and, in particular, climate change scenarios to be examined.

The latest set of Global Circulation Model (GCM) experiments run for the recent Fourth Assessment Report on Climate Change (IPCC, 2007) are available via the IPCC data distribution website (www.IPCC-DDC.org). However, limitations remain in the way the data can be used. In line with understanding changes in the seasonal deficits of water, the impact study will focus on examining the effects of changes in the mean monthly precipitation, temperature and potential evaporation derived from GCMs centred on 2020, 2050 and 2080. In the GWAVA scheme, these changes can be provided as inputs to GWAVA so that climate change scenarios can be examined easily. As well as running climate change scenarios two demand scenarios of increasing demand for domestic water supply will be developed and examined.

9.5 Model development

The model extent was selected to incorporate the whole of mainland South America. With a grid cell resolution of 0.5 degrees, this covers 85W to 32W and 14N to 57S. The river network is taken from DDM30 (Lehner & Döll, 2004) with some manual adjustments made e.g. in the Baker basin. There are some discrepancies between the land cover mask derived from GLCC, the CRU land-sea mask and the river network mask which affect certain coastal cells. In these cases the cell was either removed from the model, where there is no land cover or few adjacent cells containing climate data or, where there is land cover, the climate data were interpolated from adjacent cells. The final model mask contains 6524 cells.

9.5.1 Runoff generation

The probability distributed moisture (PDM; Moore, 1985) rainfall-runoff model was developed as a catchment model and represents the catchment (or cell) as a distribution of soil stores. The PDM parameters defining the soil moisture stores are linked to soil texture and land cover according to relationships with saturation and field capacities based on work by Vorosmarty *et al.* (1989) and Saxton *et al.* (1986). The parameters used are shown in Table 8.3. Surface runoff is routed through a linear reservoir and the baseflow through a non-linear reservoir. The routing parameters for each (srout and grout) require calibration. Fast surface runoff and slower baseflow are summed together at the cell outlet.

Other sub-models include an empirical interception loss model (Calder, 1990) applied to tree and shrub classes, and a snowmelt model (Bell & Moore, 1999) which provides a degree-day temperature based method for estimating snowmelt.

Upstream cells are identified from the drainage network and the flows are routed and summed to give an accumulated flow. Finally, the demands are computed for the current cell and net monthly abstractions are deducted.

Table 9.3 Parameter values used to define soil moisture stores

Soil texture class	Root depth (m)				Field capacity (mm)				Saturation capacity (mm)			
	forest	shrub	grass	bare soil	forest	shrub	grass	bare soil	forest	shrub	grass	bare soil
Sand	2.5	2.0	1.0	0.5	369	296	148	74	886	709	354	177
Sandy loam	2.0	1.6	1.0	0.5	420	336	210	105	825	660	412	206
Silt loam	2.0	1.7	1.3	0.5	590	501	383	147	935	795	608	234
Clay loam	1.6	1.4	1.0	0.5	533	466	333	167	806	705	504	252
Clay	1.2	1.0	0.7	0.5	580	484	339	242	653	544	381	272
Lithosol	0.1	0.1	0.1	0.1	27	27	27	27	50	50	50	50
Organic	-	-	-	-	50	50	50	50	100	100	100	100

Lakes, reservoirs and wetlands are taken into account in broadly similar ways with each being treated as a tank with storage, S and outflows (Q_{out}) a function of storage:

$$S = S + P - PE - Q_{out} + Q_{in}$$

Where: S is storage, P is precipitation, PE is potential evapotranspiration, Q_{out} are outflows and Q_{in}

Evaporation losses are assumed to occur at the potential rate for lakes and 1.4 times the potential rate for wetlands. Contributions to direct runoff generation are reduced by the proportion of cell that is a lake, wetland or reservoir. Where a lake occupies more than one cell then the lake water balance and outflows are computed at the outlet cell.

9.5.2 Water demand estimation

For application to South America, domestic water demands, where annual volumetric demands are not available at the cell scale, are calculated from the population in a cell and an estimated per capita water use according to rural or urban consumption rates. Meigh *et al.* (1998) reviewed estimates of water use across Eastern and Southern Africa and selected the ideal water consumption rates of 25l/h/d for rural areas and 60 l/h/d in urban areas. Network losses are assumed to amount to 40 % in urban areas and 20% in rural areas.

Irrigation demands are strongly seasonal and vary year to year whereas water demands for livestock watering are assumed to be constant throughout the year. Irrigation demands and other agricultural demands are therefore treated separately in GWAVA.

Water demand for irrigation are estimated following the FAO guidelines for estimating crop water requirements (Doorenbos & Pruitt, 1977). Crop coefficients enable crop water requirements to vary throughout the growing season and are defined for different crop types. As species adapt to a particular climate, soil or growing season, so multiple crop coefficients may be reported for a single crop type. However, there is insufficient spatial information to be able to allocate a particular crop type (and hence crop coefficient) to a given cell. New crop coefficients added to the model reflect crops grown in South America and are shown in Table 9.4. A value is provided for each month with month 1 being the month the crop is planted. Irrigation efficiencies are assumed to be 50%.

A constant monthly profile of livestock water demands is assumed and computed from the number of animals per cell multiplied by the per head water consumption per day. The per head consumption of water is assumed to be 37.5 l/h/day for cattle and 20 l/h/d for sheep and goats based on estimates by Meigh *et al.* (1998).

Table 9.4 Cropping coefficients for six major irrigated crops grown in South America

Crop	Month											
	1	2	3	4	5	6	7	8	9	10	11	12
Cotton	0.35	0.35	0.6	0.6	0.6	0.9	0.0	0.0	0.0	0.0	0.0	0.0
Maize	0.3	1.2	0.5	0.0	0.0	0.0	0.0	0.0	0.0	0.0	0.0	0.0
Potatoes	0.8	0.8	1.05	0.7	0.0	0.0	0.0	0.0	0.0	0.0	0.0	0.0
Rice	1.1	1.1	1.05	1.05	1.05	1.05	0.95	0.0	0.0	0.0	0.0	0.0
Sugarcane	0.48	0.78	0.93	1.05	1.15	1.15	1.15	1.15	1.15	1.15	0.88	0.65
Vegetables	0.55	0.55	0.96	0.84	0.79	0.0	0.0	0.0	0.0	0.0	0.0	0.0

It is assumed in this model configuration that all water demands are met by surface water supply alone. However, in reality there are significant regions in Southern Brazil and Argentina whose supply is supplemented by the abstraction of groundwater pumped from the large regional Guarani aquifer.

9.6 Calibration and validation

The rainfall-runoff model parameters that define the soil moisture storages are linked to soil texture and land cover, yet a degree of model calibration is still required. The key parameters requiring calibration are a soil store multiplier ν_{fact} , the pareto shape parameter which determines the distribution of soil moisture stores in a cell, b , and surface runoff and sub-surface routing parameters, s_{rout} and g_{rout} . The model setup is such that each cell is a rainfall-runoff model and could have its own set of parameters potentially leading to complex and unidentifiable model structure. Instead these four parameters are calibrated across all cells in a sub-basin.

The calibration process is carried out along the line of typical calibration procedure for any rainfall-runoff model, whereby gauged flow records are selected which meet criteria of length and reliability as well as those imposed by the geometric constraints. Observed monthly flow data for South America have been collated under a number projects with the main sources being the Global Runoff Data Centre (GRDC) and the Centre for Sustainability and the Global Environment (SAGE) River Discharge Database (RivDis2.0), a Regional Electronic Hydrometeorological Data Network for South America, Central America, and the Caribbean (R-Hydronet) collated by Vorosmarty *et al.* (1998) and the Atmospheric Research (NCAR) Monthly Discharge Data for World Rivers (except former Soviet Union) (dss552.1).

Basins for calibration are selected according to the following criteria:

- Gauge must be on a main river not a tributary;
- Basin area $> 10,000 \text{ km}^2$ (to reduce errors in approximating to a grid);
- Record length of at least 30 years, ideally to encompass the baseline period 1961–1990;
- Spatial coverage

The main sources of data were the RivDis2.0 and R-Hydronet datasets supplemented by data from dss552.1. There were few gauges that spanned the entire baseline period, although many have sufficiently long records. Ultimately, to have a reasonable coverage of calibrated basins, it was necessary that these criteria were relaxed to include gauges with as little as 10 years of data. Initially some 126 gauges were identified; however further problems were encountered. The main issues related to defining the sub-basins are:

- Missing gauge basin areas or discrepancies between published gauge basin areas of different sources;
- Errors in the gridded river network leading to errors in sub-basin area estimates (a particular problem in the Amazonian headwaters);
- Gauges actually being located on tributaries;
- Inherent errors arising from the geometry of the problem.

The first point is resolved in most cases by comparing with GRDC metadata. The second point could be solved, either by correcting the gridded river network, or by selecting gauges that are far enough downstream that the error in the gridded basin area is minimised and the directions of flow from individual cells are not a significant factor. The third point requires a visual check of each gauging station and can be identified by comparing basin areas. Finally, errors may be reduced by selecting large enough sub-basins. The selected gauge locations and basins are shown in Figure 9.7 and listed in Table 9.5.

Overall 43 basins have been calibrated accounting for roughly 75% of the land surface. There are, however, notable omissions in the coverage which include coastal zones which were below the basin area threshold, and northern parts of Argentina and parts of Chile for which there is an absence of gauge records to choose from.

Calibration of monthly flows was performed using simple optimisation procedure based on the Simplex method (Nelder & Mead, 1965) and minimising the standard error computed over the monthly time series. This did not work particularly well with the optimisation procedure failing to find solution for many catchments, and for many other basins the low flow portions of the hydrographs were not captured. To make it easier for the optimisation procedure to find a solution, the model was calibrated against the mean monthly flows which lead to all catchments being optimised, although this is at the expense of very good calibrations for some catchments. A further improvement was to use a different objective function in this case a relative deviation version of the

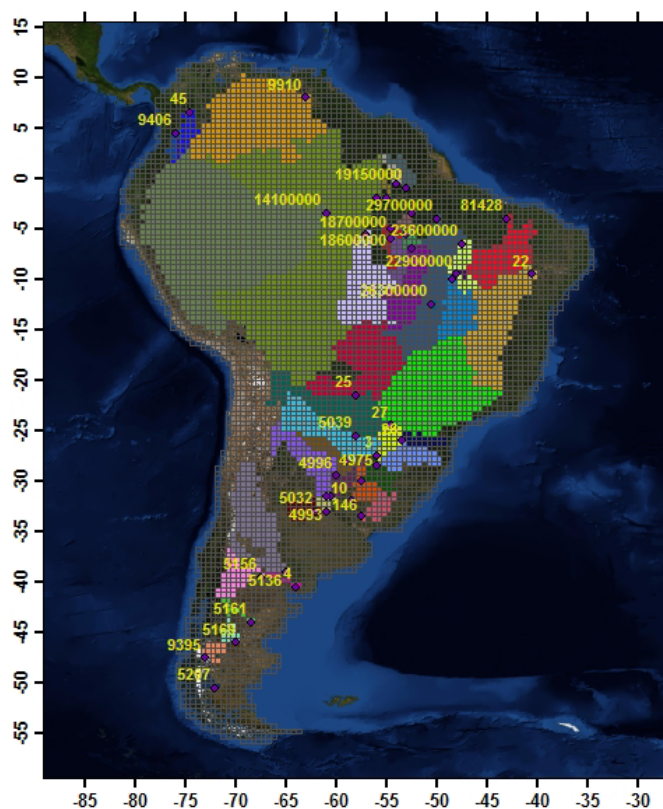


Figure 9.7 Location and coverage of calibration basin

Table 9.5 Summary of gauges and data used to calibrate the model

Gauge	Source*	Long	Lat	Station Name	Start Year	End Year
3	1	-56	-27.5	Parana at Posadas	1965	1979
4	1	-64	-40.5	Negro at P. Angostura	1965	1979
10	1	-58.5	-32	Uruguay at Concordia	1969	1979
22	1	-40.5	-9.5	Sao_Francisco at Juazeiro	1929	1979
25	1	-58	-21.5	Paraguay at Fecho Dos Morros	1966	1978
26	1	-53.5	-26	Iguacu at Salto Osorio	1941	1975
27	1	-54.5	-24.5	Parana at Guaira	1920	1979
45	1	-74.5	6.5	Magdalena at Pto Berrio	1969	1984
146	1	-57.5	-33.5	Negro at Palmar	1910	1979
4974	1	-57.5	-30	Uruguay at Paso De Los Libres	1909	1994
4975	1	-56	-28.5	Uruguay at Garabi	1930	1994
4993	1	-61	-33	Parana at Timbues	1905	1994
4995	1	-59	-28	Parana at Corrientes	1904	1990
4996	1	-60	-29.5	Parana B._Princ at Isla Pati	1975	1990
5016	1	-60.5	-31.5	Leyes at Ruta Provincial 1	1977	1994
5020	1	-61	-31.5	Salado at Ruta Prov. 70	1952	1994
5032	1	-62	-33	Tortugas at Puente Km 38	1939	1955
5039	1	-58	-25.5	Paraguay at Puerto Pilcomayo	1980	1994
5136	1	-65	-39	Colorado at Pichi Mahuida	1918	1994
5156	1	-67.5	-39.5	Negro at Paso Cordova (Roca)	1922	1994
5161	1	-68.5	-44	Chubut at Los Altares	1943	1994
5169	1	-70	-46	Senguerr at Vuelta Del Senguerr	1937	1959
5207	1	-72	-50.5	Santa Cruz at Charles Fuhr	1955	1994
9395	3	-73	-47.5	Baker at La Colonia	1963	1984
9406	3	-76	4.5	Cauca at La Virginia	1947	1994
9910	3	-63	8	Orinoco at Pte Angostura	1923	1989
81428	3	-43	-4	Paranaiba at Porto Formoso	1973	1996
14100000	2	-61	-3.5	Solimões at Manacapuru	1972	1983
17050000	2	-56.5	-2	Amazonas at Óbidos	1927	1995
17090000	2	-55	-2	Curua at Boca do Inferno	1973	1994
17650000	2	-57	-5.5	Tapajós at Jatobá	1972	1994
18300000	2	-54	-0.5	Paru de Este at Fazenda Paquira	1973	1988
18510000	2	-52.5	-7	Xingu at São Felix do Xingu	1975	1997
18520000	2	-53	-5.5	Xingu at Belo Horizonte	1976	1997
18600000	2	-54.5	-6	Iriri at Laranjeiras	1976	1988
18700000	2	-54.5	-5	Iriri at Pedra do Ó	1976	1994
18850000	2	-52.5	-3.5	Xingu at Altamira	1971	1997
19150000	2	-53	-1	Jari at São Francisco	1968	1997
22500000	2	-48.5	-10	Tocantins at Miracema	1969	1983
22900000	2	-48	-9.5	Sono at Porto Real	1969	1983
23600000	2	-47.5	-6.5	Tocantins at Tocantinópolis	1955	1980
26300000	2	-51	-12.5	Mortes at Santo Antônio do Leverger	1969	1996
29700000	2	-50	-4	Tocantins at Tucuruí	1978	1994

*Source: 1) SAGE – RivDis2.0 2) R-Hydronet and 3) dss552.1

Nash-Sutcliffe efficiency (Krause *et al.*, 2005) applied to the monthly mean flows, and this yielded good simulations. The relative efficiency criteria E_{rel} is given as:

$$E_{rel} = 1 - \frac{\sum_{i=1}^n \left(\frac{O_i - P_i}{O_i} \right)^2}{\sum_{i=1}^n \left(\frac{O_i - \bar{O}}{\bar{O}} \right)^2}$$

where: O are the observed and P the predicted values.

The effect of this equation is to reduce the influence of large absolute errors and, thus, the bias towards fitting peak flows. To illustrate the results of the calibration, Figure 9.8 shows four examples selected to show a good model fit (Orinoco at Pte Angostura), moderate fit (Uruguay at Paso de Los Libres and Negro at Paso Cordova (Roca)) and a poor model fit (Paraguay at Fecho dos Morros). The pairs of plots for the four gauges compare the seasonal pattern for flows (left) and the total annual flows for modelled and observed data (right). For the Orinoco at Pte Angostura, a basin that had a good model fit, the monthly time series is also plotted (Figure 9.9) to highlight the ability to capture the year on year variability. The effect of the choice of the objective function is also apparent in that the low flows are generally very well fitted but with a degree of over or underestimation in the high flows.

For 17 gauges, the seasonal pattern and the annual variability were well reproduced. Those performing less well tend to have nested sub-basins for which errors in the upstream basin were compounded requiring the calibration process to compensate for these. Other problems, particularly in the Baker and Paraguay basins are the presence of a large lake and a wetland system, respectively, which have a greater impact on the movement of the water, cell to cell, than the runoff generation in the cell. Some additional manual calibration was carried out comparing flows at of the Paraguay at Fechos dos Morros which is downstream of the Pantanal, and it was evident that the model could not simulate the slow travel time of water over such large areas or the subsequent losses of water that occur and, hence, overestimated the annual variability in flows.

The process of selecting basins for calibration puts large constraints on the number of gauges that can be used for the comparison. Gauges that are excluded are generally inappropriately located and from those available, full records have been used to calibrate against. Therefore, validation against streamflow data has not been carried out.

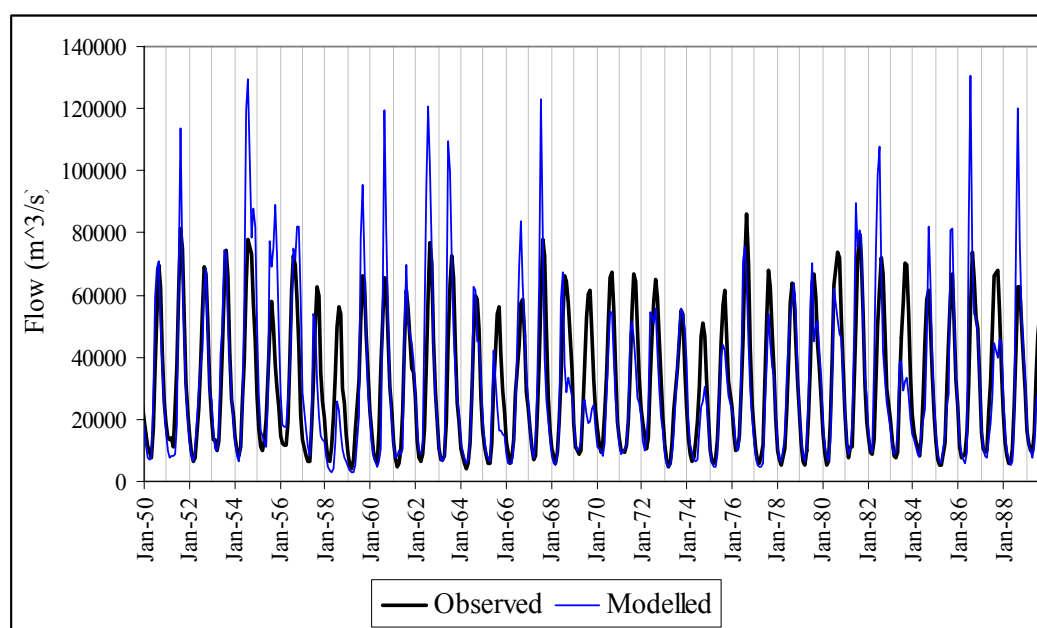


Figure 9.8 Observed and modelled monthly streamflow for the Orinoco at Pte Angostura

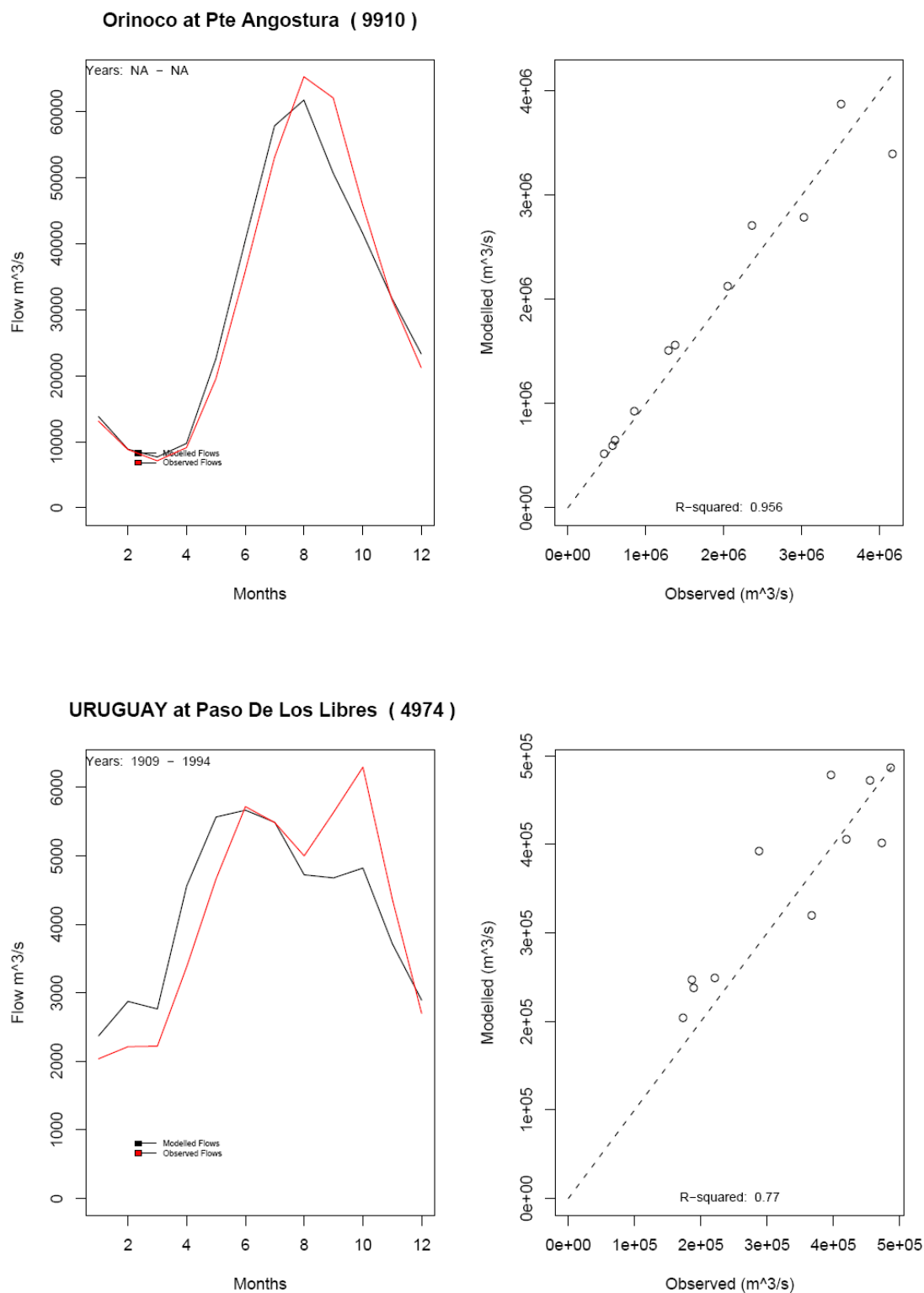
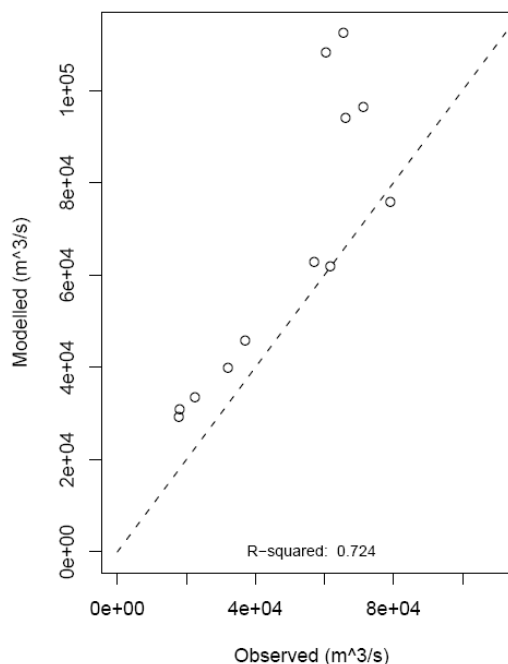
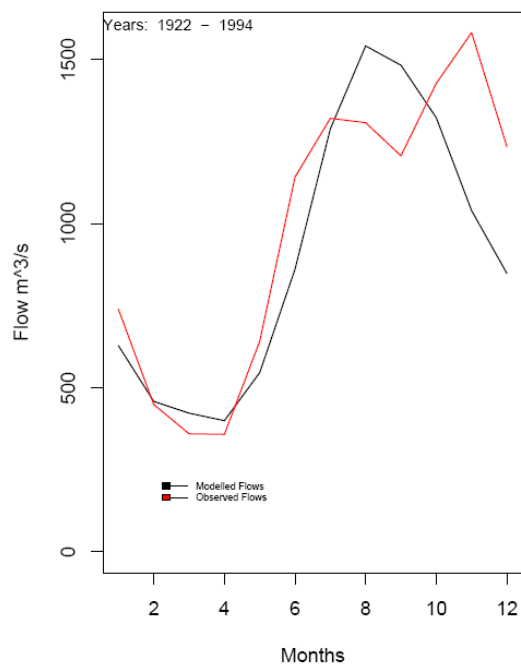


Figure 9.9 Plots comparing the mean monthly flows (left) and annual biases between modelled and observed flows (right) for four basins in South America

NEGRO at Paso Cordova (Roca) (5156)



Paraguay at Fecho Dos Morros (25)

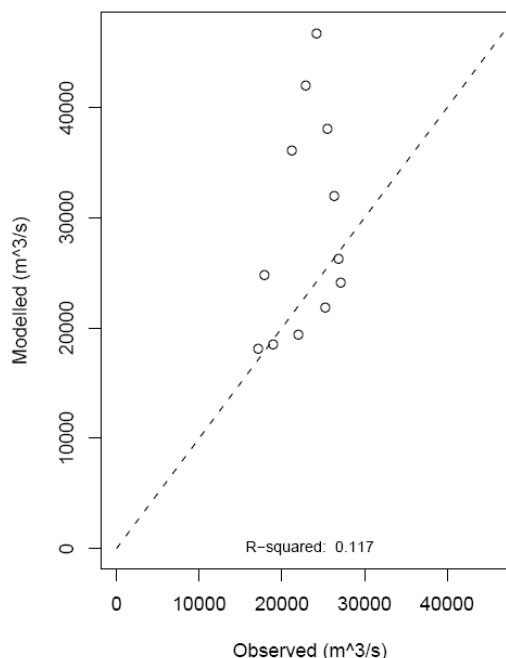
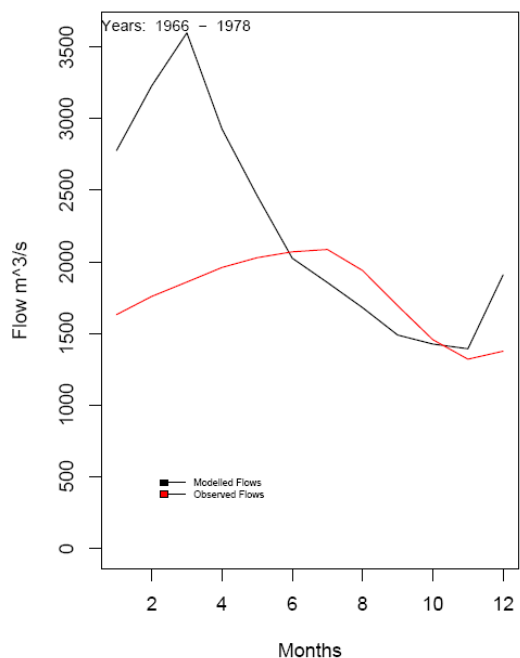


Figure 9.9 continued Plots comparing the mean monthly flows (left) and annual biases between modelled and observed flows (right) for four basins in South America

9.7 Results

The two key model outputs are the monthly streamflow series generated at each cell and the water availability indices (WAIs) summarised below in Table 9.6. Other supplementary maps can be produced to examine changes to low flows and standard deviation of flows in cells.

9.7.1 Water availability indices

Comparisons on a cell by cell basis of water yield and demands can be made in different ways. The simplest Type 1 index divides the annual volumetric water yield by the annual volumetric demand; however, this does not capture the seasonal or inter-annual variation in water demand and supply. The Type 2 index calculates the actual supply available for use, estimated as the driest month in each year which occurs with 90% reliability. This value, termed Qdryav, can also be plotted to examine changes to low flows. This value is compared to the minimum monthly demand i.e. assumes demands are constant throughout the year. The Type 3 index for surface water is found by calculating the 90% reliable flow for each month of the year separately, rather than calculating a single value based on the driest month in each year. The index is then the minimum (over all months in the year) of this value minus the demand in the same month. This index reflects the critical point in the year whether or not there are variable irrigation demands. The index is expressed as a volume, with positive values indicating an excess of supply over demand and negative values a shortfall. An advantage of this index is that it helps to distinguish areas where demands are large and there is a large shortfall (for instance) from those where both supply and demands are small and, therefore, the shortfall is small. Thus, areas of large-scale water availability problems are picked out from those where the problems are relatively small-scale. The Type 4 index was developed so that results could be expressed as a ratio which ranges from -1 (negligible water available to meet demand), through zero (available water meets demand), to 1 (available water exceeds demand).

Examples of these outputs produced for South America are plotted in ArcGIS and shown in Figure 9.10.

Table 9.6 Summary of water availability indices for surface water, groundwater and combined sources as computed in GWAVA

	Index	Definition
Surface water only	SWAI-type 1	Total annual runoff / Total annual demand
	SWAI-type 2	90% reliable driest month runoff / Minimum monthly demand
	SWAI-type 3	Minimum over all months of: (90% reliable monthly runoff – Demand for that month)
	SWAI-type 4	(SWAI-type 3) / (90% Reliable monthly runoff + Demand for that month)
Ground water only	GWAI-type 1	Annual groundwater yield / Total annual demand
	GWAI-type 2	Minimum monthly groundwater yield / Minimum monthly demand
	GWAI-type 3	Minimum over all months of: (Monthly groundwater yield – Demand for that month)
	GWAI-type 4	(GWAI-type 3) / (Monthly groundwater yield + Demand for that month)
Combined	TWAI-type 1	(Total annual runoff + Annual groundwater yield) / Total annual demand
	TWAI-type 2	(90% Reliable driest month runoff + Minimum monthly groundwater yield) / Minimum monthly demand
	TWAI-type 3	Minimum over all months of: (90% Reliable monthly runoff + Monthly groundwater yield – Demand for that month)
	TWAI-type 4	(TWAI-type 3) / (90% Reliable monthly runoff + Monthly groundwater yield + Demand for that month)

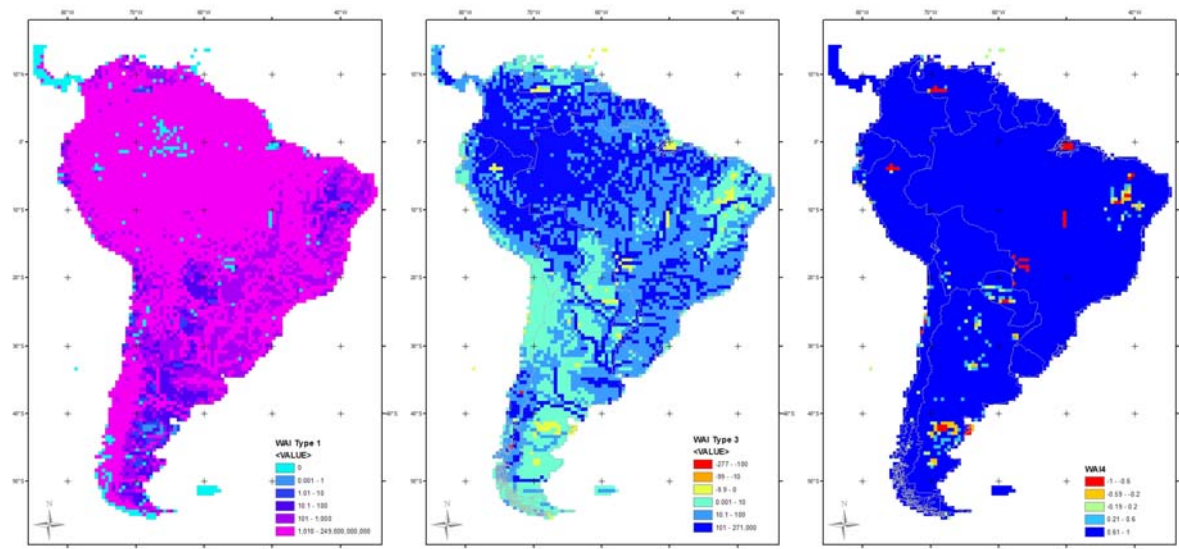


Figure 9.10 Maps illustrating a) WAI Type 1 b) WAI Type 3 and c) WAI Type 4 for South America computed for the baseline period 1961-1990

9.7.2 Baseline period

The model was run for a baseline period of 1961 to 1990. It should be noted that landcover, and all information used to compute the water demands, are assumed to be constant over the baseline period with data used to derive the water demands centred on 1990. Figure 9.10a shows the straightforward Type 1 index as a simple ratio of the annual demand to runoff where 76 cells have an annual deficit of water. As expected the cells with highest runoff volume, i.e. those in the main river channel, have flows considerably in excess of demands annually. In the second plot (Figure 9.10b), the Type 3 index is plotted. The more complex Type 4 index is shown in Figure 9.10c which compares the water availability to the demand such that across most of South America the demand is met (A positive value for the Type 4 index shown as blue on the map indicates a ample supply of water to meet demand whereas a negative value denoted by orange and red indicates cells insufficient water to meet demand i.e. water stress with red indicating a more severe deficit). Overall for the baseline period, there are 152 cells experiencing water shortfalls with two main clusters of cells: one in north-east Brazil, a region of intense agriculture, and the second in southern Argentina, plus another smaller grouping in Paraguay. Water supply in southern Brazil, Argentina, Uruguay and Paraguay is supplemented by the use of groundwater pumped from the large regional Guaraní aquifer. In these simulations however, no account has been taken of water supply by groundwater and these maps should be treated as a worst case view if groundwater were to become unusable due to either insufficient recharge or contamination.

9.8 Evaluation of hydrological modelling (D3.2)

The GWAVA model has been applied to South America on a half degree grid. It has been calibrated at 43 locations against observed monthly streamflow records and has been rerun for the baseline period 1961–1990. The model has reproduced monthly flows reasonably well across a range of climates and flow regimes. Some particular issues were encountered in capturing the large wetland area of the Pantanal; whilst ultimately a reasonable annual water balance was achieved the seasonal outflow from the model was not captured and is due largely to the simplicity of routing algorithm used within GWAVA. It has not been possible to make a proper assessment of the model in basins whose regime is characterised by glacial melt and, in particular, the Baker basin for the following reasons:

- 0.5 degrees too coarse to resolve the basin accurately enough;
- Scarcity of independent information to validate the input precipitation;

- Presence of the very large Lake General Carrera obscuring the effects of snowmelt as viewed from the very downstream gauging station at La Colonia.

9.9 Summary and recommendations

Whilst the GWAVA modelling scheme is designed to be a generalised approach capturing large-scale hydrological processes, there are a number of improvements that could be made to refine the model:

- A finer spatial resolution on the western Andes watersheds would enable more accurate modelling of the mountainous and small catchments through a more detailed river routing network and fewer errors between the gridded and natural basin areas;
- A better approach of implementing large wetlands into the model using the existing method, developing a large-scale inundation model, or perhaps incorporating an empirically-based solution.

The calibration procedure could also be improved by the use of a multivariate approach to model optimisation when examining nested sub-basins, and this would overcome some of the problems of propagating errors from basin to basin that were encountered.

In terms of the estimates of water demands and water scarcity mapping, the accuracy of the results depends largely upon the availability of data both to validate the model and as inputs. Better information on the cropping patterns in South America is needed and mapping of crop types with climate and altitude would lead to a more realistic distribution of particular crop types (and hence the crop coefficients) across the region.

Incorporating information on groundwater supply and, if available, groundwater availability would enable a fuller examination of water resources availability for South America to be carried out. Again this is in possible within the GWAVA scheme but relies on the availability of data, ideally standardised across the continent.

10. Summary and recommendations

Work Package 3 “Hydrological modelling and extremes” was formulated to provide methods and tools to be used by other WPs in TWINLATIN. The application of hydrological (rainfall-runoff) models is specifically relevant for as a basis for identification and analysis of mitigation actions (WP6) and the assessment of potential future impacts caused by global change (WP8). WP3 activities very much followed the five stages in hydrological modelling applications, namely: data collation and pre-processing, model set-up and configuration, calibration, validation and evaluation. Development of improved hydrological modelling was an important task in all Latin American basins, and major advances were made in all cases. Table 10.1 summaries the outcomes from the modelling and section 10.1 highlights the key achievements in each basin and for the continental modelling.

Table 10.1 Outcomes from hydrological modelling

Issue	Baker/Biobío Chile	Catamayo-Chira Ecuador-Peru	Cauca Colombia	Lake Cocibolca Nicaragua	Cuareim/Quaraí Brazil-Uruguay
Model applications					
Choice of model	SWAT to Lonquimay sub-basin of BioBío to further develop snow/ glacier/ TWINBAS work	SWAT to 4 sub-basins in upper & mid basin, & outlet	HBV/IHMS to basin – for TWINLATIN work to Tulua sub-basin of Cauca	Simple WB & WASMOD WB for basin WATSHMAN-PCRaster in Mayales sub-basin & GLUE uncertainty	SWAT, MODSIM to Tres-Cruces sub-basin MGB-IPH large-scale distributed hydrological model to basin
Data availability	Very poor in Baker, mixed in amount & quality in BioBío	Poor amount & quality	OK amount of data, quality poor	Poor amount & quality	Global datasets available, local data mixed in amount & quality
Time interval	Daily	Monthly	Daily	Daily/monthly/annual	Daily
Spatial scale	1 sub-basin of Biobío	Basin & 4 sub-basins	1 sub-basin	Basin & 1 sub-basin	Basin & 1 sub-basin
Model results					
Calibration & validation	Calib good: $R^2=0.87$, $EFF=0.81$ Valid satisfactory: $R^2=0.57$, $EFF=0.56$	Calib good to satisfactory: $R^2=0.47$ to 0.77 , $EF=0.02$ to 0.76 Valid similar: $R^2=0.47$ to 0.76 , $EF=-3.10$ to 0.75	Calib poor Valid similar: $R^2=0.46$	WASMOD calib satisfactory: $EFF=0.65$ Valid similar: $EFF=0.60$ WATSHMAN poor: $EFF=0.5$	MGB-IPH calib & valid good SWAT calib poor: $R^2=0.45$, $EFF=0.44$ Valid poor: $R^2=0.45$, $EFF=0.43$
Issues	Underestimation of high flows, overestimation of low flows	Performance varies, general overestimation of flow	Performance varies from year-to-year	WASMOD over-estimation of low flows	MGB-IP: some high flows underestimated in calib & over-estimated in valid SWAT: under-estimation of high flows
Hoped for but not achieved	WB for Baker basin	-	-	-	WQ modelling using MGB-IPH

where: calib – calibration period, valid – validation period, R^2 =goodness of fit, EFF – efficiency criterion

10.1 Key results and achievements

10.1.1 Baker/Biobío

The SWAT model was successfully applied to the Lonquimay basin in the Biobío, representing the major intra- and inter-annual variability of flow values in the basin relatively well and thus enabling first assessments of the possible impacts of climate change scenarios in a mixed-regime (rainfall and snow-fed) river basin from central Chile in WP8. Outcomes from such assessments can be used to foresee potential impacts under similar climate change scenarios in similar sub-basins of the Baker (see WP8 report).

For the calibration period, SWAT model performance was good with R^2 of 0.87, efficiency of 0.81 and 4.88% deviation from observed streamflow. The results were not so good for the validation period, with equivalent values of 0.57, 0.56 and 7.86%, respectively. Examination of the results reveals that the model tends to underestimate the high flows and overestimate the low flows, with overall best model performance occurring in winter.

The main problems encountered in model application related to data issues, specifically the limited amount and spatial coverage of input and calibration and validation datasets (e.g. precipitation, soil, snowcover), and the poor representation of hydrological processes within the model (e.g. snowmelt).

10.1.2 Catamayo-Chira

Application of the SWAT model to four sub-basins of the Catamayo-Chira basin proved successful in three cases, as it did for the overall basin. The results obtained can be considered a useful tool for management and planning activities, by allowing a first assessment of the impacts on water and sediment production due to soil use and climatic changes in the basin.

SWAT model performance varied in the different sub-basins. For the calibration period, model performance was good to satisfactory with R^2 of 0.77 to 0.47, efficiency of 0.76 to 0.02, and 0.96 to 13.10% deviation from observed streamflow volume. For the validation period, with equivalent values were 0.76 to 0.47, 0.75 to -3.10, and 6.67 to 27.16%, respectively. The negative efficiency, for one of the sub-basins, indicates a result worse than substituting the modelled values with the mean flow.

Examination of the results reveals that the model tends to overestimate the flows, most likely caused by the rainfall interpolation method from the limited number of rainfall stations. Indeed, the gathering and digitisation of climatic, hydrologic and physical (e.g. sediments, soils, vegetation) information for the basin proved extremely time-consuming. It was also noted that data availability in the Ecuadorian part of the basin was more limited than in the Peruvian part. This uncertainty has a direct consequence on the quantity and quality of the model results.

10.1.3 Cauca

The HBV/IHMS model was applied to the Tulua sub-basin in the Cauca. For the validation period, HBV/IHMS model performance was relatively poor with R^2 of 0.46. The equivalent figure for the calibration period was not available; however, examination of the mean monthly modelled and observed flows for each year of the calibration shows that model performance varies from year-to-year with no consistent over- or underestimation of high or low flows apparent.

The main problems encountered in model application again related to data issues, specifically the limited amount and spatial coverage of precipitation data and initially poor topographical information. In addition the rating curve used to convert water level data into flows was believed to be suspect at high flows.

One of the model's potential applications as a management tool for hydrology is the generation of a series of short, medium and long-term forecasts for tributaries to Salvajina Dam, as well as flow generation at ungauged sites.

10.1.4 Lake Cocibolca

Three modelling approaches were adopted in the Lake Cocibolca basin. The simple annual water balance method revealed that water resources are especially scarce in the north-western part of the basin during the dry season. The monthly water balance modelling using WASMOD had relatively low efficiency criteria (0.65 for the calibration period and 0.60 for the validation period) indicating that there are high uncertainties in the input and/or validation data. Uncertainty estimation was important because the data quality and availability were often low. A limits-of-acceptability approach was found to be a useful way of accounting for uncertainties in discharge data, which may have wider application in the region.

The main problems encountered in model application again related to data uncertainty, specifically relating to the precipitation data - several different rainfall interpolation methods were used in the basin to assess which worked best - and the rating curve used to convert water level data into flows.

The daily hydrological modelling using WATSHMAN was problematic, because of the same data limitations and high spatial and temporal variability, with the efficiency criterion around 0.5. Modelling results from such daily-scale modelling could be a useful tool for quality control of discharge data, as well as for evaluation of the coherence and quality of the hydrometeorological data, one of the most likely causes of error being underestimation of the evapotranspiration, though groundwater seepage could also be a problem.

10.1.5 Cuareim/Quaraí

Two modelling approaches were also adopted in the Cuareim/Quaraí basin, results from which will provide the basis for analysis in several other work packages. The MGB-IPH model, which was adapted to include hundreds of small farm reservoirs and rice fields, was successfully applied and results of the model analysis have already been presented to both stakeholders in the basin, and government institutions. The National Water Agency is using results of the model to support decisions concerning water permits.

For the calibration period, SWAT model performance was poor with R^2 of 0.45 and efficiency of 0.44. The results in the validation period were similar, with equivalent values of 0.45 and 0.43, respectively. Examination of the results reveals that the model tends to underestimate the high flows. It is, however, recommended for use as a tool to validate daily data of precipitation and flow, and to model erosion and water quality in a basin with diffuse source pollution. MODISM, a water allocation model, is recommended for management of the basin water resources.

Limitations of the modelling work identified include the low availability and quality of hydrological data, both rainfall and streamflow.

10.1.6 Norrström

The good hydrological modelling results at Norrström have allowed achieving better and satisfying Nutrient modelling. SWAT model was satisfyingly calibrated and validated using Swedish parameters/conditions. However, more data is needed in areas such as: soil parameters, soil nutrient content. Another key result from the work done at Norrström is that IVL have set up two stations for flow proportional measuring of Nitrogen and Phosphor. Need for improved modelling of the P cycle and better estimates of the internal load of Phosphorus from Lake Mälaren are substantial in the basin to have a better understanding on how the eutrophication process affect the water quality conditions.

The conclusions that can be drawn from this work package regarding the hydrological modelling are that it is possible with available data to get a good overview of the situation and produce reliable data.

10.1.7 Continental modelling

The GWAVA model was successfully applied to the South American continent. The model has reproduced monthly flows reasonably well across a range of climates and flow regimes. Some

particular issues were encountered in capturing the large wetland area of the Pantanal; whilst ultimately a reasonable annual water balance was achieved the seasonal outflow from the model was not captured and is due largely to the simplicity of routing algorithm used within GWAVA. It has not been possible to make a proper assessment of the model in basins whose regime is characterised by glacial melt and, in particular, the Baker basin.

The continent-wide approach means that a consistent methodology can be applied across four of the subject basins in the TWINLATIN project (Baker, Catamayo-Chira, Cauca and Quaraí/Cuareim) as well as the areas in between, in order to provide a wider regional context for some of the problems faced, in particular water resources. It can also provide an opportunity for climate change impacts to be examined and compared at the continental, regional and basin scales.

10.2 Discussions and recommendations

The hydrological modelling work carried out in WP3 will enable modelling of climate change effects on hydrological regimes, and analyses of human development scenarios such as land use change and water resource development to satisfy a growing population. Hydrological modelling has a major role to play in Integrated Water Resources Management (IWRM), needed to solve the extensive societal problems related to lack of water and insufficient quality of water. Hence TWINLATIN will have a significant impact on the partner countries' capacity to apply sustainable water management in the region, as well as developing and strengthening the links between the countries.

The suitability of the model to solve the problems originally highlighted in section 1 was not a major issue for most partners. The choice of model applied was governed largely by factors like familiarity with model, prior success in application of the model in the region (not necessarily by that partner), support provided in model application (twinning), the opportunity to exchange experiences with other model users (twinning), and the opportunity to develop expertise in the model for future, post-TWINLATIN, applications. TWINLATIN has facilitated increased familiarity with models, support in model application and opportunities to exchange experiences with others, particularly with regard to the SWAT model. The formation of the Binational Technical Group (Grupo Técnico Binacional, GTB) in the Catamayo-Chira basin to support SWAT applications is a welcome development to assist in the transference of planning and decision-making tools used under TWINLATIN to local institutions involved in the basin's management to make the modelling more useful for other basins in the region.

There is also an acknowledged need to create awareness among government departments and stakeholders with regard to the possibilities and limitations of modelling work, to help them to better evaluate the model outcome, and better direct and specify requests for further work. In the Baker basin, a first stage in this awareness building has been achieved through public participation workshops, but it needs to be developed further in ongoing and future interactions between academics and authorities (or other basin stakeholders).

Poor data quality and availability were issues highlighted by all partners as having a significant impact on their hydrological modelling activities, specifically:

- Poorly distributed networks – spatially and topographically;
- Old and/or poorly maintained equipment;
- Access to records is difficult – physical access and storage media;
- Records are short and/or have gaps;
- Records lack quality control and/or show inconsistencies;
- Records require significant processing before use.

For several basins, the model results were surprisingly good given the problems inherent in the underlying data. Even in these situations, it is important to be conscious of the implications of poor data for the accuracy of and uncertainty in the results, and the limitations of the models themselves. The limits-of-acceptability approach for uncertainty estimation applied in Nicaragua may have wider

application across the region. The very limited availability of traditional input and calibration and validation datasets is typical of many Andean basins, and also of much of the continent.

With regard to rainfall and other meteorological data as well as water level/flow data, it is recommended that strategic (long-term and goal-oriented) improvements in hydrometeorological monitoring networks should urgently be considered. Long time series are generally required for model calibration and validation, and maximum benefits from improvements in the monitoring network will not be obtained immediately. These improvements can be balanced and combined with the search for alternative data sources such as, for example, those generated from remote sensing, though further research will be required to evaluate the potential importance of such alternative data sources.

Even where there were flow data to use in model calibration and validation, in many cases there were issues concerning the applicability of the rating curve used to convert water levels to flows at during high flow events. It is essential that regular river gaugings are made in order to check and improve rating curves and, if possible, more high flow measurements should be made to reduce uncertainty in peak flows. It would be useful to establish the highest measured discharges included in the current rating curves to know which flow data are based on the extrapolated parts of the rating curves.

In terms of the estimation of water demands for the continental modelling, the accuracy of the results depends largely upon the availability of input data. In the agricultural sector, better information on the cropping patterns in South America is needed, and mapping of crop types with climate and altitude would lead to a more realistic distribution of particular crop types (and hence the crop coefficients) across the region. Also in the agricultural sector there is a lack of information concerning the volume and operation rules of the small farm reservoirs, incorporated into the MGB-IPH modelling in the Cuareim/Quaraí basin. Indeed a lack of knowledge of the locations where water is being stored and/or abstracted from rivers is one of the most important obstacles to hydrological modelling. It is recommended that an inventory of water users in each basin be made, including very detailed information on how much and where water is be taken from the rivers. Finally, incorporating information on groundwater supply and, if available, groundwater availability, would enable a fuller assessment of water resources uses and availability within each basin and across the continent.

References

- Aguilar, E., Peterson, T.C., Obando, P.R., Frutos, R., Retana, J.A., Solera, M., Soley, J., Garcia, I.G., Araujo, R.M., Santos, A.R., Valle, V.E., Brunet, M., Aguilar, L., Alvarez, L., Bautista, M., Castanon, C., Herrera, L., Ruano, E., Sinay, J.J., Sanchez, E., Oviedo, G.I.H., Obed, F., Salgado, J.E., Vazquez, J.L., Baca, M., Gutierrez, M., Centella, C., Espinosa, J., Martinez, D., Olmedo, B., Espinoza, C.E.O., Nunez, R., Haylock, M., Benavides, H. & Mayorga, R. 2005. Changes in precipitation and temperature extremes in Central America and northern South America, 1961-2003. *Journal of Geophysical Research-Atmospheres*, **110(D23)**, D23107.
- Alavi, G. 1999. Climate, leaf area, soil moisture and tree growth in spruce stands in SW Sweden – Field experiments and modeling. Doctoral thesis, Swedish University of Agricultural Sciences, Agraria 175.
- Alfaro, E. J. 2000. Some characteristics of the precipitation annual cycle in Central America and their relationships with its surrounding tropical oceans. *Tópicos Meteorológicos y Oceanográficos* **7(2)**, 99 -115.
- Allasia, D.G., Collischonn, W., Silva, B.C. & Tucci, C.E.M. 2005. Large basin simulation experience in South America. *IAHS Publication No 303*, 360-370.
- Allen, R.G., Pereira, L.S., Raes, D. & Smith, M. 1998. *Crop evapotranspiration – guidelines for computing crop water requirements*. FAO Irrigation and Drainage Paper. 300 pp.
- Amador, J.A., Alfaro, E.J., Lizano, O.G. & Magana, V.O. 2006. Atmospheric forcing of the eastern tropical Pacific: A review. *Progress in Oceanography*, **69(2-4)**, 101-142.
- Arnold, J.G., Srinivasan, R., Muttiah, R.S. & Williams, J.R. 1998. Large area hydrologic modelling and assessment - Part I: model development. *JAWRA* **34(1)**, 73-89.
- ASCE. 2005. The ASCE reference evapotranspiration equation. Allen, R.G. (ed). Prepared by the Task Committee on Standardization of Reference Evapotranspiration of the Environmental and Water Resources Institute of the American Society of Civil Engineers.
- Baethgen, W.E. 1997. “Relaciones entre la temperatura superficial del Pacífico tropical y los rendimientos de cultivos en Uruguay”, Workshop and Conference on the 1997-1998 El Niño: Impacts and Potencial Applications of Climate Prediction in Southeast South America, December 1997, Montevideo, Uruguay.
- Baethgen, W.E. & Giménez, A.E. Applying seasonal climate forecasts and satellite information for improving decisions in the agricultural sector: the 1999-2000 drought in Uruguay”, INIA, Estanzuela, Uruguay. Available at: www.inia.org.uy/disciplinas/agroclima/publicaciones/sistemas/uso_informacion_satelital.doc
- Baethgen, W.E. & Giménez A.E. 2002. Seasonal Climate Forecast and the Agricultural Sector of Uruguay. ENSO and Society – Examples of ENSO-Society Interactions: Agricultural Sector of Uruguay. International Research Institute for Climate Prediction. Available at: <http://iri.columbia.edu/climate/ENSO/societal/example/Baethgen.html>
Accessed June 11, 2003
- Bell, V.A. & Moore, R.J. 1999. An elevation-dependent snowmelt model for upland Britain. *Hydrological Processes* **12**, 1887-1903.
- Belward, A.S. (ed). 1996. The IGBP-DIS global 1 km land cover dataset (DISCover)-proposal and implementation plans: IGBP-DIS Working Paper No. 13, Toulouse, France, 61pp.
- Beven, K., & Binley, A. 1992. The Future of Distributed Models - Model Calibration and Uncertainty Prediction. *Hydrological Processes* **6(3)**, 279-298.

- Beven, K.J. 2001. *Rainfall-runoff modelling – The primer*. Wiley, Chichester, 360pp.
- Beven, K. 2006. A manifesto for the equifinality thesis. *Journal of Hydrology* **320(1-2)**, 18-36.
- Blombäck, K. 1998. Carbon and Nitrogen in Catch Crop Systems – Modeling of seasonal and long-term dynamics in plant and soil. Doctoral thesis, Swedish University of Agricultural Sciences, Agraria 134.
- Bossi, J. *et al.* 2001. Carta geológica del Uruguay a escala 1/500.000. Facultad de Agronomía, Catedra de Geología, Montevideo, Versión 2, 2001.
- Bremicker, M. 1998. *Aufbau eines Wasserhaushaltsmodells für das Weser und das Ostsee Einzugsgebiet als Baustein eines Atmosphären-Hydrologie-Modells*. Dissertation Doktorgrad, Geowissenschaftlicher Fakultät der Albert-Ludwigs-Universität. Freiburg. Juli.
- Cáceres, H.A. 2003. Dinámica del uso de la tierra y de la oferta hídrica en la Cuenca del río guacerique, tegucigalpa, honduras. Centro Agronómico Tropical de Investigación y Enseñanza, Turrialba, Costa Rica.
- Calder I.R. 1990. *Evaporation in uplands*. Wiley, Chichester.
- Campos, A. 2005. Modelo Hidrológico integrado a un sistema de información geográfico para una cuenca agroforestal de la VIIIª Región. Thesis, Universidad de Concepción, Concepción, Chile.
- Chaubey, I., Haan, C.T., Salisbury, J.M. & Grunwald, S. 1999. Quantifying model output uncertainty due to the spatial variability of rainfall. *JAWRA* **35(5)**, 1113-1123.
- Chow, V.T., Maidment, D.R. & Mays, L.W. 1988. *Applied hydrology*. McGraw-Hill Book Company, New York.
- CIESIN (Center for International Earth Science Information Network), Columbia University; and Centro Internacional de Agricultura Tropical (CIAT). 2005. Gridded Population of the World Version 3 (GPWv3): Population Grids. Palisades, NY: Socioeconomic Data and Applications Center (SEDAC), Columbia University. Available at: <http://sedac.ciesin.columbia.edu/gpw>.
- CIESIN (Center for International Earth Science Information Network), Columbia University; The International Food Policy Research Institute (IFPRI); The World Bank; and The International Center for Tropical Agriculture (CIAT). 2004. Global Rural-Urban Mapping Project (GRUMP): Urban Mask. Available at: <http://beta.sedac.ciesin.columbia.edu/gpw/>.
- CIREN. 1999^a. Estudio Agrológico, VIII Región, Tomos I y II., Centro de Información de Recursos Naturales, Chile. *Estudio Agrológico, VIII Región, Tomos I y II., Centro de Información de Recursos Naturales, Chile*.
- CIREN. 1999^b. Estudio Agrológico, IX Región. Centro de Información de Recursos Naturales, Chile. *Estudio Agrológico, IX Región. Centro de Información de Recursos Naturales, Chile*.
- Climate Prediction Center Internet Team. 2007. Cold and warm episodes by season NOAA/ National Weather Service. Available at http://www.cpc.ncep.noaa.gov/products/analysis_monitoring/ensostuff/ensoyears.shtml Accessed 07-03-2007.
- Collischonn, B, Collischonn, W., Agra, S. & Bortoli, C. 2007b. Reconstituição das vazões naturais do Rio Caí (RS) a jusante da transposição de vazões do Sistema Salto. XVII Simpósio Brasileiro de Recursos Hídricos, São Paulo, 25 a 29 de novembro.
- Collischonn, W., Allasia, D., Silva, B.C. & Tucci, C.E.M. 2007a. The MGB-IPH model for large-scale rainfall-runoff modelling. *Hydrological Sciences Journal* **52(5)**, 878-895.
- Collischonn, W. & Tucci, C.E.M. 2001. Simulação hidrológica de grandes bacias. *Revista Brasileira de Recursos Hídricos*. Vol. 6 No. 1.
- Comisión Río Cuareim: <http://www.crc.gub.uy/indice.htm>.

- CONAMA-CONAF-BIRF (Corporación Nacional Forestal - Comisión Nacional del Medio Ambiente - Banco Interamericano de Reconstrucción y Fomento). 1999. Catastro y evaluación de los recursos vegetacionales nativos de Chile. Informe Regional: Octava Región. CONAF-CONAMA, Santiago, Chile.
- CONAMA-DGF. 2006. Estudio de la variabilidad climática en Chile para el siglo XXI, Comisión Nacional del Medio Ambiente. Departamento de Geofísica. Facultad de Ciencias. Físicas y Matemáticas. Universidad de Chile.
- Consorcio ATA – UNP – UNL. 2003. Caracterización territorial y documentación básica en el ámbito de la cuenca binacional Catamayo-Chira. Volumen III Estudios Básicos, Tomo 3.6 Estudio de Suelos. Loja – Piura.
- Consorcio ATA – UNP – UNL. 2003. Caracterización Hídrica y Adecuación entre la Oferta y la Demanda en el Ámbito de la Cuenca Binacional Catamayo Chira. Volumen III Estudios Basicos, Tomo 3.2 Estudio Climático. Loja – Piura.
- Consorcio ATA – UNP – UNL. 2003. Caracterización Hídrica y Adecuación entre la Oferta y la Demanda en el Ámbito de la Cuenca Binacional Catamayo Chira. Volumen I Resumen Ejecutivo. Loja – Piura.
- Cosgrove, W. & Rijsberman, F. 2002. *World Water Vision: Making Water Everybody's Business*". Earthscan, London. <http://www.watercouncil.org/>
- Crespo, P., de Bievre, B. & Cisneros, F. 2006, Modelos Hidrológicos: Guía para su implementación y análisis de escenarios. PROMAS - Universidad de Cuenca. Loja – Ecuador.
- Crisci, M., Fernández, M. & Trambauer, P. 2007. Viabilidad económico – ambiental de un sistema regional de riego por gravedad en la cuenca del Río Cuareim para la producción de arroz–pasturas. Proyecto Hidráulica Ambiental, Instituto de Mecánica de los Fluidos e Ingeniería Ambiental, Facultad de Ingeniería, Universidad de la República, Tutor Dr. Rafael Terra, 335pp.
- CVC–Environmental Technical Direction, Water Resources Group. 2000. Rain Hydrology Model – IHMS Flow. Sandovan, M.C., Mayorquin, J.A. & Aristizabal, H.F. (ed). Santiago de Cali.
- CVC-Universidad del Valle. 2001. PMC - Phase I. Cauca River Mathematical Modelling - Volume VIII. Technical Report. Santiago de Cali.
- CVC-Universidad del Valle. 2005. PMC - Phase II . Calibration and Applications of the Cauca River Water Quality Model -Volume VIII. Technical Report. Santiago de Cali.
- Davies, H. & Bell, V. 2008 Assessment of methods for extracting low resolution river networks from high resolution digital data. *Hydrological Sciences Journal*. In press.
- Di Luzio, M., Srinivasan, R., Arnold, J.C. & Neitsch, S.L. 2002. ArcView Interface for SWAT2000 User's Guide. Texas, Texas Water Resources Institute, College Station.
- Di Luzio, M., Mitchell, G. & Sammons, N. 2005. Watershed Modelling using SWAT2003. Texas, Texas Water Resources Institute, College Station.
- Diaz, H.F., Hoerling, M.P. & Eischeid, J.K. 2001. ENSO variability, teleconnections and climate change. *International Journal of Climatology* **21(15)**, 1845-1862
- Dirección Nacional de Meteorología (DNM): <http://www.meteorologia.com.uy/>
- Dirks, K.N., Hay, J.E., Stow, C.D. & Harris, D. 1998. High-resolution studies of rainfall on Norfolk Island Part II: Interpolation of rainfall data. *Journal of Hydrology* **208(3-4)**, 187-193.
- Döll P. & Lehner B. 2002. Validation of a new global 30-min drainage direction map. *Journal of Hydrology* **258(1-4)**, 214-231.
- Doorenbos J. & Pruitt W.O. 1977. Guidelines for predicting crop water requirements. Irrigation and Drainage Paper 24 (revised), Food and Agriculture Organization, Rome.

- Enfield, D.B. & Alfaro, E.J. 1999. The dependence of Caribbean rainfall on the interaction of the tropical Atlantic and Pacific oceans. *Journal of Climate* **12(7)**, 2093-2103.
- Eriksson, J., Andersson, A., and Andersson, R. 1997. Current status of Swedish arable soils. Naturvårdsverket rapport 4778.
- Escobar, F. 1992. Aplicación del modelo "SRM3-11" (Snowmelt runoff model) en cuencas de los Andes centrales. Segundas Jornadas de Hidráulica Francisco Javier Domínguez, Santiago, Chile.
- ESRI. 1993. Digital chart of the world.
- FAO. 1995. Digital Soil Map of the World and Derived Soil Properties (Version 3.5). CD-ROM, FAO, Rome.
- FAO. 2003. Review of world water resources by country. FAO Water Report 23. FAO, Rome. 71pp.
- FAO. 2007. Gridded livestock of the world 2007. Wint, G.R.W. & Robinson, T.P. (ed). FAO, Rome. 131pp.
- Feijó, U.F. F. & Chalán, B.L. 2008. Análisis multitemporal de la cobertura vegetal de la cuenca Catamayo, Universidad Nacional de Loja.
- Genta, J.L., Pérez-Iribarren, G. & Mechoso, C.T. 1998. A recent increasing trend in the streamflow of rivers in Southeastern South America. *Journal of Climatology* **11**, 2858-2862.
- Genta J.L. *et al.* 2005. Balances Hídricos superficiales en la cuenca del Río Cuareim con fines de gestión del recurso agua y el impacto en las crecientes. Instituto de Mecánica de los Fluidos e Ingeniería Ambiental – Dirección Nacional de Hidrografía – Comisión Río Cuareim.
- Genta J.L. 2005. Cambio climático. Grupo de dinámica de la atmósfera y el océano, Instituto de Mecánica de los Fluidos e Ingeniería Ambiental, Facultad de Ingeniería, Universidad de la República.
- Ghil, M. *et al.* 2002. Advanced spectral methods for climatic time series. *Rev. Geophys.*, **10.1029/2000GR000092**.
- Goovaerts, P. 2000. Geostatistical approaches for incorporating elevation into the spatial interpolation of rainfall. *Journal of Hydrology* **228(1-2)**, 113-129.
- Grip, H. & Rodhe, A. 1985. *Vattnets väg från regn till bäck*. Forskningsrådets förlagstjänst, Karlshamn.
- Gruber, P., 2008. Analisis and Modelling of Land Use Changes in the Río Quiroz river catchment, Peru, Hochschule für Forstwirtschaft Rottenburg, Rottenburg am Neckar.
- Guzmán E., Bonini J., & Matamoros D. 2004. Aplicación Del Modelo Hidrológico SWAT (Soil & Water Assessment Tool) Para La Predicción de Caudales y Sedimentos en una Cuenca hidrográfica caso de estudio: cuenca del río Chaguana. El oro – Ecuador.
- Hall, D.K., Riggs, G.A. & Salomonson, V.V. 2006, updated weekly. MODIS/Terra snow cover 8-day L3 global 500m grid V004, [March 2000 to December 2003]. Boulder, Colorado USA: National Snow and Ice Data Center. Digital media.
- Hall, D.K., Riggs, G.A., Salomonson, V.V., DiGirolamo, N.E. & Bayr, K.J. 2002. MODIS snow-cover products. *Remote Sensing of the Environment*. **83**, 181-194.
- Hastenrath, S.L. 1967. Rainfall distribution and regime in Central America. *Arch. Meteor. Geophys. Bioklimatol.* **15B**, 201-241.
- Heuvelmans, G., Garcia-Qujano, J.F., Muys, B., Feyen, J. & Coppin, P. 2005. Modelling the water balance with SWAT as part of the land use impact evaluation in a life cycle study of CO₂ emission reduction scenarios. *Hydrological Processes* **19**, 729-748.

- Hattermann, F., Krysanova, V., Wechsung, F. & Wattenbach, M. 2005. Runoff simulations on the macroscale with the ecohydrological model SWIM in the Elbe catchment - validation and uncertainty analysis. *Hydrological Processes*, **19**, 693-714.
- IPCC. 2007. Climate Change 2007: The Physical Science Basis. Contribution of Working Group I to the Fourth Assessment Report of the Intergovernmental Panel on Climate Change. Solomon, S., Qin, D., Manning, M., Chen, Z., Marquis, M., Averyt, K.B., Tignor, M. & Miller, H.L. (ed). Cambridge University Press, Cambridge, United Kingdom and New York, NY, USA, 996pp.
- Isaaks, E.H. & Srivastava, R.M. 1989. *Applied Geostatistics* xix. Oxford University Press, New York. 561pp.
- Johnson, R.R. 1998. An investigation of curve number applicability to watersheds in excess of 25000 hectares (250 km²). *Journal of Environmental Hydrology* **6** (Paper 7), 10.
- Johnsson, H. and Mårtensson, K. 2002. Kväveläckage från svensk åkermark – beräkning av normalutlakning för 1995 och 1999. Naturvårdsverket Rapport 5248.
- Jordbruksverket. 2002. Markkartering. Jordbruksinformation 6.
- Kouwen, N., Soulis, E.D., Pietroniro, A., Donald, J., & Harrington, R.A. 1993. Grouped response units for distributed hydrologic modelling. *Journal of Water Resources Planning & Management - ASCE*, **119(3)**, 289-305.
- Krause, P., Boyle, D.P. & Base, F. 2005. Comparison of different efficiency criteria for hydrological model assessment. *Advances in Geosciences* **5**, 89 – 97
- Labadie, J.W. 2007. MODSIM 8.1: River Basin Management Decision Support System, User Manual and Documentation. 128pp. Available at: <http://www.engr.colostate.edu/~labadie/projects/MODSIMv8.1UserManual.pdf>
- Lantbrukarnas Riksförbund, Statistiska Centralbyrån Miljöredovisning för Svenskt Jordbruk 2000. Projektledare Erik Bendz, LRF. 2001
- Larentis, D.G., Collischonn, W. & Tucci, C.E.M. 2008. Simulação da qualidade de água em grandes bacias: Rio Taquari-Antas, RS. *Revista Brasileira de Recursos Hídricos*, v. 13, 5-22.
- Leff, B., Ramankutty, N., & Foley, J.A. 2004. Geographic distribution of major crops across the world *Global Biogeochemical Cycles* **18(1)**.
- Lehner, B. & Döll, P. 2004. Development and validation of a global database of lakes, reservoirs and wetlands. *Journal of Hydrology* **296(1-4)**, 1-22.
- Liang, X., Lettenmaier, D.P., Wood, E.F. & Burges, S.J. 1994. A simple hydrologically based model of land surface water and energy fluxes for general circulation models. *Journal of Geophysical Research* **99(D7)**, 14415-14428.
- Lui, Y., Gembremeskel, S., De Smedt, F. & Pfister, L. 2002. Flood prediction with wetspa model on catchment scale. Flood Defense 2002, Science Press New York Ltd.
- Magaña, V., Amador, J.A. & Medina, S. 1999. The midsummer drought over Mexico and Central America. *Journal of Climate* **12(6)**, 1577-1588.
- Malaquín I. 2006. La adaptación de las empresas ganaderas a la variabilidad del entorno. 8pp. Available at: http://www.eemac.edu.uy/dmdocuments/seminarios_discusion/El_Entorno_Ganadero_2006.pdf
- McGregor, G.R. & Nieuwolt, S. 1998. *Tropical Climatology : An Introduction to the Climates of the Low Latitudes*, 2nd ed. xi. Wiley, New York. 339pp.
- Meigh J.R., McKenzie A.A., Austin B.N., Bradford R.B. & Reynard N.S. 1998. Assessment of global water resources – Phase II, Estimates of present and future water availability for Eastern and Southern Africa. Institute of Hydrology / Department for International Development, 104 pp.

- Meigh J.R., McKenzie A.A. & Sene K.J. 1999. A grid-based approach to water scarcity estimates for eastern and southern Africa. *Water Resources Management* **13**, 85-115.
- Mitchell, T.D. & Jones, P.D. 2005. An improved method of constructing a database of monthly climate observations and associated high-resolution grids. *International Journal of Climatology* **25**, 693 – 712.
- Molfino J.H. & Califra, A. 2002. Agua Disponible de las Tierras del Uruguay. División de Suelos y Aguas, Ministerio de Ganadería Agricultura y Pesca. 12pp. Available at: http://www.mgap.gub.uy/Renare/SuelosyAguas/EstudiosBasicosdeSuelos/agua_disponible.pdf
- Molfino J.H., Morelli, C., Califra, A., Clerici, C. & Petraglia, C. 2000. Zonificación de Tierras de la cuenca del Río Cuareim-Evaluación de dos sistemas de producción bajo riego-Aportes a su regulación hídrica. Proyecto FAO GCP/RLA126/JPN. Available at: <http://www.rlc.fao.org/proyecto/139jpn/document/3dctos/sirtplan/06urutx.PDF>
- Monteith, J.L. 1965. Evaporation and the Environment. In: Fogg, G.E. (ed.) *The State and Movement of Water in Living Organisms*. Cambridge University Press. 205-234.
- Montenegro-Guillén, S. 2006. *Lake Cocibolca/Nicaragua - Experience and Lessons Learned Brief*, International Lake Environment Comité.
- Moore, R.J. & Clarke, R.T. 1981. A distribution function approach to rainfall-runoff modelling. *Water Resources Research* **17(5)**, 1367-1382.
- Moore R.J. 1985. The probability-distributed principle and runoff production at point and basin scales. *Hydrological Sciences Journal* **30(2)**, 273-297
- Mota, F.S. 2000. Influência dos fenômenos El Niño e La Niña sobre a necessidade de irrigação do arroz em Pelotas (RS). *Revista Brasileira de Agrometeorologia*, v. 8, nº 1.
- Mu, Q., Heinsch, F.A., Zhao, M. & URNG, S.W. 2007. Development of a global evapotranspiration algorithm based on MODIS and global meteorology data. *Remote Sensing of the Environment* **111(4)**, 519-536.
- Nash, J.E. & Sutcliffe, J.V. 1970. River flow forecasting through conceptual models 1. A discussion of principles. *Journal of Hydrology* **10**, 282-290.
- Neitsch, S.L., Arnold, J.C., Kiniry, J.R., Williams, J.R. & King, K.W. 2002^a. Soil and Water Assessment Tool Theoretical Documentation. Version 2000. Texas, Texas Water Resources Institute, College Station.
- Neitsch, S.L., Arnold, J.C., Kiniry, J.R., Williams, J.R. & King, K.W. 2002^b. Soil and Water Assessment Tool User's Manual. Version 2000. Texas, Texas Water Resources Institute, College Station.
- Nealder J.A. & Mead R. 1965. A simplex method for function minimization. *Computer Journal* **7**, 308-313
- Nijssen, B, Lettenmaier, D.P., Liang, X., Wetzel, S.W. & Wood, E.F. 1997. Streamflow simulation for continental-scale river basins. *Water Resources Research* **33(4)**, 711-724.
- OAS. 2007. PROCUENCA San Juan Organization of American States (OAS). Available at: <http://www.oas.org/sanjuan/defaultesp.html>. Accessed 24-03-2007.
- Oñate Valdivieso F., Duque E., León P., Duque F. Rojas W. & Tenesaca F. 2007. Caracterización Climática, Meteorológica e hidrológica de una cuenca Binacional previo a la implementación de un Modelo Hidrológico semidistribuido de Generación Continua, Area de Hidrología UGC-SIG, Universidad de Loja - Ecuador.
- Paz, A.R., Collischonn, W. & Silveira, A.L.L. 2006. Improvements in large scale drainage networks derived from digital elevation models. *Water Resources Research* **42(8)**.

- Paz, A.R. & Collischonn, W. 2007. River reach length and slope estimates for large-scale hydrological models based on a relatively high-resolution digital elevation model. *Journal of Hydrology* **343**, 127-139.
- Pebezma, E.J. & Wesseling, C.G. 1998. Gstat: a program for geostatistical modelling, prediction and simulation. *Computers & Geosciences* **24(1)**, 17-31.
- Pebezma, E.J. 2004. Multivariable geostatistics in S: the gstat package. *Computers & Geosciences* **30**, 683-691.
- Peña, H., Vidal, F. & Escobar, F. 1985. Estimación de tasas de derretimiento de nieve. VII Congreso Nacional, Sociedad Chilena de Ingeniería Hidráulica, Concepción, Chile.
- Peña, M. & Douglas, M.W. 2002. Characteristics of wet and dry spells over the Pacific side of Central America during the rainy season. *Monthly Weather Review* **130(12)**, 3054-3073.
- Pérez, F.L. 2006. Modelamiento Hidrológico de la Cuenca del Río Piura y Río Jequetepeque con Modelo SWAT. Proyecto Compensación equitativa de los Servicios Ambientales Hídricos en las cuencas del río Jequetepeque y Piura.
- Pisciottano G., Díaz, A., Cazes, G. & Mechoso, R. 1994. El Niño-Southern Oscillation Impact on Rainfall in Uruguay. *Journal of Climatology* **7**, 1286-1302.
- PRENADER, CONEAT: <http://www.prenader.gub.uy/coneat/>
- Portig, W.H. 1976. The climate of Central America. In: Schwerdtfeger, W. (ed.) *World Survey of Climatology*. Elsevier, New York. 405-464.
- Press, W.H., Teukolsky, S.A., Vetterling, W.T. & Flannery, B.P. 1995. *Numerical Recipes in FORTRAN*. Cambridge University Press.
- Proyecto Binacional Catamayo-Chira. 2003. Cartografía digital. Mapa de cobertura Vegetal y uso actual del suelo, Mapa de tipos de suelos, Ubicación de estaciones hidrometeorológicas. Loja – Piura.
- Rawls, W.J., Ahuja, L.R., Brakensiek, D.L. & Shirmohammadi, A. 1993. Infiltration and soil water movement. In: Maidment, D. (ed) *Handbook of hydrology*.
- Reed, S.M. 2003. Deriving flow directions for coarse-resolution (1-4 km) gridded hydrologic modelling. *Water Resources Research* **39(9)**, 1238+.
- Robertson, A.W. & Mechoso, C.R. 2000. Interannual and interdecadal variability of the South Atlantic convergence zone. *Monthly Weather Review* **128**, 2947-2957.
- Roel, A. & Baethgen, W. 2005. El Niño y el arroz, Efectos en la producción uruguaya. Publicación en el suplemento del diario el País : el País Agropecuario N° 119.
- Saxton, K.E., Rawls, W.J., Romberger, J.W. & Papendick, R.I. 1986. Estimating generalised soil water characteristics from texture. *Soil Sci. Soc. Am. J.* **50(4)**, 1031-1036.
- Sharpley, A.N. & Williams, J., 1990. EPIC, Erosion/Productivity Impact Calculator, U.S. Dept. of Agriculture, Agricultural Research Service, Technical Bulletin, Washington, D.C.
- Siebert, S., Döll, P., Feick, S., Hoogeveen, J. & Frenken, K. 2007. Global Map of Irrigation Areas version 4.0.1. Johann Wolfgang Goethe University, Frankfurt am Main, Germany / Food and Agriculture Organization of the United Nations, Rome, Italy.
- Sofini, A., Holvoet, K. & van Griensven, A. 2006. The Soil and Water Assessment Tool - The Nil Catchment. UNESCO – IHE, Institute for Water Education.
- Soulis, E.D., Kouwen, N., Pietroniro, A., Seglenieks, F.R., Snelgrove, K.R., Pellerin, P., Shaw, D.W. & Martz, L.W. 2004. A framework for hydrological modelling in MAGS. In: Spence, C., Pomeroy, J.W. & Pietroniro, A. (ed) *Prediction in Ungauged Basins: Approaches for Canada's Cold Regions*. CWRA ACRH Press, Ontario, Canada.

- Srinivasan, R. 2006. Training Manual for ArcView interface with the SWAT model. Blackland Research and Extension Center and Spatial Sciences Laboratory Texas A&M University System.
- Sincich, T.L., Levine, D.M. & Stephan, D. 1999. *Practical Statistics by Example using Microsoft Excel*. Prentice Hall, Upper Saddle River, NJ, 1999. 789pp.
- SMHI. 2005. Integrated Hydrological Modelling System IHMS Manual 5.6. Version, Sweden.
- Stehr, A., Debels, P., Romero, F. & Alcayaga, H. 2008. Hydrological modelling with SWAT under conditions of limited data availability: evaluation of results from a Chilean case study. *Hydrological Sciences Journal*. **53(3)**, 588-601.
- Teegavarapu, R.S.V. & Chandramouli, V. 2005. Improved weighting methods, deterministic and stochastic data-driven models for estimation of missing precipitation records *Journal of Hydrology* **312(1-4)**, 191-206.
- Todini, E. 1996. The ARNO rainfall-runoff model. *Journal of Hydrology* **175(1-4)**, 339-382.
- Tucci, C.E.M., Clarke, R.T., Collischonn, W., Dias, P.L.S. & Sampaio, G. 2003. Long Term Flow Forecast based on Climate and Hydrological Modelling: Uruguay river basin. *Water Resources Research* **39(7)**, SWC3.1-3.11.
- Turner K.J., Fogwill, C.J., McCulloch, R.D. & Sugden, D.E. 2005. Deglaciation of the eastern flank of the North Patagonian Icefield and associated continental-scale lake diversions. *Geografiska Annaler: Series A, Physical Geography* **87**, 363-374.
- UNESCO Instituto de Mécanica de los Fluidos e Ingeniería Ambiental, Facultad de Ingeniería; Universidad de la República - Ministerio de Transporte y Obras Públicas -Dirección Nacional de Hidrografía. 2002. Balances Hídricos superficiales del Uruguay. 115pp. Available at: <http://www.unesco.org/uy/phi/biblioteca/bitstream/123456789/450/1/balanceuy.pdf>
- Universidad Nacional Agraria La Molina. Escuela de Posgrado. Maestría de Recursos Hídricos. 2004. Clase III: MODSIM. 2004. Available at: http://tarwi.lamolina.edu.pe/~echavarr/ clase_iii_mod_modelo_modsim.pdf
- USDA. 1986. Urban Hydrology for small Watersheds, TR 55.
- USGS. 1999. Swat Model Calibration 1999. USGS Water Resources of the United States. USA.
- USGS. 2000. HYDRO1k. Available at: <http://edcdaac.usgs.gov/gtopo30/hydro/>.
- USGS. 2002. *Activities in Nicaragua In Support of the Hurricane Mitch Reconstruction Program*, USGS.
- USGS. 2005. EROS (GLCC). Available at: <http://eros.usgs.gov/products/landcover/glcc.html>.
- USGS. 2006. Inter-American Biodiversity Information Network (IABIN) DGF Project USGS EROS. Available at: http://edcintl.cr.usgs.gov/iabin_datadownload.html#Honduras. Accessed 31-08-2006.
- Valarezo González J. I. 2007. Validación y Complementación de los Estudios de Suelos de la Cuenca Binacional Catamayo-Chira con miras a implementar el modelo SWAT. Proyecto Binacional Catamayo-Chira. Loja – Ecuador.
- van Deursen, W.P.A. 1995. *Geographical Information Systems and Dynamic Models: development and application of a prototype spatial modelling language.*, Doctor's dissertation thesis. Utrecht University, Utrecht.
- van Griensven, A. 2005. Sensitivity, auto-calibration, uncertainty and model evaluation in SWAT2005. UNESCO – IHE, Institute for Water Education.
- van Griensven, A. & Bauwens, W. 2003. Multiobjective autocalibration for semidistributed water quality models. *Water Resources Research* **39(12)**, 1348+.

- van Griensven, A., Meixner, T., Grunwald, S., Bishop, T. & Sirinivasan, R. 2006. A global sensitivity analysis tool for the parameters of multi-variable catchment models. *Journal of Hydrology* **324**, 10-23.
- Vorosmarty, C.J., Jauregui, C.F. & Donoso, M.C. 1998. A Regional, Electronic Hydrometeorological Data Network for South America, Central America, and the Caribbean (R-Hydronet). Available at: <http://www.r-hydronet.sr.unh.edu/english/point.html>.
- Vörösmarty, C.J., Moore, B., Grace, A.L., Gildea, M.P., Melillo, J.M., Peterson, B.J., Rastetter, E.B., & Steudler, P.A. 1989. Continental scale models of water balance and fluvial transport: an application to South America. *Global Biogeochemical Cycles* **3(3)**, 241-265.
- Vorosmarty, C.J., Green, P., Salisbury, J. & Lammers, R.B. 2000. Global water resources: vulnerability from climate change and population growth. *Science* **289**, 284-288.
- Wallin, M. (ed.), 2000. Mälaren miljö tillstånd och utveckling 1965-98. SLU, Mälarens vattenvårdsförbund.
- Walter, M.T., Brooks, E.S., McCool, D.K., King, L.G., Molnau, M. & Boll, J. 2005. Process-based snowmelt modelling: does it require more input data than temperature-index modelling? *Journal of Hydrology*. **300**, 65-75.
- Westerberg, I. 2005. *Utveckling och tillämpning av en GIS-baserad hydrologisk modell*. Institutionen för geovetenskaper, Uppsala university, Uppsala. 42pp.
- Widen-Nilsson, E., Halldin, S. & Xu, C.Y. 2007. Global water balance modelling with WASMOD-M: Parameter estimation and regionalisation. *Journal of Hydrology* **340(1-2)**, 105-118.
- Wigmosta, M.S., Vail, L.W. & Lettenmaier, D.P. 1994. A distributed hydrology-vegetation model for complex terrain. *Water Resources Research* **30(6)**, 1665-1679.
- Wiklert, P., Andersson, S. and Weidow B. 1983. Studier av markprofiler i svenska åkerjordar – en faktasammanställning. Department of soil sciences, Swedish university of agricultural sciences.
- Westman, Y. and Gyllander, A., 2005. Vattendirektivet Rapport och metodbeskrivning för indelning av sjöar, vattendrag, kustvatten och havsområden i vattenförekomster. Naturvårdsverket. Naturvårdsverket D-nr 721-5506-04Mm
- WMO. 2003. Projeto Piloto Gestão Integrada de Cheias na Bacia Hidrográfica transfronteiriça (Brasil/Uruguai) do Rio Quaraí/Cuareim. IPH-DNH.
- Wood, E.F., Lettenmaier, D.P. & Zartarian, V.G. 1992. A land surface hydrology parameterization with subgrid variability for general circulation models. *Journal of Geophysical Research* **97(D3)**, 2717-2728.
- Xu, C.Y. 2002. WASMOD - The water and snow balance modelling system. In: Singh, V.J. & Singh, F. (ed.) *Mathematical Models of Small Watershed Hydrology and Applications*. Water Resources Publications LLC, Highlands Ranch, Colorado, U.S. 555-590.
- Xu, C.Y. & Halldin, S. 1997. The effect of climate change on river flow and snow cover in the NOPEX area simulated by a simple water balance model. *Nordic Hydrology* **28(4-5)**, 273-282.
- Xu, C.Y. & Singh, V.P. 1998. Dependence of evaporation on meteorological variables at different time-scales and intercomparison of estimation methods. *Hydrological Processes* **12(3)**, 429-442.
- Yang, D., Kanae, S., Oki, T., Koike, T. & Musiak, K. 2003. Global potential soil erosion with reference to land use and climate changes. *Hydrological Processes* **17**, 2913 – 2928.
- Yapo, P.O., Gupta, H.V. & Sorooshian, S. 1998. Multi-objective global optimization for hydrologic models. *Journal of Hydrology* **204**, 83-97.
- Zakrisson, J. Ekstrand, S., Huang, B. 2004. Kväve- och fosformodellering i Svartån och Tyresån – Slutrapport. Rapport B 1551, IVL Svenska Miljöinstitutet AB.

Zhao, R.J., Zuang, Y.L., Fang, L.R., Liu, X.,R. & Zhang, Q.S. 1980. The Xinanjiang model. *Hydrological forecasting*. IAHS Publication No. **129**, 351-356.